Evidence-Based Complementary and Alternative Medicine

Underlying Mechanisms of the Cardioprotective Effects of Natural Products on Endothelial Function and Arteriosclerosis

Lead Guest Editor: Arquimedes Gasparotto Junior
Guest Editors: Denise Brentan Silva, Francislaine Aparecida dos Reis Lívero, and Laurent Picot

Underlying Mechanisms of the Cardioprotective Effects of Natural Products on Endothelial Function and Arteriosclerosis

Evidence-Based Complementary and Alternative Medicine

Underlying Mechanisms of the Cardioprotective Effects of Natural Products on Endothelial Function and Arteriosclerosis

Lead Guest Editor: Arquimedes Gasparotto Junior
Guest Editors: Denise Brentan Silva, Francislaine Aparecida dos Reis Lívero, and Laurent Picot

Contents

Ethyl Acetate Fraction from *Leandra dasytricha* (A. Gray) Cong. Leaves Promotes Vasodilatation and Reduces Blood Pressure in Normotensive and Hypertensive Rats
Rita de Cassia Vilhena da Silva, Luísa Nathália Bolda Mariano, Eleine Renata Bidinha, Camila Leandra Bueno de Almeida, Valdir Cechinel-Filho, Vanessa Samudio Santos Zanuncio, Denise Brentan Silva, Arquimedes Gasparotto Junior, and Priscila de Souza
Research Article (11 pages), Article ID 7203934, Volume 2021 (2021)

Efficacy and Safety of Curcumin Supplement on Improvement of Insulin Resistance in People with Type 2 Diabetes Mellitus: A Systematic Review and Meta-Analysis of Randomized Controlled Trials
Tianqing Zhang, Qi He, Yao Liu, Zhenrong Chen, and Hengjing Hu
Research Article (19 pages), Article ID 4471944, Volume 2021 (2021)

Hindawi
Evidence-Based Complementary and Alternative Medicine
Volume 2022, Article ID 3311228, 17 pages
https://doi.org/10.1155/2022/3311228

Review Article

Vascular Protective Effect and Its Possible Mechanism of Action on Selected Active Phytocompounds: A Review

Nur Aqilah Kamaruddin,[1,2] Muhammad Nazrul Hakim Abdullah,[3] Jun Jie Tan,[4] Vuanghao Lim,[4] Lai Yen Fong,[5] Siti Aisyah Abd Ghafar,[6] and Yoke Keong Yong[1]

[1]*Department of Human Anatomy, Faculty of Medicine and Health Sciences, Universiti Putra Malaysia, Serdang 43400, Selangor, Malaysia*
[2]*Department of Anatomy, Faculty of Medicine, Universiti Kebangsaan Malaysia Medical Centre, Cheras, Kuala Lumpur 56000, Malaysia*
[3]*Department of Biomedical Science, Faculty of Medicine and Health Sciences, Universiti Putra Malaysia, Serdang 43400, Selangor, Malaysia*
[4]*Advanced Medical and Dental Institute, Universiti Sains Malaysia, Bertam 13200, Kepala Batas, Penang, Malaysia*
[5]*Department of Pre-Clinical Sciences, Faculty of Medicine and Health Sciences, Universiti Tunku Abdul Rahman, Kajang 43000, Selangor, Malaysia*
[6]*Department of Oral Biology and Basic Sciences, Faculty of Dentistry, Universiti Sains Islam Malaysia, Persiaran MPAJ, Jalan Pandan Indah 55100 Pandan Indah, Ampang, Malaysia*

Correspondence should be addressed to Yoke Keong Yong; yoke_keong@upm.edu.my

Received 8 December 2021; Revised 22 March 2022; Accepted 30 March 2022; Published 16 April 2022

Academic Editor: Arquimedes Gasparotto Junior

Vascular endothelial dysfunction is characterized by an imbalance of vasodilation and vasoconstriction, deficiency of nitric oxide (NO) bioavailability and elevated reactive oxygen species (ROS), and proinflammatory factors. This dysfunction is a key to the early pathological development of major cardiovascular diseases including hypertension, atherosclerosis, and diabetes. Therefore, modulation of the vascular endothelium is considered an important therapeutic strategy to maintain the health of the cardiovascular system. Epidemiological studies have shown that regular consumption of medicinal plants, fruits, and vegetables promotes vascular health, lowering the risk of cardiovascular diseases. This is mainly attributed to the phytochemical compounds contained in these resources. Various databases, including Google Scholar, MEDLINE, PubMed, and the Directory of Open Access Journals, were searched to identify studies demonstrating the vascular protective effects of phytochemical compounds. The literature had revealed abundant data on phytochemical compounds protecting and improving the vascular system. Of the numerous compounds reported, curcumin, resveratrol, cyanidin-3-glucoside, berberine, epigallocatechin-3-gallate, and quercetin are discussed in this review to provide recent information on their vascular protective mechanisms in vivo and in vitro. Phytochemical compounds are promising therapeutic agents for vascular dysfunction due to their antioxidative mechanisms. However, future human studies will be necessary to confirm the clinical effects of these vascular protective mechanisms.

1. Introduction

Epidemiological studies in the last few decades have demonstrated that the consumption of foods containing high levels of flavonoids such as curcumin, resveratrol, cyanidin-3-glucoside, berberine, epigallocatechin-3-gallate, and quercetin was associated with a lower risk of cardiovascular morbidity and mortality [1]. The beneficial effect of these phytocompounds in the cardiovascular system was partly due to direct effects towards the blood vessels and the endothelium. Evidence from cohort studies and pivotal research demonstrated the ability of phytocompounds to constantly modulate vasoprotective factors. These factors regulate the function of the endothelial barrier [2,3]. These compounds show promise in the management of cardiovascular disease.

Cardiovascular disease is a leading cause of mortality globally, with a projected increase in the coming years, hence placing a tremendous strain on the world's health resources

[4]. Poor diet, smoking, obesity, and physical inactivity are among the well-known modifiable risk factors for cardiovascular disease, all of which are conditions associated with inflammation [5]. Inflammatory response plays a crucial role in endothelial cell activation/dysfunction and the pathogenesis of cardiovascular diseases [6]. Therefore, new therapeutic targets are sought to prevent cardiovascular diseases.

Although effective, medications are also associated with adverse effects and cost, as well as challenges with patient compliance [7]. On the other hand, herbal medicine with adequate clinical effectiveness and low toxicity has been used as an alternative to treat diseases [8,9]. Natural compounds such as flavonoids are becoming increasingly popular. They offer a variety of therapeutic benefits, including anti-inflammatory and antioxidizing properties, which are critical in the treatment of cardiovascular disorders [10]. In this paper, a few phytocompounds of interest are reviewed for their vascular endothelial cell protective effects against proinflammatory mediators. These compounds were isolated from natural products such as plants, vegetables, and fruits. In addition, the possible mechanisms by which these compounds can improve vascular endothelial cell integrity were elucidated.

2. The Functions of Vascular Endothelium under Physiological and Pathological Conditions

Endothelial cells of the vascular system line the entire circulatory system from the heart to the tiniest capillaries. The endothelial layer consists of 1 to 6×10^{13} cells, covers an area of approximately 1–7 m^2, and weighs approximately 1 kg in an adult human [11]. The vascular system regulates blood fluidity and fibrosis, vascular tone, angiogenesis, vascular permeability, leukocyte adhesion, and platelet aggregation, all of which are important in maintaining the homeostasis of the cardiovascular system [12]. It is well established that a healthy vascular endothelium is an excellent predictor of cardiovascular health, whereas an aberrant vascular endothelium is invariably associated with a range of cardiovascular illnesses, including hypertension and atherosclerosis [13].

Additionally, endothelial cells form a semipermeable barrier that allows certain substances to pass through between the blood and the vascular wall. A variety of localized chemicals, including nitric oxide (NO), prostacyclin, endothelium-derived hyperpolarizing factor, and endothelin, are secreted by vascular endothelial cells to control the blood vessels [14]. These chemicals dilate blood vessels, promote anti-cell proliferation, are involved in antiagglutination, and reduce blood pressure under physiological conditions. These chemicals also alter endothelium homeostasis in pathological situations such as during hypercholesterolemia, vasoactive amine circulation, infection, and immunological conditions [15].

Endothelial cells also play an important function in blood flow regulation. This function is enhanced by the ability of quiescent endothelial cells to form an active antithrombotic surface that facilitates the flow of plasma and cellular components throughout the vasculature [16]. Endothelial cells generate a prothrombotic and antifibrinolytic milieu in response to perturbations, such as those that may occur during inflammation or high hydrodynamic shear stress [17]. Additionally, the production and absorption of vasoactive endothelial chemicals play a role in blood flow regulation. These chemicals work in a paracrine manner to constrict and dilate particular arterial beds in response to stimuli such as endotoxin [18].

The regulation of vascular tone is another essential function of the endothelium. Healthy endothelial cells help to maintain a balance between vasorelaxing and vasoconstricting factors in the blood. Endothelial cells release various vasoconstrictors such as angiotensin II, endothelin, thromboxane A2, and free radicals, while nitric oxide (NO) and prostacyclin (PGI2) are the most potent vasodilators to retain basal vascular tone. Endothelial cells synthesize these vasodilators in response to bradykinin, thrombin, adenosine triphosphate (ATP), adenosine diphosphate (ADP), and shear stress. Particularly, endothelial-derived NO stimulates the soluble guanylyl cyclase (sGC) pathway in smooth muscle cells which results in a reduction of contraction and vasodilation [14]. Hence, impaired bioavailability of NO is attributed to endothelial dysfunction, which initiates pathological events involving chronic inflammation such as atherosclerosis, hypertension, and diabetes [19].

Furthermore, the endothelium is also essential for coordinating leukocyte trafficking during vascular injuries. Lymphocytes, neutrophils, and monocytes do not adhere to the endothelium in physiological conditions due to the antiadhesive phenotype of endothelial cells. However, stimuli such as proinflammatory cytokines, shear stress, oxidized LDL (ox-LDL), and vasoconstrictors could shift the endothelial cell phenotype to be proadhesive to leukocytes, initiating the recruitment and the subsequent migration to the subendothelial space [20]. Here, the leukocytes develop into macrophages and then foam cells, assisting in the formation and progression of atherosclerotic plaques [21]. This shows that endothelial dysfunction and monocyte-endothelial interactions are critical for atherosclerosis' start and development.

The development of vascular disease is dependent on the activation of the vascular endothelial cell. The activation increases the expression of proinflammatory mediators, chemokines, and growth factors that enhance ROS formation, inhibit eNOS expression, and decrease NO bioavailability [22], priming the blood vessels to be in a more prothrombotic and proinflammatory state [23,24]. Furthermore, the expression of cells adhesion molecules (CAM) such as E-selectin, vascular CAM-1 (VCAM-1), and intercellular adhesion molecules-1 (ICAM-1) is also upregulated, leading to leukocytes' recruitment, migration, and infiltration [25]. This mechanism occurs in many inflammatory diseases and induces endothelial cell inflammation and endothelial dysfunction [26]. The endothelial cell will have impaired vascular tone, endothelial-dependent vasodilatation, and redox imbalance as well as increased inflammatory reactions inside the wall of the blood vessel [27] (Figure 1). Proinflammatory mediators or cytokines that cause vascular endothelial cell activation and endothelial dysfunction are

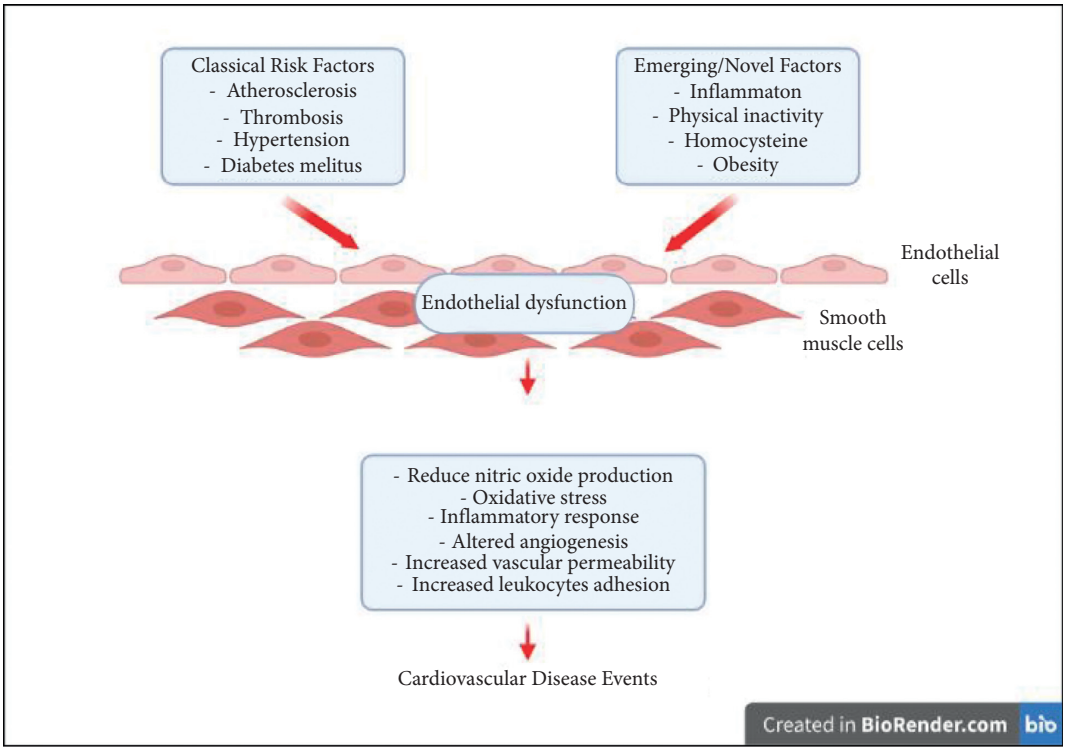

Figure 1: Mechanisms linked to endothelial dysfunction. Adapted from [26].

listed in Table 1. Identification of endothelial cell-derived inflammatory inducing factors and its underlying mechanisms may be beneficial in preventing the onset of cardiovascular diseases.

3. Vascular Protective Effects of Active Phytocompounds

3.1. Curcumin. Curcumin, a flavonoid compound derived from the roots of the plant *Curcuma longa,* is a major component of turmeric. Turmeric is commonly a spice and food-coloring agent. Curcumin's β-diketone group, carbon-carbon double bonds, and phenyl rings with numerous hydroxyl groups and methoxy substituents make it a strong antioxidant [46]. Curcumin also has anti-inflammatory [47], antiviral, antibacterial, antifungal [48], anticancer, and antitumor effects [47,49], making it a promising phytochemical for treating cancer, diabetes, allergies, arthritis, Alzheimer's disease, and other chronic conditions [50,51].

Curcumin may also help protect endothelial cells from the negative vascular effects stimulated by TNF-α which modulates p38, signal transducer and activator of transcription-3 (STAT-3), nuclear factor kappa B (NF-κB), and c-Jun N-terminal kinase (JNK) in endothelial cells [52]. Lee et al. [53] also report that curcumin significantly inhibited TNF-α-induced lectin-like oxidized LDL receptor-1 (LOX-1) expression and suppressed endothelial activation and dysfunction against TNF-α. Specifically, the authors demonstrated that curcumin treatment inhibited the formation of ROS, along with the degradation of IκBα and the translocation of NF-B. Curcumin also simultaneously induced eNOS to ensure sufficient production and availability of NO for optimal endothelial function were not adversely affected [53]. Kim et al. [52] additionally found that curcumin reduced the production of ICAM-1 mRNA and its associated TNF-α-activated protein in human umbilical vein endothelial cells (HUVECs).

One of the prominent effects of curcumin on the endothelium is the inhibition of leukocyte adhesion. An *in vitro* study has shown that human umbilical vein endothelial cells (HUVECs) pretreated with 40 μM curcumin for 1h completely inhibited endothelial cell adhesion to monocytes. The effect was induced by tumor necrosis factor-alpha (TNF-α) [52,54] and associated with the suppression of cell surface molecules. Particularly, ICAM-1, VCAM-1, E-selectin [54], monocyte chemoattractant protein (MCP)-1, and interleukin (IL)-8 were suppressed by curcumin at both the mRNA and protein level [52]. Leukocyte recruitment and adhesion are inflammatory hallmarks in the vasculature and probably the first stage in atherosclerotic plaque development [55]. Leukocytes adhered to the endothelial cells then differentiate into tissue macrophages, resulting in the development and stabilization of local inflammation. The matured macrophages, as well as their transition into foam cells, eventually form plaque. Hence, the vascular protective effect exhibited by curcumin is derived from the compound's ability to prevent leukocytes' recruitment, modulate lipoprotein composition, and attenuate oxidative stress through antioxidative processes.

Another factor that increases the risk of cardiovascular morbidity and mortality is environmental pollutants. [56].

Table 1: Summary of the type of endothelial cell damaging factors with its effects on respective vascular endothelial cells.

Source	Type of endothelial cell	Effect/mechanism	Ref.
Tumor necrosis factor-alpha (TNF-α)	Human umbilical vein endothelial cells (HUVECs)	(i) Induction of oxidative stress, inflammation, and apoptosis (ii) Induction of inflammation and monocytes adhesion	[28,29]
Glycated low-density lipoprotein (glyLDL)	Porcine aortic EC (PAEC)	(i) Induction of oxidative stress and apoptosis	[30]
Bradykinin	HUVECs	(i) Induction of endothelial hyperpermeability (ii) Stimulation of angiogenesis via increased endothelial permeability and remodeling	[31,32]
Histamine	HUVEC Human dermal microvascular endothelial cells (HDMEC)	(i) Increased endothelial permeability through PLC-NO-cGMP signaling cascade (ii) Induction of endothelial dysfunction by activating Ca2+-mediated RhoA and adherens junctions' tension	[33,34]
α-Thrombin	HUVECs	(i) Increased endothelial macromolecular permeability	[35]
IFNγ	HUVEC	(i) Induction of endothelial hyperpermeability via activation of p38 MAP kinase and actin cytoskeleton alteration	[36]
IL-1α	Brain microvascular endothelial cells (BECs)	Activation and induction of angiogenic markers in endothelial cells	[37]
IL-1β	Human glomerular endothelial cell (HRGEC)	Induction of vascular hyperpermeability and upregulation of vascular endothelial-cadherin	[38]
IL-4	Human coronary artery endothelial cells (HCAEC) and human pulmonary artery endothelial cells (HPAEC)	Induction of vascular hyperpermeability through Wnt5A signaling	[39]
Lipopolysaccharide (LPS)	HUVECs HUVECs and human lung microvascular endothelial cells (HMVEC-L)	(i) Induction of apoptosis, injury, JNK phosphorylation, decreased MCL-1 expression and SOD activity, and increased proinflammatory cytokine production. (ii) Activation of endothelial cells' inflammatory responses	[40,41]
Thrombin	Primary human dermal microvascular endothelial cells (HDMECs) Human pulmonary microvascular endothelial cells (HPMVECs)	(i) Induction of microvessel leakage (ii) Induction of vascular hyperpermeability via dysregulation of vascular endothelial (VE-)cadherin and alteration of small rho GTPases	[42,43]
Angiotensin II (Ang II)	HUVECs	Induced vascular endothelial cells' injury and oxidative stress	[44]
Glucose	Rat aortic endothelial cells (RAOECs)	Induces cyclin D2 upregulation and miR-98 downregulation	[45]

For instance, the presence of high bisphenol A levels in urine and serum is associated with an increased risk and atherogenic alterations in the carotid artery, respectively [57]. Di-(2-ethylhexyl) phthalate (DEHP), on the other hand, is a popular plasticizer used in flexible polyvinyl chloride goods including soft-squeeze toys, food packaging, clothes, medical tubing, and blood storage bags. A growing body of epidemiological research indicates a favourable relationship between circulating levels of phthalate metabolites and cardiovascular diseases [58]. DEHP promoted atherosclerosis in mice model [59] and may enhance the expression of inflammatory mediators such as ICAM-1 and IL-8 in HUVECs via ERK and p38 MAPK signaling pathway. Increase in these markers increases the likelihood of allergic inflammatory reactions leading to hospitalization [60]. Interestingly, the same study reported that curcumin significantly inhibited ICAM-1 and IL-8 production stimulated by DEHP.

Extensive studies indicate that ambient exposure to environmental pollution is strongly associated with an increased risk of cardiovascular morbidity and mortality [56]. For instance, the presence of high urine bisphenol A levels relates to an increased risk of cardiovascular disease, and the elevated serum bisphenol A level is associated with atherogenic alterations in the carotid artery [57]. Di-(2-ethylhexyl) phthalate (DEHP), considered as one of the common environmental pollutants, is a popular plasticizer used in flexible polyvinyl chloride goods including soft-squeeze toys, food packaging, clothes, medical tubing, and blood storage bags. A growing body of epidemiological research indicates a favourable relationship between circulating levels of phthalate metabolites and cardiovascular diseases [58]. DEHP not only promoted atherosclerosis in mice model [59], study from in vitro also found that it may enhance inflammatory mediator expressions such as ICAM-1 and IL-8 in HUVECs via ERK and p38 MAPK signaling pathway, which increases the likelihood of allergic inflammatory reaction admissions [60]. Interestingly, Wang and Dong [60] reported that curcumin significantly inhibited ICAM-1 and IL-8 production which was stimulated by DEHP in the same study.

Pathogens have also been associated with disrupting the normal function of endothelial cells. Lipopolysaccharide (LPS) of Gram-negative bacteria cell walls is also a powerful monocyte/macrophages activator. The activation alters the production of important mediators including inflammatory cytokines and chemokines, leading to acute inflammation in many cell types including endothelial cells [61]. Furthermore, LPS-mediated release of high-mobility group box-1 (HMGB1) from macrophages and dendritic cells plays an important role in vascular inflammation [62,63]. A study revealed that curcumin inhibits LPS-mediated release of HMGB1 and HMGB1-mediated proinflammatory responses in human endothelial cells through downregulation of the cell surface expression of HMGB1 receptors TLR2 and TLR4 [64].

Curcumin injection has also been shown to reduce ICAM-1 expression using a mouse model of lung damage. The compound inhibited neutrophil sequestration by inhibiting the activation of endothelial-derived ICAM-1, which is normally observed in an endotoxemia mice model with induction of heme oxygenase (HO-1) [65]. Boola and colleagues [66] have shown that curcumin therapy for 6 weeks in male renovascular hypertensive rats inhibited the development of hypertension by reducing endothelial dysfunction, vascular remodeling, and oxidative stress. It has also been discovered that curcumin as a daily diet increases antioxidant activity, NO bioavailability, and decreases angiotensin-converting enzyme (ACE) and metalloproteinase-2 (MMP2) and MMP9 expression [66]. Curcumin supplementation at 300 mg/kg body weight reduced diabetic vascular inflammation in diabetes-induced endothelial dysfunction male Wistar rats [67]. The production of both ICAM-1 and the pro-oxidative NOX-2 enzymes was achieved by a reduction in ROS generation and leukocyte/endothelium interaction [67].

Moreover, in stroke-prone spontaneously hypertensive rats (SHRsp), treatment of curcumin at 100 mg/kg/day significantly delayed the onset of stroke and increased survival. These effects were a result of decreased ROS and improved endothelial-dependent relaxation of carotid arteries. In this study, both curcumin-mediated decrease of ROS and increase of NO production were blocked in the presence of UCP2 inhibitor genipin. This result was consistent with the *in vitro* study in which curcumin increased NO levels and decreased ROS levels in the HUVECs [68].

3.2. Resveratrol. Resveratrol (trans-3, 4, 5-trihydroxystilbene), a natural polyphenolic compound, is abundantly found in grape skin, peanuts, mulberries, and red wine. It is a phytoalexin that plants employ to protect themselves against fungus and other types of aggression. Epidemiological research connecting red wine to decreased mortality from cardiovascular diseases in the French population despite the high intake of dietary cholesterol and saturated fats was later associated with resveratrol [69]. Resveratrol has antioxidative, modulatory lipoprotein metabolism, antiplatelet aggregatory, anti-inflammatory, and antitumor properties [70–72]. Resveratrol also protected the cardiovascular system in a multidimensional way, including vasculature. The protective effect of resveratrol against vascular dysfunction has been demonstrated in *in vitro* and *in vivo* studies.

Human coronary artery endothelial cells treated with resveratrol significantly suppressed reactive oxygen species (ROS) production and NF-κB activation while concurrently downregulated the ICAM-1, iNOS, IL-6, and TNF-α inflammatory markers against induction from TNF-α and cigarette smoke extract [73,74]. Resveratrol also protects vascular inflammation by targeting cyclooxygenease-1 (COX-1) and cyclooxygenase-2 (COX-2) that also reduces prostaglandin activity [71]. COX-1 is a constitutive isoform of COX regularly secreted in different sites including vasculature while COX-2 is an inducible isoform that releases prostaglandins, prostacyclines, and thromboxane, all of which cause inflammation [75]. In healthy blood vessels, endothelial and smooth muscle cells express COX-1, with COX-2 a distant second. However, in endothelial cells of both healthy and diseased blood vessels, COX-1 is a significant source of prostaglandins [76]. Overproduction of prostaglandins leads to the formation of prostaglandin D_2 and E_2, prostacyclin, and thromboxane A_2 which eventually promote vascular inflammation and platelet aggregation [76]. Thus, the suppression of COX-1, COX-2, prostaglandin activity, and other inflammatory mediators by resveratrol protects vasculature from phlogistic agent-induced damage. Another study has also shown that resveratrol activates anti-inflammatory pathways, including sirtuin 1, [69] while *in vitro* studies demonstrated the compound's antioxidant potential.

Resveratrol reduces ROS generation by inhibiting nicotinamide adenine dinucleotide phosphate oxidases and scavenges hydroxyl, superoxide, metal-induced radicals, and hydrogen peroxide [77–80]. A study by Chen and team [81] demonstrated that high-glucose-induced oxidative stress and apoptosis in murine brain microvascular endothelial cell bEnd3 through the NF-κB/NADPH oxidase/ROS pathway was significantly abrogated by resveratrol treatment. Resveratrol also attenuated oxidative injury in human vascular endothelial cells through the regulation of mtROS homeostasis, which in part was mediated through the activation of the SIRT3 signaling pathway [82]. Although resveratrol was capable to counter oxidative stress-induced vascular injury, the vascular protective effects are likely attributed to the indirect upregulation of the endogenous cellular antioxidant systems rather than its direct ROS scavenging activity. Additionally, resveratrol causes the increase of endogenous antioxidant enzymes in endothelial cells, including superoxide dismutases (SOD) [83], SOD1, glutathione peroxidase 1 (GPx1) and NADPH oxidase subunit (NO×4) [84], thioredoxin-1 (Trx-1) [85], heme oxygenase-1 [86], and NAD(P)H:quinone oxidoreductase (NQO1 and NQO2) [87].

Apart from abovementioned mechanism, resveratrol was also reported to protect the vascular system via the antiapoptotic effect. Specifically, resveratrol prevented circulating endothelial cells from oxLDL-induced apoptotic insults by downregulating Lox-1-mediated activation of the

Bax-mitochondria-cytochrome c-caspase protease pathway [88], and increasing the expression of endothelial nitric oxide synthase (eNOS), which results in increased nitric oxide generation from endothelial cells [89]. Increased endothelial nitric oxide production can improve endothelial function and acutely reduce systolic blood pressure, which may be critical in preventing cardiovascular disease [90].

The vascular protective effect of resveratrol in animal models is also well documented. Male Wistar rats treated with 50 mg/L of resveratrol for 10 weeks significantly prevented high-fructose corn syrup-induced vascular dysfunction associated with a metabolic syndrome [91]. In addition to insulin resistance, hypertriglyceridemia, and hepatic steatosis, rats on a high-fructose diet also developed endothelial dysfunction [92]. The related mechanisms are decrease in nitric oxide synthase (NOS) activity and increase in ROS generation mediated by the vascular renin angiotensin system, which possibly results in lower NO bioavailability [92]. Resveratrol also significantly mitigated high-fat diet-induced vascular dysfunction in male C57BL/6 mice [93]. As obesity has a strong link with insulin resistance [94], insulin signal loss in endothelial cells promotes leukocyte-endothelial cell interactions, triggering inflammation associated with the development of vascular dysfunction [95]. The vascular protective effect of resveratrol in both metabolic disorders might be attributed to the increased expression of the eNOS and SIRT1 protein [91,93]. Moreover, resveratrol also promoted the integrity of epithelial cell lining, as well as suppressed leukocyte extravasation, which eventually prevented injury of the vascular [93].

3.3. Cyanidin-3-Glucoside (C3G). Anthocyanins are polyphenols of the flavonoid family, a natural pigment responsible for the blue, purple, red, and orange colours widely present in fruits and vegetables. Anthocyanins are claimed to have potential health-promoting effects. In recent decades, the relatively high intake of anthocyanins is investigated for roles in health promotion and illness prevention. Cyanidin-3-glucoside (C3G), one of the major components of anthocyanins commonly found in black currant, red cabbages, red raspberry, blueberry, blackberry, and purple rice bran, contributes to the violet, blue, and red colours [96]. *In vitro* and *in vivo* studies demonstrated the antioxidant and anti-inflammatory properties of C3G [97,98], as well as providing protection against endothelial dysfunction, vascular failure, and myocardium damage [99,100]. It also has been shown to prevent obesity and hyperglycemia [101] and appear to help prevent cardiovascular diseases [102]. C3G and its phenolic metabolites also exhibited distinct biological properties and potentially beneficial effects in various human pathologies [103]. The vascular protective effect of C3G was mainly reported in cell culture models.

Sivasinprasasn et al. [104] and Pantan et al. [105] evaluated the effect of C3G on vascular endothelial cells (EA.hy926) and human aortic vascular smooth muscle cells (HASMCs) in an inflammation model against angiotensin II. Both studies reported that C3G pretreatment significantly suppressed NF-kB signaling pathway through downregulation of NF-kB p65, decreased the expression of inducible nitric oxide synthase (iNOS), enhanced nuclear erythroid-related factor 2 (Nrf2), increased superoxide dismutase (SOD), and increased heme oxygenase (HO-1) activities [104,105]. Pantan and team further investigated the possible vascular protective effect of C3G on angiotensin II-induced human aortic smooth muscle cells (HASMCs) inflammation. C3G significantly suppressed angiotensin II-induced HASMCs proliferation and migration through MAPK and PI3K/Akt pathways [106]. Furthermore, a combination of low-dose statins and C3G possessed a synergistic effect on inhibiting angiotensin II-induced inflammation in vascular smooth muscle cells [105,106]. A combination of atorvastatin and C3G successfully decreased the expression of ICAM-1 and VCAM-1, nitric oxide (NO) production, and NOX1 while concurrently increased NAD(P)H:quinone oxidoreductase (NQO-1) and glutamate-cysteine ligase catalytic subunit (γ-GCLC) [106].

Inflammation and oxidative stress-induced vascular endothelial dysfunction and phenotypic switch of vascular smooth muscle cells are the main factors contributing to the early stage of atherosclerosis [107,108]. Atherosclerosis is established to be a vascular inflammatory disease. Lesion areas in the vascular smooth muscle cells exhibited increased permeability, leukocytes' migration, foam cells' formation, and release of proinflammatory cytokines, which trigger a deleterious event such as myocardial infarction [109]. Vascular smooth muscle cells' proliferation and migration are also triggered by angiotensin II which promotes the formation of reactive oxygen species (ROS) by activating NADH/NADPH and subsequent activation of the NF-kB signaling pathway [110,111], leading to vascular dysfunction. Furthermore, angiotensin II promoted cellular hypertrophy, induced the release of various growth factors, altered the extracellular environment by modifying the matrix composition, and stimulated apoptosis in vascular smooth muscle cells [112]. Thus, the ability of C3G to suppress angiotensin II potentiates the compound against atherosclerosis.

Studies have also found that C3G modulates anti-inflammation in human umbilical vein endothelial cells' injury caused by TNF-α and lipopolysaccharide (LPS) both *in vitro* and *in vivo* [113,114]. Speciale and team [113] demonstrated that pretreatment of C3G at 20–40 μM significantly suppressed TNF-α-induced HUVECs injury in a dose-dependent manner. The protective effects were associated with suppression of adhesion molecules expression, leukocyte adhesion, and antioxidative stress via the NF-kB signaling pathway. C3G also prevented oxidative stress, enhanced the endogenous antioxidant system, and activated the NrF2/ARE signaling pathway [115]. In addition, C3G inhibited vascular smooth muscle cells' proliferation through the repression of NOX activator 1, which is associated with the involvement of the STAT3 signaling induced by TNF-α [116]. Ma et al. [114] demonstrated that C3G positively reversed the effects of LPS by inhibiting NF-κB and MAPK pathways on HUVECs and in mice models. The vascular protective effects of C3G were also documented against different types of vascular damaging factors, including

peroxynitrite [99] and palmitate [117,118]. These studies demonstrate that C3G exhibited vascular protective effects through antioxidant activities by directly or indirectly blocking oxidative stress and enhancing the endogenous antioxidant system.

More recent study by Wang and his team [119] demonstrated the vascular protective effect of C3G in high-fat diet plus balloon catheter injured rabbit model. Based on the data obtained, C3G improved the function of endothelial cells and suppressed blood lipids. In this experiment, C3G may have downregulated miR-204-5p, which led to the upregulation of sirtuin 1 (SIRT1) and the restoration of endothelial cell functions [119]. In addition to this, mice supplemented with C3G significantly reversed hypercholesterolemia-induced endothelial dysfunction in both prevention and intervention studies [120]. Data from the animal studies fully supported the hypothesis from previous *in vitro* studies. The data suggested that the C3G reduces cholesterol and 7-oxysterol levels through the ATP binding cassette subfamily G member 1 (ABCG1) pathway, lowering superoxide generation and increasing eNOS activity and NO bioavailability, therefore alleviating hypercholesterolemia-induced endothelial dysfunction and atherosclerosis [120].

3.4. Berberine. Berberine (BBR), or 5,6-dihydro-9,10-dimethoxybenzo[g]-1,3-benzodioxolo [5,6-á] quinolizinium, is an isoquinoline alkaloid mainly found in rhizomes, roots, and stem bulk of plants such as the Berberidaceae and Ranunculaceae families, and Chinese herb Huanglian. Based on the chemical formula of BBR, $C_{20}H_{18}NO_4$ is a protozoan morphinane alkaloid [121]. It has long been used in the treatment of gastrointestinal infections and diarrhoea but more recently is reported to be used in treating cardiovascular complications [122]. BBR has been extensively studied on its pharmacological activity *in vivo* and *in vitro* settings, in which it exhibited anticancer [123], anti-inflammatory [124], antileishmanial [125], anti-human immunodeficiency virus [126], and neuroprotective agent [127]. Cardiovascular protective effects were revealed based on evidence that BBR suppressed proliferation and migration of vascular smooth muscle cells [128], blocked macrophages-derived foam cell formation [129], anti-inflammatory functions, inactivated inflammasome [130], inhibited platelet activation [131], and normalized vascular endothelial function [132].

BBR treatment also intervened oxidized low-density lipoprotein (oxLDL)-stimulated endothelial dysfunction. oxLDL is a proatherogenic lipoprotein that leads to excessive or abnormal proliferation of vascular endothelial cells eventually leading to atherosclerotic plaque formation [133]. Hsieh and his team [132] documented that BBR perturbed ROS production triggered by oxLDL on HUVECs. Moreover, BBR protected the HUVECs by reducing cytotoxicity and apoptosis induced by oxLDL. This effect was attributed to the regulation of mitochondrial transmembrane permeability, reducing proapoptotic protein while increasing antiapoptotic proteins [132]. Xu et al. [134] further reported that the antiproliferative and anti-inflammatory activities of BBR were exerted by lowering the expression of NF-κB, lectin-like oxidized low-density lipoprotein (LDL) receptor-1 (LOX-1), proliferating cell nuclear antigen (PCNA), and inhibiting the phosphorylation of the PI3K/Akt, extracellular signal-regulated protein kinase (ERK1/2), and p38 mitogen-activated protein kinases (MAPKs) on HUVECs, as stimulated by oxLDL.

Similar to other proinflammatory cytokines, oxLDL is capable of activating vascular endothelial cells and subsequently the expression of a series of adhesion molecules, which leads to leukocyte migration and adhesion [135]. HUVECs were also reported to be protected by BBR when challenged with oxLDL through the inhibition of VCAM-1 and ICAM-1 expression and adhesion of monocytes [136]. Interaction between oxLDL with its scavenger receptor, the lectin-like oxLDL receptor 1 (LOX1), was shown to stimulate endothelial expression and secretion of proatherogenic enzymes as well as the production of NOX (nicotinamide adenine dinucleotide oxidase)-derived ROS, thereby decreasing local NO level [137]. Interestingly, BBR suppressed LOX1 expression in the HUVECs through counterreaction with NOX2-derived ROS, MAPK/Erk1/2, and NF-κB activation [138]. More surprisingly, BBR exhibited higher activity compared to that of the reference drug, lovastatin [138].

Studies have also revealed that BBR effectively inhibited inflammatory effects caused by TNF-α in cultured human aortic endothelial cells (HAECs) and HUVECs [138,139]. BBR could prevent TNF-α-induced LOX1 expression and oxidative stress, possibly through the NOX, MAPK/Erk1/2, and NF-κB signaling cascade [138]. BBR was shown to abrogate the vascular endothelial damaging effect of TNF-α by attenuating the production of ICAM-1 and MCP-1 through suppression of NF-κB following AMPK activation in the HAECs [139]. BBR also significantly reverted vascular endothelial cell injury caused by other damaging factors. For instance, BBR suppressed leukocyte adhesion and expression of adhesion molecules in both *in vivo* and *in vitro* endothelial cell models. In these models, the damage was induced by LPS via blocking the NF-κB signaling pathway [140].

BBR protected vascular endothelial cells against angiotensin II by reducing intracellular ROS production, MCP-1, and monocyte adhesion [141]. In addition, BBR was also capable of enhancing NO production in vascular endothelial cells via upregulation of eNOS expression and its activity, in which the underlying mechanism might involve upregulation of AMP-activated protein kinase (AMPK) and downregulation of NOX4 activities [142]. Furthermore, Cheng and his team [143] revealed the vascular endothelial protective effect of BBR via a clinical trial and *in vitro* model. According to the data, BBR significantly reduced serum malondialdehyde (MDA) level and circulating endothelial microparticles in human sample, which were correlated with improvement of flow-mediated vasodilation [143]. Moreover, CD31+/CD42 circulating endothelial microparticles have emerged as a sensitive marker for endothelial damage in response to a variety of stimuli, including inflammation, partially via increasing oxidative stress in endothelial cells

[144,145]. In a cell culture setting, BBR also significantly reversed the vascular endothelial injury caused by endothelial microparticles, by altering the oxidative stress level [143].

3.5. Epigallocatechin-3-Gallate. Green tea (Camellia sinensis), a beverage widely diffused and consumed in the Asian population, has long been known for its extensive health benefits, which are mainly attributed to its polyphenol content [146]. In fresh leaf in dry weight, approximately 30% is made up of polyphenol contents, particularly flavanols and flavonols [147]. Catechins are the major flavonoids found in green tea [147], and among the catechins, epigallocatechin-3-gallate (EGCG) is mainly present in green tea. Extensive research has revealed that EGCG exhibited antioxidative stress [148], anti-inflammation [149], anticancer [150,151], antimicrobial [152], neuroprotective [153], hepatoprotective [154], renal protective [155], and cardiovascular protective effects [156].

The phenol rings in EGCG's structure trap electrons and scavengers' free radicals [157], conferring the capability to inhibit the formation of ROS, and consequently the harming effects of oxidative stress [158]. EGCG had also effectively suppressed platelet activation induced by collagen or thrombin [159] and improved the function of mitochondria [160]. However, studies have shown that EGCG at high concentrations can cause self-oxidization and function as a prooxidant [161,162]. This occurs via the production of hydroxyl radicals, hydrogen peroxide, and quinonoid intermediates which can cause cytotoxicity [163]. Therefore, more evidence is required to evaluate the relationship between dose and antioxidant signaling pathways in cellular activity.

The vascular protective effect of EGCG was observed in a TNF-α-induced inflammation cell culture study with HUVECs. EGCG significantly reduced MCP-1 and monocyte adhesion in a dose-dependent manner via inhibition of NF-κB signaling cascade against [164]. Furthermore, Yang and team demonstrated that EGCG suppressed the inflammatory response of vascular endothelial cells by increasing the cytosolic calcium (Ca^{2+}) triggered by TNF-α [165]. Elevation of cytosolic Ca^{2+} causes the activation of disintegrin and cleavage of metalloprotease 10 (ADAM10), followed by ectodomain shedding of tumor necrosis factor receptor 1 (TNFR1) [165]. By decreasing the number of receptors on the endothelial cell surface, the shedding of TNFR1 ectodomain reduces the cell's sensitivity towards TNF-α. Furthermore, the released ectodomain part of TNFR1 may bind to TNF-α in the extracellular space and negate its action [166]. A study revealed that EGCG potentially suppressed the inflammatory response of vascular endothelial cells against TNF-α via ADAM-mediated ectodomain shedding of TNFR1 [167]. Moreover, treatment of EGCG on human coronary artery endothelial cells caused the downregulation of multiple cytokines, chemokines, and transcription factor activity, including NF-κB-p65 DNA-binding activity, MCP1, IL-6, and IL-8 stimulated by TNF-α [168]. Moreover, EGCG also significantly reversed endothelial hyperpermeability and monocytes stimulated by TNF-α [168].

The treatment of HUVECs with EGCG caused a reduction of oxidative stress factors including ROS, nitrite, and MDA, while concurrently enhancing the SOD and GSH antioxidant enzymes [169]. EGCG significantly prevented HUVECs apoptosis and expression of adhesion molecules by inhibiting NF-κB activation [169]. A study has additionally shown that EGCG abrogated MC-LR-induced apoptosis of HUVECs through activation of NRF2/HO-1 signaling [170]. Microcystin-LR (MC-LR) is a toxin released from aquatic cyanobacteria and causes a variety of adverse effects on different cell types, tissues, and organs, including liver [171], kidney [172], cardiovascular, lung, intestine, and spleen [173]. MC-LR has also been shown to cause apoptosis in HUVECs by inducing oxidative stress via NF-κB activation [174]. EGCG counteracted NADPH oxidase, particularly $p47^{phox}$, in which this angiotensin II-mediated oxidase was responsible to initiate and develop inflammatory vascular diseases and inhibited the expression of iNOS induced by angiotensin II in HUVECs [175,176]. However, EGCG failed to suppress ROS in angiotensin II-stimulated HUVECs [175,176]. EGCG has also been reported to effectively protect vascular endothelial function from high-glucose stress-induced injury [177].

In addition to vascular protective effects in the *in vitro* models, EGCG also ameliorated endothelial dysfunction in animal models. For instance, Potenza and team evaluated the impact of EGCG administration on the ability of spontaneously hypertensive rats (model of metabolic syndrome with hypertension, insulin resistance, and overweight) to enhance both their cardiovascular and metabolic performances at the same time [178]. Here, EGCG exhibited a vasodilator effect in mesenteric vascular beds *ex vivo*, in both acute and chronic studies. The study suggested that the vasodilator effect was in part attributed to the stimulation of nitric oxide production from the endothelium through the PI 3-kinase-dependent pathway [178]. Furthermore, obese mice fed with EGCG at 50 mg/kg/day for 10 weeks showed improved insulin sensitivity, glucose tolerance, and endothelial function [177]. As obesity is highly associated with various metabolic and cardiovascular disorders, including insulin resistance, diabetes, and atherosclerosis [179], the pathogenesis of diabetes and its associated cardiovascular consequences is heavily influenced by reciprocal interactions between insulin resistance and endothelial dysfunction [180]. Thus, altering high-fed-diet-induced inflammatory response in obese mice, especially the amelioration of insulin resistance by EGCG, might be beneficial for endothelial function.

3.6. Quercetin. Quercetin (3,3′,4′,5,7 pentahydroxy flavone) is a natural flavonoid widely and abundantly found in almost all plant food such as tea, onion, lettuce, broccoli, beans, fruits, and buckwheat. It is also one of the effective components of ginkgo leaves, mulberry parasitic, sandalwood, and other Chinese herbs [181]. Accumulating evidence suggests that quercetin exhibits antioxidant, anti-inflammatory, and antimicrobial activities [182,183]. Moreover,

recent studies have found that quercetin can restrain the proliferation and metastasis of multiple cancer cell types such as breast cancer and colon cancer [181]. The presence of five hydroxyl groups in the structure of quercetin confers a significant level of antioxidant activity. Furthermore, the pyrocatechol type of the benzene ring makes it a strong scavenger of free radicals [184]. Quercetin is one of the most often consumed members of the flavonoid family, accounting for around 65–75% of our daily intake of flavonoids [185]. Quercetin may be found in nature in the form of ramifications that attach to glucose and rutinose [186]. Once consumed, quercetin can be swiftly degraded by the glucosidase enzyme in the digestive system, making it simpler for absorption by the mucosa of the large intestine and subsequently transported to the entire body through the portal circulation [187]. Quercetin is nontoxic and nonlethal to animals, even at large dosages (4000 mg/day), making it a safe supplement for human use [188].

Quercetin protects vascular endothelial injury through multiple approaches, for instance through its antioxidative effects. Treatment of quercetin protected the vascular endothelial cells by scavenging ROS, increasing the level of SOD and HO-1, while concurrently decreasing MDA and XO-1 levels in TNF-α and homocysteine-induced vascular endothelial cells [189,190]. Moreover, quercetin significantly opposed tunicamycin-induced HUVECs injury by reducing endoplasmic reticulum stress, possibly through the poly (ADP-ribose) polymerase (PARP) signaling [191].

Quercetin also demonstrated encouraging benefits for vascular endothelial cells' dysfunction and endothelial cell activation triggered by diabetes-related high-glucose levels in the circulation. Endothelial cells exposed to a hyperglycemic environment produce less nitric oxide but had increased cell adhesion molecules and inflammatory gene expressions caused by activation of NF-κB signaling [192]. In addition, the hexosamine biosynthesis pathway becomes overactive in diabetic individuals, leading to elevated levels of glucosamine in the blood circulation [193]. Increased glucosamine will cause endoplasmic reticulum stress, which may lead to exacerbation of endothelial cell damage. The damage eventually leads to increased inflammation and lipid metabolic abnormalities, which eventually accelerate the development of atherosclerosis [194]. A study done by Ozyel and the team [192] reported that quercetin was capable of regulating the balance of HUVECs metabolites towards a less inflamed phenotype when challenged with high-glucose stimuli. Furthermore, findings from Cai et al. [195] revealed that quercetin's protective benefits against high-glucosamine-induced HUVECs damage may be mediated through the ER/CHOP and ER/JNK pathways. PERK may also be a crucial component of the molecular mechanism responsible for these protective effects. More recently, quercetin was shown to inhibit vascular endothelial inflammation in diabetic vasculature, via suppression of myeloperoxidase/high-glucose-dependent hypochlorous acid formation. The acid formation plays an important role in diabetic vascular complications [196].

Quercetin also showed promising data in animal models. Male Sprague-Dawley rats orally treated with quercetin at doses of 25 or 50 mg/kg/day for 6 days significantly ameliorated vascular dysfunction challenged by phenylhydrazine (PHZ) [197]. PHZ is widely used for inducing haemolytic disorders and investigating anemic mechanisms [198]. It is a strong oxidant that exhibits a number of toxic effects, and the free radicals generated from PHZ might directly impact vascular tissues via oxidative stress-induced inflammation and reduction in NO bioactivity, eventually resulting in vascular dysfunction [197]. It is widely known that quercetin possesses a very strong antioxidant activity, capable of scavenging free radicals generated from PHZ and thus decreasing oxidative stress. In addition, quercetin restored arterial blood pressure and vascular responsiveness to endothelium-dependent vasodilators and vasoconstrictors, which ultimately prevent the vascular from PHZ damage [197]. Furthermore, oral administration of quercetin at 50 or 100 mg/kg either prior to or after exposure to LPS protected vascular function as measured by blood pressure, heart rate, and vascular responsiveness, which were all recovered to near-normal levels [199]. These effects were highly associated with upregulation of eNOS expression, a decrease of oxidative stress, and maintenance of the blood GSH redox ratio [199]. Quercetin also reduced inflammatory cardiovascular risk factors, such as serum amyloid A (SAA), C-reactive protein, and fibrinogen levels, when administered to mice fed with an atherogenic 1% cholesterol-containing diet [200]. Quercetin also significantly decreased histological atherosclerotic lesion growth. However, no effect was seen on monocyte adherence to the endothelium and on the lesion macrophage content [200]. The vascular protective effect of quercetin in animal models is mostly similar to other antioxidant compounds, as previously described through antioxidant activities.

4. Conclusion and Future Prospective

Natural herbs are rich sources of potential therapeutic candidates for various diseases including cardiovascular diseases, neurodegenerative disorders, and metabolic dysregulation. Repurposing the existing medications for alternative applications is an important way to discover new therapies with known safety profiles. For cardiovascular diseases, the pivotal components of pathogenesis are ROS production and inflammation, which are targeted by many phytocompounds and existing medications. Although extensive studies have been carried out to determine the vascular protective effects of active phytocompounds reviewed in this paper, there are ongoing developments and research studies on other human diseases. Active phytocompounds isolated from natural resources often face challenges in bioavailability and stability. Thus, improving extraction and formulation techniques to maintain biological activities is crucial. Furthermore, biosafety, long-term bioactivity, degrading properties, interactions with immune cells, the ability to sustainably circulate in humans, and excretion must be thoroughly evaluated before consumption. In addition, further research is needed to minimize the cost of industrial-scale manufacturing, develop better methods for synthesis or extract, and discover the optimal

route of administration. New phytochemical agents to treat cardiovascular diseases particularly vascular endothelial cells are expected to surface with the progress of research.

Data Availability

The data sets supporting the conclusions of this study are included within the manuscript.

Conflicts of Interest

The authors declare that there are no conflicts of interest.

Acknowledgments

Nur Aqilah Kamaruddin was supported by (HLP) Hadiah Latihan Persekutuan from Ministry of Education, Malaysia. The authors wish to thank supporting staff from Anatomy and Histology Laboratory, Physiology Laboratory, and Cell Signaling Laboratory from Faculty of Medicine and Health Sciences, Universiti Putra Malaysia for their excellent technical support. This work was supported by the Ministry of Higher Education, Malaysia, under Fundamental Research Grant Scheme with the code project of FRGS/1/2020/SKK0/UPM/02/1 and reference number under Universiti Putra Malaysia 04-01-20–2271FR.

References

[1] B. H. Parmenter, K. D. Croft, J. M. Hodgson et al., "An overview and update on the epidemiology of flavonoid intake and cardiovascular disease risk," *Food & Function*, vol. 11, no. 8, pp. 6777–6806, 2020.

[2] C. D. Kay, L. Hooper, P. A. Kroon, E. B. Rimm, and A. Cassidy, "Relative impact of flavonoid composition, dose and structure on vascular function: a systematic review of randomised controlled trials of flavonoid-rich food products," *Molecular Nutrition & Food Research*, vol. 56, no. 11, pp. 1605–1616, 2012.

[3] D. Zhang, M. Du, Y. Wei, C. Wang, and L. Shen, "A review on the structure–activity relationship of dietary flavonoids for protecting vascular endothelial function: current understanding and future issues," *Journal of Food Biochemistry*, vol. 42, no. 5, pp. 1–14, 2018.

[4] in*The Top 10 Causes of Death," the Top 10 Causes of Death*, https://www.who.int/news-room/fact-sheets/detail/the-top-10-causes-of-death, 2020.

[5] M. Z. Allende-Vigo, "Pathophysiologic mechanisms linking adipose tissue and cardiometabolic risk," *Endocrine Practice*, vol. 16, no. 4, pp. 692–698, 2010.

[6] P. Welsh, G. Grassia, S. Botha, N. Sattar, and P. Maffia, "Targeting inflammation to reduce cardiovascular disease risk: a realistic clinical prospect?" *British Journal of Pharmacology*, vol. 174, no. 22, pp. 3898–3913, 2017.

[7] N. Mohebbi, G. Shalviri, M. Salarifar, J. Salamzadeh, and K. Gholami, "Adverse drug reactions induced by cardiovascular drugs in cardiovascular care unit patients," *Pharmacoepidemiology and Drug Safety*, vol. 19, no. 9, pp. 889–894, 2010.

[8] Y. H. Wu, H. Y. Chen, and C. H. Lai, "Use of Chinese herbal medicine improves chemotherapy-induced thrombocytopenia among gynecological cancer patients: an observational study," *Evidence-based Complementary and Alternative Medicine*, vol. 2018, Article ID 4201325, 2018.

[9] B.-Y. Lai, A.-J. Chu, B.-W. Yu et al., "Clinical effectiveness and safety of Chinese herbal medicine compound kushen injection as an add-on treatment for breast cancer: a systematic review and meta-analysis," *Evidence-based Complementary and Alternative Medicine*, vol. 2022, Article ID 8118408, 16 pages, 2022.

[10] K. Yamagata and Y. Yamori, "Inhibition of endothelial dysfunction by dietary flavonoids and preventive effects against cardiovascular disease," *Journal of Cardiovascular Pharmacology*, vol. 75, no. 1, pp. 1–9, 2019.

[11] H. G. Augustin, D. H. Kozian, and R. C. Johnson, "Differentiation of endothelial cells: analysis of the constitutive and activated endothelial cell phenotypes," *BioEssays*, vol. 16, no. 12, pp. 901–906, 1994.

[12] P. Rajendran, T. Rengarajan, J. Thangavel et al., "The vascular endothelium and human diseases," *International Journal of Biological Sciences*, vol. 9, no. 10, pp. 1057–1069, 2013.

[13] S. Jamwal and S. Sharma, "Vascular endothelium dysfunction: a conservative target in metabolic disorders," *Inflammation Research*, vol. 67, no. 5, pp. 391–405, 2018.

[14] A. Sandoo, J. J. C. S. Veldhuijzen van Zanten, G. S. Metsios, D. Carroll, and G. D. Kitas, "The endothelium and its role in regulating vascular tone," *The Open Cardiovascular Medicine Journal*, vol. 4, no. 1, pp. 302–312, 2015.

[15] D. H. Endemann and E. L. Schiffrin, "Endothelial dysfunction," *Journal of the American Society of Nephrology*, vol. 15, no. 8, pp. 1983–1992, 2004.

[16] A. Krüger-Genge, A. Blocki, R. P. Franke, and F. Jung, "Vascular endothelial cell biology: an update," *International Journal of Molecular Sciences*, vol. 20, no. 18, 2019.

[17] O. Guipaud, C. Jaillet, K. Clément-Colmou, A. François, and F. Milliat, *The Importance of the Vascular Endothelial Barrier in the Immune-Inflammatory Response Induced by Radiotherapy*, 2018.

[18] G. Russo, J. A. Leopold, and J. Loscalzo, *Vasoactive Substances: Nitric Oxide and Endothelial Dysfunction in Atherosclerosis $*.

[19] J. yi Chen, Z. xin Ye, X. fen Wang et al., "Nitric oxide bioavailability dysfunction involves in atherosclerosis," *Biomedicine and Pharmacotherapy*, vol. 97, pp. 423–428, 2018.

[20] M. Félétou and P. M. Vanhoutte, "Endothelium-derived hyperpolarizing factor: where are we now?" *Arteriosclerosis, Thrombosis, and Vascular Biology*, vol. 26, no. 6, pp. 1215–1225, 2006.

[21] E. J. Baker, M. H. Yusof, P. Yaqoob, E. A. Miles, and P. C. Calder, "Omega-3 fatty acids and leukocyte-endothelium adhesion: novel anti-atherosclerotic actions," *Molecular Aspects of Medicine*, vol. 64, pp. 169–181, 2018.

[22] H. He, Y. Qiao, Q. Zhou et al., "Iron overload damages the endothelial mitochondria via the ROS/ADMA/DDAHII/eNOS/NO pathway," *Oxidative Medicine and Cellular Longevity*, vol. 2019, Article ID 2340392, 19 pages, 2019.

[23] C. Park-Windhol and P. A. D'Amore, "Disorders of vascular permeability," *Annual Review of Pathology: Mechanisms of Disease*, vol. 11, no. 1, pp. 251–281, 2016.

[24] T. C. Baghai, G. Varallo-Bedarida, and C. Born, "Classical risk factors and inflammatory biomarkers: one of the missing biological links between cardiovascular disease and major depressive disorder," *International Journal of Molecular Sciences*, vol. 19, no. 6, 2018.

[25] D.-H. Zhang, "Tripterine inhibits the expression of adhesion molecules in activated endothelial cells," *Journal of Leukocyte Biology*, vol. 80, no. 2, pp. 309–319, 2006.

[26] H. J. Sun, Z. Y. Wu, X. W. Nie, and J. S. Bian, "Role of endothelial dysfunction in cardiovascular diseases: the link between inflammation and hydrogen sulfide," *Frontiers in Pharmacology*, vol. 10, pp. 1–15, 2020.

[27] B. K. Ooi, K. G. Chan, B. H. Goh, and W. H. Yap, "The role of natural products in targeting cardiovascular diseases via Nrf2 pathway: novel molecular mechanisms and therapeutic approaches," *Frontiers in Pharmacology*, vol. 9, no. NOV, pp. 1308–1318, 2018.

[28] P. Zhou, S. Lu, Y. Luo et al., "Attenuation of TNF-α-induced inflammatory injury in endothelial cells by ginsenoside Rb1 via inhibiting NF-κB, JNK and p38 signaling pathways," *Frontiers in Pharmacology*, vol. 8, no. AUG, p. 464, 2017.

[29] T. Bian, H. Li, and Q. Zhou, "Human β-defensin 3 reduces TNF-α-induced inflammation and monocyte adhesion in human umbilical vein endothelial cells," *Mediators of Inflammation*, vol. 2017, Article ID 8529542, 11 pages, 2017.

[30] X. Xie, R. Zhao, and G. Shen, "Impact of cyanidin-3-glucoside on glycated LDL-induced NADPH oxidase activation, mitochondrial dysfunction and cell viability in cultured vascular endothelial cells," *International Journal of Molecular Sciences*, vol. 13, no. 12, pp. 15867–15880, 2012.

[31] Z. A. Yoke Keong Yong, "Muhd nazrul somchit, "anti-inflammatory properties of bixa orellana leaves extract are associated with suppression of bradykinin-induced endothelial hyperpermeability," *Pharmacognosy Magazine*, vol. 14, pp. S352–S357, 2018.

[32] E. Terzuoli, S. Meini, P. Cucchi et al., "Antagonism of bradykinin B2 receptor prevents inflammatory responses in human endothelial cells by quenching the NF-kB pathway activation," *PLoS ONE*, vol. 9, no. 1, Article ID e84358, 2014.

[33] Y. K. Yong, H. S. Chiong, M. N. Somchit, and Z. Ahmad, "Bixa orellana leaf extract suppresses histamine-induced endothelial hyperpermeability via the PLC-NO-cGMP signaling cascade," *BMC Complementary and Alternative Medicine*, vol. 15, no. 1, p. 356, 2015.

[34] D. Kugelmann, L. T. Rotkopf, and M. Y. Radeva, "Histamine causes endothelial barrier disruption via Ca2+-mediated RhoA activation and tension at adherens junctions," *Scientific Reports*, vol. 8, no. 1, pp. 1–14, 2018.

[35] W. D. Ehringer, O.-L. Wang, A. Haq, and F. N. Miller, "Bradykinin and α-thrombin increase human umbilical vein endothelial macromolecular permeability by different mechanisms," *Inflammation*, vol. 24, no. 2, pp. 175–193, 2000.

[36] C. T. Ng, L. Y. Fong, M. R. Sulaiman et al., "Interferon-gamma increases endothelial permeability by causing activation of p38 MAP kinase and actin cytoskeleton alteration," *Journal of Interferon and Cytokine Research*, vol. 35, no. 7, pp. 513–522, 2015.

[37] K. Salmeron, T. Aihara, E. Redondo-Castro, E. Pinteaux, and G. Bix, "IL-1alpha induces angiogenesis in brain endothelial cells in vitro: implications for brain angiogenesis after acute injury," *Journal of Neurochemistry*, vol. 136, no. 3, pp. 573–580, 2016.

[38] L. Du, F. Dong, L. Guo et al., "Interleukin-1β increases permeability and upregulates the expression of vascular endothelial-cadherin in human renal glomerular endothelial cells," *Molecular Medicine Reports*, vol. 11, no. 5, pp. 3708–3714, 2015.

[39] T. Skaria, J. Burgener, E. Bachli, and G. Schoedon, "IL-4 causes hyperpermeability of vascular endothelial cells through Wnt5A signaling," *PLoS ONE*, vol. 11, no. 5, Article ID e0156002, 2016.

[40] J. Guo, L. Wang, and L. Wang, "Berberine protects human umbilical vein endothelial cells against LPS-induced apoptosis by blocking JNK-mediated signaling," *Evidence-based Complementary and Alternative Medicine*, vol. 2016, Article ID 6983956, 11 pages, 2016.

[41] E. Z. Dayang, J. Plantinga, B. ter Ellen, M van Meurs, G Molema, and J Moser, "Identification of LPS-activated endothelial subpopulations with distinct inflammatory phenotypes and regulatory signaling mechanisms," *Frontiers in Immunology*, vol. 10, p. 1169, 2019.

[42] Y. Liu, X. L. Chen, L. Wang, and M. Martins-Green, "Insulin antagonizes thrombin-induced microvessel leakage," *Journal of Vascular Research*, vol. 54, no. 3, pp. 143–155, 2017.

[43] M. van der Heijden, G. P. van Nieuw Amerongen, and J. van Bezu, "Opposing effects of the angiopoietins on the thrombin-induced permeability of human pulmonary microvascular endothelial cells," *PLoS One*, vol. 6, no. 8, 2011.

[44] L. Zhang, J. Wang, J. Liang et al., "Propofol prevents human umbilical vein endothelial cell injury from Ang II-induced apoptosis by activating the ACE2-(1-7)-Mas axis and eNOS phosphorylation," *PLoS ONE*, vol. 13, no. 7, Article ID e0199373, 2018.

[45] X. X. Li, Y. M. Liu, Y. J. Li et al., "High glucose concentration induces endothelial cell proliferation by regulating cyclin-D2-related miR-98," *Journal of Cellular and Molecular Medicine*, vol. 20, no. 6, pp. 1159–1169, 2016.

[46] E. M. Tanvir, M. S. Hossen, and M. F. Hossain, "Antioxidant properties of popular turmeric (Curcuma longa) varieties from Bangladesh," *Journal of Food Quality*, vol. 2017, Article ID 8471785, 8 pages, 2017.

[47] A. J. Ruby, G. Kuttan, K. Dinesh Babu, K. N. Rajasekharan, and R. Kuttan, "Anti-tumour and antioxidant activity of natural curcuminoids," *Cancer Letters*, vol. 94, no. 1, pp. 79–83, 1995.

[48] S. Zorofchian Moghadamtousi, H. Abdul Kadir, and P. Hassandarvish, "A review on antibacterial, antiviral, and antifungal activity of curcumin," *BioMed Research International*, vol. 2014, Article ID 186864, 12 pages, 2014.

[49] J.-K. Lin, "Suppression of protein kinase C and nuclear oncogene expression as possible action mechanisms of cancer chemoprevention by curcumin," *Archives of Pharmacal Research*, vol. 27, no. 7, pp. 683–692, 2004.

[50] B. Salehi, Z. Stojanović-Radić, J. Matejić et al., "The therapeutic potential of curcumin: a review of clinical trials," *European Journal of Medicinal Chemistry*, vol. 163, pp. 527–545, 2019.

[51] S. J. Hewlings and D. S. Kalman, "Curcumin: a review of its effects on human health," *Foods*, vol. 6, no. 10, pp. 1–11, 2017.

[52] Y. S. Kim, Y. Ahn, M. H. Hong et al., "Curcumin attenuates inflammatory responses of TNF-α-stimulated human endothelial cells," *Journal of Cardiovascular Pharmacology*, vol. 50, no. 1, pp. 41–49, 2007.

[53] H.-S. Lee, M.-J. Lee, H. Kim et al., "Curcumin inhibits TNFα-induced lectin-like oxidised LDL receptor-1 (LOX-1) expression and suppresses the inflammatory response in human umbilical vein endothelial cells (HUVECs) by an antioxidant mechanism," *Journal of Enzyme Inhibition and Medicinal Chemistry*, vol. 25, no. 5, pp. 720–729, 2010.

[54] A. Kumar, S. Dhawan, N. J. Hardegen, and B. B. Aggarwal, "Curcumin (diferuloylmethane) inhibition of tumor necrosis

factor (TNF)-Mediated adhesion of monocytes to endothelial cells by suppression of cell surface expression of adhesion molecules and of nuclear factor-κb activation," *Biochemical Pharmacology*, vol. 55, no. 6, pp. 775–783, 1998.

[55] S. Čejková, I. Králová-Lesná, and R. Poledne, "Monocyte adhesion to the endothelium is an initial stage of atherosclerosis development," *Cor et Vasa*, vol. 58, no. 4, p. e419, 2016.

[56] T. Münzel, M. R. Miller, and M. Sørensen, "Reduction of environmental pollutants for prevention of cardiovascular disease: it's time to act," *European Heart Journal*, vol. 41, no. 41, pp. 3989–3997, 2020.

[57] C. Fang, B. Ning, A. B. Waqar et al., "Bisphenol A exposure enhances atherosclerosis in WHHL rabbits," *PLoS ONE*, vol. 9, no. 10, pp. 1–11, 2014.

[58] S. Singh and S. S.-L. Li, "Bisphenol A and phthalates exhibit similar toxicogenomics and health effects," *Gene*, vol. 494, no. 1, pp. 85–91, 2012.

[59] J.-F. Zhao, S.-H. Hsiao, M.-H. Hsu et al., "Di-(2-ethylhexyl) phthalate accelerates atherosclerosis in apolipoprotein E-deficient mice," *Archives of Toxicology*, vol. 90, no. 1, pp. 181–190, 2016.

[60] J. Wang and S. Dong, "ICAM-1 and IL-8 are expressed by DEHP and suppressed by curcumin through ERK and p38 MAPK in human umbilical vein endothelial cells," *Inflammation*, vol. 35, no. 3, pp. 859–870, 2012.

[61] M. M. Tucureanu, D. Rebleanu, C. A. Constantinescu et al., "Lipopolysaccharide-induced inflammation in monocytes/macrophages is blocked by liposomal delivery of Gi-protein inhibitor," *International Journal of Nanomedicine*, vol. 13, pp. 63–76, 2018.

[62] Y. Hirata, H. Kurobe, M. Higashida et al., "HMGB1 plays a critical role in vascular inflammation and lesion formation via toll-like receptor 9," *Atherosclerosis*, vol. 231, no. 2, pp. 227–233, 2013.

[63] J. Yang, Y. Zhao, P. Zhang et al., "Hemorrhagic shock primes for lung vascular endothelial cell pyroptosis: role in pulmonary inflammation following LPS," *Cell Death & Disease*, vol. 7, no. 9, pp. 1–16, 2016.

[64] D.-C. Kim, W. Lee, and J.-S. Bae, "Vascular anti-inflammatory effects of curcumin on HMGB1-mediated responses in vitro," *Inflammation Research*, vol. 60, no. 12, pp. 1161–1168, 2011.

[65] R. Olszanecki, A. Gebska, and R. Korbut, "The role of haem oxygenase-1 in the decrease of endothelial intercellular adhesion molecule-1 expression by curcumin," *Basic and Clinical Pharmacology and Toxicology*, vol. 101, no. 6, pp. 411–415, 2007.

[66] O. Boonla, U. Kukongviriyapan, P. Pakdeechote et al., "Curcumin improves endothelial dysfunction and vascular remodeling in 2K-1C hypertensive rats by raising nitric oxide availability and reducing oxidative stress," *Nitric Oxide*, vol. 42, pp. 44–53, 2014.

[67] N. Wongeakin, P. Bhattarakosol, and S. Patumraj, "Molecular mechanisms of curcumin on diabetes-induced endothelial dysfunctions: txnip, ICAM-1, and NOX2 expressions," *BioMed Research International*, vol. 2014, Article ID 161346, 14 pages, 2014.

[68] C. Lan, X. Chen, Y. Zhang et al., "Curcumin prevents strokes in stroke-prone spontaneously hypertensive rats by improving vascular endothelial function," *BMC Cardiovascular Disorders*, vol. 18, no. 1, pp. 43–10, 2018.

[69] M. J. Banez, M. I. Geluz, A. Chandra et al., "A systemic review on the antioxidant and anti-inflammatory effects of resveratrol, curcumin, and dietary nitric oxide supplementation on human cardiovascular health," *Nutrition Research*, vol. 78, pp. 11–26, 2020.

[70] S. Bradamante, L. Barenghi, and A. Villa, "Cardiovascular protective effects of resveratrol," *Cardiovascular Drug Reviews*, vol. 22, no. 3, pp. 169–188, 2004.

[71] S. Das and D. Das, "Anti-inflammatory responses of resveratrol," *Inflammation and Allergy - Drug Targets*, vol. 6, no. 3, pp. 168–173, 2007.

[72] B. Tadolini, C. Juliano, L. Piu, F. Franconi, and L. Cabrini, "Resveratrol inhibition of lipid peroxidation," *Free Radical Research*, vol. 33, no. 1, pp. 105–114, 2000.

[73] A. Csiszar, K. Smith, and N. Labinskyy, "Resveratrol attenuates TNF-α-induced activation of coronary arterial endothelial cells: role of NF-κB inhibition," *American Journal of Physiology - Heart and Circulatory Physiology*, vol. 291, no. 4, pp. 1694–1699, 2006.

[74] A. Csiszar, N. Labinskyy, A. Podlutsky et al., "Vasoprotective effects of resveratrol and SIRT1: attenuation of cigarette smoke-induced oxidative stress and proinflammatory phenotypic alterations," *American Journal of Physiology - Heart and Circulatory Physiology*, vol. 294, no. 6, pp. H2721–H2735, 2008.

[75] L. A. Abdulkhaleq, M. A. Assi, R. Abdullah, M. Zamri-Saad, Y. H. Taufiq-Yap, and M. N. M. Hezmee, "The crucial roles of inflammatory mediators in inflammation: a review," *Veterinary World*, vol. 11, no. 5, pp. 627–635, 2018.

[76] M. Félétou, Y. Huang, and P. M. Vanhoutte, "Endothelium-mediated control of vascular tone: COX-1 and COX-2 products," *British Journal of Pharmacology*, vol. 164, no. 3, pp. 894–912, 2011.

[77] M. Yousefian, N. Shakour, and H. Hosseinzadeh, "The natural phenolic compounds as modulators of NADPH oxidases in hypertension," *Phytomedicine*, vol. 55, pp. 200–213, 2019.

[78] L.-M. Hung, M.-J. Su, W.-K. Chu, C.-W. Chiao, W.-F. Chan, and J.-K. Chen, "The protective effect of resveratrols on ischaemia-reperfusion injuries of rat hearts is correlated with antioxidant efficacy," *British Journal of Pharmacology*, vol. 135, no. 7, pp. 1627–1633, 2002.

[79] S. S. Leonard, C. Xia, B.-H. Jiang et al., "Resveratrol scavenges reactive oxygen species and effects radical-induced cellular responses," *Biochemical and Biophysical Research Communications*, vol. 309, no. 4, pp. 1017–1026, 2003.

[80] Z. Ungvari, Z. Orosz, A. Rivera et al., "Resveratrol increases vascular oxidative stress resistance," *American Journal of Physiology. Heart and Circulatory Physiology*, vol. 292, no. 5, pp. H2417–H2424, 2007.

[81] F. Chen, L.-H. Qian, B. Deng, Z.-M. Liu, Y. Zhao, and Y.-Y. Le, "Resveratrol protects vascular endothelial cells from high glucose-induced apoptosis through inhibition of nadph oxidase activation-driven oxidative stress," *CNS Neuroscience and Therapeutics*, vol. 19, no. 9, pp. 675–681, 2013.

[82] X. Zhou, M. Chen, X. Zeng et al., "Resveratrol regulates mitochondrial reactive oxygen species homeostasis through Sirt3 signaling pathway in human vascular endothelial cells," *Cell Death & Disease*, vol. 5, no. 12, pp. 1–13, 2014.

[83] N. Xia, A. Daiber, A. Habermeier et al., "Resveratrol reverses endothelial nitric-oxide synthase uncoupling in apolipoprotein E knockout mice," *Journal of Pharmacology and Experimental Therapeutics*, vol. 335, no. 1, pp. 149–154, 2010.

[84] G. Spanier, H. Xu, and N. Xia, "Resveratrol reduces endothelial oxidative stress by modulating the gene expression of

superoxide dismutase 1 (SOD1), glutathione peroxidase 1 (GPx1) and NADPH oxidase subunit (Nox4)," *Journal of Physiology and Pharmacology: An Official Journal of the Polish Physiological Society*, vol. 60, no. 11, pp. 111–116, 2009.

[85] S. Kaga, L. Zhan, M. Matsumoto, and N. Maulik, "Resveratrol enhances neovascularization in the infarcted rat myocardium through the induction of thioredoxin-1, heme oxygenase-1 and vascular endothelial growth factor," *Journal of Molecular and Cellular Cardiology*, vol. 39, no. 5, pp. 813–822, 2005.

[86] S.-H. Juan, T.-H. Cheng, H.-C. Lin, Y.-L. Chu, and W.-S. Lee, "Mechanism of concentration-dependent induction of heme oxygenase-1 by resveratrol in human aortic smooth muscle cells," *Biochemical Pharmacology*, vol. 69, no. 1, pp. 41–48, 2005.

[87] Z. Ungvari, Z. Bagi, A. Feher et al., "Resveratrol confers endothelial protection via activation of the antioxidant transcription factor Nrf2," *American Journal of Physiology. Heart and Circulatory Physiology*, vol. 299, no. 1, pp. H18–H24, 2010.

[88] H.-C. Chang, T.-G. Chen, Y.-T. Tai, T.-L. Chen, W.-T. Chiu, and R.-M. Chen, "Resveratrol attenuates oxidized LDL-evoked Lox-1 signaling and consequently protects against apoptotic insults to cerebrovascular endothelial cells," *Journal of Cerebral Blood Flow and Metabolism*, vol. 31, no. 3, pp. 842–854, 2011.

[89] T. Wallerath, G. Deckert, T. Ternes et al., "Resveratrol, a polyphenolic phytoalexin present in red wine, enhances expression and activity of endothelial nitric oxide synthase," *Circulation*, vol. 106, no. 13, pp. 1652–1658, 2002.

[90] N. S. Bryan, "Functional nitric oxide nutrition to combat cardiovascular disease," *Current Atherosclerosis Reports*, vol. 20, no. 5, p. 21, 2018.

[91] F. Akar, O. Uludağ, A. Aydın et al., "High-fructose corn syrup causes vascular dysfunction associated with metabolic disturbance in rats: protective effect of resveratrol," *Food and Chemical Toxicology*, vol. 50, no. 6, pp. 2135–2141, 2012.

[92] M. D. Nyby, K. Abedi, V. Smutko, P. Eslami, and M. L. Tuck, *Vascular Angiotensin Type 1 Receptor Expression Is Associated with Vascular Dysfunction, Oxidative Stress and Inflammation in Fructose-Fed Rats*, 2007.

[93] J.-P. Huang, S.-C. Hsu, D.-E. Li, K.-H. Chen, C.-Y. Kuo, and L.-M. Hung, "Resveratrol mitigates high-fat diet-induced vascular dysfunction by activating the akt/eNOS/NO and Sirt1/ER pathway," *Journal of Cardiovascular Pharmacology*, vol. 72, no. 5, pp. 231–241, 2018.

[94] Y. T. Wondmkun, "Obesity, insulin resistance, and type 2 diabetes: associations and therapeutic implications," *Diabetes, Metabolic Syndrome and Obesity: Targets and Therapy*, vol. 13, pp. 3611–3616, 2020.

[95] M. M. Adeva-Andany, E. Ameneiros-Rodríguez, C. Fernández-Fernández, A. Domínguez-Montero, and R. Funcasta-Calderón, "Insulin resistance is associated with subclinical vascular disease in humans," *World Journal of Diabetes*, vol. 10, no. 2, pp. 63–77, 2019.

[96] M. Ding, R. Feng, S. Y. Wang et al., "Cyanidin-3-glucoside, a natural product derived from blackberry, exhibits chemopreventive and chemotherapeutic activity," *Journal of Biological Chemistry*, vol. 281, no. 25, pp. 17359–17368, 2006.

[97] N. Tena, J. Martín, and A. G. Asuero, "State of the art of anthocyanins: antioxidant activity, sources, bioavailability, and therapeutic effect in human health," *Antioxidants*, vol. 9, no. 5, 2020.

[98] M. Banach, M. Wiloch, K. Zawada, W. Cyplik, and W. Kujawski, "Evaluation of antioxidant and anti-inflammatory activity of anthocyanin-rich water-soluble aronia dry extracts," *Molecules*, vol. 25, no. 18, pp. 1–15, 2020.

[99] I. Serraino, L. Dugo, P. Dugo et al., "Protective effects of cyanidin-3-O-glucoside from blackberry extract against peroxynitrite-induced endothelial dysfunction and vascular failure," *Life Sciences*, vol. 73, no. 9, pp. 1097–1114, 2003.

[100] A. M. Amorini, G. Lazzarino, F. Galvano, G. Fazzina, B. Tavazzi, and G. Galvano, "Cyanidin-3- O -β-glucopyranoside protects myocardium and erythrocytes from oxygen radical-mediated damages," *Free Radical Research*, vol. 37, no. 4, pp. 453–460, 2003.

[101] T. Tsuda, F. Horio, K. Uchida, H. Aoki, and T. Osawa, "Dietary cyanidin 3-O-β-D-Glucoside-Rich purple corn color prevents obesity and ameliorates hyperglycemia in mice," *Journal of Nutrition*, vol. 133, no. 7, pp. 2125–2130, 2003.

[102] M. Zhang, J. Ma, H. Bi et al., "Characterization and cardioprotective activity of anthocyanins from Nitraria tangutorum Bobr. by-products," *Food & Function*, vol. 8, no. 8, pp. 2771–2782, 2017.

[103] J. Tan, Y. Li, D. X. Hou, and S. Wu, "The effects and mechanisms of cyanidin-3-glucoside and its phenolic metabolites in maintaining intestinal integrity," *Antioxidants*, vol. 8, no. 10, pp. 1–16, 2019.

[104] S. Sivasinprasasn, R. Pantan, S. Thummayot, J. Tocharus, A. Suksamrarn, and C. Tocharus, "Cyanidin-3-glucoside attenuates angiotensin II-induced oxidative stress and inflammation in vascular endothelial cells," *Chemico-Biological Interactions*, vol. 260, pp. 67–74, 2016.

[105] R. Pantan, J. Tocharus, A. Suksamrarn, and C. Tocharus, "Synergistic effect of atorvastatin and Cyanidin-3-glucoside on angiotensin II-induced inflammation in vascular smooth muscle cells," *Experimental Cell Research*, vol. 342, no. 2, pp. 104–112, 2016.

[106] R. Pantan, J. Tocharus, M. Phatsara, A. Suksamrarn, and C. Tocharus, "Synergistic effect of atorvastatin and cyanidin-3-glucoside against angiotensin II-mediated vascular smooth muscle cell proliferation and migration through MAPK and PI3K/Akt pathways," *Archives of Pharmacal Research*, pp. 1–12, 2016.

[107] M. Y. Wu, C. J. Li, M. F. Hou, and P. Y. Chu, "New insights into the role of inflammation in the pathogenesis of atherosclerosis," *International Journal of Molecular Sciences*, vol. 18, no. 10, 2017.

[108] G. L. Basatemur, H. F. Jørgensen, M. C. H. Clarke, M. R. Bennett, and Z. Mallat, "Vascular smooth muscle cells in atherosclerosis," *Nature Reviews Cardiology*, vol. 16, no. 12, pp. 727–744, 2019.

[109] L. Dowsett, E. Higgins, S. Alanazi, N. A Alshuwayer, F. C Leiper, and J Leiper, "ADMA: a key player in the relationship between vascular dysfunction and inflammation in atherosclerosis," *Journal of Clinical Medicine*, vol. 9, no. 9, pp. 1–17, 2020.

[110] S. Masi, M. Uliana, and A. Virdis, "Angiotensin II and vascular damage in hypertension: role of oxidative stress and sympathetic activation," *Vascular Pharmacology*, vol. 115, pp. 13–17, 2019.

[111] L. Piqueras and M. J. Sanz, "Angiotensin II and leukocyte trafficking: new insights for an old vascular mediator. Role of redox-signaling pathways," *Free Radical Biology and Medicine*, vol. 157, pp. 38–54, 2020.

[112] K. M. Schmidt-Ott, S. Kagiyama, and M. I. Phillips, "The multiple actions of angiotensin II in atherosclerosis," *Regulatory Peptides*, vol. 93, no. 1–3, pp. 65–77, 2000.

[113] A. Speciale, R. Canali, J. Chirafisi, A. Saija, F. Virgili, and F. Cimino, "Cyanidin-3-O-glucoside protection against TNF-α-induced endothelial dysfunction: involvement of nuclear factor-κb signaling," *Journal of Agricultural and Food Chemistry*, vol. 58, no. 22, pp. 12048–12054, 2010.

[114] M.-M. Ma, Y. Li, X.-Y. Liu et al., "Cyanidin-3-O-Glucoside ameliorates lipopolysaccharide-induced injury both in vivo and in vitro suppression of NF-κB and MAPK pathways," *Inflammation*, vol. 38, no. 4, pp. 1669–1682, 2015.

[115] A. Speciale, S. Anwar, and R. Canali, "Cyanidin-3-O-glucoside counters the response to TNF-alpha of endothelial cells by activating Nrf2 pathway," *Molecular Nutrition and Food Research*, vol. 57, no. 11, pp. 1979–1987, 2013.

[116] X. Luo, S. Fang, Y. Xiao et al., "Cyanidin-3-glucoside suppresses TNF-α-induced cell proliferation through the repression of Nox activator 1 in mouse vascular smooth muscle cells: involvement of the STAT3 signaling," *Molecular and Cellular Biochemistry*, vol. 362, no. 1–2, pp. 211–218, 2012.

[117] D. Fratantonio, A. Speciale, D. Ferrari, M. Cristani, A. Saija, and F. Cimino, "Palmitate-induced endothelial dysfunction is attenuated by cyanidin-3-O-glucoside through modulation of Nrf2/Bach1 and NF-κB pathways," *Toxicology Letters*, vol. 239, no. 3, pp. 152–160, 2015.

[118] D. Fratantonio, F. Cimino, and M. S. Molonia, "Cyanidin-3-O-glucoside ameliorates palmitate-induced insulin resistance by modulating IRS-1 phosphorylation and release of endothelial derived vasoactive factors," *Biochimica et Biophysica Acta (BBA) - Molecular and Cell Biology of Lipids*, vol. 1862, no. 3, pp. 351–357, 2017.

[119] Z. Wang, M. Zhang, Z. Wang, Z. Guo, Z. Wang, and Q. Chen, "Cyanidin-3- O -glucoside attenuates endothelial cell dysfunction by modulating miR -204-5p/SIRT1 -mediated inflammation and apoptosis," *BioFactors*, vol. 46, no. 5, pp. 803–812, 2020.

[120] Y. Wang, Y. Zhang, X. Wang, Y. Liu, and M. Xia, "Supplementation with cyanidin-3-O-β-Glucoside protects against hypercholesterolemia-mediated endothelial dysfunction and attenuates atherosclerosis in apolipoprotein E-deficient mice," *Journal of Nutrition*, vol. 142, no. 6, pp. 1033–1037, 2012.

[121] H. Ruan, Y. Y. Zhan, J. Hou et al., "Berberine binds RXRα to suppress β-catenin signaling in colon cancer cells," *Oncogene*, vol. 36, no. 50, pp. 6906–6918, 2017.

[122] L. Liu, J. Liu, Z. Huang et al., "Berberine improves endothelial function by inhibiting endoplasmic reticulum stress in the carotid arteries of spontaneously hypertensive rats," *Biochemical and Biophysical Research Communications*, vol. 458, no. 4, pp. 796–801, 2015.

[123] Y. Wang, Y. Liu, X. Du, H. Ma, and J. Yao, "The anti-cancer mechanisms of berberine: a review," *Cancer Management and Research*, vol. 12, pp. 695–702, 2020.

[124] S. M. Ehteshamfar, M. Akhbari, J. T. Afshari et al., "Anti-inflammatory and immune-modulatory impacts of berberine on activation of autoreactive T cells in autoimmune inflammation," *Journal of Cellular and Molecular Medicine*, vol. 24, no. 23, pp. 13573–13588, 2020.

[125] S. de Sarkar, D. Sarkar, A. Sarkar et al., "Berberine chloride mediates its antileishmanial activity by inhibiting Leishmania mitochondria," *Parasitology Research*, vol. 118, no. 1, pp. 335–345, 2019.

[126] H. S. Bodiwala, S. Sabde, D. Mitra, K. K. Bhutani, and I. P. Singh, "Synthesis of 9-substituted derivatives of berberine as anti-HIV agents," *European Journal of Medicinal Chemistry*, vol. 46, no. 4, pp. 1045–1049, 2011.

[127] H. M. Hussien, A. Abd-Elmegied, and D. A. Ghareeb, "Neuroprotective effect of berberine against environmental heavy metals-induced neurotoxicity and Alzheimer's-like disease in rats," *Food and Chemical Toxicology*, vol. 111, pp. 432–444, 2018.

[128] H. Qiu, Y. Wu, Q. Wang et al., "Effect of berberine on PPARα-NO signalling pathway in vascular smooth muscle cell proliferation induced by angiotensin IV," *Pharmaceutical Biology*, vol. 55, no. 1, pp. 227–232, 2017.

[129] S. Guan, B. Wang, W. Li, J. Guan, and X. Fang, "Effects of berberine on expression of LOX-1 and SR-BI in human macrophage-derived foam cells induced by ox-LDL," *The American journal of Chinese medicine*, vol. 38, no. 6, pp. 1161–1169, 2010.

[130] L. Chi, L. Peng, X. Hu, N. Pan, and Y. Zhang, "Berberine combined with atorvastatin downregulates LOX-1 expression through the ET-1 receptor in monocyte/macrophages," *International Journal of Molecular Medicine*, vol. 34, no. 1, pp. 283–290, 2014.

[131] M.-y. Gao, L. Chen, L. Yang, X. Yu, J.-p. Kou, and B.-y. Yu, "Berberine inhibits LPS-induced TF procoagulant activity and expression through NF-κB/p65, Akt and MAPK pathway in THP-1 cells," *Pharmacological Reports*, vol. 66, no. 3, pp. 480–484, 2014.

[132] Y.-S. Hsieh, W.-H. Kuo, T.-W. Lin et al., "Protective effects of berberine against low-density lipoprotein (LDL) oxidation and oxidized LDL-induced cytotoxicity on endothelial cells," *Journal of Agricultural and Food Chemistry*, vol. 55, no. 25, pp. 10437–10445, 2007.

[133] R. Wang, Y. Zhang, L. Xu et al., "Protein inhibitor of activated STAT3 suppresses oxidized LDL-induced cell responses during atherosclerosis in apolipoprotein E-deficient mice," *Scientific Reports*, vol. 6, Article ID 36790, 2016.

[134] R. X. Xu, X. C. Sun, C. Y. Ma et al., "Impacts of berberine on oxidized LDL-induced proliferation of human umbilical vein endothelial cells," *American Journal of Tourism Research*, vol. 9, no. 10, pp. 4375–4389, 2017.

[135] A. Takei, Y. Huang, and M. F. Lopes-Virella, "Expression of adhesion molecules by human endothelial cells exposed to oxidized low density lipoprotein Influences of degree of oxidation and location of oxidized LDL," *Atherosclerosis*, vol. 154, no. 1, pp. 79–86, 2001.

[136] Z. Huang, X. Cai, S. Li et al., "Berberine-attenuated monocyte adhesion to endothelial cells induced by oxidized low-density lipoprotein via inhibition of adhesion molecule expression," *Molecular Medicine Reports*, vol. 7, no. 2, pp. 461–465, 2013.

[137] J. P. Gaut and J. W. Heinecke, "Mechanisms for oxidizing low-density lipoprotein. Insights from patterns of oxidation products in the artery wall and from mouse models of atherosclerosis," *Trends in Cardiovascular Medicine*, vol. 11, no. 3–4, pp. 103–112, 2001.

[138] C. Caliceti, P. Rizzo, R. Ferrari et al., "Novel role of the nutraceutical bioactive compound berberine in lectin-like OxLDL receptor 1-mediated endothelial dysfunction in comparison to lovastatin," *Nutrition, Metabolism, and Cardiovascular Diseases*, vol. 27, no. 6, pp. 552–563, 2017.

[139] S.-J. Liu, C.-X. Yin, M.-C. Ding, Y.-Z. Wang, and H. Wang, "Berberine inhibits tumor necrosis factor-α-induced expression of inflammatory molecules and activation of

nuclear factor-κB via the activation of AMPK in vascular endothelial cells," *Molecular Medicine Reports*, vol. 12, no. 4, pp. 5580–5586, 2015.

[140] Y.-H. Wu, S.-Y. Chuang, W.-C. Hong, Y.-J. Lai, G.-J. Chang, and J.-H. S. Pang, "Berberine reduces leukocyte adhesion to lps-stimulated endothelial cells and vcam-1 expression both in vivo and in vitro," *International Journal of Immunopathology and Pharmacology*, vol. 25, no. 3, pp. 741–750, 2012.

[141] Y. J. Ko, J. S. Lee, B. C. Park, H. M. Shin, and J. A. Kim, "Inhibitory effects of Zoagumhwan water extract and berberine on angiotensin II-induced monocyte chemoattractant protein (MCP)-1 expression and monocyte adhesion to endothelial cells," *Vascular Pharmacology*, vol. 47, no. 2–3, pp. 189–196, 2007.

[142] M. Zhang, C.-M. Wang, J. Li et al., "Berberine protects against palmitate-induced endothelial dysfunction: involvements of upregulation of AMPK and eNOS and downregulation of NOX4," *Mediators of Inflammation*, vol. 2013, Article ID 260464, 8 pages, 2013.

[143] F. Cheng, Y. Wang, J. Li et al., "Berberine improves endothelial function by reducing endothelial microparticles-mediated oxidative stress in humans," *International Journal of Cardiology*, vol. 167, no. 3, pp. 936–942, 2013.

[144] P. Puddu, G. M. Puddu, E. Cravero, S. Muscari, and A. Muscari, "The involvement of circulating microparticles in inflammation, coagulation and cardiovascular diseases," *Canadian Journal of Cardiology*, vol. 26, no. 4, pp. 140–145, 2010.

[145] K. R. Paudel, N. Panth, and D. W. Kim, "Circulating endothelial microparticles: a key hallmark of atherosclerosis progression," *Scientific*, vol. 2016, Article ID 8514056, 9 pages, 2016.

[146] J. M. Hodgson and K. D. Croft, "Tea flavonoids and cardiovascular health," *Molecular Aspects of Medicine*, vol. 31, no. 6, pp. 495–502, 2010.

[147] M. G.-P. Claudia Musial, "Beneficial properties of green tea catechins," *International Journal of Molecular Medicine*, vol. 21, p. 1744, 2020.

[148] J. Ouyang, K. Zhu, Z. Liu, and J. Huang, "Prooxidant effects of epigallocatechin-3-gallate in health benefits and potential adverse effect," *Oxidative Medicine and Cellular Longevity*, vol. 2020, Article ID 9723686, 14 pages, 2020.

[149] E.-B. Byun, W. S. Kim, N.-Y. Sung, and E.-H. Byun, "Epigallocatechin-3-Gallate regulates anti-inflammatory action through 67-kDa laminin receptor-mediated tollip signaling induction in lipopolysaccharide-stimulated human intestinal epithelial cells," *Cellular Physiology and Biochemistry*, vol. 46, no. 5, pp. 2072–2081, 2018.

[150] T. W. Kwak, S. B. Park, H. J. Kim, Y. I. Jeong, and D. H. Kang, "Anticancer activities of epigallocatechin-3-gallate against cholangiocarcinoma cells," *OncoTargets and Therapy*, vol. 10, pp. 137–144, 2017.

[151] B. A. Mir, S. Rasool, M. U. Rehman, I. Amin, and R. Ali, "Anticancer mechanistic insights of epigallocatechin-3-gallate, an active ingredient of green tea (camellia sinensis)," *Plant and Human Health, Volume 2*, vol. 2, pp. 139–157, 2019.

[152] M. Nikoo, J. M. Regenstein, and H. Ahmadi Gavlighi, "Antioxidant and antimicrobial activities of (-)-Epigallocatechin-3-gallate (EGCG) and its potential to preserve the quality and safety of foods," *Comprehensive Reviews in Food Science and Food Safety*, vol. 17, no. 3, pp. 732–753, 2018.

[153] M. A. El-Missiry, A. I. Othman, M. R. El-Sawy, and M. F. Lebede, "Neuroprotective effect of epigallocatechin-3-gallate (EGCG) on radiation-induced damage and apoptosis in the rat hippocampus," *International Journal of Radiation Biology*, vol. 94, no. 9, pp. 798–808, 2018.

[154] D. Bhatia, M. Bansal, S. Bhangu, G. Singh, and G. Singh, "Hepatoprotective effects of epigallocatachin gallate via mitochondrial permeability transition pore in paracetamol induced hepatotoxicity," *Plant Archives*, vol. 19, pp. 2162–2167, 2019.

[155] R. Kanlaya and V. Thongboonkerd, "Protective effects of epigallocatechin-3-gallate from green tea in various kidney diseases," *Advances in Nutrition*, vol. 10, no. 1, pp. 112–121, 2019.

[156] Q. Zhang, L. Hu, L. Chen et al., "(−)-Epigallocatechin-3-gallate, the major green tea catechin, regulates the desensitization of β1 adrenoceptor via GRK2 in experimental heart failure," *Inflammopharmacology*, vol. 26, no. 4, pp. 1081–1091, 2018.

[157] J. E. Chung, M. Kurisawa, Y.-J. Kim, H. Uyama, and S. Kobayashi, "Amplification of antioxidant activity of catechin by polycondensation with acetaldehyde," *Biomacromolecules*, vol. 5, no. 1, pp. 113–118, 2004.

[158] G. Tipoe, T.-M. Leung, M.-W. Hung, and M.-L. Fung, "Green tea polyphenols as an anti-oxidant and anti-inflammatory agent for cardiovascular protection," *Cardiovascular & Haematological Disorders - Drug Targets*, vol. 7, no. 2, pp. 135–144, 2012.

[159] M. Sabetkar, S. Y. Low, N. J. Bradley, M. Jacobs, K. M. Naseem, and K. Richard Bruckdorfer, "The nitration of platelet vasodilator stimulated phosphoprotein following exposure to low concentrations of hydrogen peroxide," *Platelets*, vol. 19, no. 4, pp. 282–292, 2008.

[160] Q. Meng, C. N. Velalar, and R. Ruan, "Regulating the age-related oxidative damage, mitochondrial integrity, and antioxidative enzyme activity in Fischer 344 rats by supplementation of the antioxidant epigallocatechin-3-gallate," *Rejuvenation Research*, vol. 11, no. 3, pp. 649–660, 2008.

[161] L. Elbling, R.-M. Weiss, O. Teufelhofer et al., "Green tea extract and (−)-epigallocatechin-3-gallate, the major tea catechin, exert oxidant but lack antioxidant activities," *The FASEB Journal*, vol. 19, no. 7, pp. 1–26, 2005.

[162] G.-X. Li, Y.-K. Chen, Z. Hou et al., "Pro-oxidative activities and dose-response relationship of (−)-epigallocatechin-3-gallate in the inhibition of lung cancer cell growth: a comparative study in vivo and in vitro," *Carcinogenesis*, vol. 31, no. 5, pp. 902–910, 2010.

[163] H. Nakagawa, K. Hasumi, J. T. Woo, K. Nagai, and M. Wachi, "Generation of hydrogen peroxide primarily contributes to the induction of Fe(II)-dependent apoptosis in Jurkat cells by (-)-epigallocatechin gallate," *Carcinogenesis*, vol. 25, no. 9, pp. 1567–1574, 2004.

[164] Z.-M. Wang, W. Gao, H. Wang et al., "Green tea polyphenol epigallocatechin-3-gallate inhibits TNF-a-induced production of monocyte chemoattractant protein-1 in human umbilical vein endothelial cells," *Cellular Physiology and Biochemistry*, vol. 33, no. 5, pp. 1349–1358, 2014.

[165] W. S. Yang, H. Yu, J. J. Kim, M. J. Lee, and S.-K. Park, "Vitamin D-induced ectodomain shedding of TNF receptor 1 as a nongenomic action: D3 vs D2 derivatives," *The Journal of Steroid Biochemistry and Molecular Biology*, vol. 155, pp. 18–25, 2016.

[166] C. Zhang, "The role of inflammatory cytokines in endothelial dysfunction," *Basic Research in Cardiology*, vol. 103, no. 5, pp. 398–406, 2008.

[167] W. S. Yang, S. Y. Moon, M. J. Lee, and S. K. Park, "Epigallocatechin-3-gallate attenuates the effects of TNF-α in vascular endothelial cells by causing ectodomain shedding of TNF receptor 1," *Cellular Physiology and Biochemistry*, vol. 38, no. 5, pp. 1963–1974, 2016.

[168] A. T. Reddy, S. P. Lakshmi, E. Maruthi Prasad, N. C. Varadacharyulu, and L. D. Kodidhela, "Epigallocatechin gallate suppresses inflammation in human coronary artery endothelial cells by inhibiting NF-κB," *Life Sciences*, vol. 258, Article ID 118136, 2020.

[169] J. Shi, H. Deng, H. Pan, Y. Xu, and M. Zhang, "Epigallocatechin-3-gallate attenuates microcystin-LR induced oxidative stress and inflammation in human umbilical vein endothelial cells," *Chemosphere*, vol. 168, pp. 25–31, 2017.

[170] J. Shi, M. Zhang, L. Zhang, and H. Deng, "Epigallocatechin-3-gallate attenuates microcystin-LR-induced apoptosis in human umbilical vein endothelial cells through activation of the NRF2/HO-1 pathway," *Environmental Pollution*, vol. 239, pp. 466–472, 2018.

[171] R. C. Su, A. Lad, J. D. Breidenbach et al., "Assessment of diagnostic biomarkers of liver injury in the setting of microcystin-LR (MC-LR) hepatotoxicity," *Chemosphere*, vol. 257, Article ID 127111, 2020.

[172] Z. Wang, G. Li, and Q. Wu, "Microcystin-LR exposure induced nephrotoxicity by triggering apoptosis in female zebrafish," *Elsevier*, vol. 214, 2019.

[173] A. Al-hazmi, "N-acetylcysteine as a therapeutic extract for cardiac, lung, intestine and spleen injuries induced by microcystin-LR in mice," *Journal of King Saud University Science*, vol. 32, no. 1, pp. 934–938, 2020.

[174] J. Shi, J. Zhou, and M. Zhang, "Microcystins induces vascular inflammation in human umbilical vein endothelial cells via activation of NF-B," *Mediators of Inflammation*, vol. 2015, Article ID 942159, 7 pages, 2015.

[175] H. Y. Ahn, C. H. Kim, and T.-S. Ha, "Epigallocatechin-3-gallate regulates NADPH oxidase expression in human umbilical vein endothelial cells," *KOREAN JOURNAL OF PHYSIOLOGY and PHARMACOLOGY*, vol. 14, no. 5, pp. 325–329, 2010.

[176] H. Y. Ahn and C. H. Kim, "Epigallocatechin-3-gallate regulates inducible nitric oxide synthase expression in human umbilical vein endothelial cells," *Laboratory Animal Research*, vol. 27, no. 2, p. 85, 2011.

[177] H. J. Jang, S. D. Ridgeway, and J. A. Kim, "Effects of the green tea polyphenol epigallocatechin-3-gallate on high-fat diet-induced insulin resistance and endothelial dysfunction," *American journal of physiology. Endocrinology and metabolism*, vol. 305, no. 12, pp. E1444–E1451, 2013.

[178] M. A. Potenza, F. L. Marasciulo, M. Tarquinio et al., "EGCG, a green tea polyphenol, improves endothelial function and insulin sensitivity, reduces blood pressure, and protects against myocardial I/R injury in SHR," *American journal of physiology. Endocrinology and metabolism*, vol. 292, no. 5, pp. E1378–E1387, 2007.

[179] D. Drozdz, J. Alvarez-Pitti, and M. Wójcik, "Obesity and cardiometabolic risk factors: from childhood to adulthood," *Nutrients*, vol. 13, no. 11, pp. 1–20, 2021.

[180] C. Manrique, G. Lastra, and J. R. Sowers, "New insights into insulin action and resistance in the vasculature," *Annals of the New York Academy of Sciences*, vol. 1311, no. 1, pp. 138–150, 2014.

[181] A. Rauf, M. Imran, I. A. Khan et al., "Anticancer potential of quercetin: a comprehensive review," *Phytotherapy Research*, vol. 32, no. 11, pp. 2109–2130, 2018.

[182] M. Lesjak, I. Beara, and N. Simin, "Antioxidant and anti-inflammatory activities of quercetin and its derivatives," *Journal of Functional Foods*, vol. 40, pp. 68–75, 2018.

[183] L. R. Braga, L. M. Pérez, M. del v. Soazo, and F. Machado, "Evaluation of the antimicrobial, antioxidant and physicochemical properties of Poly(Vinyl chloride) films containing quercetin and silver nanoparticles," *Lebensmittel-Wissenschaft & Technologie*, vol. 101, pp. 491–498, 2019.

[184] D. Xu, M. J. Hu, Y. Q. Wang, and Y. L. Cui, "Antioxidant activities of quercetin and its complexes for medicinal application," *Molecules*, vol. 24, no. 6, 2019.

[185] N. Suganthy, K. P. Devi, S. F. Nabavi, N. Braidy, and S. M. Nabavi, "Bioactive effects of quercetin in the central nervous system: focusing on the mechanisms of actions," *Biomedicine & Pharmacotherapy*, vol. 84, pp. 892–908, 2016.

[186] J. Terao, "Factors modulating bioavailability of quercetin-related flavonoids and the consequences of their vascular function," *Biochemical Pharmacology*, vol. 139, pp. 15–23, 2017.

[187] L. Zhang, M. Dong, G. Guangyong Xu, fnm Yuan Tian, H. Tang, and Y. Wang, "Metabolomics reveals that dietary ferulic acid and quercetin modulate metabolic homeostasis in rats," *Journal of Agricultural and Food Chemistry*, vol. 66, no. 7, pp. 1723–1731, 2018.

[188] W. Jiang, H. Zhang, J. Wu et al., "CuS@MOF-Based well-designed quercetin delivery system for chemo-photothermal therapy," *ACS Applied Materials & Interfaces*, vol. 10, no. 40, pp. 34513–34523, 2018.

[189] R. Lin, J. Liu, W. Gan, and C. Ding, "Protective effect of quercetin on the homocysteine-injured human umbilical vein vascular endothelial cell line (ECV304)," *Basic and Clinical Pharmacology and Toxicology*, vol. 101, no. 3, pp. 197–202, 2007.

[190] W.-Y. Huang, L. Fu, C.-Y. Li, L.-P. Xu, L.-X. Zhang, and W.-M. Zhang, "Quercetin, hyperin, and chlorogenic acid improve endothelial function by antioxidant, antiinflammatory, and ACE inhibitory effects," *Journal of Food Science*, vol. 82, no. 5, pp. 1239–1246, 2017.

[191] N. Suganya, E. Bhakkiyalakshmi, S. Suriyanarayanan, R. Paulmurugan, and K. M. Ramkumar, "Quercetin ameliorates tunicamycin-induced endoplasmic reticulum stress in endothelial cells," *Cell Proliferation*, vol. 47, no. 3, pp. 231–240, 2014.

[192] B. Ozyel, G. le Gall, P. W. Needs, and P. A. Kroon, "Anti-inflammatory effects of quercetin on high-glucose and pro-inflammatory cytokine challenged vascular endothelial cell metabolism," *Molecular Nutrition and Food Research*, vol. 65, no. 6, pp. 1–11, 2021.

[193] G. H. Werstuck, M. I. Khan, G. Femia et al., "Glucosamine-induced endoplasmic reticulum dysfunction is associated with accelerated atherosclerosis in a hyperglycemic mouse model," *Diabetes*, vol. 55, no. 1, pp. 93–101, 2006.

[194] R. A. DeFronzo, "Insulin resistance, lipotoxicity, type 2 diabetes and atherosclerosis: the missing links," *The Claude Bernard Lecture*, vol. 53, no. 7, pp. 1270–1287, 2010.

[195] X. Cai, L. Bao, Y. Ding, X. Dai, Z. Zhang, and Y. Li, "Quercetin alleviates cell apoptosis and inflammation via the ER stress pathway in vascular endothelial cells cultured in high concentrations of glucosamine," *Molecular Medicine Reports*, vol. 15, no. 2, pp. 825–832, 2017.

[196] R. Tian, Z. Jin, L. Zhou, X.-P. Zeng, and N. Lu, "Quercetin attenuated myeloperoxidase-dependent HOCl generation and endothelial dysfunction in diabetic vasculature," *Journal of Agricultural and Food Chemistry*, vol. 69, no. 1, pp. 404–413, 2021.

[197] S. Luangaram, U. Kukongviriyapan, P. Pakdeechote, V. Kukongviriyapan, and P. Pannangpetch, "Protective effects of quercetin against phenylhydrazine-induced vascular dysfunction and oxidative stress in rats," *Food and Chemical Toxicology*, vol. 45, no. 3, pp. 448–455, 2007.

[198] O. E. Kale, O. Awodele, and A. J. Akindele, "Protective effects of acridocarpus smeathmannii (DC.) guill. & perr. Root extract against phenylhydrazine-induced haematotoxicity, biochemical changes, and oxidative stress in rats," *Biochemistry Insights*, vol. 12, p. 117862641988324, 2019.

[199] U. Kukongviriyapan, K. Sompamit, P. Pannangpetch, V. Kukongviriyapan, and W. Donpunha, "Preventive and therapeutic effects of quercetin on lipopolysaccharide-induced oxidative stress and vascular dysfunction in mice," *Canadian Journal of Physiology and Pharmacology*, vol. 90, no. 10, pp. 1345–1353, 2012.

[200] R. Kleemann, L. Verschuren, M. Morrison et al., "Anti-inflammatory, anti-proliferative and anti-atherosclerotic effects of quercetin in human in vitro and in vivo models," *Atherosclerosis*, vol. 218, no. 1, pp. 44–52, 2011.

Hindawi
Evidence-Based Complementary and Alternative Medicine
Volume 2022, Article ID 8738435, 12 pages
https://doi.org/10.1155/2022/8738435

Research Article

Protective Effects of *Alternanthera sessilis* Ethanolic Extract against TNF-α or H_2O_2-Induced Endothelial Activation in Human Aortic Endothelial Cells

Nur Nadia Mohd Razali,[1] Soek Sin Teh,[2] Siau Hui Mah,[3] Yoke Keong Yong,[4] Chin Theng Ng,[5] Yang Mooi Lim,[1] and Lai Yen Fong[1]

[1]*Department of Pre-Clinical Sciences, Faculty of Medicine and Health Sciences, Universiti Tunku Abdul Rahman, Kajang 43000, Selangor, Malaysia*
[2]*Engineering and Processing Division, Malaysia Palm Oil Board, Kajang 43000, Selangor, Malaysia*
[3]*School of Biosciences, Faculty of Health and Medical Sciences, Taylor's University, Subang Jaya 47500, Selangor, Malaysia*
[4]*Department of Human Anatomy, Faculty of Medicine and Health Sciences, Universiti Putra Malaysia, Serdang 43400, Selangor, Malaysia*
[5]*Unit of Physiology, Faculty of Medicine, AIMST University, Bedong 08100, Kedah, Malaysia*

Correspondence should be addressed to Lai Yen Fong; fongly@utar.edu.my

Received 18 August 2021; Revised 2 January 2022; Accepted 26 January 2022; Published 24 February 2022

Academic Editor: Arquimedes Gasparotto Junior

Activation of the endothelium has been shown to contribute to the early stage of vascular diseases such as atherosclerosis and hypertension. In endothelial activation, excess reactive oxygen species (ROS) production and increased expression of cell adhesion molecules cause an increase in vascular permeability. *Alternanthera sessilis* (L.) R. Br. is an edible traditional herbal plant, which has previously been shown to possess antioxidant and anti-inflammatory effects. However, the effect of *A. sessilis* on the activation of human aortic endothelial cells (HAECs) remains unknown. This study aimed to investigate the effects of *A. sessilis* on endothelial permeability, vascular cell adhesion-1 (VCAM-1) expression, production of ROS and hydrogen peroxide (H_2O_2), and superoxide dismutase (SOD) and catalase (CAT) activities. The viability of HAECs was first determined using the MTT viability assay. The effect of *A. sessilis* on endothelial permeability was examined using the FITC-dextran permeability assay. Besides, enzyme-linked immunosorbent assay (ELISA) was done to assess soluble VCAM-1 (sVCAM-1) expression. The production of ROS and H_2O_2 was studied using 2′,7′-dichlorodihydrofluorescein diacetate (H_2-DCFDA) and Amplex Red fluorescent dyes, respectively. SOD and CAT activities were also measured using commercial kits. Our results showed that 25–200 μg/mL of *A. sessilis* ethanolic extract did not cause significant death in HAECs. *A. sessilis* at 200 μg/mL significantly inhibited TNF-α-induced hyperpermeability of HAECs. However, *A. sessilis* did not reduce increased VCAM-1 expression induced by TNF-α. *A. sessilis* also significantly reduced TNF-α-induced increased ROS production, but not H_2O_2 production. Furthermore, 100 μM of H_2O_2 decreased both SOD and CAT activities in HAECs at 2 h. *A. sessilis* ethanolic extract dramatically increased both reduced SOD and CAT activities caused by H_2O_2. The liquid chromatography-mass spectrometry (LC-MS) analysis of *A. sessilis* ethanolic extract demonstrated the presence of arachidonic acid, azadirachtin, astaxanthin, flavanole base + 3O, 2Prenyl, and vicenin 2, while the gas chromatography-mass spectrometry (GC-MS) analysis showed that the extract contains 1,3,5-dihydroxy-6-methyl-2,3-dihydro-4H-pyran-4-one, 3-deoxy-d-mannoic lactone, 4-pyrrolidinobenzaldehyde, and *n*-hexadecanoic acid. In conclusion, our findings suggest that *A. sessilis* ethanolic extract protects against endothelial hyperpermeability and oxidative stress elicited by pro-inflammatory or prooxidant stimulus. This study reveals a therapeutic potential of *A. sessilis* in preventing endothelial activation, which is a key event in early atherosclerosis.

1. Introduction

The inner wall of blood vessels is lined by the endothelium, which functions as a semipermeable barrier that regulates permeability, inflammatory responses, and hemostasis [1]. Pro-inflammatory mediators such as tumor necrosis factor-alpha (TNF-α) have evidently been shown to induce endothelial activation, which is a key early event implicated in chronic inflammatory diseases such as atherosclerosis [2]. In endothelial activation, TNF-α and interleukins trigger vascular cell adhesion molecule 1 (VCAM-1) to be highly expressed on endothelial cells and stimulate increased endothelial permeability, thereby enhancing leukocyte attachment and migration to the site of inflammation [3]. Previous studies have highlighted the role of VCAM-1, as well as oxidative stress, in mediating endothelial activation [4]. Oxidative stress occurs when there is an imbalance between the release of prooxidant molecules such as reactive oxygen species (ROS) and hydrogen peroxide (H_2O_2), and the activity of antioxidant enzymes such as catalase (CAT) and superoxide dismutase (SOD). An overproduction of oxidants, which exceeds the ability of the antioxidant system to scavenge them, causes oxidative stress. The increased expression of adhesion molecules and oxidative stress in the activated endothelium initiate multiple signaling cascades that impair the endothelial barrier, resulting in increased endothelial permeability [5].

The current treatment for atherosclerosis focuses on the use of statins including simvastatin and atorvastatin, which act through the lipid-lowering approach. However, apart from adverse effects caused by statins, there is also evidence of relapses [6]. Thus, other alternative approaches such as targeting endothelial activation might be useful in the prevention and treatment of atherosclerosis. *Alternanthera sessilis* (L.) R. Br., popularly known as "sessile joy weed" or "dwarf copperleaf," is a traditional herbal plant commonly found in Southeast Asia and other Asian countries such as Malaysia, Indonesia, India, and Pakistan [7]. The plant, belonging to the Amaranthaceae family, is used traditionally to treat a variety of conditions such as asthma, diabetes, wounds, diarrhea, and bronchitis [8, 9]. In Malaysia, *A. sessilis* is one of the commonly consumed *ulam* (salad), which is usually eaten raw or boiled with rice [10].

Previous *in vitro* studies showed that *A. sessilis* possesses a number of pharmacological activities such as antioxidant, anti-inflammatory, analgesic, and wound healing effects [11–13]. In RAW 264.7 cells, *A. sessilis* exhibited anti-inflammatory effect by inhibiting the production of pro-inflammatory mediators such as TNF-α, prostaglandin E2, interleukin-6, and interleukin-1β triggered by lipopolysaccharide [12]. Besides, a few *in vivo* studies also demonstrated hepatoprotective, antioxidant, analgesic, and anti-hyperglycemic effects of *A. sessilis* [14, 15]. *A. sessilis* was also demonstrated to suppress serum cholesterol and bilirubin levels, as well as lipid peroxidation in carbon tetrachloride (CCl_4)-induced Wistar albino rats [7]. Activities of antioxidant enzymes such as CAT and glutathione peroxidase were also increased in the Wistar albino rat pretreated with *A. sessilis* methanolic extract. To date, no study has highlighted the protective effect of A. *sessilis* against barrier dysfunction and oxidative stress in the endothelium. Thus, this study aimed to investigate the effect of *A. sessilis* ethanolic extract in endothelial activation induced by TNF-α or H_2O_2 by examining endothelial permeability, VCAM-1 expression, production of ROS and H_2O_2, and activities of SOD and CAT. Identification of compounds in *A. sessilis* extract was also done using liquid chromatography-mass spectrometry (LC-MS) and gas chromatography-mass spectrometry (GC-MS).

2. Materials

Human recombinant TNF-α was purchased from PeproTech (NJ, USA). H_2O_2 was purchased from Merck. Simvastatin, 2′,7′-dichlorodihydrofluorescein diacetate (H_2-DCFDA), fluorescein isothiocyanate (FITC)-dextran, dexamethasone, and N-acetyl cysteine (NAC) were purchased from Sigma-Aldrich (MO, USA). 10X trypsin-EDTA was purchased from Biowest (Nuaille, France). 3-(4,5-dimethylthiazol-2-yl)-2,5-diphenyltetrazolium bromide (MTT), dimethyl sulfoxide (DMSO), and phosphate-buffered saline (PBS) were obtained from Oxoid (UK).

3. Methods

3.1. Preparation of A. sessilis Ethanolic Extract. *A. sessilis* whole plant was collected from the herb garden of Persatuan Memperbaiki Akhlak Che Ru, Endau, Johor, Malaysia (2°38′56.8″N 103°37′49.7″E), in July 2014. A sample of the plant with voucher specimen number RG5040 was deposited at the Department of Biology, Faculty of Science, Universiti Putra Malaysia, and the plant was verified by Dr. Rusea Go. Approximately 104.4 g of air-dried *A. sessilis* was ground to fine powder and extracted in a Soxhlet apparatus with ethanol for 4 h [16]. The extract was evaporated to dryness under vacuum to give 31.3 g of ethanolic extract. To prepare a stock solution of *A. sessilis* ethanolic extract, the extract was dissolved in endothelial basal media to a concentration of 5 mg/mL. The stock was filter-sterilized through a 0.2 μm polyethersulfone (PES) membrane filter before being stored at 4°C for a maximum of 3 months. The working solutions were freshly prepared using endothelial cell media on the day of usage. Any leftover was discarded.

3.2. Cell Culture. Primary human aortic endothelial cells (HAECs) were purchased from American Type Culture Collection (VA, USA). HAECs were cultured in endothelial cell media supplemented with 5% (v/v) fetal bovine serum (FBS), 100 U/mL penicillin/streptomycin, and 1% endothelial cell growth factor (ScienCell, CA, USA) and were grown in T-25 culture flasks at a starting density of 2.5×10^3 cells/cm^2. The cells were maintained at 37°C in a 5% CO_2 incubator. The media were changed the next day after thawing and subsequently every two days until the cells reached a confluency of about 70%. Then, the media were changed every day until the cells were 80–90% confluent. The cells were subcultured until the desired passage. Cells at passages 3 to 5 were used for assays.

3.3. MTT Viability Assay. The cell viability was determined according to the procedures described previously [17]. HAECs were seeded onto 96-well plates at a density of 1×10^4 cells/well overnight. The medium was removed, and the cells were then incubated with 25, 50, 100, 200, 400, and 800 μg/mL of *A. sessilis* ethanolic extract for 24 h.

Then, 10 μl of 5 mg/mL MTT (Sigma-Aldrich, MO, USA) in PBS was added to each well, and the cells were incubated for another 4 h. Lastly, all solution was removed from the well, and 100 μL of dimethyl sulfoxide (DMSO) was added to each well. The absorbance was read using a microplate reader (Infinite M200pro, Tecan, Switzerland) at 450 nm. The cell viability was expressed as a percentage of untreated control.

3.4. FITC-Dextran Permeability Assay. This assay was performed according to the procedure previously described with some modifications [18]. Cell culture inserts with a pore size of 1.0 μm (Falcon, USA) were coupled with 24-well companion plates. 2×10^5 cells were seeded on each cell culture insert precoated with 1.5 mg/mL of type 1 rat tail collagen (BD Biosiences, USA). Each bottom chamber was filled with 500 μL of endothelial cell media. The cells were grown for 3 to 4 days until a monolayer was formed. After the cells formed a monolayer, the cells were then treated with *A. sessilis* ethanolic extract (25–200 μg/mL) or simvastatin (2 μM) for 24 h. Then, the cells were induced with 10 ng/mL of TNF-α for 6 h. Following treatment, the media in the insert and in the bottom well were removed. The bottom well was filled with 500 μLof endothelial basal media, while 150 μL of 0.04 mg/mL FITC-dextran (2000 kDa) was added to the insert and incubated at room temperature. After 20 mins, the permeation of FITC-dextran was stopped by removing the culture insert from the well. The fluorescence intensity was then measured using a fluorescent microplate reader (Infinite M200pro, Tecan, Switzerland) at an excitation wavelength of 485 nm and an emission wavelength of 530 nm.

3.5. Measurement of Soluble VCAM-1 (sVCAM-1) Production. The assay was performed using DuoSet VCAM-1/CD106 enzyme-linked immunosorbent assay (ELISA) and ancillary reagent kit (R&D System, Minnesota, USA) according to the manufacturer's protocol. HAECs were seeded in 24-well plates at a density of 2×10^5 cells/well overnight. The cells were then treated with *A. sessilis* ethanolic extract at 25, 50, 100, and 200 μg/mL, 2 μM of simvastatin, or 10 mM of DeletedNAC for 24 h. Then, the cells were induced with 10 ng/mL TNF-α for 6 h. The supernatant was collected and was centrifuged at 1500 rpm for 10 mins at 4°C. Then, the supernatant was collected in new tubes and stored at −80°C if not assayed on the same day. To perform the assay, samples were first diluted at a dilution factor of 2 and were added to mouse antihuman VCAM-1 capture antibody-coated ELISA plate. Then, biotinylated sheep antihuman VCAM-1 detection antibody was added to each well, and this was followed by the addition of streptavidin-horseradish peroxidase. H_2O_2 and tetramethylbenzidine mixture was added to each well, and the reaction was stopped by the addition of 2 N H_2SO_4. The absorbance was read at 450 nm and corrected at 540 nm using a microplate reader (Infinite M200pro, Tecan, Switzerland).

3.6. Intracellular Reactive Oxygen Species (ROS) Quantitative Assay. This assay was done according to the method of Ganji et al. with some modifications [19]. HAECs were seeded in 96-well plates at a density of 1×10^4 cells/well, and the plate was incubated overnight. To optimize the duration of TNF-α required to induce maximal ROS level production, the medium in each well was removed and the cells were incubated with 10 μM of H_2-DCFDA (Sigma-Aldrich, MO, USA) for 30 mins. After that, 10 ng/mL of TNF-α (PeproTech, NJ, USA) was added to the well and the plate was further incubated for 30 mins, 1 h, 2 h, 4 h, 6 h, and 24 h. The fluorescence intensity was measured at excitation and emission wavelengths of 480 nm and 570 nm, respectively, using a fluorescent microplate reader (Infinite M200pro, Tecan, Switzerland). The results were expressed as a percentage of control.

To study the effect of *A. sessilis* on TNF-α-induced ROS production, the cells were pretreated with 25, 50, 100, and 200 μg/mL of *A. sessilis* ethanolic extract for 24 h before the addition of H_2-DCFDA fluorescent dye. Then, the cells were induced with 10 ng/mL of TNF-α for 4 h.

3.7. Hydrogen Peroxide (H_2O_2) Assay. The assay was performed using Amplex Red H_2O_2/peroxidase assay kits (Invitrogen, USA) according to the manufacturer's protocol. HAECs were cultured overnight in 6-well plates at a density of 3×10^5 cells/well. First, the TNF-α concentration and induction time required to increase H_2O_2 level were optimized. The cells were induced with 10, 20, 100, and 200 ng/mL of TNF-α for 30 mins, 1 h, 2 h, 4 h, and 6 h. The supernatant was collected and was immediately assayed using the kit. The samples were mixed with 0.1 mM of Amplex Red and 0.2 U/mL of horseradish peroxidase solution diluted in 1X reaction buffer. After 30 mins, fluorescence intensities were measured using a microplate reader at excitation/emission wavelengths of 540/590 nm (Infinite M200pro, Tecan, Switzerland). To study the effects of *A. sessilis* on H_2O_2 production, the cells were treated with 25, 50, 100, and 200 μg/mL of *A. sessilis* or 2 μM of simvastatin for 24 h before an induction with 20 ng/mL of TNF-α for 1 h.

3.8. Measurement of Superoxide Dismutase (SOD) Activity. The SOD activity was detected using SOD Assay Kits (Cayman, USA). Briefly, HAECs were seeded onto 12-well plates at a density of 2×10^5 cells/well. To optimize the concentration and induction time of H_2O_2, the cells were induced with H_2O_2 at concentrations of 50, 100, 200, and 400 μM for 30 mins, 1 h, and 2 h. To assess the effects of *A. sessilis* on SOD production, the cells were treated with 25, 50, 100, and 200 μg/mL of *A. sessilis* ethanolic extract or 2 μM of simvastatin or 10 μM of NAC or 10 μM of dexamethasone

for 24 h, followed by an induction with 100 μM of H_2O_2 for 2 h. After the indicated treatment, the medium was removed from each well and replaced with ice-cold buffer. The cells were harvested using rubber cell scrapers, and the cell lysates were centrifuged at 1500 ×g for 5 mins at 4°C. The supernatant was collected and stored at −80°C. To measure SOD activity, the samples were first added to tetrazolium salt radical detector. Then, xanthine oxidase was added to initiate the reaction. After 30 mins, the absorbance was read at 440 nm using a microplate reader (Infinite M200pro, Tecan, Switzerland).

3.9. Measurement of Catalase (CAT) Activity. CAT activity was detected using CAT Assay Kits (Cayman, USA) according to the manufacturer's protocol. Briefly, HAECs were seeded onto 6-well plates at a density of 3×10^5 cells/well. In optimization experiments, the cells were induced with 50, 100, 200, and 500 μM of H_2O_2 for 30 mins, 1 h, and 2 h. To study the effects of *A. sessilis* on CAT activity, the cells were treated with 25, 50, 100, and 200 μg/mL of*A. sessilis* or 2 μM of simvastatin for 24 h, followed by induction with 100 μM of H_2O_2 for 2 h.

The cells were harvested in ice-cold buffer and were centrifuged at 10,000 ×g for 15 mins at 4°C. The supernatant was collected and used for the assay. Briefly, samples, methanol, and assay buffer were added to 96-well assay plates. Then, 20 μL of H_2O_2 was added to each well to initiate the reaction, which was stopped with 30 μL of potassium hydroxide after 20 mins. Catalase potassium periodate was then added at a volume of 10 μL, and the absorbance was read at 540 nm.

3.10. Liquid Chromatography-Mass Spectrometry (LC-MS). *A. sessilis* ethanolic extract was separated using Thermo Scientific C18 Column (3 × 150 mm, 3 μm particle size; Acclaim™ Polar Advantage II, Thermo Scientific, USA) with an UltiMate 3000 UHPLC System (Dionex, Thermo Fisher Scientific, USA). Gradient elution was run at this setting: 0.4 mL/min and 40°C using water and 0.1% formic acid (A) and 100% acetonitrile (B) with a total run time of 22 mins. The sample was injected at a volume of 1 μL. The gradient began at 5% B (0–3 mins); 80% B (3–10 mins); 80% B (10–15 mins); and 5% B (15–22 mins). High-resolution mass spectrometry was performed with micrOTOF-QIII (Bruker Daltonics GmbH, Germany) using an ESI-positive ionization and the following conditions: capillary voltage: 4500 V; nebulizer pressure: 1.2 bar; and drying gas: 8 L/min at 200°C. The mass range was set at 50–1000 m/z. The mass data of molecular ions were then processed and analyzed using Compass Data Analysis 4.1 software (Bruker Daltonics GmbH, Germany).

3.11. Gas Chromatography-Mass Spectrometry (GC-MS). *A. sessilis* ethanolic extract was analyzed using GC-MS (Agilent J&W, USA) equipped with GC column HP-5MS (30 m × 0.25 mm × 0.25 μm). The temperature of the column was first set to 60°C, was gradually increased to 250°C at a rate of 15°C/min, and was then kept constant for 8 mins. The injector temperature was fixed at 200°C (split mode with ratio 10 : 1, injection volume 1 μL) with a total run time of 20 mins. The mass spectra were obtained between the range m/z 50 and 550 and the electron ionization at 70 eV. The mass spectra were then compared with the NIST17 library data to identify chromatograms of the sample.

3.12. Statistical Analysis. All experiments were performed in triplicates and repeated for at least three times. The results were analyzed and presented as the means of readings and standard error of means (mean ± S.E.M). Statistical analysis was performed using one-way analysis of variance (ANOVA) and Dunnett's test in GraphPad Prism 7 (CA, USA). The statistical difference of $P < 0.05$ was considered as significant.

4. Results

4.1. A. sessilis Does Not Affect Viability of HAECs at 6.25–200 μg/mL. HAECs were treated with 6.25–800 μg/mL of *A. sessilis* ethanolic extract for 24 h, and the MTT assay was used to evaluate whether *A. sessilis* ethanolic extract would affect the cell viability. *A. sessilis* ethanolic extract, at 400 and 800 μg/mL, was found to cause significant cell death with mean cell viabilities of 23.74 ± 0.83 and 33.42 ± 0.81% of control, respectively (Figure 1) ($P < 0.05$), whereas 6.25–200 μg/mL of*A. sessilis* ethanolic extract did not affect the viability of HAECs. Therefore, the four highest concentrations (25, 50, 100, and 200 μg/mL), which did not cause significant cell death, were used in subsequent experiments.

4.2. A. sessilis Suppresses Increased Endothelial Permeability Caused by TNF-α. *In vitro* vascular permeability assay is an assay used to assess the permeability of endothelial cells by measuring the passage of fluorescent probes across a cell monolayer grown on collagen-coated inserts. The effect of *A. sessilis* ethanolic extract on endothelial cell permeability was studied. As shown in Figure 2, 10 ng/mL of TNF-α significantly increased the permeability of HAEC monolayer to 175.8 ± 15.03% of control ($P < 0.05$) (Figure 2) at 6 h. Pretreatment with 200 μg/mL of *A. sessilis* ethanolic extract for 24 h significantly reduced the increased permeability stimulated by TNF-α to a level, which was comparable to the control group (101.0 ± 8.26% of control) ($P < 0.05$). Simvastatin, the positive control, administered at 2 μM, also significantly decreased TNF-α-induced hyperpermeability to 88.64 ± 13.32% of control ($P < 0.05$). However, 25, 50, and 100 μg/mL of *A. sessilis* ethanolic extract did not have a significant effect on the increased endothelial permeability. These results showed that *A. sessilis* ethanolic extract prevents the impairment of the endothelial barrier induced by TNF-α, which is indicated by the suppression of FITC-dextran permeability.

4.3. A. sessilis Does Not Inhibit TNF-α-Induced Release of sVCAM-1. sVCAM-1 released in the cell culture supernatant was measured using commercial ELISA kits. The

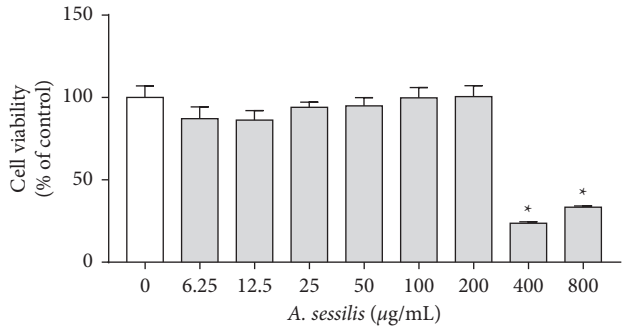

Figure 1: Effect of *A. sessilis* ethanolic extract on HAEC viability. HAECs were treated with various concentrations of *A. sessilis* ethanolic extract (6.25–800 μg/mL) for 24 h. The percentage of cell viability was determined using the MTT assay. Data are presented as the mean ± SEM of three independent experiments. $^{*}P < 0.05$ as compared to the untreated control.

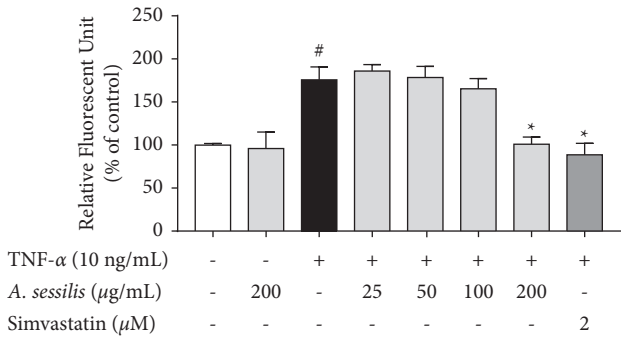

Figure 2: Effect of *A. sessilis* ethanolic extract on TNF-α-induced hyperpermeability of HAECs. HAECs cultured on collagen-coated transwell inserts were pretreated with various concentrations of *A. sessilis* (25–200 μg/mL) or simvastatin (2 μM) for 24 h followed by stimulation with TNF-α (10 ng/mL) for 6 h. At the end of the experiment, the media in the bottom well was collected, and fluorescence intensities of the bottom well were measured. Data are presented as the mean ± SEM of three independent experiments, where each was performed in triplicates. $^{\#}P < 0.05$ as compared to the unstimulated control. $^{*}P < 0.05$ as compared to the TNF-α-treated group.

sVCAM-1 production was dramatically increased by 10 ng/mL of TNF-α to 890.2 ± 6.87% ($P < 0.05$), compared with unstimulated control (Figure 3). Pretreatment with *A. sessilis* ethanolic extract at all concentrations (25–200 μg/mL) did not inhibit TNF-α-induced sVCAM-1 production. Surprisingly, treatment with 200 μg/mL of*A. sessilis* ethanolic extract alone significantly increased VCAM-1 expression to 251.5 ± 31.01% ($P < 0.05$) in HAECs. The experiment was also validated with the use of NAC, which is a ROS inhibitor. 10 mM of NAC dramatically reduced sVCAM-1 expression induced by TNF-α to 67.17 ± 4.61% of control ($P < 0.05$). These data suggested that *A. sessilis* does not alter the secretion of sVCAM-1 caused by TNF-α.

4.4. A. sessilis Reduces TNF-α-Induced Increased Intracellular ROS Levels. Intracellular ROS production was measured using H_2-DCFDA dye. This nonfluorescent dye penetrates

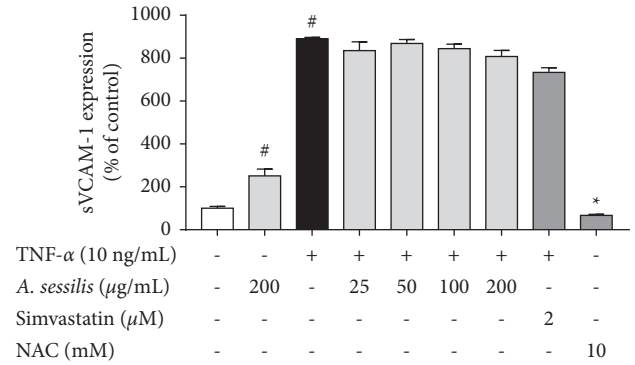

Figure 3: Effect of *A. sessilis* ethanolic extract on TNF-α-induced increased sVCAM-1 release in HAECs. HAECs were pretreated with various concentrations of *A. sessilis* (25–200 μg/mL), simvastatin (2 μM), or NAC (10 mM) for 24 h followed by stimulation with 10 ng/mL of TNF-α for 6 h. The supernatant was collected for assay using VCAM-1 ELISA kits. The absorbance was measured at 450 nm and corrected at 540 nm. $^{\#}P < 0.05$ as compared to the unstimulated control. $^{*}P < 0.05$ as compared to the TNF-α-treated group.

cell membranes and is converted to a fluorescent molecule, 2′, 7’-dichlorofluorescein (DCF), in the presence of ROS. To determine at which time point TNF-α induces the highest ROS accumulation in HAECs, the cells were stimulated with 10 ng/mL of TNF-α for 30 mins, 1 h, 2 h, 4 h, 6 h, and 24 h prior to the measurement of ROS production. We showed that 10 ng/mL of TNF-α significantly increased intracellular ROS levels at 4 h (134 ± 2.27% of control), compared with unstimulated control (Supplementary Figure 1). Therefore, 4 h incubation time for TNF-α was used in the subsequent experiment to study the effect of *A. sessilis* ethanolic extract in increased intracellular ROS levels stimulated by TNF-α.

In Figure 4, the results showed that TNF-α significantly increased intracellular ROS levels to 116.6 ± 1.67 of control ($P < 0.05$) at 4 h and this was inhibited by pretreatment of 200 μg/mL of *A. sessilis* ethanolic extract (98.1 ± 1.84% of control) ($P < 0.05$). Consistent with the finding from the permeability assay, pretreatment with 25–100 μg/mL of *A. sessilis* ethanolic extract did not alter TNF-α-induced ROS release in HAECs. In summary, *A sessilis* suppresses the release of intracellular ROS stimulated by TNF-α.

4.5. A. sessilis Fails to Reduce Extracellular H_2O_2 Production Induced by TNF-α. As the ROS assay did not indicate the type of ROS produced in cells, we then measured the release of H_2O_2, one of the most important ROS that causes endothelial activation, in cell culture supernatant using Amplex Red dye. The optimization data showed that 20 and 100 ng/mL of TNF-α significantly increased extracellular H_2O_2 levels at 1 h (138.6 ± 4.69% of control and 171.6 ± 10.66% of control, respectively) (Supplementary Figure 2). It has been reported that 100 ng/mL of TNF-α caused apoptosis of human lung endothelial cells [20]. To exclude the apoptotic effect of TNF-α, 20 ng/mL of TNF-α and 1 h incubation time were used in the subsequent

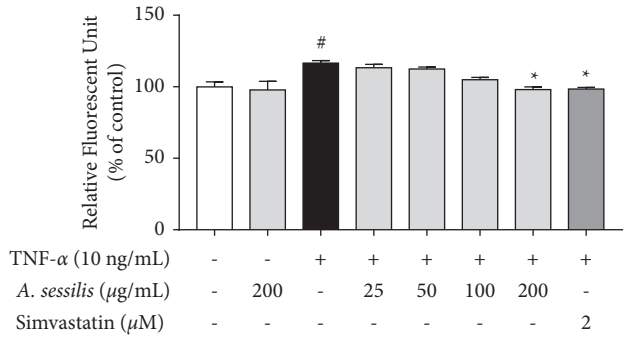

Figure 4: Effect of *A. sessilis* ethanolic extract on TNF-α-induced increased ROS levels in HAECs. HAECs were pretreated with various concentrations of *A. sessilis* (25–200 μg/mL) or simvastatin (2 μM) for 24 h prior to TNF-α (10 ng/mL) induction for 4 h. After staining the cells with H_2-DCFDA for 30 mins, the relative fluorescence unit of each well was measured. Data are presented as the mean ± SEM of three independent experiments ($n = 3$). $^{\#}P < 0.05$ as compared to the unstimulated control. $^{*}P < 0.05$ as compared to the TNF-α-treated group.

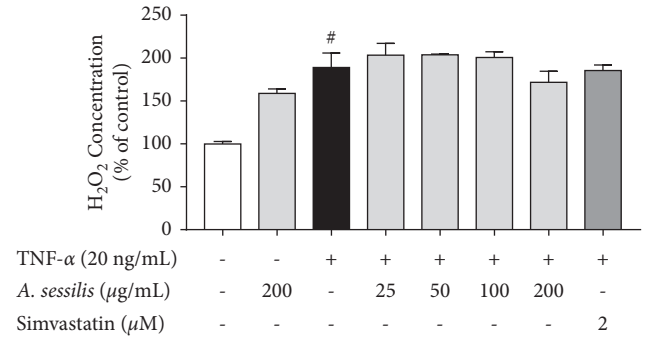

Figure 5: Effect of *A. sessilis* ethanolic extract on TNF-α-induced extracellular H_2O_2 production. HAECs were pretreated with various concentrations of *A. sessilis* (25–200 μg/mL) or 2 μM of simvastatin for 24 h followed by stimulation with 20 ng/mL of TNF-α for 1 h. The assay was performed immediately using H_2O_2 assay kits after the collection of cell culture supernatant. The results are presented as the mean ± SEM from three independent experiments ($n = 3$). $^{\#}P < 0.05$ as compared to the unstimulated control.

experiment to measure the effect of *A. sessilis* ethanolic extract on TNF-α-stimulated H_2O_2 production.

In the subsequent experiment, HAECs induced with 20 ng/mL TNF-α for 1 h showed an increase in H_2O_2 production (189 ± 16.95% of control) (Figure 5). However, neither *A. sessilis* ethanolic extract nor simvastatin reduced the elevated H_2O_2 production induced by TNF-α.

4.6. A. sessilis Improves H_2O_2-Stimulated Reduced SOD Activity. Based on our preliminary study, TNF-α did not cause a significant decrease in SOD activity in HAECs at the concentration range of 10–200 ng/mL and the incubation period of 1–6 h (data not shown). Therefore, H_2O_2 was used to study SOD activity in HAECs. To identify the optimum induction period of H_2O_2, HAECs were treated with 50–400 μM of H_2O_2 for 30 mins, 2 h, and 4 h. The data showed that 100 μM of H_2O_2 significantly reduced SOD activity at 2 h (19.92 ± 7.1% of control), compared with unstimulated control (Supplementary Figure 3). HAECs were induced with 100 μM of H_2O_2 for 2 h in the subsequent experiment, which measured the effect of *A. sessilis* ethanolic extract on H_2O_2-induced reduced SOD activity.

In the subsequent experiment, we demonstrated that 100 μM of H_2O_2 significantly reduced SOD activity in HAECs to 66.78 ± 3.37 of control ($P < 0.05$) (Figure 6(a). Pretreatment of 50, 100, and 200 μg/mL of *A. sessilis* ethanolic extract significantly increased H_2O_2-stimulated decreased SOD activity in a dose-dependent manner (120.7 ± 3.15%, 123.2 ± 6.67%, and 136.1 ± 4.01% of control, respectively). HAECs that were pretreated with 10 μM of dexamethasone also showed an increase in SOD activity (117.4 ± 5.8% of control) ($P < 0.05$). Besides, 200 μg/mL of *A. sessilis* ethanolic extract alone was also found to alter the activity of SOD.

4.7. A. sessilis Elevates Reduced CAT Activity Induced by H_2O_2. The optimization result showed that 100 μM and 500 μM of H_2O_2 significantly reduced CAT activity at 2 h, compared with unstimulated control (Supplementary Figure 4). The concentration of 100 μM and 2 h incubation time were chosen to be used in the subsequent experiment. 100 μM of H_2O_2 was chosen as 500 μM of H_2O_2 has previously been demonstrated to affect cell viability [21].

As shown in Figure 6(b), 100 μM of H_2O_2 significantly lowered CAT activity in HAECs to 74.08 ± 2.07 of control ($P < 0.05$). *A. sessilis* ethanolic extract, at 25, 50, and 200 μg/mL, significantly elevated the lowered CAT activity caused by H_2O_2 to 112.5 ± 8.65%, 96.84 ± 8.46%, and 110.1 ± 1.28% of control, respectively. A non-dose-dependent effect was observed, though. Taken together, *A. sessilis* ethanolic extract ameliorates the reduced activities of antioxidant enzymes elicited by H_2O_2.

4.8. Identification of Compounds through LC-MS Analysis. LC-MS analysis on *A. sessilis* ethanolic extract chromatogram showed the presence of 81 peaks (Figure 7). Of the 81 peaks, five compounds were successfully identified using the MassBank library. The compounds identified were arachidonic acid, azadirachtin, astaxanthin, flavanole base + 3O, 2Prenyl, and vicenin 2 [22–24]. The retention time, m/z values, and molecular formula of the compounds are presented in Table 1. The MS/MS spectra of the compounds identified are shown in Supplementary Figures 5.

4.9. Identification of Compounds through GC-MS Analysis. GC-MS analysis on *A. sessilis* ethanolic extract chromatogram showed the presence of eight prominent peaks (Figure 8). Of the eight peaks identified, four compounds were found to match with the library and the compounds identified were 1,3,5-dihydroxy-6-methyl-2,3-dihydro-4H-pyran-4-one, 3-deoxy-d-mannoic lactone, 4-pyrrolidinobenzaldehyde, and n-hexadecanoic acid. The retention time, percentage of peak area concentration, and the molecular formula of the compounds are presented in Table 2.

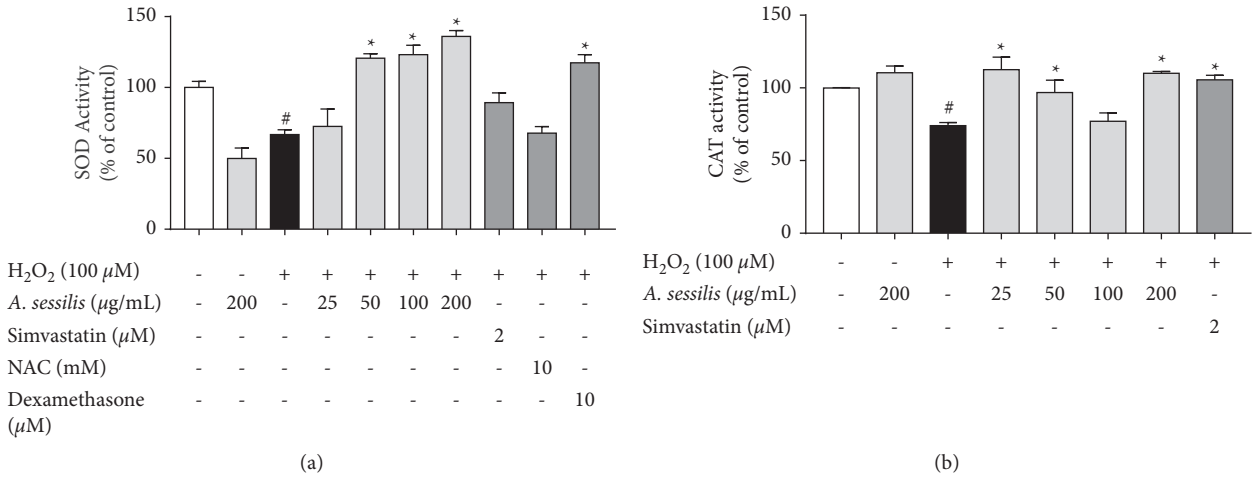

Figure 6: Effect of *A. sessilis* ethanolic extract on H_2O_2-induced reduced (a) SOD and (b) CAT activities. HAECs were pretreated with various concentrations of *A. sessilis* (25–200 μg/mL), simvastatin (2 μM), NAC (10 mM), or dexamethasone (10 μM) for 24 h followed by stimulation with 100 μM of H_2O_2 for 2 h. Cell lysates were collected, and the assay was performed immediately using SOD or CAT assay kits. The results are presented as the mean ± SEM from three independent experiments ($n = 3$). $^{\#}P < 0.05$ as compared to the unstimulated control. $^{*}P < 0.05$ as compared to the H_2O_2-induced group.

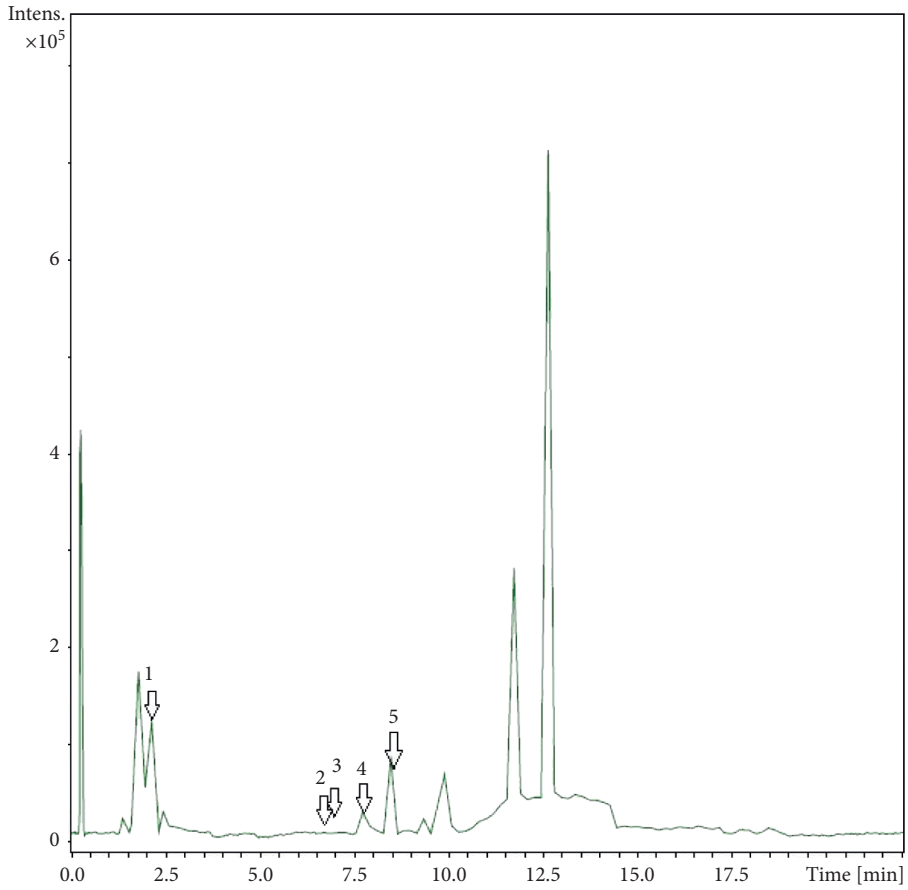

Figure 7: Liquid chromatogram of *A. sessilis* ethanolic extract.

Table 1: Compounds identified in *A. sessilis* crude extract using LC-MS analysis with the retention time, m/z value, and molecular formula.

Peak number	Compound	RT (min)	$[M\text{-}H]^+$ (m/z)	Molecular formula
1	Arachidonic acid	2.1	305.1351	$C_{20}H_{32}O_2$
2	Azadirachtin	6.9	720.0604	$C_{35}H_{44}O_{16}$
3	Astaxanthin	7.0	597.179	$C_{40}H_{52}O_4$
4	Flavanole base + 3O, 2Prenyl	7.7	409.3437	$C_{25}H_{28}O_5$
5	Vicenin 2	8.5	595.167	$C_{27}H_{30}O_{15}$

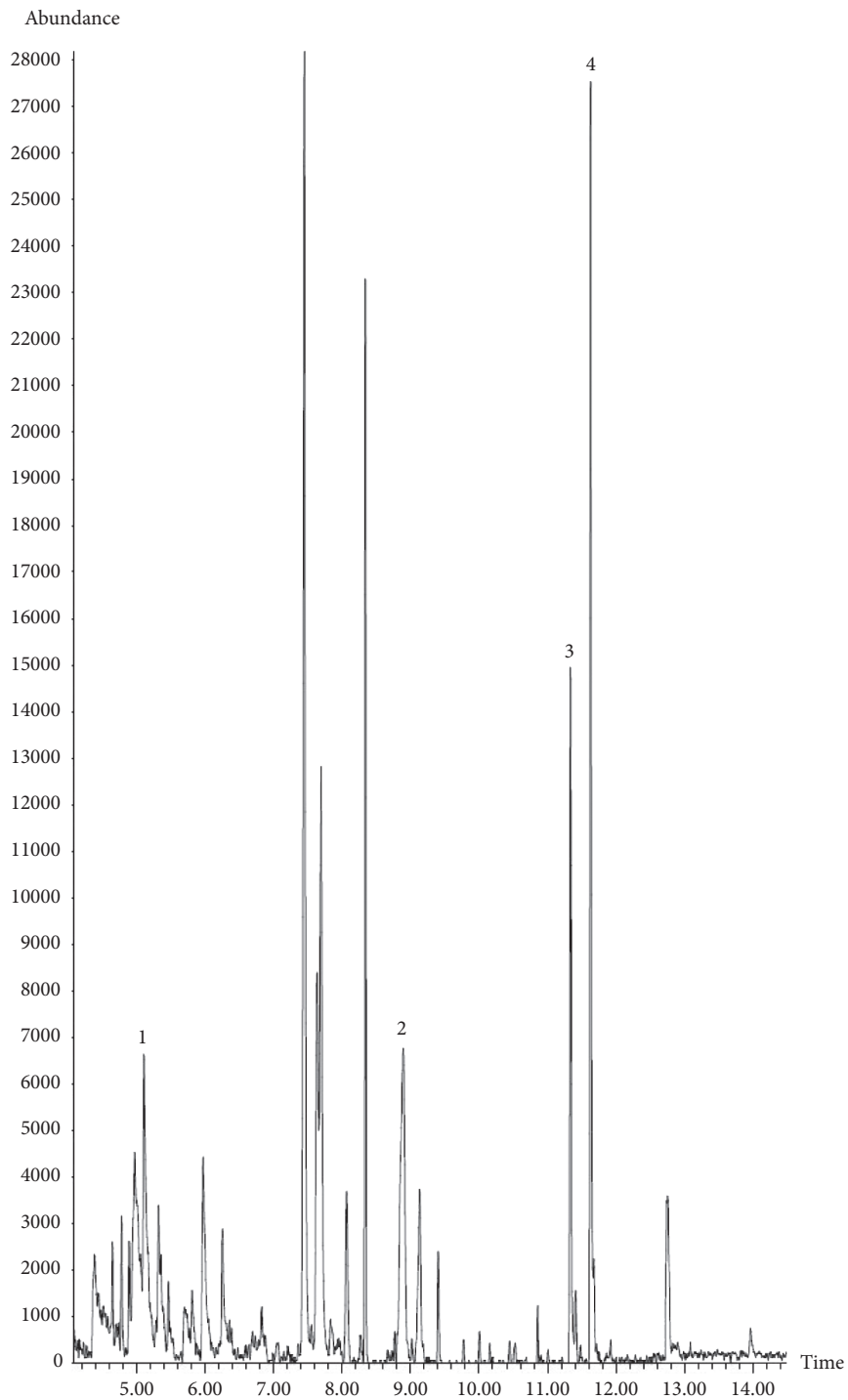

Figure 8: Gas chromatogram of *A. sessilis* ethanolic extract.

Table 2: Compounds identified in *A. sessilis* crude extract using GC-MS analysis with the retention time, peak area percentage, and molecular formula.

Peak number	Compound	RT (min)	Peak area (%)	Molecular formula
1	1,3,5-Dihydroxy-6-methyl-2,3-dihydro-4H-pyran-4-one	5.116	7.152	$C_6H_8O_4$
2	3-Deoxy-d-mannoic lactone	8.898	5.877	$C_6H_{10}O_5$
3	4-Pyrrolidinobenzaldehyde	11.336	7.069	$C_{11}H_{13}NO$
4	*n*-Hexadecanoic acid	11.629	10.69	$C_{16}H_{32}O_2$

5. Discussion

A. sessilis extracts have been demonstrated to suppress inflammatory responses in endotoxin-induced macrophages and to scavenge free radicals [12, 13]. However, the effect of *A. sessilis* on pro-inflammatory mediator-stimulated endothelial activation, particularly in terms of endothelial permeability, oxidative stress, and adhesion molecule expressions, remains poorly understood. In this study, we explored the protective effects of *A. sessilis* ethanolic extract against endothelial activation induced by TNF-α or H_2O_2. The optimization data showed that TNF-α induces increased endothelial permeability, sVCAM-1 expression, and production of both ROS and H_2O_2, but the cytokine does not stimulate significant reductions in both CAT and SOD activities. Therefore, H_2O_2 was used as an inducer to decrease CAT and SOD activities in this study. We demonstrated that *A. sessilis* ethanolic extract inhibits both endothelial hyperpermeability and increased ROS production stimulated by TNF-α in HAECs. However, *A. sessilis* fails to abrogate both the increased sVCAM-1 and H_2O_2 secretions. Importantly, *A. sessilis* ethanolic extract also elevates the reduced SOD and CAT activities caused by H_2O_2.

Paracellular permeability is regulated by tight junctions and adherens junctions that connect adjacent endothelial cells together to maintain the endothelial barrier. In endothelial activation, remodeling of interendothelial junctions takes place, causing increased endothelial permeability. In a dose- and time-response study of TNF-α, the cytokine has been shown to induce endothelial hyperpermeability in HAECs [17]. The disruption of endothelial barrier by TNF-α, which is characterized by increased endothelial permeability, results either from the direct action of TNF-α upon endothelial cells, or through the indirect effect triggered by leukocyte recruitment and adherence [25]. The results in this study showed that *A. sessilis* ethanolic extract protects against TNF-α-induced increased endothelial permeability (Figure 2), suggesting a barrier protective effect of *A. sessilis*.

VCAM-1 is one of the major regulators of leukocyte adhesion. The binding of integrins with VCAM-1 causes the production of O_2^- and the resulting increased oxidative stress in endothelial cells [26]. VCAM-1 is also implicated as a key mediator in atherosclerosis, where its expression was abundantly detected at atherosclerotic lesion sites [26]. TNF-α is a well-known positive regulator of VCAM-1 as it was demonstrated to upregulate VCAM-1 mRNA expression [27]. However, this study showed that *A. sessilis* does not reduce the expression of sVCAM-1 induced by TNF-α (Figure 3). Besides that, simvastatin also failed to reduce the increased sVCAM-1 expression, and therefore, NAC was used as a control drug in the assay. Previous data imply that the effect of simvastatin on the endothelium is greatly dependent on shear stress levels applied to endothelial cells [28]. A previous study also demonstrated that simvastatin enhances CAM expressions in TNF-α-treated HUVECs [29].

In vascular endothelial cells, increased oxidative stress contributes to the development of vascular diseases including atherosclerosis and hypertension. ROS are molecules that have one or more unpaired electrons in their orbital. Among all, ROS, H_2O_2, and O_2^- are known to contribute the most as signaling molecules that initiate oxidative stress [30]. Previous studies showed that TNF-α triggers increased ROS production in vascular cells, which results in increased endothelial permeability [31]. H_2O_2 functions as an important intracellular signaling molecule that maintains vascular homeostasis at physiological concentrations. In contrast, the excessive production of H_2O_2 causes endothelial barrier dysfunction, rearrangement of actin cytoskeleton, and apoptosis [32]. Furthermore, the free radical scavenging activity of *A. sessilis* extracts has been demonstrated previously using cell-free assays such as the 2,2-diphenyl-1-picryl-hydrazyl-hydrate (DPPH) assay, the reducing power assay, and many other methods [13, 33]. However, these assays do not mimic the *in vivo* environment of vascular beds where ROS is produced by several intracellular enzymes including nicotinamide adenine dinucleotide phosphate (NADPH) oxidases, xanthine oxidases, and uncoupled endothelial nitric oxide synthases. Our results showed that *A. sessilis* reduces intracellular ROS production, but not the release of H_2O_2, induced by TNF-α in the endothelium. This implies that *A. sessilis* may inhibit the generation of ROS other than H_2O_2.

We then attempted to investigate whether the protective effect of *A. sessilis* against endothelial activation are also mediated by the enzymatic antioxidant mechanism. CAT and SOD are intracellular antioxidant enzymes that abrogate overproduction of ROS in cells. SOD converts O_2^- to H_2O_2, which is less reactive, while CAT acts by reducing H_2O_2 into water and oxygen [34]. In this study, *A. sessilis* ethanolic extract successfully restored H_2O_2-induced decreased SOD and CAT activities (Figures 6(a) and 6(b)). Our results are in agreement with other previous findings. It has been reported that *A. sessilis* red ethyl acetate fraction dramatically increased pancreatic total SOD activity in diabetic rats [35]. Besides, dexamethasone was used as a positive control in the SOD assay of this study, as simvastatin and NAC did not prevent the reduced SOD activity induced by H_2O_2. Taken

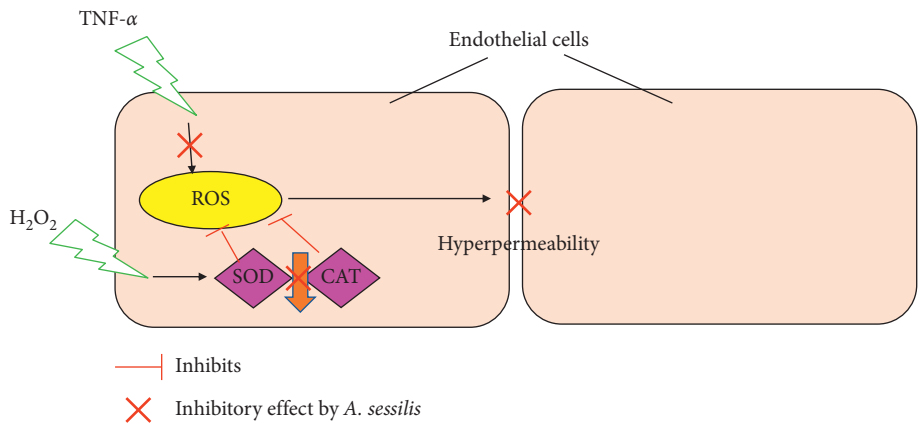

Figure 9: *A. sessilis* suppresses both TNF-α-induced endothelial hyperpermeability and increased ROS production. *A. sessilis* also prevents the reduction in SOD and CAT activities induced by H_2O_2. The endothelial barrier protective effect of *A. sessilis* might be attributed to its inhibitory effect on oxidative stress.

together, *A. sessilis* prevents oxidative stress by suppressing ROS generation and enhancing the antioxidant defense system in the endothelium. ROS has been shown to impair the endothelial barrier, which in turn causes increased vascular permeability. We suggest that the endothelial barrier protective effect of *A. sessilis* might be attributed to its inhibitory effect on oxidative stress (Figure 9).

Based on the LC-MS and GC-MS results, a total of five and four compounds were identified, respectively, in *A. sessilis* ethanolic crude extract, of which four were found to possess antioxidant and anti-inflammatory effects in *in vitro*, *in vivo*, and clinical studies (azadirachtin, astaxanthin, vicenin 2, and n-hexadecanoic acid) [36–39]. These compounds could be the active compounds, which are responsible for the positive effects of *A. sessilis* observed in this study.

There are some limitations in this study. Firstly, this study only evaluates the biological activity of *A. sessilis* crude extract and identifies compounds that are present in the crude extract. Bioassay-guided extraction, fractionation, and isolation of pure compounds should be done in the future to identify the active compound, which is responsible for the endothelial protective effect of *A. sessilis*. Secondly, the signaling pathway that underlies the endothelial protective effect of *A. sessilis* has not been identified in this study and further studies need to be done to address this. Lastly, this study provides only *in vitro* data, and therefore, *in vivo* studies also should be conducted in the future to better understand the *in vivo* effect of *A. sessilis* in suppressing vascular dysfunction and vascular oxidative stress.

6. Conclusion

In conclusion, this study shows that *A. sessilis* ethanolic extract protects against endothelial activation induced by TNF-α or H_2O_2. This is demonstrated by the protective effect of *A. sessilis* against TNF-α-induced increased endothelial permeability. In addition, *A. sessilis* also reduces intracellular ROS production and increases antioxidant enzyme activities (SOD and CAT). However, our data showed that *A. sessilis* does not inhibit sVCAM-1 secretion. An increase in endothelial permeability and oxidative stress are known to be indicators of endothelial activation, which plays an important role in the early stage of atherosclerosis. Therefore, this study suggests a new pharmacological activity of *A. sessilis* in preventing endothelial activation through inhibition of oxidative stress and endothelial hyperpermeability. Our data also support the medicinal use of this edible plant.

Data Availability

The data of this study can be obtained from the corresponding author upon request.

Conflicts of Interest

The authors declare no conflicts of interest.

Acknowledgments

This project was funded under Universiti Tunku Abdul Rahman (UTAR) Research Fund (Project no. IPSR/RMC/UTARRF/2020-01/F01).

Supplementary Materials

Supplementary Figure 1. Time response of TNF-α on ROS levels. HAECs were stimulated with 10 ng/mL of TNF-α for different durations (30 mins–24 h). After staining the cells with H_2-DCFDA for 30 mins, the relative fluorescence unit of each well was measured. Data are presented as the mean ± SEM of three independent experiments ($n = 3$). $^*P < 0.005$ compared with the unstimulated control. *Supplementary Figure 2.* Effect of TNF-α on extracellular H_2O_2 production in HAECs. HAECs were pretreated with various concentrations of TNF-α (10, 20, 100, or 200 ng/mL) for (a) 30 mins, (b) 1 h, (c) 2 h, (d) 4 h, and (e) 6 h. The supernatant was collected, and the assay was performed immediately using H_2O_2 assay kits. The results are presented as the mean ± SEM from three independent experiments ($n = 3$).

$^{\#}P < 0.05$ as compared to the unstimulated control. *Supplementary Figure 3.* Effect of H_2O_2 on SOD activity in HAECs. HAECs were pretreated with various concentrations of H_2O_2 (50, 100, 200, and 400 μM) for (a) 30 mins, (b) 2 h, and (c) 4 h. Then, the cells were lysed in iced-cold buffer. The cell lysates were collected, and the assay was performed using SOD assay kits. Data are presented as the mean ± S.E.M of three independent experiments ($n = 3$). $^{\#}P < 0.05$ as compared to the unstimulated control. *Supplementary Figure 4.* Effect of H_2O_2 on CAT activity in HAECs. HAECs were pretreated with various concentrations of H_2O_2 (50, 100, 200, and 500 μM) for (a) 30 mins, (b) 2 h, and (c) 4 h. Cell lysates were collected, and CAT activity was measured using CAT assay kits. Data are presented as the mean ± SEM of three independent experiments ($n = 3$). $\#P < 0.05$ as compared to the unstimulated control. Supplementary Figure 5: MS/MS spectrum of peaks 1–5. (*Supplementary Materials*)

References

[1] M. A. Gimbrone and G. García-Cardeña, "Endothelial cell dysfunction and the pathobiology of atherosclerosis," *Circulation Research*, vol. 118, no. 4, pp. 620–636, 2016.

[2] P. R. Clark, R. K. Kim, J. S. Pober, and M. S. Kluger, "Tumor necrosis factor disrupts claudin-5 endothelial tight junction barriers in two distinct NF-κB-Dependent phases," *PLoS One*, vol. 10, no. 3, Article ID 1020075, 2015.

[3] R. W. Pierce, J. S. Giuliano, and J. S. Pober, "Endothelial cell function and dysfunction in critically ill children," *Pediatrics*, vol. 140, no. 1, Article ID 20170355, 2017.

[4] M. Vockel and D. Vestweber, "How T cells trigger the dissociation of the endothelial receptor phosphatase VE-PTP from VE-cadherin," *Blood*, vol. 122, no. 14, pp. 2512–2522, 2013.

[5] M. Margaritis, K. M. Channon, and C. Antoniades, "Statins as regulators of redox state in the vascular endothelium: beyond lipid lowering," *Antioxidants and Redox Signaling*, vol. 20, no. 8, pp. 1198–1215, 2014.

[6] I. Broniarek, K. Dominiak, L. Galganski, and W. Jarmuszkiewicz, "The influence of statins on the aerobic metabolism of endothelial cells," *International Journal of Molecular Sciences*, vol. 27, no. 1485, pp. 1–17, 2020.

[7] B. Bhuyan, K. Baishya, and P. Rajak, "Effects of Alternanthera sessilis on liver function in carbon tetra chloride induced hepatotoxicity in wister rat model," *Indian Journal of Clinical Biochemistry: Indian Journal of Clinical Biochemistry*, vol. 33, no. 3, pp. 190–195, 2018.

[8] R. Gupta and H. K. Singh, "Nootropic potential of *Alternanthera sessilis* and *Clerodendrum infortunatum* leaves on mice," *Asian Pacific Journal of Tropical Disease*, vol. 2, no. 1, pp. 465–470, 2012.

[9] F. Saqib and K. H. Janbaz, "Rationalizing ethnopharmacological uses of *Alternanthera sessilis*: a folk medicinal plant of Pakistan to manage diarrhea, asthma and hypertension," *Journal of Ethnopharmacology*, vol. 182, pp. 110–121, 2016.

[10] M. F. Bachok, B. N. Yusof, A. Ismail, and A. A. Hamid, "Effectiveness of traditional Malaysian vegetables (ulam) in modulating blood glucose levels," *Asia Pacific Journal of Clinical Nutrition*, vol. 23, no. 3, pp. 369–376, 2014.

[11] K. Muniandy, S. Gothai, and W. S. Tan, "In vitro wound healing potential of stem extract of *Alternanthera sessilis*," *Evidence-based Complementary and Alternative Medicine*, vol. 201813 pages, Article ID 3142073, 2018.

[12] K. Muniandy, S. Gothai, K. M. H. Badran, S. S. Kumar, N. M. Esa, and P. Arulselvan, "Suppression of proinflammatory cytokines and mediators in LPS-induced RAW 264.7 macrophages by stem extract of *Alternanthera sessilis* via the inhibition of the NF-κB pathway," *Journal of Immunology Research*, vol. 2018, Article ID 3430684, 2018a.

[13] S. Kota, V. R. Govada, R. K. Anantha, and M. K. Verma, "An investigation into phytochemical constituents, antioxidant, antibacterial and anti-cataract activity of Alternanthera sessilis, A predominant wild leafy vegetable of South India," *Biocatalysis and Agricultural Biotechnology*, vol. 10, pp. 197–203, 2017.

[14] A. I. Hossain, M. Faisal, S. Rahman, R. Jahan, and M. Rahmatullah, "A preliminary evaluation of anti-hyperglycemic and analgesic activity of *Alternanthera sessilis* aerial parts," *BMC Complementary and Alternative Medicine*, vol. 14, no. 169, pp. 169–175, 2014.

[15] H. Mondal, S. Saha, K. Awang et al., "Central-stimulating and analgesic activity of the ethanolic extract of *Alternanthera sessilis* in mice," *BMC Complementary and Alternative Medicine*, vol. 14, no. 1, p. 398, 2014.

[16] S. H. Mah, S. S. Teh, and G. C. L. Ee, "Anti-inflammatory, anticholinergic and cytotoxic effects of *Sida rhombifolia*," *Pharmaceutical Biology*, vol. 55, no. 1, pp. 920–928, 2017.

[17] L. Y. Fong, C. T. Ng, Z. L. Cheok, M. A. Mohd Moklas, M. N. Hakim, and Z. Ahmad, "Barrier protective effect of asiatic acid in TNF-α-induced activation of human aortic endothelial cells," *Phytomedicine*, vol. 23, no. 2, pp. 191–199, 2016.

[18] L. Y. Fong, C. T. Ng, Y. K. Yong, M. N. Hakim, and Z. Ahmad, "Asiatic acid stabilizes cytoskeletal proteins and prevents TNF-α-induced disorganization of cell-cell junctions in human aortic endothelial cells," *Vascular Pharmacology*, vol. 117, pp. 15–26, 2018.

[19] S. H. Ganji, S. Qin, L. Zhang, V. S. Kamanna, and M. L. Kashyap, "Niacin inhibits vascular oxidative stress, redox-sensitive genes, and monocyte adhesion to human aortic endothelial cells," *Atherosclerosis*, vol. 202, no. 1, pp. 68–75, 2009.

[20] R. C. Oita, S. M. Camp, W. Ma et al., "Novel mechanism for nicotinamide phosphoribosyltransferase inhibition of TNF-α-mediated apoptosis in human lung endothelial cells," *American Journal of Respiratory Cell and Molecular Biology*, vol. 59, no. 1, pp. 36–44, 2018.

[21] S. Al-Ruzzeh, I. Schmidt, K. Nakamura, A. Chester, C. Ilsley, and M. Amrani, "Cerivastatin does not prevent oxidative injury of human aortic endothelial cells," *Texas Heart Institute Journal*, vol. 31, no. 2, pp. 127–131, 2004.

[22] H. Tsugawa, R. Nakabayashi, T. Mori et al., "A cheminformatics approach to characterize metabolomes in stable-isotope-labeled organisms," *Nature Methods*, vol. 16, no. 4, pp. 295–298, 2019.

[23] M. Kohlhoff, "Azadirachtin," Massbank, 2020.

[24] T. Maoka, "Structural studies of carotenoids in plants, animals, and food products," in *Carotenoids: Nutrition, Analysis and Technology*, A. Kaczor and M. Baranska, Eds., Wiley Backwell, New York, NY, USA, pp. 103–129, 2016.

[25] L. A. Madge and J. S. Pober, "TNF signaling in vascular endothelial cells," *Experimental and Molecular Pathology*, vol. 70, no. 3, pp. 317–325, 2001.

[26] M. E. Vogel, G. Idelman, E. S. Konaniah, and S. D. Zucker, "Bilirubin prevents atherosclerotic lesion formation in low-density lipoprotein receptor-deficient mice by inhibiting endothelial

VCAM-1 and ICAM-1 signaling," *Journal of American Heart Association*, vol. 6, no. 4, Article ID 004820, 2017.

[27] D. Zapolska-Downar, D. Bryk, M. Małecki, K. Hajdukiewicz, and D. Sitkiewicz, "Aronia melanocarpa fruit extract exhibits anti-inflammatory activity in human aortic endothelial cells," *European Journal of Nutrition*, vol. 51, no. 5, pp. 563–572, 2012.

[28] J. Rossi, L. Rouleau, A. Emmott, J. C. Tardif, and R. L. Leask, "Laminar shear stress prevents simvastatin-induced adhesion molecule expression in cytokine activated endothelial cells," *European Journal of Pharmacology*, vol. 649, no. 1–3, pp. 268–276, 2010.

[29] M. M. Sadeghi, M. Collinge, R. Pardi, and J. R. Bender, "Simvastatin modulates cytokine-mediated endothelial cell adhesion molecule induction: involvement of an inhibitory G protein," *The Journal of Immunology*, vol. 165, no. 5, pp. 2712–2718, 2000.

[30] Y. Wang, R. Branicky, A. Noë, and S. Hekimi, "Superoxide dismutases: dual roles in controlling ROS damage and regulating ROS signaling," *Journal of Cell Biology*, vol. 217, no. 6, pp. 1915–1928, 2018.

[31] D. H. Kong, Y. K. Kim, M. R. Kim, J. H. Jang, and S. Lee, "Emerging roles of vascular cell adhesion molecule-1 (VCAM-1) in immunological disorders and cancer," *International Journal of Molecular Sciences*, vol. 19, no. 4, p. 1059, 2018.

[32] R. Bretón-Romero and S. Lamas, "Hydrogen peroxide signaling in vascular endothelial cells," *Redox Biology*, vol. 2, pp. 529–534, 2014.

[33] S. Aryal, M. K. Baniya, K. Danekhu, P. Kunwar, R. Gurung, and N. Koirala, "Total phenolic content, flavonoid content and antioxidant potential of wild vegetables from western Nepal," *Plants*, vol. 8, no. 4, p. 96, 2019.

[34] A. V. Poznyak, A. V. Grechko, V. A. Orekhova, Y. S. Chegodaev, W.-K. Wu, and A. N. Orekhov, "Oxidative stress and antioxidants in atherosclerosis development and treatment," *Biology*, vol. 9, no. 3, p. 60, 2020.

[35] K. K. Tan and K. H. Kim, "*Alternanthera sessilis* red ethyl acetate fraction exhibits antidiabetic potential on obese type 2 diabetic rats," *Evidence-based Complementary and Alternative Medicine*, vol. 2013, Article ID 845172, 2013.

[36] J.-B. He, M.-J. Fang, X.-Y. Ma, W.-J. Li, and D.-S. Lin, "Angiogenic and anti-inflammatory properties of azadirachtin A improve random skin flap survival in rats," *Experimental Biology and Medicine*, vol. 245, no. 18, pp. 1672–1682, 2020.

[37] M. X. Chang and F. Xiong, "Astaxanthin and its effects in inflammatory responses and inflammation-associated diseases: recent advances and future directions," *Molecules*, vol. 25, no. 22, p. 5342, 2020.

[38] X. Duan, T. Wu, T. Liu et al., "Vicenin-2 ameliorates oxidative damage and photoaging via modulation of MAPKs and MMPs signaling in UVB radiation exposed human skin cells," *Journal of Photochemistry and Photobiology B: Biology*, vol. 190, pp. 76–85, 2019.

[39] V. Aparna, K. V. Dileep, P. K. Mandal, P. Karthe, C. Sadasivan, and M. Haridas, "Anti-inflammatory property of n-hexadecanoic acid: structural evidence and kinetic assessment," *Chemical Biology & Drug Design*, vol. 80, no. 3, pp. 434–439, 2012.

Hindawi
Evidence-Based Complementary and Alternative Medicine
Volume 2022, Article ID 4560607, 8 pages
https://doi.org/10.1155/2022/4560607

Research Article

Boldine, an Alkaloid from *Peumus boldus* Molina, Induces Endothelium-Dependent Vasodilation in the Perfused Rat Kidney: Involvement of Nitric Oxide and Small-Conductance Ca^{2+}-Activated K^+ Channel

Priscila de Souza,[1] **Rita de Cássia Vilhena da Silva**,[1] **Luisa Mota da Silva**,[1] **Viviane Miranda Bispo Steimbach**,[1] **Karyne Garcia Tafarelo Moreno**,[2] **and Arquimedes Gasparotto Junior**[2]

[1]*Graduate Program in Pharmaceutical Sciences, Nucleus of Chemical-Pharmaceutical Investigations (NIQFAR), University of Vale do Itajaí, Itajaí, SC, Brazil*
[2]*Laboratory of Electrophysiology and Cardiovascular Pharmacology, Faculty of Health Sciences, Universidade Federal da Grande Dourados, Dourados, Mato Grosso do Sul, Brazil*

Correspondence should be addressed to Priscila de Souza; priscilasouza_rc@yahoo.com.br

Received 11 September 2021; Revised 11 January 2022; Accepted 17 January 2022; Published 16 February 2022

Academic Editor: Adolfo Andrade-Cetto

Boldine, 2,9-dihydroxy-1,10-dimethoxyaporphine, is the main alkaloid found in the leaves and bark of *Peumus boldus* Molina. In recent years, boldine has demonstrated several pharmacological properties that benefit endothelial function, blood pressure control, and reduce damage in kidney diseases. However, the renal vasodilator effects and mechanisms remain unknown. Herein, perfused rat kidneys were used to study the ability of boldine to induce vasodilation of renal arteries. For that, left kidney preparations with and without functional endothelium were contracted with phenylephrine and received 10–300 nmol boldine injections. The preparations were then perfused for 15 min with phenylephrine plus L-NAME, indomethacin, KCl, tetraethylammonium, glibenclamide, apamin, charybdotoxin, or iberiotoxin. In 30, 100, and 300 nmol doses, boldine induced a dose-and endothelium-dependent relaxing effect on the renal vascular bed. No vasodilator effects were observed in preparations lacking functional endothelium. While the inhibition of the cyclooxygenase enzyme through the addition of indomethacin did not cause any change in the vasodilating action of boldine, the nonselective nitric oxide synthase inhibitor L-NAME fully precluded the vasodilatory action of boldine at all doses tested. The perfusion with KCl or tetraethylammonium (nonselective K^+ channels blocker) also abolished the vasodilatory effect of boldine, indicating the participation of K^+ channels in the renal action of boldine. The perfusion with glibenclamide (selective ATP-sensitive K^+ channels blocker), iberiotoxin (selective high-conductance Ca^{2+}-activated K^+ channel blocker), and charybdotoxin (selective high- and intermediate-conductance Ca^{2+}-activated K^+ channel blocker) did not modify the vasodilatory action of boldine. On the other hand, the perfusion with apamin (selective small-conductance Ca^{2+}-activated K^+ channel blocker) completely prevented the vasodilatory action of boldine at all doses tested. Together, the present study showed the renal vasodilatory properties of boldine, an effect dependent on the generation of nitric oxide and the opening of a small-conductance Ca^{2+}-activated K^+ channel.

1. Introduction

Peumus boldus Molina, popularly known as "boldo" or "boldu", is a tree species belonging to the Monimiaceae family and native to central and southern Chile, where it occurs abundantly. In addition to popular use for the treatment of several ailments, widely known for gastric and liver disorders, boldo-based preparations are described in several official pharmacognostic texts, such as official pharmacopeias in Brazil, Chile, Germany, Portugal, Romania, Spain, and Switzerland [1, 2].

Boldo's active principles have been described in essential oils (ascaridol, cineol, esters, aldehydes, ketones, and hydrocarbons), alkaloids (boldine, isoboldine, and others), glycosides, and others (flavonoids, citric acid, gum, sugars, tannins, minerals, lipids, etc.). The barks are richer in alkaloids [3]. Most of the pharmacological studies of boldo describe the activities observed for the alkaloid boldine, defined as the main component of boldo tea [4]. The concentration of alkaloids in boldo leaves is estimated at 0.4%, and the concentration of boldine can reach more than 12% [5].

Indeed, a wide range of biological effects has been attributed to boldine. Boldine has been shown to possess antioxidant activity and anti-inflammatory effects, which is why it is often studied for oxidative stress-associated diseases. For instance, the protective effect of boldine on oxidative mitochondrial damage in streptozotocin-induced diabetic rats has been described [6], and the reduction on oxidative stress to induce its gastroprotective properties [7]. As for the pharmacological action on the cardiovascular and renal systems to control hypertension and pathologies such as diabetes, studies have shown the action of boldine in improving the endothelial function in diabetic mice through the inhibition of vascular oxidative stress and endothelial dysfunction [8]. In addition, studies have demonstrated that boldine treatment exerts endothelial protective effects in spontaneously hypertensive rats through the inhibition of NADPH-mediated superoxide production [9]. Boldine improved kidney damage in renovascular hypertension induced by the Goldblatt two-kidney one-clip model [10] and showed a renoprotective action in streptozotocin-induced diabetes in rats [11].

Despite the widespread use of the alkaloid boldine, its mechanism of action on renal function remains unclear. Considering the need for new approaches to the treatment of hypertension or contributing to the renoprotective actions against hypertension, this study aimed to investigate boldine's vasodilatory action by using an isolated and perfused rat kidney model to verify the hypothesis that boldine causes the direct relaxation of renal arteries. The mechanisms responsible for renal vasodilator actions were also explored.

2. Materials and Methods

2.1. Drugs. Boldine (≥98% purity) was purchased from Sigma-Aldrich (St. Louis, MO, USA). Heparin was obtained from Cristália, (São Paulo, SP, Brazil). Xylazine and ketamine hydrochloride were obtained from Vetec (Vetec, Duque de Caxias, RJ, Brazil). Acetylcholine chloride, apamin, charybdotoxin, dextrose, glibenclamide, iberiotoxin, indomethacin, tetraethylammonium chloride (TEA), Nω-nitro-L-arginine methyl ester (L-NAME), phenylephrine, sodium deoxycholate, NaCl, $NaHCO_3$, KCl, $CaCl_2$, $MgSO_4$, KH_2PO_4, and ethylenediaminetetraacetic acid (EDTA) were purchased from Sigma-Aldrich (St. Louis, MO, USA).

2.2. Animals. Male Wistar rats, 3 months old, were obtained from the animal facility of the University of Vale do Itajaí (UNIVALI). The animals were kept at controlled room temperature (22 ± 2°C), 12-hour light/dark cycle, with free access to water and chow. All methodologies and procedures used here were submitted and approved by the Ethics Committee on Animal Use of UNIVALI, under authorization number 022/19p and followed all the National Control Council of Animal Experimentation recommendations.

2.3. Isolation and Perfusion of the Rat Kidney. To avoid the appearance of clots in the renal vascular bed during the kidney isolation and perfusion procedure, the animals were previously treated with heparin (30 UI, by intraperitoneal route), 5 to 10 min before the administration of the anesthetic agent. The rats were then anesthetized with 80 mg/kg ketamine plus 10 mg/kg xylazine by intraperitoneal route. After obtaining deep anesthesia, a laparotomy was performed, allowing access to all the animal's viscera. The intestine was shifted to the right side, allowing visualization of the left kidney and dissection of the abdominal aorta. During these procedures, the viscera, especially the left kidney, were kept moist with surgical gauze soaked in physiological saline solution. With the aid of a surgical thread, the left ureter was ligated, preventing urinary flow and, consequently, the production of urine by the kidney. Another surgical wire was placed in the abdominal aorta artery, between the right and left renal arteries, to direct blood flow only to the left side. Blood flow in the aorta artery was interrupted below the right renal artery. Then, a small incision was made in the aorta artery, allowing the insertion of a catheter-directed to the left renal artery and fixed to the aorta artery with surgical threads. The surgical thread positioned over the abdominal aorta was tied, interrupting the renal flow, and a peristaltic perfusion pump was activated, starting the perfusion process. In the continuous perfusion process, the kidney was removed from the abdominal cavity and placed in a plate to remove the adjacent fat and adrenal gland, to avoid the influence of the adrenal on the renal vascular bed during the experimentation period. Then, the kidney was placed in a chamber containing 100 ml of physiological saline solution (PSS; 119 mM NaCl, 4.7 mM KCl, 2.4 mM $CaCl_2$, 1.2 mM $MgSO_4$, 25.0 mM $NaHCO_3$, 1.2 mM KH_2PO_4, 11.1 mM dextrose, and 0.03 mM EDTA) and coupled to the perfusion system, kept at a temperature of 37°C, constantly aerated with 95% O_2 and 5% CO_2, with a constant flow of 4 ml/min. A period of 30 min was respected before starting the experimental evaluation. The recording of perfusion pressure was performed through a pressure transducer coupled to the perfusion system, connected to a computerized polygraph with specific integration software (PowerLab system and Chart 7.1 software, ADInstruments, Castle Hill, Australia). A diagram of the isolated perfused kidney experimental setup is displayed in Figure 1.

2.4. Evaluation of the Effects and Mechanisms of Boldine on the Renal Arteries. After a stabilization time of 30 min, tissue integrity was verified with a bolus injection of 120 mmol KCl. The integrity of the endothelium was checked 20 min

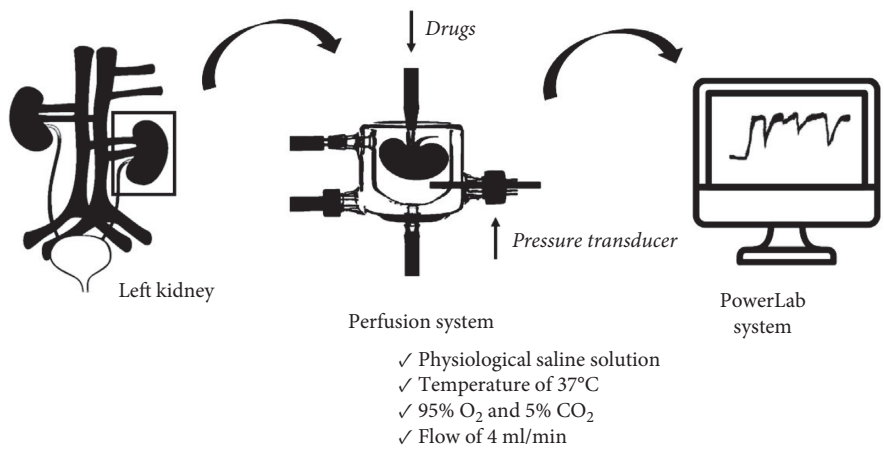

Figure 1: Diagram of the isolated perfused kidney experimental setup.

later with the addition of phenylephrine (300 nmol) followed by acetylcholine (300 nmol). A further 20 min period waited, and then the preparations were continuously perfused with PSS containing phenylephrine (3 μM), which is enough to induce a sustained increase in renal perfusion pressure. After stabilization in the increase in perfusion pressure, the preparations received bolus injections containing 10, 30, 100, and 300 nmol of boldine, and the reduction in perfusion pressure was evaluated. The bolus injections of the tested substances were made in a final volume of 10 or 30 μl through access close to the preparation, with a minimal time interval of 3 min between doses. Some kidney preparations were perfused with PSS that contained sodium deoxycholate (1.8 mg/ml) for 30 s to chemically remove the renal arteries' endothelium. After the infusion of sodium deoxycholate, regular PSS was perfused for 40 min for stabilization. The lack of vasodilatation confirmed the endothelium removal after a bolus injection of acetylcholine. A dose-response curve (30, 100, and 300 nmol) of boldine was generated for preparations without an endothelium. Responses were recorded 10 s after administration. Changes in perfusion pressure (in mmHg) were recorded and compared between groups.

In another experimental set, using preparations with an intact endothelium, the preparations were perfused with PSS that contained 3 μM phenylephrine *plus* the following agents: 100 μML-NAME (nonselective nitric oxide synthase inhibitor), 1 μM indomethacin (nonselective cyclooxygenase inhibitor), 40 mM KCl (K^+-mediated depolarization), 10 mM TEA (nonspecific potassium channel blocker), 10 μM glibenclamide (selective ATP-sensitive K^+ channels blocker), apamin 10 nM (selective small-conductance Ca^{2+}-activated K^+ channel blocker), iberiotoxin (selective high-conductance Ca^{2+}-activated K^+ channel blocker), 1 nM charybdotoxin (selective high- and intermediate-conductance Ca^{2+}-activated K^+ channel blocker). After 15 min of perfusion, boldine (30, 100, and 300 nmol) was injected. Its ability to reduce perfusion pressure was compared with the results obtained with the control preparations perfused only with the vehicle.

2.5. Statistical Analysis. The results are expressed as the mean ± standard error of the mean from six preparations in each group. The statistical analyses were performed using a one-way analysis of variance (ANOVA) followed by Bonferroni's *post hoc* test. Values of $p < 0.05$ were considered statistically significant. The statistical analyses were performed using the GraphPad Prism software version 6.00 for Windows (GraphPad, La Jolla, CA, USA).

3. Results and Discussion

The vasodilator effect on renal arteries using isolated and perfused rat kidneys has been a heavily used strategy to assess the hemodynamic actions of isolated compounds, with a closer approximation to the mechanism of action, given the ability to assess different molecular targets [12]. In the present study, the administration of boldine (30, 100, and 300 nmol) in the vascular bed of the kidney induced a dose-dependent dilatory result (Figure 2(c)), thus answering the initial hypothesis of the work that discussed the possibility of boldine having a vasodilating action in the renal arterial bed. This is the first study to demonstrate the relaxing effects of boldine on the renal vascular bed. However, the relaxing effect of boldine on other vascular tissues was first described in 1996, where Chen et al. demonstrated the vasodilating action of this alkaloid in isolated rat thoracic aorta [13].

Based on this positive result, investigations were carried out on the involvement of the endothelium and the underlying mechanisms related to relaxing actions. As depicted in Figure 2(d), the effects of boldine in the preparations previously administered with sodium deoxycholate (i.e., to remove the endothelium) were completely absent (Figure 2(d)), indicating that the functional endothelium is essential for its vasodilatory action. Correspondingly, the effects of all doses of boldine were prevented in preparations that were treated with the nonselective nitric oxide synthase inhibitor L-NAME (Figure 3(a)), while in the preparations perfused with the nonselective cyclooxygenase enzyme inhibitor indomethacin, the vasorelaxant effects of boldine

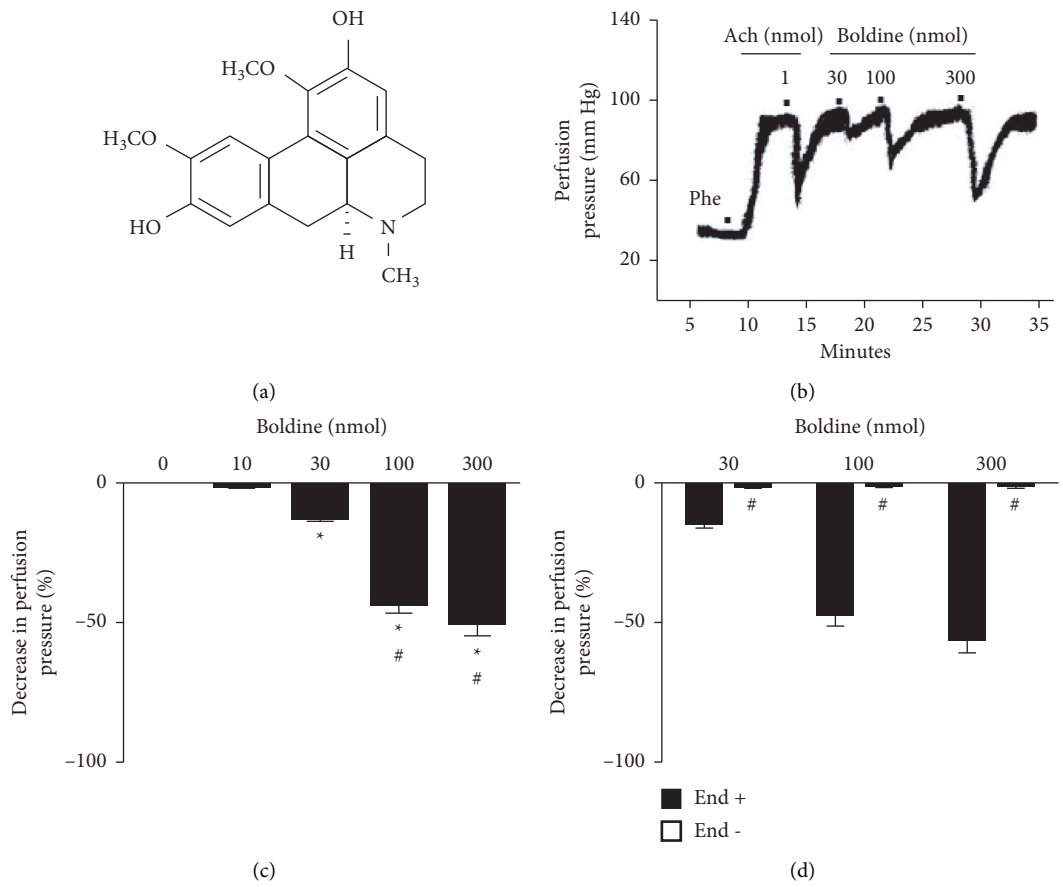

Figure 2: Boldine dose-dependently induced vasorelaxation in isolated and perfused kidneys. (a) Molecular structure of boldine. (b) Trace recording of kidney perfusion pressure showing the effects of acetylcholine (ACh) and boldine. (c) Effects of boldine on perfusion pressure in endothelium-intact isolated kidneys. (d) Effects of boldine on endothelium-intact (End+) and endothelium-denuded (End-) preparations. The data are expressed as the mean ± SEM from six experiments. $^{*}p < 0.05$, compared with perfusion pressure after PSS administration (identified as the number 0); $^{\#}p < 0.05$, compared with the previous dose of boldine (a) or endothelium-denuded preparations (b).

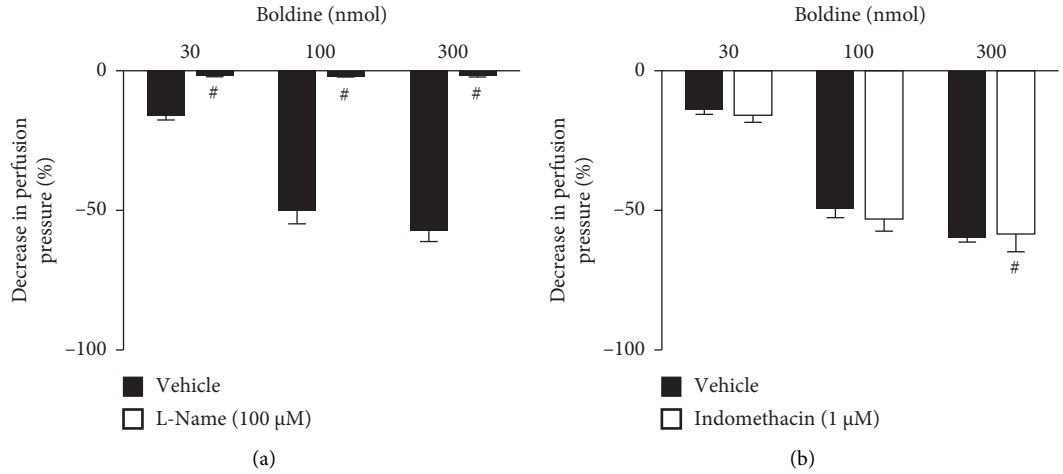

Figure 3: Role of nitric oxide and prostanoids in the vasodilatory effects of boldine. Effects of boldine on endothelium-intact kidney preparations that were perfused with (a) L-NAME or (b) indomethacin. The data are expressed as the mean ± SEM from six experiments. $^{\#}p < 0.05$, compared with the vehicle-only perfused preparations.

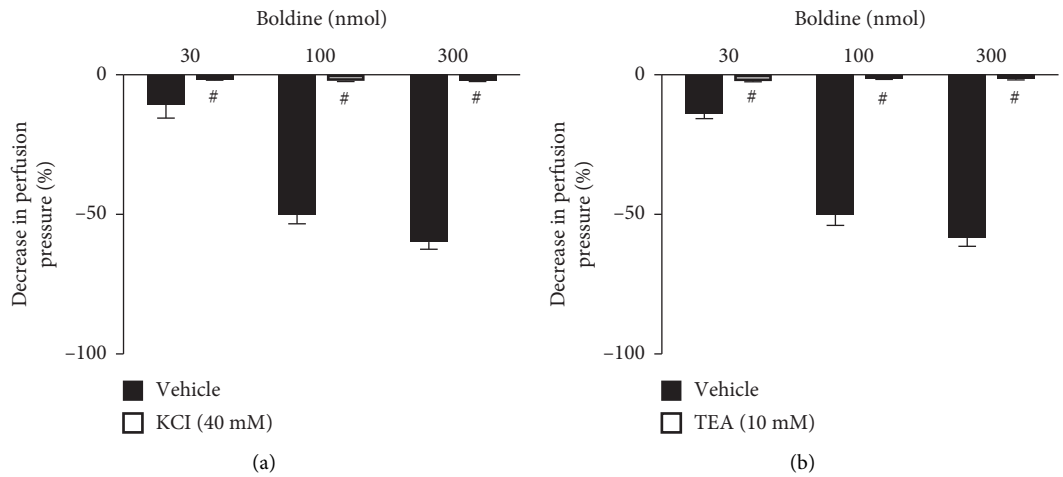

Figure 4: Effect of potassium channels on the vasodilatory effect of boldine. Effects of boldine on endothelium-intact kidney preparations that were perfused with (a) KCl or (b) TEA. The data are expressed as the mean ± SEM from six experiments. $^{\#}p < 0.05$, compared with the vehicle-only perfused preparations.

remained unchanged (Figure 3(b)), indicating that endothelium-dependent relaxant properties of boldine were dependent of nitric oxide (NO) generation and independent of prostanoids production.

The main endothelium-derived relaxant factor is NO, which is considered one of the main mediators of cellular processes. In blood vessels, NO is produced in endothelial cells from L-arginine, having a vasodilating action. It diffuses to the smooth muscle cells interacting with the soluble guanylate cyclase enzyme making it active, causing the formation of cyclic guanosine monophosphate, which results in the relaxation of the vascular smooth muscle cell [14, 15]. Considering that endothelial removal or the suppression of NO production through the administration of L-NAME completely prevented the vascular effects of boldine, our findings suggest that the endothelium performed a crucial function in decreasing perfusion pressure induced by boldine. Indeed, the actions of boldine on vascular endothelium have already been described in the literature. Boldine treatment enhanced the maximal relaxation to acetylcholine in spontaneously hypertensive rats aorta [9], improved the endothelium-dependent relaxation in the aortas of streptozotocin-treated diabetic rats [16], and improved endothelium-dependent relaxation in aortas of diabetic mice [17].

To verify the actions related to K^+ channels, the preparations were perfused with a nutrient solution in which 40 mM KCl was added, which induces K^+-mediated depolarization, and TEA, a nonselective K^+-channel blocker (Figures 4(a) and 4(b), respectively). It was observed that both treatments blocked the vasorelaxant effects induced by boldine, suggesting a predominant role of K^+ channels in the vasodilatory effects of this compound. K^+ channels are protein structures present in different types of cells, function as pores in membranes that allow the passage of K^+. They are divided into 4 major classes: voltage-dependent K^+ channels, ATP-sensitive K^+ channels, inward-rectifier K^+ channels, and Ca^{2+}-activated K^+ channels [18–20]. The treatment with glibenclamide, an ATP-sensitive K^+ channel blocker, maintained the vasorelaxant action of boldine unchanged in all doses used (Figure 5(a)). Similarly, the perfusion with charybdotoxin, a selective high- and intermediate-conductance Ca^{2+}-activated K^+ channel blocker (Figure 6(a)), and iberiotoxin, a selective high-conductance Ca^{2+}-activated K^+ channel blocker (Figure 6(b)), did not modify the vasodilatory action of boldine. On the other hand, the perfusion with apamin, a selective small-conductance Ca^{2+}-activated K^+ channel blocker, completely prevented the vasodilatory action of boldine at all doses tested (Figure 5(b)), indicating that this K^+ channel subtype appears to be crucial for the relaxing actions evoked by boldine. In summary, considering that the downstream targets of the nitric oxide pathway in vessels include the opening of K^+ channels [21, 22], this set of results suggests that boldine-mediated endothelium-dependent vasodilation in renal arteries depends on the opening of small-conductance Ca^{2+}-activated K^+ channels induced by nitric oxide in smooth muscle cells.

It is noteworthy that, in recent years, many compounds isolated from medicinal plants have been studied about their renal actions, revealing important vasodilating, diuretic, antiurolithic, and protective actions against hypertensive damage. Nothofagin, a mono-C-glycoside of 4,2′,4′,6′-tetrahydroxy-dihydrochalcone found in *Leandra dasytricha* leaves, demonstrated the ability to induce diuresis [23], renoprotection [24], vasodilation [12], and hypotensive effect [25]. Different compounds from the xanthone classes isolated from *Garcinia achachairu* branches revealed acute diuretic actions [26, 27], prolonged diuretic and renoprotective effects [28], and antiurolithic properties [29]. Besides, glycosylated flavonoids obtained from the leaves of *Bauhinia forficata* revealed vasodilator [30], diuretic, and kidney protective effects [31].

However, although the results described herein undoubtedly point toward the participation of Ca^{2+}-activated K^+ channels in the renal effects induced by boldine, further studies are needed to investigate other molecular targets and subtypes of channels by using different inhibitors combined approaches. Besides, another important limitation of the

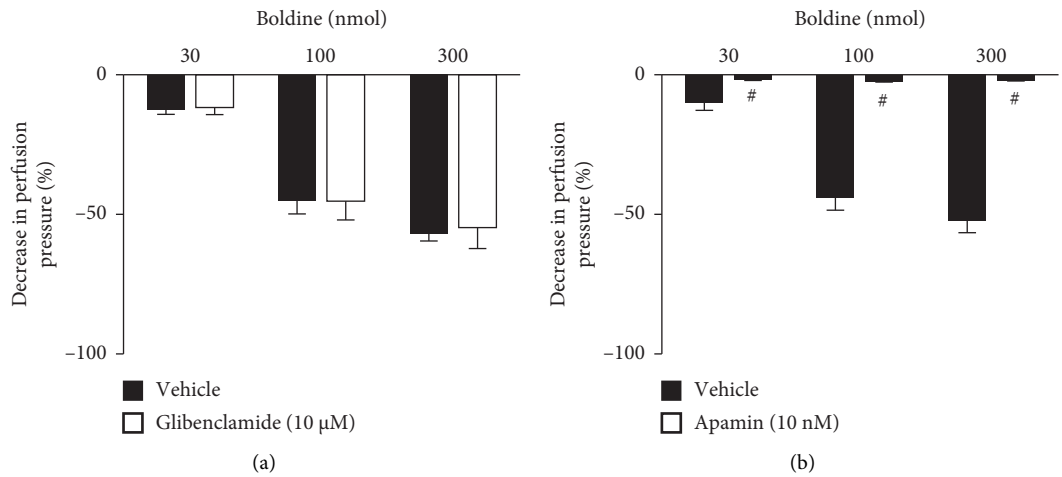

Figure 5: Effect of potassium channel subtype blockers on the vasodilatory effect of boldine. Effects of boldine on endothelium-intact kidney preparations that were perfused with (a) glibenclamide or (b) apamin. The data are expressed as the mean ± SEM from six experiments. $^{\#}p < 0.05$, compared with the vehicle-only perfused preparations.

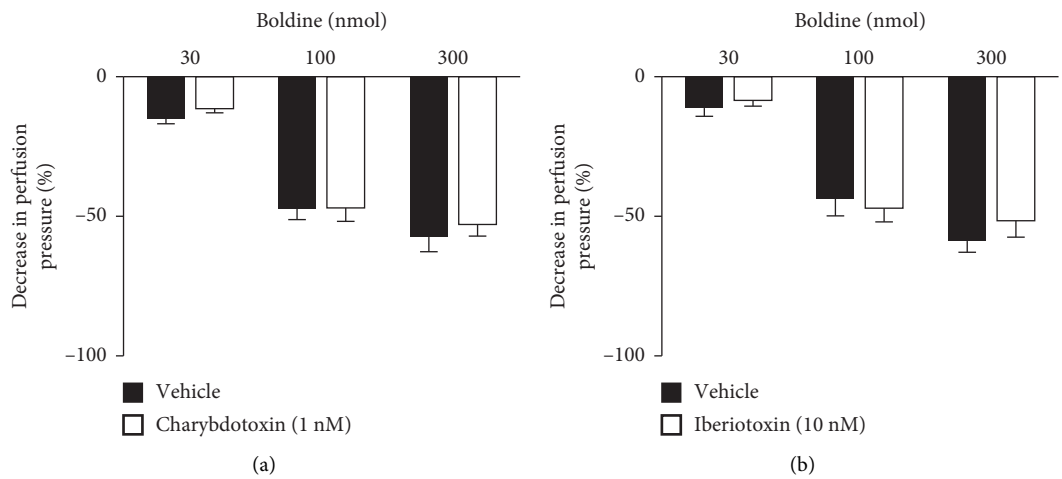

Figure 6: Effect of potassium channel subtype blockers on the vasodilatory effect of boldine. Effects of boldine on endothelium-intact kidney preparations that were perfused with (a) charybdotoxin or (b) iberiotoxin. The data are expressed as the mean ± SEM from six experiments.

study is that we were unable to explore the receptor involved in the vasodilatory effect of boldine, which remains to be studied in the future. Considering the actions already described in the literature for this alkaloid, this study adds about the renal vasodilator effect, contributing to a better understanding of boldine's potential to be used as pharmacotherapy or dietary supplement.

Data Availability

The data used to support the findings of this study are available on request to the corresponding author.

Conflicts of Interest

The authors declare that they have no conflicts of interest to disclose.

Authors' Contributions

PDS and AGJ designed the study, acquired funding, and prepared the article. KGTM, VMBS, LMS, and RCVS performed the experiments and generated and analyzed the data. All authors read and approved the final version of the article.

Acknowledgments

This work was supported by grants from the National Council for Scientific and Technological Development (CNPq; no. 449464/2014-8 and 407685/2018-9), Higher Education Personnel Improvement Coordination (CAPES), Scientific Research Support Foundation and Technological Sciences of the State of Santa Catarina (FAPESC), and University of Vale do Itajaí (UNIVALI).

References

[1] M. d. F. Agra, P. F. d. Freitas, and J. M. Barbosa-Filho, "Synopsis of the plants known as medicinal and poisonous in Northeast of Brazil," *Revista Brasileira de Farmacognosia*, vol. 17, no. 1, pp. 114–140, 2007.

[2] M. G. L. Brandão, G. P. Cosenza, R. A. Moreira, and R. L. M. Monte-Mor, "Medicinal plants and other botanical products from the Brazilian Official Pharmacopoeia," *Rev Bras Farmacogn*, vol. 16, pp. 408–420, 2006.

[3] C. Viegas, V. S. Bolzani, J. Eliezer, and E. J. Barreiro, "The natural products and the modern medicinal chemistry," *Quimica Nova*, vol. 29, no. 2, 2006.

[4] A. L. T. G. Ruiz, D. Tafarello, V. H. S. Souza, and J. E. Carvalho, "Pharmacology and toxicology of *Peumus boldus* and *Baccharis genistelloides*," *Rev. bras. Farmacognosia*.vol. 18, no. 2, 2008.

[5] P. O'Brien, C. Carrasco-Pozo, and H. Speisky, "Boldine and its antioxidant or health-promoting properties," *Chemico-Biological Interactions*, vol. 159, pp. 1–17, 2006.

[6] Y. Y. Jang, J. H. Song, Y. K. Shin, E. S. Han, and C. S. Lee, "Protective effect of boldine on oxidative mitochondrial damage in streptozotocin-induced diabetic rats," *Pharmacological Research*, vol. 42, no. 4, pp. 361–371, 2000.

[7] T. Boeing, L. N. B. Mariano, A. C. Dos Santos et al., "Gastroprotective effect of the alkaloid boldine: involvement of non-protein sulfhydryl groups, prostanoids and reduction on oxidative stress," *Chemico-Biological Interactions*, vol. 327, Article ID 109166, 2020.

[8] Y. S. Lau, W. C. Ling, D. Murugan, and M. R. Mustafa, "Boldine ameliorates vascular oxidative stress and endothelial dysfunction," *Journal of Cardiovascular Pharmacology*, vol. 65, no. 6, pp. 522–531, 2015.

[9] Y.-S. Lau, A. Machha, F. I. Achike, D. Murugan, and M. R. Mustafa, "The aporphine alkaloid boldine improves endothelial function in spontaneously hypertensive rats," *Experimental Biology and Medicine*, vol. 237, no. 1, pp. 93–98, 2012.

[10] G. I. Gómez and V. Velarde, "Boldine improves kidney damage in the Goldblatt 2K1C model avoiding the increase in TGF-β," *International Journal of Molecular Sciences*, vol. 19, no. 7, p. 1864, 2018.

[11] R. Hernández-Salinas, A. Z. Vielma, M. N. Arismendi, M. P. Boric, J. C. Sáez, and V. Velarde, "Boldine prevents renal alterations in diabetic rats," *Journal of Diabetes Research*, vol. 2013, Article ID 593672, , 2013.

[12] A. A. M. Marques, C. H. F. da Silva, P. de Souza et al., "Nitric oxide and Ca2+-activated high-conductance K+ channels mediate nothofagin-induced endothelium-dependent vasodilation in the perfused rat kidney," *Chemico-Biological Interactions*, vol. 327, Article ID 109182, 2020.

[13] K. S. Chen, F. N. Ko, C. M. Teng, and Y. C. Wu, "Antiplatelet and vasorelaxing actions of some aporphinoids," *Planta Medica*, vol. 62, no. 2, pp. 133–136, 1996.

[14] G. A. Shiekh, T. Ayub, S. N. Khan, R. Dar, and K. I. Andrabi, "Reduced nitrate level in individuals with hypertension and diabetes," *Journal of Cardiovascular Disease Research*, vol. 2, no. 3, pp. 172–176, 2011.

[15] E. S. Underbakke, A. T. Iavarone, M. J. Chalmers et al., "Nitric oxide-induced conformational changes in soluble guanylate cyclase," *Structure*, vol. 22, no. 4, pp. 602–611, 2014.

[16] Y. S. Lau, X. Y. Tian, Y. Huang, D. Murugan, F. I. Achike, and M. R. Mustafa, "Boldine protects endothelial function in hyperglycemia-induced oxidative stress through an antioxidant mechanism," *Biochemical Pharmacology*, vol. 85, no. 3, pp. 367–375, 2013a.

[17] Y. S. Lau, X. Y. Tian, M. R. Mustafa et al., "Boldine improves endothelial function in diabeticdb/dbmice through inhibition of angiotensin II-mediated BMP4-oxidative stress cascade," *British Journal of Pharmacology*, vol. 170, no. 6, pp. 1190–1198, 2013b.

[18] M. Baranowska, H. Kozłowska, A. Korbut, and B. Malinowska, "Potassium channels in blood vessels: their role in health and disease," *Postepy Higieny I Medycyny Doswladczalnej*, vol. 61, pp. 596–605, 2007.

[19] W. F. Jackson, "Potassium channels in the peripheral microcirculation," *Microcirculation*, vol. 12, no. 1, pp. 113–127, 2005.

[20] B. F. Palmer and D. J. Clegg, "Physiology and pathophysiology of potassium homeostasis," *Advances in Physiology Education*, vol. 40, no. 4, pp. 480–490, 2016.

[21] S. L. Archer, J. M. Huang, V. Hampl, D. P. Nelson, P. J. Shultz, and E. K. Weir, "Nitric oxide and cGMP cause vasorelaxation by activation of a charybdotoxin-sensitive K channel by cGMP-dependent protein kinase," *Proceedings of the National Academy of Sciences*, vol. 91, no. 16, pp. 7583–7587, 1994.

[22] V. M. Bolotina, S. Najibi, J. J. Palacino, P. J. Pagano, and R. A. Cohen, "Nitric oxide directly activates calcium-dependent potassium channels in vascular smooth muscle," *Nature*, vol. 368, no. 6474, pp. 850–853, 1994.

[23] C. L. B. de Almeida, T. Boeing, L. B. Somensi et al., "Diuretic, natriuretic and potassium-sparing effect of nothofagin isolated from *Leandra dasytricha* (A. Gray) Cogn. leaves in normotensive and hypertensive rats," *Chemico-Biological Interactions*, vol. 268, pp. 103–110, 2017.

[24] C. L. B. de Almeida, V. Cechinel-Filho, T. Boeing et al., "Prolonged diuretic and saluretic effect of nothofagin isolated from *Leandra dasytricha* (A. Gray) Cogn. leaves in normotensive and hypertensive rats: role of antioxidant system and renal protection," *Chemico-Biological Interactions*, vol. 279, pp. 227–233, 2018.

[25] C. H. da Silva, R. A. Palozi, P. de Souza et al., "Nitric oxide/cGMP signaling pathway and potassium channels contribute to hypotensive effects of nothofagin," *Minerva Cardioangiologica*, vol. 68, no. 6, pp. 602–608, 2020.

[26] L. N. Bolda Mariano, T. Boeing, R. d. C. M. V. d. A. F. da Silva et al., "1,3,5,6-Tetrahydroxyxanthone, a natural xanthone, induces diuresis and saluresis in normotensive and hypertensive rats," *Chemico-Biological Interactions*, vol. 311, Article ID 108778, 2019.

[27] L. N. Bolda Mariano, T. Boeing, V. Cechinel-Filho, R. Niero, L. Mota da Silva, and P. de Souza, "The acute diuretic effects with low-doses of natural prenylated xanthones in rats," *European Journal of Pharmacology*, vol. 884, Article ID 173432, 2020.

[28] L. N. Bolda Mariano, T. Boeing, V. Cechinel Filho et al., "Prolonged diuretic and renoprotective effects of a xanthone obtained from *Garcinia achachairu* rusby in normotensive and hypertensive rats," *Evid-based Complement Alternative Medicine*, vol. 2021, Article ID 5510053, 9 pages, 2021.

[29] L. N. B. Mariano, T. Boeing, V. Cechinel Filho, R. Niero, L. Mota da Silva, and P. de Souza, "1,3,5,6-tetrahydroxyxanthone promotes diuresis, renal protection and antiurolithic properties in normotensive and hypertensive rats," *Journal of Pharmacy and Pharmacology*, vol. 73, no. 5, pp. 700–708, 2021.

[30] C. C. Cechinel-Zanchett, R. d. C. M. V. d. A. F. da Silva, A. Tenfen et al., "*Bauhinia forficata* link, a Brazilian medicinal

plant traditionally used to treat cardiovascular disorders, exerts endothelium-dependent and independent vasorelaxation in thoracic aorta of normotensive and hypertensive rats," *Journal of Ethnopharmacology*, vol. 243, p. 112118, 2019.

[31] C. C. Cechinel-Zanchett, L. N. Bolda Mariano, T. Boeing et al., "Diuretic and renal protective effect of kaempferol 3-O-Alpha-l-rhamnoside (afzelin) in normotensive and hypertensive rats," *Journal of Natural Products*, vol. 83, no. 6, pp. 1980–1989, 2020.

Hindawi
Evidence-Based Complementary and Alternative Medicine
Volume 2022, Article ID 2671343, 14 pages
https://doi.org/10.1155/2022/2671343

Research Article

The Improvement of Cardiac and Endothelial Functions of Xue-Fu-Zhu-Yu Decoction for Patients with Acute Coronary Syndrome: A Meta-Analysis of Randomized Controlled Trials

Shiqi Chen,[1,2] **Xiaoxiao Wu**,[2] **Tong Li**,[2] **Weiting Cheng**,[2] **Xiaowan Han**,[1] **Yang Li**,[2] **Baofu Wang**,[1,2] **Yu Teng**,[2] **Mingjing Zhao**,[2] **and Yahong Wang**[1]

[1]*Department of Cardiology, Dongzhimen Hospital Affiliated to Beijing University of Chinese Medicine, Beijing 100700, China*
[2]*Key Laboratory of Chinese Medicine of Ministry of Education and Beijing, Dongzhimen Hospital Affiliated to Beijing University of Chinese Medicine, Beijing 100700, China*

Correspondence should be addressed to Mingjing Zhao; mjgx2004@163.com and Yahong Wang; wyh411@hotmail.com

Received 11 November 2021; Revised 4 January 2022; Accepted 17 January 2022; Published 10 February 2022

Academic Editor: Arquimedes Gasparotto Junior

Background. Xue-Fu-Zhu-Yu decoction (XFZYD) is a traditional Chinese prescription that has been used to treat patients with blood stasis in China for many years. The present study aimed to evaluate the improvement of cardiac and endothelial functions of XFZYD for patients with acute coronary syndrome (ACS) through a systematic review and meta-analysis. *Methods.* Six databases were searched to collect RCTs related to the treatment of XFZYD for ACS. The primary outcomes were cardiac and endothelial functions, including the levels of left ventricular ejection fraction (LVEF), left ventricular end-diastolic diameter (LVEDD), and left ventricular end-systolic diameter (LVESD) in echocardiography, as well as the changes in the levels of nitric oxide (NO), endothelin-1 (ET-1), intercellular adhesion molecule-1 (ICAM-1), and vascular cell adhesion molecule-1 (VCAM-1) in the serum. The secondary outcomes were the blood levels of oxidative damage markers (including superoxide dismutase (SOD) and malondialdehyde (MDA)), C-reactive protein (CRP), brain natriuretic peptide (BNP), creatine kinase-MB (CK-MB), and cardiac troponin I (cTnI) as well as the incidence of adverse drug reactions (ADRs). Weighted mean difference (WMD) was estimated for all the outcomes with the random effects model. This type of analysis was conducted in the subgroups of the ACS subtypes, and the methodological quality was assessed using the handbook of Cochrane Collaboration. *Results.* A total of 1,658 records were identified, and 16 randomized controlled trials (1,171 patients) were included. The primary outcomes suggested that XFZYD combined with routine treatment improved LVEF, reduced LVEDD and LVESD, and also improved the serum levels of NO, and reduced the levels of ET-1 and ICAM-1. XFZYD combination therapy significantly ameliorated the blood levels of SOD, MDA, BNP, CK-MB, and cTnI. However, the results indicated no significant difference between XFZYD plus routine treatment and routine treatment for the levels of VCAM-1 and CRP. Moreover, all the ADRs reported in the included studies were slight and the patients recovered soon. *Conclusions.* The present study suggested that XFZYD may improve the cardiac and endothelial functions of ACS patients without serious ADRs. However, based on the mediocre methodological quality, the aforementioned conclusion should be confirmed in a multicenter, large-scale, and accurately designed clinical trial.

1. Introduction

Coronary heart disease (CHD) has been a leading cause of the incidence and mortality worldwide, and it can be divided into acute coronary diseases and stable angina pectoris [1, 2]. Acute coronary syndrome (ACS), which contains three conditions, including ST-elevation myocardial infarction (STEMI), non-ST-elevation myocardial infarction (NSTEMI), and unstable angina (UA), can obstruct the balance of myocardial oxygen supply and demand and result in myocardial ischemia [3]. Untreated UA (without serologic elevation of troponin or creatine kinase-MB (CK-MB) isoenzyme concentration) may dynamically progress to myocardial infarction (MI); both NSTEMI and STEMI,

which can be distinguished by the ST-segment elevation in the electrocardiogram (ECG), exhibit serological evidence of myonecrosis [3]. ACS is mainly caused by the rupture of vulnerable atherosclerotic coronary plaques or the acute formation of the thrombus. Arterial thrombosis due to superficial erosion can activate the endothelium leading to endothelial apoptosis and detachment and induce inflammation and oxidative stress, which affects endothelial dysfunction and platelet aggregation [4, 5]. Transient or long-term myocardial ischemia also results in impaired cardiac function. Recent studies have shown that the western therapies for ACS are related to inhibition of angina, platelet aggregation, and thrombosis, lowering of cholesterol levels by statin medications, as well as percutaneous coronary intervention (PCI) surgery [3, 6]. However, these therapies may be inappropriate for certain individuals and can produce specific adverse drug reactions (ADRs) [7–9]. Traditional Chinese medicine (TCM) plays a more extensive therapeutic role in patients who do not undergo PCI surgery and improve the functions of the heart and blood vessels. Under these circumstances, remedies of complementary and alternative medicine are used so as to enhance the therapeutic effect and reduce adverse reaction-associated toxicity.

Xue-Fu-Zhu-Yu decoction (XFZYD) is a well-known TCM formula, which was originally founded by the famous TCM doctor Qingren Wang from the Qing dynasty. XFZYD consists of the following 11 Chinese herbs: *Angelicae sinensis* (Oliv.), Diels (Danggui), *Rehmannia glutinosa* Libosch. (Dihuang), *Prunus persica* (L.) Batsch (Taoren), *Carthamus tinctorius* L. (Honghua), *Glycyrrhiza uralensis* Fisch. (Gancao), Aurantii Fructus (Zhiqiao), *Paeonia lactiflora* Pall. (Chishao), *Bupleurum chinense* DC. (Chaihu), *Ligusticumi chuanxiong* Hort. (Chuanxiong), *Platycodon grandiflorum* (Jacq.) A. DC. (Jiegeng), and *Achyranthes bidentata* Bl. (Niuxi). The decoction contains at least 34 major constituents including 21 flavonoids, 5 terpenoids, 3 organic acids, 2 lactones, 1 alkaloid, 1 amino acid, and 1 cyanogenic glycoside, which play important roles in the prevention of various cardiovascular diseases [10]. XFZYD has been identified to treat UA patients with blood stasis and Qi stagnation symptoms [11, 12], and a variety of its dosage forms have also been approved by the National Medical Products Administration of the Chinese government for clinical practice. Previous studies [13–15] have shown that the integration of XFZYD and Western medicines can improve the angina symptoms and the blood levels of lipids in patients with CHD. However, the amelioration of the cardiac and endothelial functions due to the combination of XFZYD with routine treatment (RT) in ACS has not been fully explored. The indicators detecting these functions are objective in nature and the results are beneficial to assess the authentic efficacy of XFZYD. Considering that a number of clinical trials have examined the use of XFZYD to treat ACS in recent years, we sought to evaluate its efficacy in improving cardiac and endothelial functions through a systematic review and meta-analysis.

2. Materials and Methods

This review protocol was registered on PROSPERO (CRD 42021253651).

2.1. Criteria for considering the Studies in This Review

2.1.1. Types of Studies. Randomized controlled trials (RCTs) with no limit of publishing language were included.

2.1.2. Types of Participants. The patients that were identified according to accurate ACS diagnostic criteria, which were similar to previously published guidelines [16, 17], were eligible for inclusion in this study. According to the International Classification of Diseases 10th revision (ICD-10) codes, the patients with STEMI, NSTEMI, or UA with or without PCI could be included in the present study [1, 18].

2.1.3. Types of Interventions in the Experimental and Control Groups. The intervention in the experimental group included XFZYD without addition or subtraction of any herbs and should be combined with the routine treatment (RT) of the control group. The intervention in the control group was the conventional therapy without any other traditional Chinese medicines. RT should be the regular medications of inhibition of angina, platelet aggregation, thrombosis, arrhythmia, hypertension, and diabetes as well as statins according to the guidelines [3, 6].

2.1.4. Types of Outcome Measures. The primary outcomes were defined as measures of cardiac and endothelial functions. The levels of left ventricular ejection fraction (LVEF), left ventricular end-diastolic diameter (LVEDD), and left ventricular end-systolic diameter (LVESD) in the echocardiography measurement were used to identify the cardiac function, and the changes in the levels of nitric oxide (NO), endothelin-1 (ET-1), intercellular adhesion molecule-1 (ICAM-1), and vascular cell adhesion molecule-1 (VCAM-1) in the serum were representative of the endothelial function. The additional outcomes observed included the blood levels of the oxidative damage markers (superoxide dismutase (SOD) and malondialdehyde (MDA)), C-reactive protein (CRP), brain natriuretic peptide (BNP), and the myocardial enzymes (CK-MB and cardiac troponin I (cTnI)) and ADRs.

2.2. Information Sources and Search Strategy. The search was applied to the following six databases: Cochrane Library, PubMed, Web of Science, the Chinese National Knowledge Infrastructure (CNKI), Wanfang Database, and Weipu Database (VIP), from the inception of each electronic database to February 15, 2021. Additional identification was conducted for all eligible trials by other searching methods from websites and citations. The following terms were used as the mesh terms or the free terms: "acute coronary syndrome," "ACS," "myocardial infarction," "MI," "ST-segment elevation myocardial infarction," "STEMI," "non-ST-segment elevation myocardial infarction," "NSTEMI," "unstable angina," "UA," "unstable angina pectoris," "UAP," "Xuefuzhuyu," "xue-fu-zhu-yu," "xuefuzhuyu," and "xue fu zhuyu." The searching strategy in PubMed was performed as ("acute coronary syndrome"[MeSH Terms] OR "acute coronary

syndrome"[All Fields] OR "ACS"[All Fields] OR "myocardial infarction"[MeSH Terms] OR "myocardial infarction"[All Fields] OR "ST elevation myocardial infarction"[MeSH Terms] OR "ST elevation myocardial infarction"[All Fields] OR "ST segment elevation myocardial infarction"[All Fields] OR "STEMI"[All Fields] OR "non ST elevated myocardial infarction"[MeSH Terms] OR "non ST elevated myocardial infarction"[All Fields] OR "NSTEMI"[All Fields] OR "angina, unstable"[MeSH Terms] OR ("angina"[All Fields] AND "unstable"[All Fields]) OR "unstable angina"[All Fields] OR ("unstable"[All Fields] AND "angina"[All Fields] AND "pectoris"[All Fields]) OR "unstable angina pectoris"[All Fields] OR "UAP"[All Fields] OR "UA"[All Fields]) AND ("Xuefuzhuyu"[All Fields] OR "xue-fu-zhu-yu"[All Fields] OR "xue fu zhu yu"[All Fields] OR "xuefu zhuyu"[All Fields]).

2.3. Study Selection. Two investigators (SQC and TL) independently carried out a literature search using the predetermined criteria in the NoteExpress 3.2 software. Initially, duplications were found in all databases and removed from the original search results. Furthermore, the apparently irrelevant studies were excluded following the reading of the titles and abstracts. Finally, the full texts were screened to identify the related studies, and the unqualified studies were excluded. The process of study selection was cross-checked by two researchers. Any disagreement was discussed and resolved in a consensus meeting with the corresponding author (YHW and MJZ).

2.4. Data Extraction. After the selection, two authors (XXW and WTC) independently extracted data from the included studies by using a standardized sheet, which was prepared for this review. The extracted data included the study title, name of the first author, year of publication, the diagnostic criteria of the patients, age of participants, baseline, disease types, sample size, interventions in the treatment and control groups, treatment duration, treatment dose, and outcome measures.

2.5. Risk of Bias in Individual Studies. Two authors (XWH and YL) independently assessed the risk of bias using assessment tools provided by the handbook of Cochrane Collaboration to evaluate the methodological quality of included studies, involving the blinding of outcomes assessment (i.e., detection bias), the blinding of participants and personnel (i.e., performance bias), the random sequence generation (i.e., selection bias), the allocation concealment (i.e., selection bias), the incomplete outcomes data (i.e., attrition bias), the selective reporting (i.e., reporting bias), and other biases. Disagreements were resolved by consensus with the corresponding author (YHW and MJZ).

2.6. Strategy for Data Synthesis

2.6.1. Statistical Analysis. Review Manager 5.3 software provided by the Cochrane Collaboration was used to conduct data analysis. Dichotomous data were calculated as the risk ratios (RR) and the 95% confidence interval (CI). Continuous outcomes were expressed as weighted mean difference (WMD) or standardized mean difference (SMD) with 95% CI. SMD would be applied in preference if the included studies used different units or rating instruments [19]. $P < 0.05$ was considered to indicate a statistically significant difference.

2.6.2. Assessment of Heterogeneity. The heterogeneity of the included studies was analyzed with the χ^2 test. When $I^2 \leq 50\%$, a small heterogeneity was considered among the studies, and the fixed effects model was used for data analysis. In case the statistical heterogeneity was $I^2 > 50\%$, the sources of heterogeneity were measured. Subgroup analysis was performed in the presence of clinical heterogeneity, such as the subtypes of ACS, including STEMI, NSTEMI, and UA. In case of significant heterogeneity, the random effects model was considered, or only the descriptive analysis was performed.

2.6.3. Sensitivity Analysis. The studies with high weight and low quality were excluded. Following the comparison of the pooled statistics prior to and following exclusion of these studies, certain differences could be found. Subgroup and sensitivity analyses were also conducted to explore the stability of the results if necessary.

3. Results

3.1. Study Selection. A total of 1,658 articles were retrieved from six literature databases. Following the removal of 722 duplicates, 936 potentially relevant articles remained for subsequent assessment. Following evaluation of titles and abstracts, 830 articles were excluded. A total of 90 out of 106 remaining studies were excluded following the investigation of the full texts. Finally, 16 studies [20–35] were included in the meta-analysis. A flow chart (Figure 1) indicated the search process and study selection.

3.2. Study Characteristics. A total of 1,658 records were identified and 16 RCTs [20–35] were included, covering 1,171 participants. All the studies were conducted in China and almost all of them were published in Chinese. Only one was published in English. They were published from 2004 to 2020. The sample size varied from 49 to 104 subjects, and the duration of the XFZYD treatment ranged from 1 to 12 weeks. The disease diagnoses of these studies were AMI, STEMI, UNSTEMI, and UA with or without PCI. Further details regarding the characteristics of the included studies are shown in Table 1 and supplementary Table S1.

3.3. Risk of Bias and Methodological Quality. According to the assessment tools provided by the handbook of Cochrane Collaboration, the included studies displayed methodological bias (Figure 2). All the included studies were described as "randomized" studies; among them, five studies reported

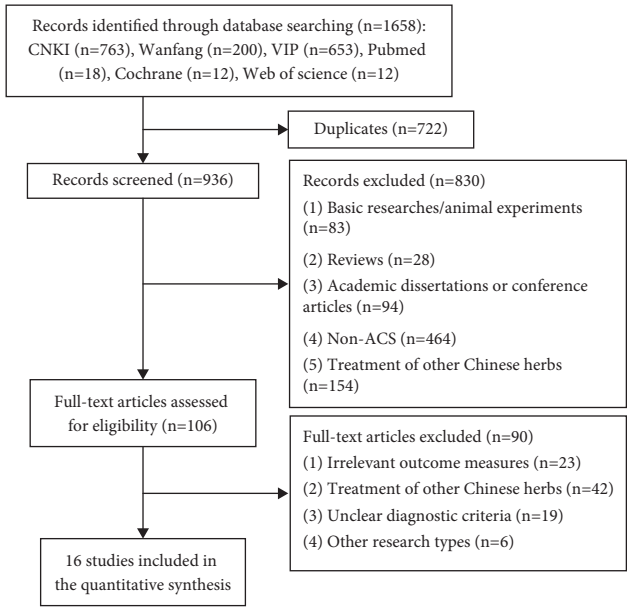

Figure 1: Flow chart for searching and screening of the studies.

using the "random number table" [21, 26, 27, 29, 31], and one study used the toss method [23]. However, the allocation concealment, the blinding of the participants, and the outcome assessment were not clear in any of the studies investigated. The data reported in the results were complete according to the methods used. Therefore, the incomplete outcome data were identified as low risks. Although not all the studies included provided protocols, the expected outcome indicators were reported and the selective reporting bias was defined as low risk. The results indicated that the methodological quality of the 16 literature studies included in this meta-analysis was generally mediocre.

3.4. Outcome Measures

3.4.1. Cardiac Functions. In total, six studies [20–23, 25, 35] reported the outcome of LVEF from the ECG. Three studies [20, 22, 25] included AMI patients with PCI, one study [21] included only UA patients, one study [35] included AMI patients, and one study [23] explicitly included STEMI patients with PCI. Subgroup meta-analysis was performed due to the high total heterogeneity ($I^2 = 62\%$), and the random effects model was used in the meta-analysis. As shown in Figure 3, the combination of XFZYD with RT therapy performed better in improving LVEF (MD 6.35, 95% CI 4.20 to 8.50; $P < 0.00001$; $I^2 = 62\%$). Therefore, it could be used to maintain the cardiac function, and the heterogeneity among AMI with the PCI subgroup was reduced to 0%.

LVEDD and LVESD were also collected from the echocardiography data and were used to indicate cardiac functions. Among the included studies, five studies [20, 21, 23, 25, 35] reported LVEDD and three [23, 25, 35] reported LVESD. As shown in Figure 4, five studies demonstrated a high heterogeneity ($I^2 = 98\%$), and the subgroup meta-analysis was applied to identify the AMI patients with PCI [20, 25], the STEMI patients with PCI [23], the UA patients [21], and the AMI patients [35]. The results indicated that the combination of XFZYD with RT therapy could decrease LVEDD (MD −3.48, 95% CI −5.68 to −1.29; $P = 0.002$; $I^2 = 98\%$). The subgroup of AMI patients with PCI reduced the heterogeneity to 38% and resulted in a positive result. Following analysis of LVESD, the three studies included AMI patients with PCI [25], STEMI patients with PCI [23], and AMI patients [35], respectively. Therefore, they were not merged in the meta-analysis. Each of the three studies indicated a significant difference in improving LVESD following comparison of XFZYD plus RT with RT (26.19 ± 0.87 vs. 29.03 ± 2.05; 32.4 ± 3.3 vs. 39.5 ± 3.4; 27.96 ± 1.56 vs. 29.28 ± 1.38).

3.4.2. The Endothelial Functions. In total, four studies [25, 27, 31, 34] reported the serum levels of NO, and three of them included UA patients [27, 31, 34]. One study included AMI patients with PCI [25]. A meta-analysis with a random effects model was conducted in all four studies. The results indicated that the serum levels of NO were significantly increased following the comparison of XFZYD plus RT with RT (MD 12.57, 95% CI 2.95 to 22.19; $P = 0.01$; $I^2 = 95\%$). However, the heterogeneity was high and the subgroups were performed in the meta-analysis so as to reduce the heterogeneity to 0% as shown in Figure 5.

The serum levels of ET-1 were also related to the endothelial functions, and a total of five studies [25, 27, 29, 31, 34] reported this index. As shown in Figure 6, a meta-analysis in the random effects model was performed in the five studies. XFZYD plus RT significantly reduced the serum levels of ET-1 compared with those noted for RT (MD −30.93, 95% CI −56.59 to −5.27; $P = 0.02$; $I^2 = 99\%$). In the subgroup meta-analysis, the heterogeneity was still high ($I^2 = 85\%$) in the UA group [27, 31, 34] and the outcome was also stable.

In total, three studies [26, 31, 34] related to UA patients reported measurement of ICAM-1 and VCAM-1 levels in the serum. These studies were applied in the meta-analysis. The results are shown in Figures 7 and 8. XFZYD plus RT significantly reduced the serum levels of ICAM-1 compared with those of RT alone (MD −50.42, 95% CI −92.36 to -8.48; $P = 0.02$; $I^2 = 97\%$), while XFZYD plus RT did not significantly lower the serum levels of VCAM-1 compared with those of RT alone (MD −41.07, 95% CI −94.39 to 12.25; $P = 0.13$; $I^2 = 98\%$).

3.4.3. Assessment of CRP and Oxidative Damage Marker Levels. Three studies [30, 32, 33] reported the serum levels of CRP, and three studies [22, 23, 25] reported the determination of both SOD and MDA serum levels. One of the studies [32] indicated that XFZYD plus RT increased the serum levels of CRP compared with those of RT alone (30.88 ± 0.93 vs. 30.1 ± 0.86), which was opposite to the other two studies (3.21 ± 2.74 vs. 8.12 ± 4.39; 4.34 ± 0.95 vs. 4.91 ± 1.03) [30, 33]. In a meta-analysis (Figure 9), the levels of CRP exhibited no significant difference following comparison of XFZYD plus RT with RT (MD −1.35, 95% CI

Table 1: Characteristics of the included studies.

Study ID	Sample size (T/C)	Type of disease	Age (T/C)	Baseline	Interventions		Duration	Outcome measures
					Treatment group	Control group		
Lu (2020) [21]	43/40	UA	62.57 ± 8.42/ 63.39 ± 8.90	C	XFZYD + amiodarone	Amiodarone	4w	①②⑪
Zu (2020) [20]	38/38	AMI + PCI	59.68 ± 8.46/ 60.16 ± 8.26	C	XFZYD + RT	RT	8w	①②
Li (2019) [23]	46/45	STEMI + PCI	59.03 ± 3.62/ 58.19 ± 3.86	C	XFZYD + RT	RT	1w	①②③⑨⑩⑫
Wen (2019) [22]	52/52	AMI + PCI	60.30 ± 4.85/ 60.25 ± 4.87	C	XFZYD + RT	RT	4w	①⑨⑩⑫
Liu and Liu (2018) [24]	40/40	UA	NA/NA	C	XFZYD + RT	RT	4w	⑭
Li (2017) [26]	30/30	UA	57.9 ± 8.3/ 58.2 ± 8.5	C	XFZYD + RT	RT	2w	⑥⑦⑫⑬⑭
Wang (2017) [25]	53/53	AMI + PCI	57.36 ± 8.24/ 59.02 ± 9.78	C	XFZYD + RT	RT	2w	①②③④⑤⑨⑩⑫
Wang (2016) [27]	34/34	UA	NA/NA	C	XFZYD + RT	RT	8w	④⑤
Liu et al. (2013) [28]	30/30	AMI	NA/NA	C	XFZYD + RT	RT	2w	⑪
Zhang et al. (2012) [29]	30/30	AMI	61 ± 7/59 ± 8	C	XFZYD + RT	RT	2w	⑤
Jiang (2011) [30]	40/40	UA	NA/NA	C	XFZYD + RT	RT	4w	⑧
Guo (2009) [32]	25/24	UA	NA/NA	C	XFZYD + RT	RT	2w	⑧⑪
Zheng and Wang (2009) [31]	30/30	UA	64.8 ± 7.9/ 65.2 ± 7.4	C	XFZYD + RT	RT	8w	④⑤⑥⑦
Chen et al. (2008) [33]	42/42	USTEMI + UA	62.83 ± 10.14/ 64.83 ± 10.75	C	XFZYD + RT	RT	8w	⑧
Wang et al. (2006) [34]	32/18	UA	65.4 ± 7.6/ 65.3 ± 7.8	C	XFZYD + RT	RT	8w	④⑤⑥⑦
Tang et al. (2004) [35]	30/30	AMI	NA/NA	C	XFZYD + RT	RT	12w	①②③

① LVEF; ② LVEDD; ③ LVESD; ④ NO; ⑤ ET-1; ⑥ ICAM-1; ⑦ VCAM-1; ⑧ CRP; ⑨ SOD; ⑩ MDA; ⑪ BNP; ⑫ CK-MB; ⑬ cTnI; ⑭ ADRs. The numerical values of age are presented as mean value ± standard deviation in the treatment group (T) and the control group (C). Abbreviations: ADRs, adverse drug reactions; AMI, actue myocardial infarction; BNP, brain natriuretic peptide; C, consistent; CK-MB, creatine kinase-MB; CRP, C-reactive protein; cTnI, cardiac troponin I; ET-1, endothelin-1; ICAM-1, intercellular adhesion molecule-1; LVEF, left ventricular ejection fraction; LVEDD, left ventricular end-diastolic diameter; LVESD, left ventricular end-systolic diameter; MDA, malondialdehyde; NA, not available; NO, nitric oxide; NSTEMI, non-ST-segment elevation myocardial infarction; PCI, percutaneous coronary intervention; RT, routine treatment; SOD, superoxide dismutase; STEMI, ST-segment elevation myocardial infarction; T/C, treatment group/control group; UA, unstable angina; VCAM-1, vascular cell adhesion molecule-1; w, week; XFZYD, Xue-Fu-Zhu-Yu decoction.

−3.24 to 0.53; $P = 0.16$; $I^2 = 96\%$). Moreover, a meta-analysis was conducted to assess the changes in the levels of SOD and MDA (Figures 10 and 11). The results indicated that XFZYD plus RT caused a significant increase in SOD levels (MD 19.31, 95% CI 15.96 to 22.66; $P < 0.00001$; $I^2 = 0\%$), and they also decreased MDA levels (MD −1.61, 95% CI −1.90 to

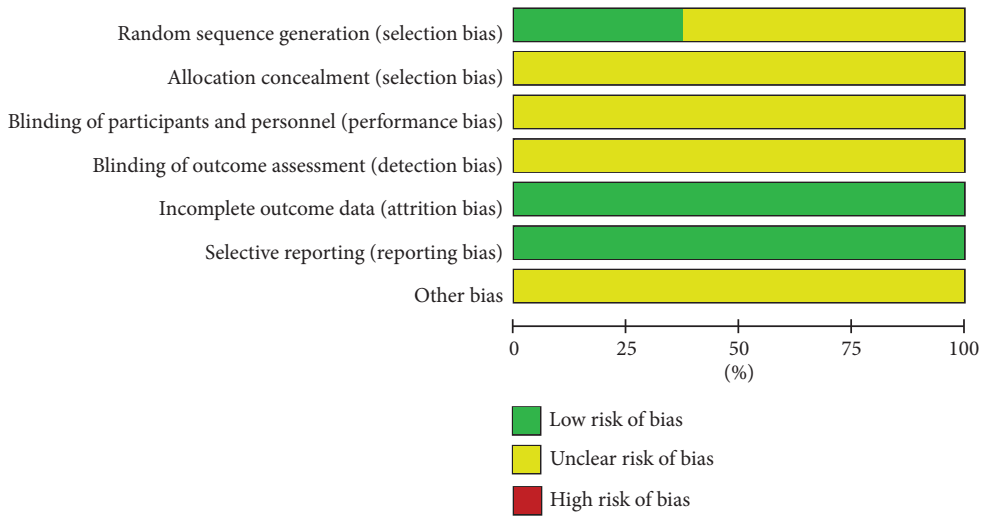

Figure 2: Risk of bias graph.

Study or Subgroup	Experimental Mean	Experimental SD	Experimental Total	Control Mean	Control SD	Control Total	Weight (%)	Mean Difference IV, Random, 95% CI
1.1.1 AMI+PCI								
Wang 2017	70.21	8.32	53	65.49	7.91	53	17.5	4.72 [1.63, 7.81]
Wen 2019	70.36	7.14	52	65.26	5.47	52	20.2	5.10 [2.66, 7.54]
Zu 2020	70.26	7.95	38	65.37	6.87	38	16.5	4.89 [1.55, 8.23]
Subtotal (95% CI)			143			143	54.3	4.94 [3.28, 6.60]
Heterogeneity: Tau^2 = 0.00; Chi^2 = 0.04, df = 2 (P = 0.98); I^2 = 0%								
Test for overall effect: Z = 5.82 (P < 0.00001)								
1.1.2 STEMI+PCI								
Li 2019	71.03	9.36	46	65.24	5.19	45	17.5	5.79 [2.69, 8.89]
Subtotal (95% CI)			46			45	17.5	5.79 [2.69, 8.89]
Heterogeneity: Not applicable								
Test for overall effect: Z = 3.66 (P = 0.0003)								
1.1.3 UA								
Lu 2020	49.72	7.65	43	43.68	8.26	40	16.1	6.04 [2.61, 9.47]
Subtotal (95% CI)			43			40	16.1	6.04 [2.61, 9.47]
Heterogeneity: Not applicable								
Test for overall effect: Z = 3.45 (P = 0.0006)								
1.1.4 AMI								
Tang et al. 2004	56.1	10.1	30	42.1	8	30	12.1	14.00 [9.39, 18.61]
Subtotal (95% CI)			30			30	12.1	14.00 [9.39, 18.61]
Heterogeneity: Not applicable								
Test for overall effect: Z = 5.95 (P < 0.00001)								
Total (95% CI)			*262*			*258*	*100.0*	*6.35 [4.20, 8.50]*
Heterogeneity: Tau^2 = 4.39; Chi^2 =13.18, df = 5 (P = 0.02); I^2 = 62%								
Test for overall effect: Z = 5.79 (P < 0.00001)								
Test for subgroup differences: Chi^2 = 13.15, df = 3 (P = 0.004), I^2 = 77.2%								

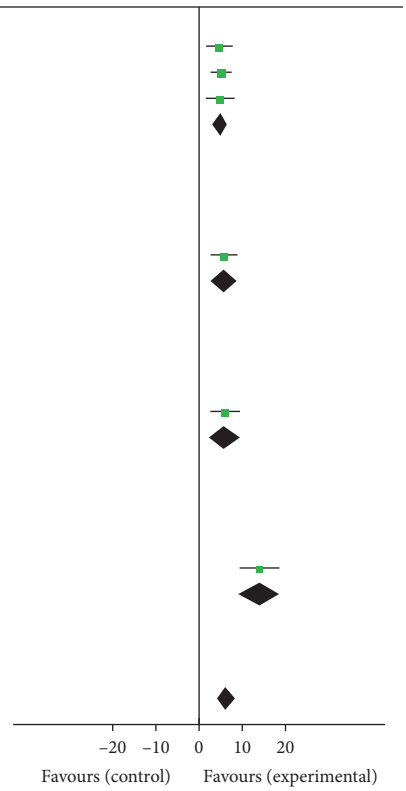

Figure 3: The LVEF of the included studies.

−1.33; $P < 0.00001$; $I^2 = 0\%$) compared with the effects noted following treatment with RT alone. The heterogeneity noted was very low.

3.4.4. The Blood Levels of BNP. Three studies [21, 28, 32] reported the blood levels of BNP. As shown in Figure 12, the levels of BNP were significantly different compared with those of RT alone (MD −49.43, 95% CI −71.18 to −27.68; $P < 0.00001$; $I^2 = 99\%$). The subgroups were performed due to the high heterogeneity, and the heterogeneity of the UA group [21, 32] was reduced to 78%.

3.4.5. Myocardial Enzymes. In total, four studies [22, 23, 25, 26] reported the assessment of CK-MB as a

Study or Subgroup	Experimental Mean	Experimental SD	Experimental Total	Control Mean	Control SD	Control Total	Weight (%)	Mean Difference IV, Random, 95% CI
1.2.1 AMI+PCI								
Wang 2017	45.26	1.08	53	46.18	1.26	53	21.2	-0.92 [-1.37, -0.47]
Zu 2020	45.04	1.03	38	46.39	1.15	38	21.2	-1.35 [-1.84, −0.86]
Subtotal (95% CI)			91			91	42.4	-1.12 [-1.54, -0.70]
Heterogeneity: Tau^2 = 0.04; Chi^2 = 1.61, df = 1 (P = 0.20); I^2 = 38%								
Test for overall effect: Z = 5.23 (P < 0.00001)								
1.2.2 STEMI+PCI								
Li 2019	40.03	0.48	46	45.02	1.25	45	21.3	-4.99 [-5.38, -4.60]
Subtotal (95% CI)			46			45	21.3	-4.99 [-5.38, -4.60]
Heterogeneity: Not applicable								
Test for overall effect: Z = 25.03 (P < 0.00001)								
1.2.3 UA								
Lu 2020	53.37	4.51	43	56.21	5.58	40	17.6	-2.84 [-5.03, -0.65]
Subtotal (95% CI)			43			40	17.6	-2.84 [-5.03, -0.65]
Heterogeneity: Not applicable								
Test for overall effect: Z = 2.54 (P < 0.01)								
1.1.4 AMI								
Tang et al. 2004	47.2	3.6	30	54.9	3.5	30	18.7	-7.70 [-9.50, -5.90]
Subtotal (95% CI)			30			30	18.7	-7.70 [−9.50, -5.90]
Heterogeneity: Not applicable								
Test for overall effect: Z = 8.40 (P < 0.00001)								
Total (95% CI)			*210*			*206*	*100.0*	*-3.48 [-5.68, -1.29]*
Heterogeneity: Tau^2 = 5.86; Chi^2 = 250.78, df = 4 (P < 0.00001); I^2 = 98%								
Test for overall effect: Z = 3.11 (P = 0.002)								
Test for subgroup differences: Chi^2 = 198.02, df = 3 (P < 0.00001), I^2 = 98.5%								

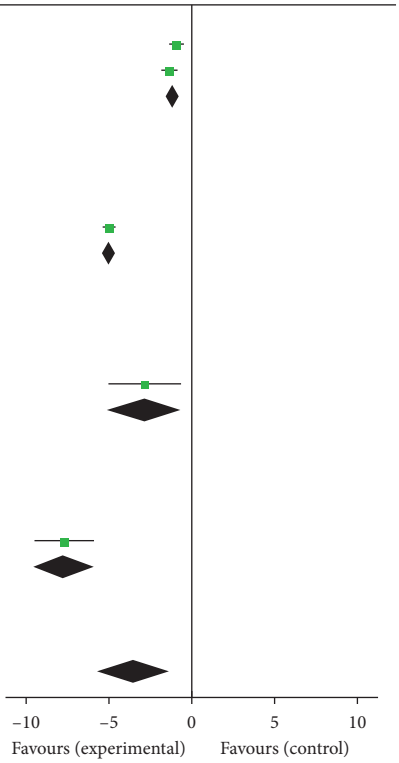

Figure 4: The LVEDD of the included studies.

Study or Subgroup	Experimental Mean	Experimental SD	Experimental Total	Control Mean	Control SD	Control Total	Weight (%)	Mean Difference IV, Random, 95% CI
2.1.1 UA								
Wang 2016	78.36	12.81	34	61.13	16.25	34	23.6	17.23 [10.27, 24.19]
Wang et al. 2006	67.7	11.3	32	52.6	8.9	18	24.6	15.10 [9.42, 20.78]
Zheng and Wang 2009	72.5	12.4	30	55.9	8.4	30	24.9	16.60 [11.24, 21.96]
Subtotal (95% CI)			96			82	73.1	16.21 [12.81, 19.61]
Heterogeneity: Tau^2 = 0.00; Chi^2 = 0.25, df = 2 (P = 0.88); I^2 = 0%								
Test for overall effect: Z = 9.35 (P < 0.00001)								
2.1.2 AMI+PCI								
Wang 2017	8.73	1.68	53	6.29	1.75	53	26.9	2.44 [1.79, 3.09]
Subtotal (95% CI)			53			53	26.9	2.44 [1.79, 3.09]
Heterogeneity: Not applicable								
Test for overall effect: Z = 7.32 (P < 0.00001)								
Total (95% CI)			*149*			*135*	*100.0*	*12.57 [2.95, 22.19]*
Heterogeneity: Tau^2 = 89.48; Chi^2 = 61.04, df = 3 (P < 0.00001); I^2 = 95%								
Test for overall effect: Z = 2.56 (P = 0.01)								
Test for subgroup differences: Chi^2 = 60.79, df = 1 (P < 0.00001), I^2 = 98.4%								

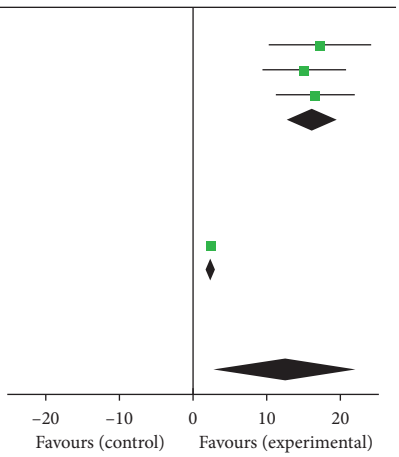

Figure 5: The serum NO levels of the included studies.

cardiac marker, and two of them [22, 25] included AMI patients with PCI, whereas one study [26] included UA patients, and one [23] STEMI patients with PCI. A total of four studies were involved in a meta-analysis (Figure 13). The results indicated that XFZYD plus RT significantly decreased the levels of CK-MB compared with those noted following RT treatment alone (MD −10.08, 95% CI −14.01 to −6.15; $P < 0.00001$; $I^2 = 96\%$). Due to the high heterogeneity, the subgroups of AMI plus PCI, UA, and STEMI plus PCI were used. The heterogeneity in the AMI plus PCI subgroup was very low ($I^2 = 0\%$). One study [26] reported on the changes in the levels of cTnI between the XFZYD plus RT

Study or Subgroup	Experimental Mean	Experimental SD	Experimental Total	Control Mean	Control SD	Control Total	Weight (%)	Mean Difference IV, Random, 95% CI
2.2.1 UA								
Wang 2016	62.48	19.57	34	73.64	25.49	34	19.7	-11.16 [-21.96, -0.36]
Wang et al. 2006	78.5	12.5	32	113	11.8	18	20.1	-34.50 [-41.46, -27.54]
Zheng and Wang 2009	77.9	12	30	100.9	13.8	30	20.2	-23.00 [-29.54, -16.46]
Subtotal (95% CI)			96			82	60.0	-23.47 [-35.39, -11.55]
Heterogeneity: Tau^2 = 93.59; Chi^2 = 13.75, df = 2 (P = 0.001); I^2 = 85%								
Test for overall effect: Z = 3.86 (P = 0.0001)								
2.2.2 AMI								
Zhang et al. 2012	56.89	2.35	30	123.19	4.27	30	20.4	-66.30 [-68.04, -64.56]
Subtotal (95% CI)			30			30	20.4	-66.30 [-68.04, -64.56]
Heterogeneity: Not applicable								
Test for overall effect: Z = 74.51 (P < 0.00001)								
2.2.3 AMI+PCI								
Wang 2017	116.23	32.79	53	134.67	30.81	53	19.5	-18.44 [-30.55, -6.33]
Subtotal (95% CI)			53			53	19.5	-18.44 [-30.55, -6.33]
Heterogeneity: Not applicable								
Test for overall effect: Z = 2.98 (P = 0.003)								
Total (95% CI)			*179*			*165*	*100.0*	*-30.93 [-56.59, -5.27]*
Heterogeneity: Tau^2 = 838.64; Chi^2 = 348.20, df = 4 (P < 0.00001); I^2 = 99%								
Test for overall effect: Z = 2.36 (P = 0.02)								
Test for subgroup differences: Chi^2 = 105.13, df = 2 (P < 0.00001), I^2 = 98.1%								

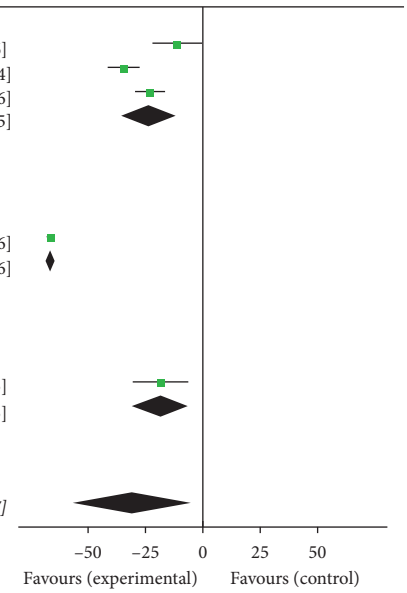

Figure 6: The serum ET-1 levels of the included studies.

Study or Subgroup	Experimental Mean	Experimental SD	Experimental Total	Control Mean	Control SD	Control Total	Weight (%)	Mean Difference IV, Random, 95% CI
Li 2017	174.82	7.55	30	194.12	7.06	30	34.9	-19.30 [-23.00, -15.60]
Wang et al. 2006	270.9	40.3	32	326.7	39.1	18	31.7	-55.80 [-78.63, -32.97]
Zheng and Wang 2009	198.9	30.7	30	276.8	32.1	30	33.3	-77.90 [-93.79, -62.01]
Total (95% CI)			*92*			*78*	*100.0*	*-50.42 [-92.36, -8.48]*
Heterogeneity: Tau^2 = 1307.28; Chi^2 = 57.60, df = 2 (P < 0.00001); I^2 = 97%								
Test for overall effect: Z = 2.36 (P = 0.02)								

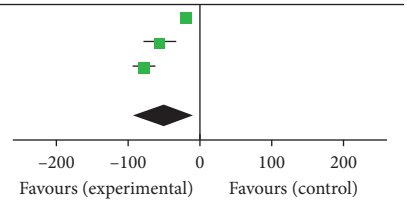

Figure 7: Assessment of the serum levels of ICAM-1 in the included studies.

Study or Subgroup	Experimental Mean	Experimental SD	Experimental Total	Control Mean	Control SD	Control Total	Weight (%)	Mean Difference IV, Random, 95% CI
Li 2017	321.1	5.12	30	333.91	4.69	30	34.3	-12.81 [-15.29, -10.33]
Wang et al. 2006	421.3	39.1	32	438.3	39.9	18	32.3	-17.00 [-39.88, 5.88]
Zheng and Wang 2009	358.4	30.6	30	451.9	32.4	30	33.3	-93.50 [-109.45, -77.55]
Total (95% CI)			*92*			*78*	*100.0*	*-41.07 [-94.39, 12.25]*
Heterogeneity: Tau^2 = 2153.57; Chi^2 = 96.05, df = 2 (P < 0.00001); I^2 = 98%								
Test for overall effect: Z = 1.51 (P = 0.13)								

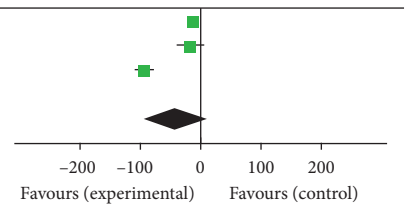

Figure 8: Assessment of the serum levels of VCAM-1 in the included studies.

and the RT groups. The results indicated that the XFZYD plus RT group performed better than the RT group alone (0.099 ± 0.019 vs. 0.106 ± 0.038, $P < 0.05$).

3.4.6. ADRs. Two studies [24, 26] on UA reported ADRs in the treatment or control groups. One study [24] reported three mild diarrhea cases in the XFZYD plus RT group and two sinus bradycardia cases in the RT group. The symptoms disappeared following simple symptomatic treatments or the absence of therapies. Another study [26] reported two cases of elevated aminotransferase levels in the control group, whereas no ADRs were noted in the treatment group.

4. Discussion

In the present review, 16 studies of ACS were included, of which eight studies reported UA cases, three AMI, three AMI with PCI, one STEMI with PCI, and one NSTE-ACS (NSTEMI + UA). Among these studies, the combination of

Study or Subgroup	Experimental Mean	Experimental SD	Experimental Total	Control Mean	Control SD	Control Total	Weight (%)	Mean Difference IV, Random, 95% CI
3.1.1 UA								
Guo 2009	30.88	0.93	25	30.1	0.86	24	35.4	0.78 [0.28, 1.28]
Jiang 2011	4.34	0.95	40	4.91	1.03	40	35.6	-0.57 [-1.00, -0.14]
Subtotal (95% CI)			65			64	71.0	0.10 [-1.22, 1.42]
Heterogeneity: Tau^2 = 0.85; Chi^2 = 15.92, df = 1 (P < 0.0001); I^2 = 94%								
Test for overall effect: Z = 0.15 (P = 0.88)								
3.1.2 USTEMI+UAP								
Chen et al. 2008	3.21	2.74	42	8.12	4.39	42	29.0	-4.91 [-6.48, -3.34]
Subtotal (95% CI)			42			42	29.0	-4.91 [-6.48, -3.34]
Heterogeneity: Not applicable								
Test for overall effect: Z = 6.15 (P < 0.00001)								
Total (95% CI)			*107*			*106*	*100.0*	*-1.35 [-3.24, 0.53]*
Heterogeneity: Tau^2 = 2.55; Chi^2 = 52.26, df = 2 (P < 0.00001); I^2 = 96%								
Test for overall effect: Z = 1.41 (P = 0.16)								
Test for subgroup differences: Chi^2 = 22.95, df = 1 (P < 0.00001), I^2 = 95.6%								

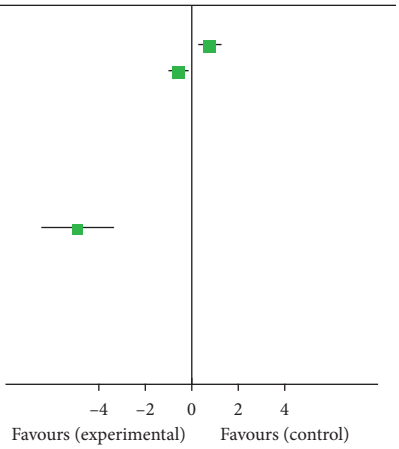

Figure 9: The serum CRP levels of the included studies.

Study or Subgroup	Experimental Mean	Experimental SD	Experimental Total	Control Mean	Control SD	Control Total	Weight (%)	Mean Difference IV, Random, 95% CI
Li 2019	179.42	27.68	46	153.72	21.35	45	10.9	25.70 [15.56, 35.84]
Wang 2017	174.82	14.25	53	156.43	13.83	53	39.3	18.39 [13.04, 23.74]
Wen 2019	174.65	13.02	52	156.02	11.68	52	49.7	18.63 [13.88, 23.38]
Total (95% CI)			*151*			*150*	*100.0*	*19.31 [15.96, 22.66]*
Heterogeneity: Tau^2 = 0.00; Chi^2 = 1.72, df = 2 (P = 0.42); I^2 = 0%								
Test for overall effect: Z = 1.51 (P < 0.00001)								

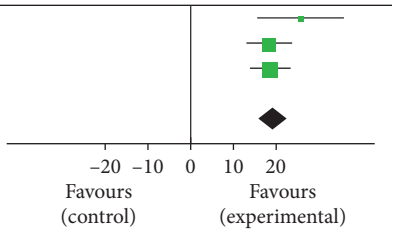

Figure 10: The serum SOD levels of the included studies.

XFZYD with RT exhibited the potential to improve cardiac and endothelial functions in ACS. The possible mechanisms of the effectiveness of this decoction are discussed below.

LVEF is positively related to the contractility of the myocardium; LVEDD and LVESD represent the diastolic and systolic functions of the left ventricle, respectively [36]. BNP is a quantitative marker of heart failure; CK-MB and cTnI are two sensitive indicators of myocardial damage [37]. The echocardiography results indicated the improvement of cardiac function, and XFZYD aided the amelioration of the levels of LVEF, LVEDD, and LVESD. In addition to these functions, XFZYD has been shown to decrease the blood levels of BNP and the myocardial enzymes (CK-MB and cTnI), representing cardioprotective effects. The cardioprotective function of XFZYD has been verified in various experimental studies. In the rat model of myocardial ischemia-reperfusion injury (MI/RI), XFZYD protected the myocardial ultrastructure [38]. Pretreatment with XFZYD demonstrated protective effects in the myocardial tissues of LPS-induced septic rats by inhibiting cardiomyocyte apoptosis and oxidative stress [39]. XFZYD demonstrated inhibition of myocardial apoptosis by increasing the expression of SIRT1 and inhibiting the expression levels of its downstream proteins p53 and NF-κB in a model of H9c2 rat myocardial cells with oxygen-glucose deprivation [40]. XFZYD was also shown to protect myocardial ischemia rats via the SIRT1-mediated signal transduction pathway [41]. The main components of XFZYD exhibited profound cardioprotective effects [10]. For example, hydroxysafflor yellow A reduced MI/RI injury, suppressed calcium overload in cardiomyocytes, and prevented the induction of their apoptosis [42]. Moreover, chlorogenic acid inhibited activation of the NF-κB and JNK pathways in cardiomyocytes [43].

Endothelial dysfunction is accompanied by the rupture of vulnerable plaques and leads to platelet aggregation and leukocyte adherence [4]. The prominent vasoactive substance NO, released by the endothelium, helps mediate the vasodilation as well as regulates adhesion of leukocytes. NO can be regarded as a protector of cardiovascular endothelial function and vascular inflammation [44]. Endothelial function is also measured by the decreased ET-1 production, which is characterized as a vasoconstrictor [44, 45]. ICAM-1 and VCAM-1 are adhesion molecules. Their expression levels are increased as a result of facilitating leukocyte adhesion and transmigration inside the endothelium, which lead to further inflammatory expansion [46]. Serum CRP levels are also widely regarded as an indicator of inflammation. According to the results, XFZYD can significantly

Study or Subgroup	Experimental Mean	Experimental SD	Experimental Total	Control Mean	Control SD	Control Total	Weight (%)	Mean Difference IV, Random, 95% CI
Li 2019	3.21	0.56	46	4.79	0.92	45	81.9	-1.58 [-1.89, -1.27]
Wang 2017	3.14	2.83	53	4.93	2.91	53	6.8	-1.79 [-2.88, -0.70]
Wen 2019	3.1	1.89	52	4.83	2.46	52	11.3	-1.73 [-2.57, 0.89]
Total (95% CI)			*151*			*150*	*100.0*	*-1.61 [-1.90, -1.33]*

Heterogeneity: Tau^2 = 0.00; Chi^2 = 0.22, df = 2 (P = 0.90); I^2 = 0%
Test for overall effect: Z = 11.12 (P < 0.00001)

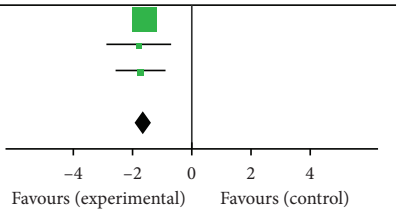

Figure 11: The serum MDA levels of the included studies.

Study or Subgroup	Experimental Mean	Experimental SD	Experimental Total	Control Mean	Control SD	Control Total	Weight (%)	Mean Difference IV, Random, 95% CI
4.1.1 UA								
Guo 2009	275	63	25	284	62	24	19.7	-9.00 [-44.00, 26.00]
Lu 2020	75.58	6.42	43	122.78	8.43	40	40.0	-47.20 [-50.44, -43.96]
Subtotal (95% CI)			68			64	59.7	-32.24 [-68.78, 4.31]
Heterogeneity: Tau^2 = 568.79; Chi^2 = 4.54, df = 1 (P = 0.03); I^2 = 78%								
Test for overall effect: Z = 1.73 (P = 0.008)								
4.1.2 AMI								
Liu et al. 2013	76.89	2.35	30	148.33	2.28	30	40.3	-71.44 [-72.61, -70.27]
Subtotal (95% CI)			30			30	40.3	-71.44 [-72.61, -70.27]
Heterogeneity: Not applicable								
Test for overall effect: Z = 119.51 (P < 0.00001)								
Total (95% CI)			*98*			*94*	*100.0*	*-49.43 [-71.18, -27.68]*

Heterogeneity: Tau^2 = 305.27; Chi^2 = 201.14, df = 2 (P < 0.00001); I^2 = 99%
Test for overall effect: Z = 4.45 (P < 0.00001)
Test for subgroup differences: Chi^2 = 4.42, df = 1 (P = 0.04), I^2 = 77.4%

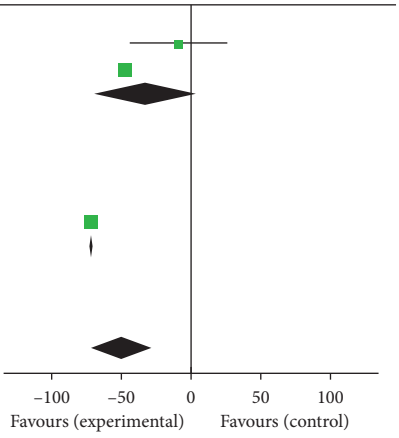

Figure 12: The blood levels of BNP in the included studies.

Study or Subgroup	Experimental Mean	Experimental SD	Experimental Total	Control Mean	Control SD	Control Total	Weight (%)	Mean Difference IV, Random, 95% CI
5.1.1 AMI+PCI								
Wang 2017	29.82	5.37	53	42.71	7.14	53	24.3	-12.89 [-15.30, -10.48]
Wen 2019	28.42	7.51	52	39.64	8.11	52	23.1	-11.22 [-14.22, -8.22]
Subtotal (95% CI)			105			105	47.5	-12.24 [-14.12, -10.36]
Heterogeneity: Tau^2 = 0.00; Chi^2 = 0.72, df = 1 (P = 0.40); I^2 = 0%								
Test for overall effect: Z = 12.77 (P < 0.00001)								
5.1.2 UA								
Li 2017	48.14	2.07	30	53.46	1.944	30	26.3	-5.32 [-6.34, -4.30]
Subtotal (95% CI)			30			30	26.3	-5.32 [-6.34, -4.30]
Heterogeneity: Not applicable								
Test for overall effect: Z = 10.27 (P < 0.00001)								
5.1.3 STEMI+PCI								
Li 2019	30.06	1.73	46	41.3	3.15	45	26.3	-11.24 [-12.29, -10.19]
Subtotal (95% CI)			46			45	26.3	-11.24 [-12.29, -10.19]
Heterogeneity: Not applicable								
Test for overall effect: Z = 21.03 (P < 0.00001)								
Total (95% CI)			*181*			*180*	*100.0*	*-10.08 [-14.01, -6.15]*

Heterogeneity: Tau^2 = 15.01; Chi^2 = 79.53, df = 3 (P < 0.00001); I^2 = 96%
Test for overall effect: Z = 5.03 (P < 0.00001)
Test for subgroup differences: Chi^2 = 78.81, df = 2 (P < 0.00001), I^2 = 97.5%

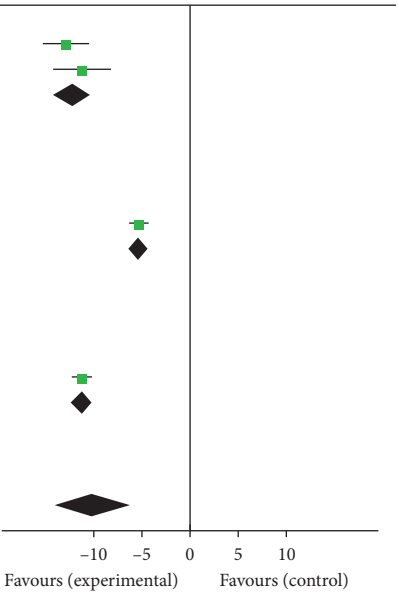

Figure 13: The blood levels of CK-MB in the included studies.

increase the serum levels of NO, and reduce serum ET-1 and ICAM-1 levels, indicating the protective effects on vascular endothelial function. However, XFZYD may not decrease serum VCAM-1 and CRP levels, which may be associated with the sample size of the included study. Therefore, additional research studies are required in the future. The systemic pharmacology of XFZYD in the prevention of atherosclerotic cardiovascular disease (ASCVD) has shown that the mechanism of XFZYD is mainly reflected in the protection of vascular endothelium, prevention of oxidative stress, and inhibition of inflammation; the effective component quercetin was also shown to protect injured endothelial cells and reduce the endothelial inflammatory response (ICAM-1, VCAM-1, and TNF-α) induced by LPS *in vitro* [47]. XFZYD has been shown to protect from ischemic necrosis, induce the migration of endothelial progenitor cells, and promote angiogenesis by improving the serum levels of NO [48]. Following XFZYD treatment, the serum levels of ET-1 were decreased and NO levels were released in MI/RI swine [49]. XFZYD can restrain inflammation, platelet aggregation, and help protect reendothelialization after PCI. The indicators reported both from clinical and experimental studies that have shown the efficacy of XFZYD in ASCVD.

SOD is an antioxidant metal enzyme that can catalyze the disproportionation of superoxide anion radicals to produce oxygen and hydrogen peroxide [50]. It plays a vital role in maintaining the balance required (pro-oxidants/antioxidants) to prevent the induction of oxidative stress in the body [50]. In several organisms, free radicals bind to lipids to induce their peroxidation, which results in the production of MDA. The latter can reflect the degree of lipid peroxidation in the body and indirectly reflect the degree of cell damage [51]. Higher SOD and lower MDA levels play inhibitory roles against the development of ACS. The results indicated that XFZYD could upregulate the serum levels of SOD and downregulate the serum levels of MDA, reducing serum oxidative stress levels and improving the function of the endothelial microenvironment. Previous studies have also shown that XFZYD plays an antioxidant role by reducing serum MDA levels and increasing serum SOD levels in CHD patients undergoing PCI surgery [52].

Endothelial dysfunction, oxidative stress, abnormal vasoconstriction, and dilation are crucial in the pathogenesis of atherosclerosis and ACS [53, 54]. XFZYD can improve cardiac function by increasing blood supply to myocardium and can ameliorate coronary microcirculation by improving endothelial function. Future studies can focus on these mechanisms for ACS to uncover more potential drug targets and long-term effects of this formula. Based on these results, the practical applications of XFZYD with conventional therapy can be used in ACS patients as soon as possible.

The limitations of this systematic review can be summarized in the following three aspects: First of all, the number of studies included in the meta-analysis was considerably small, and only six studies were involved in the meta-analysis of the primary outcome (LVEF), which could not be used for analyzing the publication bias. Moreover, the heterogeneity among all the ACS subtypes was too high in the meta-analysis. Therefore, subgroup analysis was conducted according to the ACS subtypes of STEMI, USTEMI, and UA, with or without PCI. Lower heterogeneity was detected, whereas a smaller number of studies were involved in the subgroup analysis, which may lead to unstable results. Finally, almost all the included studies were published in Chinese, while only one was published in English, and none of them reported the allocation concealment and blinding method, which augmented the risk of bias in RCTs.

5. Conclusions

In summary, the present analysis demonstrated that XFZYD can be used as a representative Chinese prescription, which may possess significant clinical applications for improving cardiac and endothelial functions and the LVEF, LVEDD, LVESD, NO, ET-1, and ICAM-1 of ACS patients when combined with RT. Moreover, it may also ameliorate the levels of oxidative stress (SOD and MDA), BNP, CK-MB, and cTnI. No serious ADRs were noted. However, XFZYD may not improve the blood levels of VCAM-1 and CRP. On the basis of these results, we prefer to confirm the amelioration of cardiac and endothelial functions of XFZYD in ACS. However, considering the mediocre methodological quality and a small number of included studies, it is deduced that multicenter, large-scale, and strictly designed trials are required to confirm these findings. This systematic review has provided evidence for the clinical efficacy of XFZYD combined with RT in treating patients with ACS.

Abbreviations

ACS: Acute coronary syndrome
ADRs: Adverse drug reactions
AMI: Actue myocardial infarction
ASCVD: Atherosclerotic cardiovascular disease
BNP: Brain natriuretic peptide
CK-MB: Creatine kinase-MB
CHD: Coronary heart disease
CI: Confidence interval
CRP: C-reactive protein
cTnI: Cardiac troponin I
ECG: Electrocardiogram
ET-1: Endothelin-1
ICAM-1: Intercellular adhesion molecule-1
ICD-10: International classification of diseases10th revision
LVEF: Left ventricular ejection fraction
LVEDD: Left ventricular end-diastolic diameter
LVESD: Left ventricular end-systolic diameter
MDA: Malondialdehyde
MI: Myocardial infarction
MI/RI: Myocardial ischemia-reperfusion injury
NO: Nitric oxide
NSTEMI: Non-ST-segment elevation myocardial infarction
PCI: Percutaneous coronary intervention
RCTs: Randomized controlled trials
RT: Routine treatment
SMD: Standardized mean difference

SOD: Superoxide dismutase
STEMI: ST-segment elevation myocardial infarction
TCM: Traditional Chinese medicine
UA: Unstable angina
VCAM-1: Vascular cell adhesion molecule-1
WMD: Weighted mean difference
XFZYD: Xue-Fu-Zhu-Yu decoction.

Data Availability

All the data generated or analyzed during this study are included in this published article and its additional files.

Disclosure

Shiqi Chen, Xiaoxiao Wu, and Tong Li are cofirst authors. Mingjing Zhao and Yahong Wang are the corresponding authors.

Conflicts of Interest

The authors declare that there are no conflicts of interest regarding the publication of this article.

Authors' Contributions

YHW and MJZ designed the research and supervised the whole process. SQC and TL conducted the literature searching and selection. XXW and WTC extracted and analyzed the outcomes. XWH and YL assessed the risk of bias. SQC drafted the manuscript with the help of BFW and YT. MJZ and YHW detected any mistakes in the entire process. All authors have approved the final manuscript for submission.

Acknowledgments

This work was supported by the National Natural Science Foundation Project of China (81774127) and the 2020 Science and Technology Innovation Project of Dongzhimen Hospital (DZMKJCX-2020-012).

Supplementary Materials

Table S1: other characteristics of the included studies. (*Supplementary Materials*)

References

[1] T. K. M. Wang, C. Grey, Y. Jiang, R. T. Jackson, and A. J. Kerr, "Nationwide trends in acute coronary syndrome by subtype in New Zealand 2006-2016," *Heart (British Cardiac Society)*, vol. 106, no. 3, pp. 221–227, 2020.

[2] E. J. Benjamin, M. J. Blaha, S. E. Chiuve et al., "Heart disease and stroke statistics-2017 update: a report from the American heart association," *Circulation*, vol. 135, no. 10, pp. e146–e603, 2017.

[3] J. C. Trost and R. A. Lange, "Treatment of acute coronary syndrome: Part 1: non-ST-segment acute coronary syndrome," *Critical Care Medicine*, vol. 39, no. 10, pp. 2346–2353, 2011.

[4] F. Crea and P. Libby, "Acute coronary syndromes: the way forward from mechanisms to precision treatment," *Circulation*, vol. 136, no. 12, pp. 1155–1166, 2017.

[5] L. Esposito, F. P. Cancro, A. Silverio et al., "COVID-19 and acute coronary syndromes: from pathophysiology to clinical perspectives," *Oxidative Medicine and Cellular Longevity*, vol. 2021, Article ID 4936571, 13 pages, 2021.

[6] K. P. Kline, C. R. Conti, and D. E. Winchester, "Historical perspective and contemporary management of acute coronary syndromes: from MONA to THROMBINS2," *Postgraduate Medicine*, vol. 127, no. 8, pp. 855–862, 2015.

[7] P. G. Steg, K. Huber, F. Andreotti et al., "Bleeding in acute coronary syndromes and percutaneous coronary interventions: position paper by the working group on thrombosis of the European society of cardiology," *European Heart Journal*, vol. 32, no. 15, pp. 1854–1864, 2011.

[8] K. K. R. Mangalpally and N. S. Kleiman, "The safety of clopidogrel," *Expert Opinion on Drug Safety*, vol. 10, no. 1, pp. 85–95, 2011.

[9] J. G. Córdoba-Soriano, M. Corbí-Pascual, I. López-Neyra et al., "Early aspirin desensitization in unstable patients with acute coronary syndrome: short and long-term efficacy and safety," *European Heart Journal: Acute Cardiovascular Care*, vol. 5, no. 7, pp. 41–50, 2016.

[10] C. Fu, Z. Xia, Y. Liu et al., "Qualitative analysis of major constituents from Xue Fu Zhu Yu decoction using ultra high performance liquid chromatography with hybrid ion trap time-of-flight mass spectrometry," *Journal of Separation Science*, vol. 39, no. 17, pp. 3457–3468, 2016.

[11] X.-J. Xiong, Z. Wang, and J. Wang, "Innovative strategy in treating angina pectoris with Chinese patent medicines by promoting blood circulation and removing blood stasis: experience from combination therapy in Chinese medicine," *Current Vascular Pharmacology*, vol. 13, no. 4, pp. 540–553, 2015.

[12] J. Wang, X. Yang, F. Chu et al., "The effects of Xuefu Zhuyu and shengmai on the evolution of syndromes and inflammatory markers in patients with unstable angina pectoris after percutaneous coronary intervention: a randomised controlled clinical trial," *Evidence-based Complementary and Alternative Medicine*, vol. 2013, Article ID 896467, 9 pages, 2013.

[13] G. Z. Yi, Y. Q. Qiu, Y. Xiao, and L. X. Yuan, "The usefulness of Xuefu Zhuyu tang for patients with angina pectoris: a meta-analysis and systematic review," *Evidence-Based Complementary and Alternative Medicine*, vol. 2014, Article ID 521602, 11 pages, 2014.

[14] D. Wang, P. Wang, R. Zhang, and X. Xi, "Efficacy and safety of Xuefu Zhuyu decoction combined with Western medicine for angina pectoris in coronary heart disease: a protocol for systematic review and meta-analysis," *Medicine (Baltimore)*, vol. 99, no. 50, Article ID e23195, 2020.

[15] F. Y. Chu, J. Wang, K. W. Yao, and Z. Z. Li, "Effect of Xuefu Zhuyu capsule on the symptoms and signs and health-related quality of life in the unstable angina patients with blood-stasis syndrome after percutaneous coronary intervention: a randomized controlled trial," *Chinese Journal of Integrative Medicine*, vol. 16, no. 5, pp. 399–405, 2010.

[16] P. T. O'Gara, F. G. Kushner, D. D. Ascheim et al., "2013 ACCF/AHA guideline for the management of ST-elevation myocardial infarction: a report of the american college of cardiology foundation/american heart association task force

on practice guidelines," *Journal of the American College of Cardiology*, vol. 61, no. 4, pp. e78–e140, 2013.

[17] H. Jneid, J. L. Anderson, R. S. Wright et al., "2012 ACCF/AHA focused update of the guideline for the management of patients with unstable angina/non-ST-elevation myocardial infarction (updating the 2007 guideline and replacing the 2011 focused update): a report of the american college of cardiology foundation/american heart association task force on practice guidelines," *Journal of the American College of Cardiology*, vol. 60, no. 7, pp. 645–681, 2012.

[18] M. M. Mafham, E. Spata, R. Goldacre et al., "COVID-19 pandemic and admission rates for and management of acute coronary syndromes in England," *The Lancet*, vol. 396, no. 10248, pp. 381–389, 2020.

[19] C. Andrade, "Mean difference, standardized mean difference (SMD), and their use in meta-analysis: as simple as it gets," *Journal of Clinical Psychiatry*, vol. 81, no. 5, 2020.

[20] X. H. Zu, "Observation on the effect of Xuefu Zhuyu decoction combined with double antiplatelet drugs after percutaneous coronary intervention in acute myocardial infarction," *Journal of Practical Traditional Chinese Medicine*, vol. 36, no. 01, pp. 49-50, 2020.

[21] C. J. Lu, "Effects of Xuefu Zhuyu decoction combined with amiodarone on unstable angina pectoris," *Shenzhen Journal of Integrated Traditional Chinese and Western Medicine*, vol. 30, no. 19, pp. 36-37, 2020.

[22] H. X. Wen, "Application of Xuefu Zhuyu decoction in myocardial infarction after percutaneous coronary intervention," *Chinese Journal of Ethnomedicine and Ethnopharmacy*, vol. 28, no. 05, pp. 97–99, 2019.

[23] G. W. Li, "Effects of Xuefu Zhuyu decoction on myocardial enzymes and cardiac function in patients with myocardial ischemia-reperfusion injury after acute myocardial infarction," *Jounal of Medical Therapy and Practice*, vol. 32, no. 23, pp. 3804-3805, 2019.

[24] P. Liu and L. Liu, "Effects of Xuefu Zhuyu granule combined with metoprolol on unstable angina pectoris in young and middle-aged people," *Chinese Journal of Integrative Medicine on Cardio-/Cerebrovascuiar Disease*, vol. 16, no. 19, pp. 2845–2847, 2018.

[25] N. Wang, "Effect of Xuefu Zhuyu decoction on myocardial reperfusion and cardiac function in patients with myocardial infarction after percutaneous coronary intervention," *Modern Journal of Integrated Traditional Chinese and Western Medicine*, vol. 26, no. 01, pp. 73–75, 2017.

[26] G. S. Li, "Effect of Xuefu Zhuyu decoction on adhesion molecules in patients with unstable angina pectoris," *Neimenggu Traditional Chinese Medicine*, vol. 36, no. 19, pp. 4-5, 2017.

[27] J. W. Wang, "Clinical effect analysis of Xuefu Zhuyu decoction on unstable angina pectoris," *Contemporary Medical Symposium*, vol. 14, no. 19, pp. 60-61, 2016.

[28] Y. F. Liu, X. H. Han, Y. H. Zhang, M. Chen, H. F. Zhou, and J. Y. Liu, "Xuefu Zhuyu decoction for acute myocardial infarction and its effects on erythrocyte immune function and B-type natriuretic peptide," *Journal of Clinical Research*, vol. 30, no. 10, pp. 2070-2071, 2013.

[29] Y. H. Zhang, Y. F. Liu, and M. Chen, "Effect of Xuefu Zhuyu decoction on acute myocardial infarction and endothelin of erythrocyte immune function," *Chinese Journal of Practical Internal Medicine*, vol. 32, no. S2, pp. 26-27, 2012.

[30] W. J. Jiang, "Clinical observation of Xuefu Zhuyu capsule in treating unstable angina pectoris," *Journal of New Chinese Medicine*, vol. 43, no. 01, pp. 15–17, 2011.

[31] G. L. Zheng and S. H. Wang, "Clinical effect and mechanism of Xuefu Zhuyu capsule in treating unstable Angina pectoris," *Chinese Journal of Integrated Traditional and Western Medicine*, vol. 29, no. 01, pp. 65–68, 2009.

[32] H. Guo, "Effects of Xuefu Zhuyu capsule on CRP and BNP in patients with unstable angina pectoris," *Tianjin Journal of Traditional Chinese Medicine*, vol. 26, no. 03, pp. 209-210, 2009.

[33] N. T. Chen, H. Chen, H. Y. Zhu, Q. Zhao, J. Liu, and D. F. Zhang, "Clinical study of Xuefu Zhuyu decoction on 42 cases of acute coronary syndrome with non-ST segment elevation," *Journal of Hubei College of Traditional Chinese Medicine*, vol. 10, no. 04, pp. 44–46, 2008.

[34] B. X. Wang, X. M. Dong, A. M. Guo, and J. Zhang, "Effects of Xuefu Zhuyu decoction on functions of vascular endothelium in patients with unstable angina pectoris," *Journal of Chinese Integrative Medicine*, vol. 4, no. 03, pp. 256–259, 2006.

[35] Y. P. Tang, Y. Liu, and P. Liang, "Clinical study on preventing and treating left ventricle remodeling after acute myocardial infarction with integrative Chinese and western medicine," *Chinese Journal of Integrative Medicine*, vol. 10, no. 1, pp. 25–28, 2004.

[36] S. Y. Yu, B. Dong, Z. F. Fang, X. Q. Hu, L. Tang, and S. H. Zhou, "Knockdown of lncRNA AK139328 alleviates myocardial ischaemia/reperfusion injury in diabetic mice via modulating miR-204-3p and inhibiting autophagy," *Journal of Cellular and Molecular Medicine*, vol. 22, no. 10, pp. 4886–4898, 2018.

[37] J. Xie, L. Zhang, X. Fan, X. Dong, Z. Zhang, and W. Fan, "MicroRNA-146a improves sepsis-induced cardiomyopathy by regulating the TLR-4/NF-κB signaling pathway," *Experimental and Therapeutic Medicine*, vol. 18, no. 1, pp. 779–785, 2019.

[38] D. Tang, Z. Liu, H. Zhang, M. Sun, and Y. Sui, "Protective effects of Xuefu Zhuyu decoction on myocardium ischemia reperfusion injury in rats," *Zhongguo Zhong Yao Za Zhi*, vol. 35, no. 22, pp. 3077–3079, 2010.

[39] F. Meng, H. Lai, Z. Luo et al., "Effect of xuefu zhuyu decoction pretreatment on myocardium in sepsis rats," *Evidence-Based Complementary and Alternative Medicine*, vol. 2018, Article ID 2939307, 10 pages, 2018.

[40] M. Q. Chen, K. W. Yao, Z. J. Liu, X. X. Feng, and Y. Xiao, "Xuefu zhuyu oral liquid prevents apoptosis of ischemic myocardium cells in rats by regulating SIRT1 and its pathway-related genes," *Chinese Journal of Integrative Medicine*, vol. 26, no. 6, pp. 442–447, 2020.

[41] F. Teng, G. Li, Z. Liu, L. Zhang, and K. Yao, "The comparative study on expression of SIRT1 signal transduction by xuefuzhuyu capsule," *Evidence-Based Complementary and Alternative Medicine*, vol. 2014, Article ID 537014, 8 pages, 2014.

[42] J. Ye, R. Wang, M. Wang et al., "Hydroxysafflor yellow A ameliorates myocardial ischemia/reperfusion injury by suppressing calcium overload and apoptosis," *Oxidative Medicine and Cellular Longevity*, vol. 2021, Article ID 6643615, 14 pages, 2021.

[43] L. Tian, C. P. Su, Q. Wang et al., "Chlorogenic acid: a potent molecule that protects cardiomyocytes from TNF-α-induced injury via inhibiting NF-κB and JNK signals," *Journal of Cellular and Molecular Medicine*, vol. 23, no. 7, pp. 4666–4678, 2019.

[44] O. Levy-Ontman, M. Huleihel, R. Hamias, T. Wolak, and E. Paran, "An anti-inflammatory effect of red microalga polysaccharides in coronary artery endothelial cells," *Atherosclerosis*, vol. 264, pp. 11–18, 2017.

[45] B. Simic, M. Hermann, S. G. Shaw et al., "Torcetrapib impairs endothelial function in hypertension," *European Heart Journal*, vol. 33, no. 13, pp. 1615–1624, 2012.

[46] A. Armoza, Y. Haim, A. Basiri, T. Wolak, and E. Paran, "Tomato extract and the carotenoids lycopene and lutein improve endothelial function and attenuate inflammatory NF-κB signaling in endothelial cells," *Journal of Hypertension*, vol. 31, no. 3, pp. 521–529, 2013.

[47] B. Liang, Y. Xiang, X. Zhang et al., "Systematic pharmacology and GEO database mining revealed the therapeutic mechanism of Xuefu Zhuyu decoration for atherosclerosis cardiovascular disease," *Frontiers In Cardiovascular Medicine*, vol. 7, Article ID 592201, 2020.

[48] D. Gao, Y. H. Jiao, and Y. M. Wu, "Experimental study of Xuefu Zhuyu decoction induced participation of endothelial progenitor cells in the angiogenesis of the ischemic region," *Zhongguo Zhong Xi Yi Jie He Za Zhi*, vol. 32, no. 2, pp. 224–228, 2012.

[49] X. Hou, B. L. Li, L. Zhao, S. D. Huang, Z. Y. Xu, and G. X. Zhang, "Effects of Xuefu Zhuyu capsule on endothelin-1 release in myocardium and vascular endothelium and nitric oxide/nitric oxide synthase system of swines after acute myocardial infarction and reperfusion," *Zhong Xi Yi Jie He Xue Bao*, vol. 6, no. 4, pp. 381–386, 2008.

[50] B. Mansuroğlu, S. Derman, A. Yaba, and K. Kızılbey, "Protective effect of chemically modified SOD on lipid peroxidation and antioxidant status in diabetic rats," *International Journal of Biological Macromolecules*, vol. 72, pp. 79–87, 2015.

[51] S. Raghavan, G. Subramaniyam, and N. Shanmugam, "Proinflammatory effects of malondialdehyde in lymphocytes," *Journal of Leukocyte Biology*, vol. 92, no. 5, pp. 1055–1067, 2012.

[52] J. Zhao, H. Liu, B. Xu et al., "The role of xuefu zhuyu decoction in prevention of contrast-induced nephropathy after percutaneous coronary intervention," *Evidence-Based Complementary and Alternative Medicine*, vol. 2020, Article ID 5419016, 7 pages, 2020.

[53] V. Lubrano, A. Pingitore, I. Traghella et al., "Emerging biomarkers of oxidative stress in acute and stable coronary artery disease: levels and determinants," *Antioxidants (Basel, Switzerland)*, vol. 8, no. 5, 2019.

[54] P. Libby, G. Pasterkamp, F. Crea, and I.-K. Jang, "Reassessing the mechanisms of acute coronary syndromes," *Circulation Research*, vol. 124, no. 1, pp. 150–160, 2019.

Hindawi
Evidence-Based Complementary and Alternative Medicine
Volume 2021, Article ID 4010607, 19 pages
https://doi.org/10.1155/2021/4010607

Review Article

Atheroprotective Effects and Mechanisms of Postmarketing Chinese Patent Formulas in Atherosclerosis Models: A Systematic Review

Shiqi Chen,[1,2] Xiaoxiao Wu,[1] Tong Li,[1] Yang Li,[1] Baofu Wang,[1,2] Weiting Cheng,[1] Yu Teng,[1] Jingjing Yang,[1] Hui Meng,[1] Lei Wang,[1] Ziwen Lu,[1] Yangyang Jiang,[1] Yahong Wang,[2] and Mingjing Zhao[1]

[1]*Key Laboratory of Chinese Medicine of Ministry of Education and Beijing, Dongzhimen Hospital Affiliated to Beijing University of Chinese Medicine, Beijing 100700, China*
[2]*Department of Cardiology, Dongzhimen Hospital Affiliated to Beijing University of Chinese Medicine, Beijing 100700, China*

Correspondence should be addressed to Yahong Wang; wyh411@hotmail.com and Mingjing Zhao; mjgx2004@163.com

Received 15 September 2021; Revised 30 October 2021; Accepted 3 November 2021; Published 27 November 2021

Academic Editor: Arquimedes Gasparotto Junior

Background. Some postmarketing Chinese patent formulas have been widely used to treat atherosclerosis (AS) and play critical roles in Chinese healthcare. However, the usage of these herbs is yet controversial due to unclear effects and lack of understanding of the mechanism of action. With the modernization of traditional Chinese formulas, we are to elucidate the atheroprotective properties of these remedies from successful postmarketing experiments *in vivo*. *Methods*. In this systematic review, we critically searched the databases, applied stringent criteria, assessed the methodological quality, and examined the current evidence *in vivo*. *Results*. Consequently, 60 studies were included in the present qualitative synthesis. Data on models, high-fat diet, intervention time, outcome measures, efficacy, and mechanisms were collected. Finally, 23 formulas that could alleviate AS were correlated to the amelioration of plaques, improvement of plaque stability, modification of lipid level and lipid metabolism, and the effects of anti-inflammation and antioxidant stress with multiple components and targets. However, the methodological quality was low and incomplete among the included literature. *Conclusions*. Thus, taken together, the studies on postmarketing Chinese patent formulas would provide a novel approach to improve the treatment of AS, and rigorously designed studies would provide high-quality evidence.

1. Introduction

Cardiovascular diseases (CVDs) are the leading causes of death worldwide, with an estimated 17.9 million deaths each year and 32% of all deaths globally [1, 2]. Compared with the high-income countries (HICs), the death rate of low- and middle-income countries is about three times higher, causing a heavy economic burden to the society [3]. Coronary heart disease (CHD) is one of the CVDs caused by atherosclerosis (AS) in blood vessels and a significant cause of death in both developing and developed countries [4–6]. AS is a multifaceted disorder involving the core mechanisms of endothelium dysfunction, lipid deposition, vascular inflammation, oxidative stress, foam cell formation, and smooth muscle cell migration [7]. In addition, AS can also be identified as an inflammatory disease characterized by immune responses [8]. Modern therapies have made significant progress in the treatment of AS; for example, the Western medicine of statins and the surgeries of percutaneous transluminal coronary intervention (PCI) or coronary artery bypass grafting (CABG). However, interventional therapy can only improve local vascular problems, and statins have been identified to cause side effects of liver damage, muscle dissolution, and new-onset type 2 diabetes mellitus [9]. Therefore, other remedies for improving the efficacy and the adverse reactions are urgent requirements.

Traditional Chinese medicine (TCM) has a history of over 2000 years and has been widely used in Chinese healthcare [10]. Unlike Western medicines, traditional Chinese herbs usually consist of various compounds and provide multiple targets for the prevention and treatment of AS [11]. With widespread clinical applications and adequate tolerance, some TCMs have been deemed as an effective approach for treating ASCVD and restoring the balance of the human body [12].

Hitherto, many Chinese patent formulas produced by pharmaceutical companies have emerged and been approved in China. Several postmarketing studies *in vivo* have been identified to understand the effects and mechanisms of Chinese patent formulas with antiatherosclerotic properties, and some reviews reported the use of Chinese patent formulas in AS [3, 13, 14]. However, most of these reviews were focused on a single formula. In this study, we critically evaluated the effects and summarized the mechanisms of all the postmarketing Chinese patent formulas in treating AS. A systematic review method was implemented by searching the databases, applying strict criteria, assessing the methodological quality, and evaluating outcomes. In this review, we focused on the formulas in the field of AS and the animal models and mechanisms in atheroprotective effects.

2. Material and Methods

2.1. Information Sources and Search Strategy. The search was applied to three databases, including PubMed, Embase, and Web of Science (publication duration was from the inception through March 29, 2021). The search strategy used the following general terms as mesh terms or free terms: "Medicine, Chinese Traditional", "Herbal Medicine", "Drugs, Chinese Herbal", "Atherosclerosis", "Chinese patent medicine", "Chinese patent drug", "Chinese traditional patent medicine", "traditional Chinese medicine or Chinese medicine", "TCM", "Chinese herb medicine", "Chinese herbal medicine", "atherosclerosis", "arteriosclerosis", "atherosis". For instance, the detailed search strategy of PubMed is as follows: (((Medicine, Chinese Traditional) OR (Herbal Medicine) OR (Drugs, Chinese Herbal)) AND (Atherosclerosis)) OR (((Chinese patent medicine or Chinese patent drug or Chinese traditional patent medicine) OR (traditional Chinese medicine or Chinese medicine or TCM or Chinese herb medicine or Chinese herbal medicine)) AND (atherosclerosis or arteriosclerosis or atherosis)). Also, we used a search filter previously developed for PubMed in order to identify all the publications on animal studies [15].

2.2. Inclusion and Exclusion Criteria. Considering the objective of our review, the inclusion criteria were listed as follows: (1) original studies were mainly related to the postmarketing Chinese patent formulas *in vivo*; (2) the patent drugs that were approved to treat the related AS diseases could be searched on the website (http://app1.nmpa.gov.cn/data_nmpa/face3/base.jsp?tableId=25&tableName=TABLE25&title=%E5%9B%BD%E4%BA%A7%E8%8D%AF%E5%93%81&bcId=152904713761213296322795806604&CbSlDlH0=qGqJcGqBhnZBhnZBhCJzH3eKIwCWYj2zliOBDl.Z9naqqcZ) of the National Medical Products Administration (NMPA) of the Chinese government; (3) any validated AS model could be applied in this review, including ApoE$^{-/-}$ mice, LDLR$^{-/-}$ mice, New Zealand white rabbits, Japanese white rabbits, Wistar rats, Sprague–Dawley (SD) rats, and C57BL/6 mice with or without a high-fat diet (HFD), balloon injury, and ligation or silastic collar implantation around a specific artery [16, 17]; and (4) language was not restricted, but the literature should have been published in official journals.

The studies were excluded if they were (1) only *in vitro* or clinical research; (2) mainly Chinese medicine monomers or other unlisted formulas; or (3) AS models combined with models of other diseases.

2.3. Study Selection and Data Extraction. Two investigators (SQC and XXW) individually conducted the literature search using the predetermined criteria in Endnote X8 software. First, duplicates were identified in various databases and removed from the initial search results. Second, the obviously irrelevant studies were eliminated after reading the titles and abstracts. Third, the full texts were screened to identify the relevant studies, and the unqualified studies were removed. The study selection was independently cross-checked by two researchers. Any disagreement was resolved by discussion in a consensus meeting with the corresponding authors (YHW and MJZ).

Subsequently, two authors (TL and YL) independently extracted data from the included literature employing a standardized sheet prepared for this review, which was further checked by BFW. The extracted data included study title, year of the research publication, drug name, approval number by NMPA, pharmaceutical company, main Chinese herbs, experimental models, HFD feeding time, drug intervention time, outcome measures, efficacy, and mechanisms.

2.4. Assessment of Risk of Bias (ROB) in Individual Studies. Two authors (WTC and YT) independently assessed the ROB using SYRCLE's ROB tool [18] for animal studies to evaluate the methodological quality of the included studies with respect to sequence generation (i.e., selection bias), baseline characteristics (i.e., selection bias), allocation concealment (i.e., selection bias), random housing (i.e., performance bias), blinding (i.e., performance bias), random outcome assessment (i.e., detection bias), blinding (i.e., detection bias), incomplete outcomes data (i.e., attrition bias), selective outcome reporting (i.e., reporting bias), and other sources of bias; it was further checked by JJY. The disagreements were resolved by consensus with the corresponding authors (YHW and MJZ).

2.5. Summary Measures and Analysis. Regarding the high heterogeneity of the various formulas and the different methodologies, all the outcome measures, which compared the experimental groups with the model groups, were

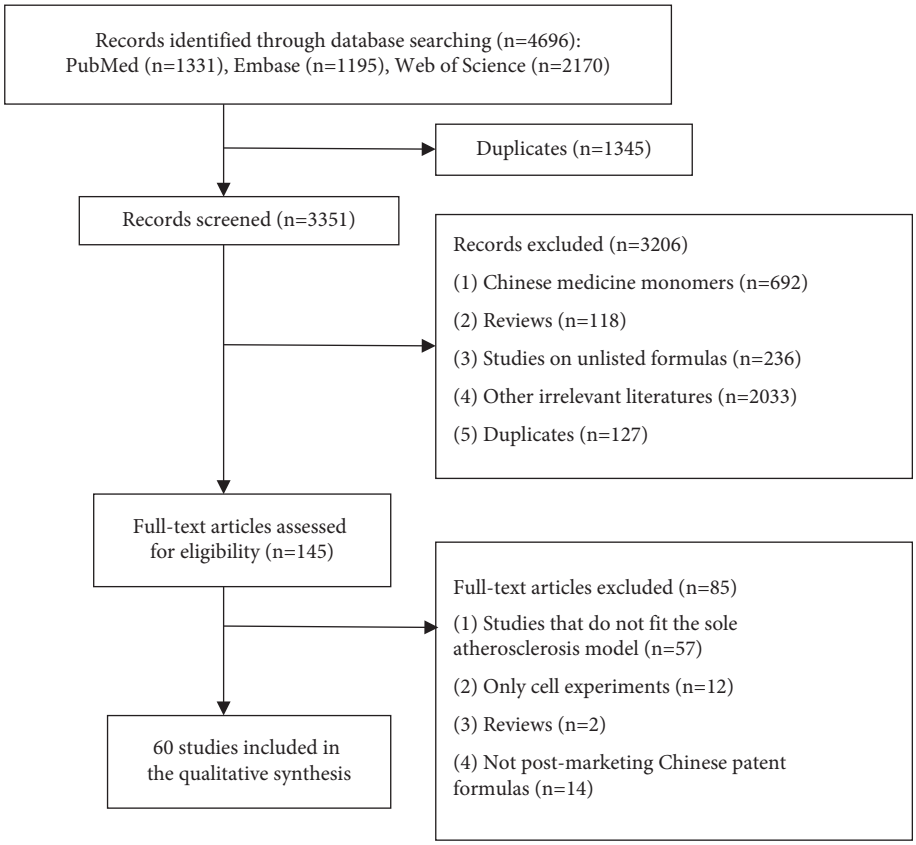

Figure 1: Flowchart of searching and screening studies.

recorded as a significant uptrend marker "↑" or a significant downtrend marker "↓". The summary analysis was presented using a qualitative synthesis.

3. Results

3.1. Study Selection. A total of 4696 articles were retrieved from three literature databases. After removing 1345 duplicates, 3351 potentially relevant articles were assessed. Subsequently, 3206 articles were excluded after the evaluation of titles and abstracts. Of the 145 remaining articles, we further excluded 85 after screening the full text. Finally, 60 studies [19–40], [41–60], [61–78] were included in this analysis. A flowchart (Figure 1) shows the search and study selection process.

3.2. Study Characteristics. Herein, 60 studies [19–40], [41–60], [61–78], encompassing 23 postmarketing Chinese patent formulas, including Danhong injection, Zhixiong capsule, Longshengzhi capsule, Tongxinluo capsule, Shexiang Baoxin pill, Danlou tablet, Angong Niuhuang pill, Longxuetongluo capsule, Longhu Rendan, Naoxintong pill/capsule, Di'ao Xinxuekang capsule, Xuezhikang, Qishenyiqi pill, ginkgo biloba tablet, Xuefu Zhuyu granule, Shexiang Tongxin dropping pill, compound Chuanxiong capsule, Yindanxinnaotong soft capsule, Dahuang Zhechong pill, Fufang Danshen dropping pill, Suxiaojiuxin pill, Xuezhitong capsule, and Guanxinshutong capsule. All the studies utilized the validated AS models and were published from 2004 to 2020. The HFD feeding time varied from 0 to 34 weeks, and the duration of different drug treatments ranged from 12 days to 34 weeks. The characteristics of the included studies and the herbal drugs of the included formulas are shown in Table 1 and Supplementary Tables S1–S3.

3.3. ROB and Methodological Quality. According to the assessment of SYRCLE's ROB tool, the included animal intervention studies displayed the methodological bias of 10 entries shown in Supplementary Table S4. All the included studies had unclear baseline characteristics, allocation concealment, blinding method, and random outcome assessment. Among these, five low-risk studies [40, 42, 43, 66, 68] used the "random number table" in the assessment of sequence generation, seven high-risk studies [24, 33, 34, 49, 59, 75, 76] did not report the entry, and the remaining 48 studies had unclear detailed random methods. Although none of the studies mentioned random housing, the outcome measures in the 19 studies [20, 23, 26, 27, 29, 30, 34–36, 38, 41, 45, 46, 48, 50, 52, 59, 73, 75] were not influenced since the feeding conditions (such as temperature, lighting, and humidity) were described, and the bias was evaluated as low risk. The incomplete outcome data were detected in 27 high-risk articles [19–21, 23, 26, 32–36, 39, 45–47, 50–53, 55, 56, 60, 61, 68, 74–77] without any reason or appropriate method for describing the

Table 1: Details of postmarketing Chinese patent formulas in the process of atherosclerosis *in vivo*.

Author, year	Postmarketing Chinese patent formulas	Experimental models	HFD feeding time	Drug intervention time	Outcome measures	Effects and mechanisms
Zhou et al. 2019 [19]	Danhong injection	HFD male apoE−/− mice	12 weeks	6 weeks	TG↓ HDL-C↑ LDL-C↓; APA↓ AI↓; NEFA↓ FBG↓ FINS↓ IR↓; GLUT-4↑ p-IRS-1↑ p-AKT↑	Attenuating AS and macrophage lipid accumulation by promoting the activation of PI3K/AKT insulin signaling pathway.
Zhai et al. 2019 [20]	Zhixiong capsule	HFD male Japanese rabbits with the silastic collar implantation around the right carotid artery	12 days	12 days	TC↓ HDL-C↑ TC/HDL-C ratio↓ log(TG/HDL-C)↓; IL-4↑; APA↓ IA↓ IA/MA↓	Preventing atherosclerotic plaque formation and intimal thickening.
Ma et al. 2019 [21]	Longshengzhi capsule	HFD female apoE−/− mice	18 weeks	10 weeks	Artery sections: APA↓; MOMA-2↓; NCA↓ CPA↑ FCA↑ SMC↑; TUNEL↓; ABCA1↑ ABCG1↑. Liver sections: lipid droplets↓ liver TG↓; FA oxidation↑ FA synthesis↓ SREBP1↓; SREBP2↓ LDLR↑ HMGCS↓; DGAT1↓ ATGL↑ MTTP↓ APOC2↑; CCR2↓ IL-6↓ MCP-1↓ TNF-α↓; CD68↓ MOMA-2↓.	Reducing AS by reducing macrophage/foam cell accumulation, maintaining the integrity of arterial wall, ameliorating hepatic lipid metabolism, and inhibiting inflammation.
Ma et al. 2019 [22]	Tongxinluo capsule	HFD male apoE−/− mice	16 weeks	16 weeks	Serum TNF-α↓ APA↓; CPA↑ SMC↑ staining of lipids and macrophages↓; IL-6↓, MMP-2↓, and TNF-α↓	Inhibiting AS development and stabilizing plaque.
Lu et al. 2019 [23]	Shexiang Baoxin pill	HFD apoE−/− mice	20 weeks	20 weeks	APA↓; SOD↑ CAT↑ GSH↑ MDA↓ H_2O_2↓ MPO↓; MCP-1↓ IFN-γ↓ IL-17A↓ IL-10↑ TGF-β1↑; VCAM-1↓ ICAM-1↓ IL-6↓ IL-2↓; macrophages↓ ABCA1↑ ABCG1↑; p38↓ JNK↓ Mfn2↑ NF-κB↓ SR-A↓ LOX-1↓ LXRα↑	Exerting antiatherosclerotic effects via improving inflammation response and inhibiting lipid accumulation.
Hao et al. 2019 [24]	Danlou tablet	HFD male apoE−/− mice	20 weeks	12 weeks	APA↓; LO↓; lipid content in artery↓ HDL-C↑ ox-LDL↓; IL-1β↓, IL-10↓, MCP-1↓, IL-18 ↓, IL-33↓; PPARα↑, PGC-1α↑, ABCA1↑, P-IKKα/β↓, P-IκBα↓, and P-NF-κBp65↓	Preventing AS via suppressing NF-κB signaling and triggering the PPARα/ABCA1 signaling pathway.
Chai et al. 2019 [25]	Angong Niuhuang pill	HFD male apoE−/− mice	8 weeks	8 weeks	Aorta: MCP-1↓ MCP-2↓ MCP-3↓ CCR2↓ CXCR3↓; ICAM-1↓ VCAM-1↓; IL-6↓ TGF-β1↑ IL-17↓; Treg cell↑; Th17/Treg cell↓. Spleen: IL-6↓ TGF-β1↑	Ameliorating the development of early AS by reducing splenic and vascular inflammation.

Table 1: Continued.

Author, year	Postmarketing Chinese patent formulas	Experimental models	HFD feeding time	Drug intervention time	Outcome measures	Effects and mechanisms
Zhou et al. 2018 [26]	Longxuetongluo capsule	HFD male SD rats	4 weeks	4 weeks	TC↓ HDL-C↑ LDL-C↓ TG↓; serum ALT↓ AST↓ serum MCP-1↓ ICAM-1↓ VCAM-1↓. Histological sections of liver and aorta↓; aortic histological sections: NF-κB↓	Preventing AS and fatty liver by controlling lipid metabolism and anti-inflammation activity.
Yin et al. 2018 [27]	Tongxinluo capsule	HFD male and female New Zealand rabbits with the silicone tube encapsulation of left carotid artery	4 weeks	4 weeks	TC↓ TG↓ LDL-C↓; serum MDA↓, SOD↑, and T-AOC↑; VEGF-A↓ VEGF-R2↓; nuclear NF-κB↓ TNF-α↓ IL-6↓; nuclear Nrf2↑ NQO1↑	Reducing carotid adventitial VV angiogenesis and alleviating early AS lesions by inhibiting carotid inflammation and oxidative stress injury.
Yan et al. 2018 [28]	Longhu Rendan	HFD male apoE−/− mice	10 weeks	10 weeks	TC↓ LDL-C↓ TG↓; APA↓; LOX-1↓	Ameliorating AS via reducing serum lipid and LOX-1 expression.
Wang et al. 2018 [29]	Naoxintong pill	HFD male apoE−/− mice	8 weeks	8 weeks	Plaque foam cell content↓	Reducing foam cell accumulation in atherosclerotic plaques.
Qu et al. 2018 [30]	Di'ao Xinxuekang capsule	HFD male apoE−/− mice	18 weeks	18 weeks	TC↓ HDL-C↑ LDL-C↓ TG↓; APA↓. Liver sections: lipid accumulation↓; PCSK9↓; liver LDLR↑ serum PCSK9↓	Alleviating lipid disorder and ameliorating AS with downregulation of the PCSK9.
Chen et al. 2018 [31]	Tongxinluo capsule	HFD male apoE−/− mice with silastic collar implantation	8 weeks	8 weeks	TUNEL↓ Lc3b dots↑; APA↓; vulnerable index↓ macrophage apoptosis↓	Improving autophagy via Beclin-1.
Yang et al. 2017 [32]	Naoxintong capsule	HFD male apoE−/− mice	18 weeks	8 weeks	APA↓ LO↓; HDL-C↑; CPA↑ SMC↑ MPO↑ CD68↓ calcification events↓ fibrous cap thickness↑. Liver sections: SREBP1↑ and SREBP2↑; ATGL↑ and LDLR↑; liver TG↓; DGAT1↓ CGI-58↑; ATGL↑ pi-AMPKa↑	Inhibiting AS development, stabilizing plaque, and reducing hepatic triglyceride levels.
Shen et al. 2017 [33]	Xuezhikang	Female apoE−/− mice combined partial ligation of the left common carotid artery and left renal artery	0	8 weeks	APA↓; CD68↓ α-SMA↑ CPA↑ vulnerable phenotype↓; p-PERK↓ p-IRE1α↓ p-eIF2α↓ and BiP↓ CHOP↓ DHE staining↓; NCA↓ TUNEL↓ caspase-3↓; TNF-α↓ MMP-8↓ MMP-13↓	Suppressing vulnerable plaque progression and rupture by mitigating lesional endoplasmic reticulum stress and inhibiting apoptosis and the NF-κB proinflammatory pathway.

Table 1: Continued.

Author, year	Postmarketing Chinese patent formulas	Experimental models	HFD feeding time	Drug intervention time	Outcome measures	Effects and mechanisms
Peng et al. 2017 [34]	Qishenyiqi pill	HFD male apoE−/− mice	8 weeks	8 weeks	APA↓ LDL-C↓ liver weight/body weight↓. Liver sections: LXRα↑ ABCG5↑. Aorta sections: CD36↓ Foxp3↑ IL-17A↓. Spleen sections: Foxp3↓ IL-17A↓ Smad2/3↓ IL-6↓ RORγ↓	Promoting regulatory T cells in atherosclerotic lesion, inhibiting T helper 17 cells in plaque and spleen, and accelerating liver cholesterol excretion.
Fu et al. 2017 [35]	Angong Niuhuang pill	HFD male SD rats with vitamin D3 injection	17 weeks	9 weeks	APA↓ IT↓ MT↓, the maximum platelet aggregation rates↓; serum TC↓ LDL-C↓ TC/HDL-C↓ LDL-C/HDL-C↓; MDA↓ hs-CRP↓ LDH↓ cTnI↓; myocardial fibers↓; Bax protein↓ Bcl-2↑	Reducing AS due to its antiplatelet aggregation, lipid regulatory, antioxidant, anti-inflammatory, and antiapoptotic properties.
Dong et al. 2017 [36]	Di'ao Xinxuekang capsule	HFD male apoE−/− mice	8 weeks	8 weeks	TC↓ LDL-C↓; APA↓. Aorta sections: ABCA1↑ and ABCG1↑. Liver and intestines: ABCA1↑ ApoA-I↑ PPARγ↑ LXRα↑. Liver sections: SR-B1↑ preB1-HDL↓ HDL3↓ HDL2↑. Serum LCAT↑	Regulating RCT by improving HDL synthesis, maturation, and catabolism.
Zhu et al. 2016 [37]	Ginkgo biloba tablet	HFD male Wistar rats with vitamin D3 injection and balloon injury in aorta.	60 days	60 days	Blood glucose and calcium↓; TC↓ TG↓ LDL-C↓; LO↓ IT↓; SR-A↓; CRP↓ ICAM-1↓ VCAM-1↓	Alleviating AS lesions by inhibiting inflammation and controlling lipid.
Zheng et al. 2016 [38]	Longxuetongluo capsule	HFD male apoE−/− mice	6 weeks	6 weeks	APA↓	Reducing plaques.
Yang et al. 2016 [39]	Naoxintong capsule	HFD male apoE−/− mice	18 weeks	8 weeks	APA↓ CPA↑ SMC↑ calcification events↓ fibrous cap thickness↑ MOMA-2 protein↓ MMP-2↓ and TNF-α↓ SM22α↑	Reducing advanced AS and enhancing the plaque stability.
Miao et al. 2016 [40]	Danlou tablet/Xuefu Zhuyu granule	HFD male Wistar rats with vitamin D3 injection	4 weeks	8 weeks	Danlou group: IT↓ TC↓ TG↓ LDL-C↓ PDGF↓ ERK1/2↓ pERK1/2↓. Xuefu Zhuyu group: IT↓ TC↓ PDGF↓ ERK1/2↓ pERK1/2↓	Reducing serum lipids, increasing PDGF, and inhibiting ERK signal pathway activation and VSMC proliferation.
Ma et al. 2016 [41]	Tongxinluo capsule	HFD male apoE−/− mice	5 weeks	5 weeks	VEGF-A↓ ANGPT-1↑; microvessels sprouting↓ VV number in plaques↓; APA↓; CPA↑ SMC↑ MOMA-2↓ FCT↑	Inhibiting early AS through regulating angiogenic factor expression and inhibiting VV proliferation in atherosclerotic plaque.
Chen et al. 2016 [42]	Danlou tablet	HFD male Wistar rats with vitamin D3 injection	4 weeks	8 weeks	TC↓ TG↓ LDL-C↓; APA↓; IL-6↓ TNF-α↓ MCP-1↓ ox-LDL↓; LP-PLA2↓ sPLA2↓	Inhibiting AS related to the reduction of blood lipid and inflammation.

Table 1: Continued.

Author, year	Postmarketing Chinese patent formulas	Experimental models	HFD feeding time	Drug intervention time	Outcome measures	Effects and mechanisms
Xiong et al. 2015 [43]	Shexiang Tongxin dropping pill	HFD male apoE−/− mice	8 weeks	8 weeks	IL-2↓ IL-6↓ TNF-α↓ INF-γ↓ ox-LDL↓ MDA↓; GSH↑ SOD↑; ROS↓; miR-21↓ miR-126↓ miR-155↓ miR-20↑ APA↓; TC↓ TG↓ LDL↓	Inhibiting AS via reducing inflammation and regulating miR-21, miR-126, miR-155, and miR-20.
Xiong et al. 2015 [44]	Shexiang Tongxin dropping pill	HFD male apoE−/− mice	8 weeks	8 weeks	ox-LDL↓ HDL↑; IL-2↓ IL-6↓ TNF-α↓ INF-γ↓ ox-LDL↓ MDA↓; GSH↑ SOD↑ ROS↓; miR-21↓ miR-126↓ miR-155↓ miR-132↓ miR-20↑	Inhibiting AS via reducing inflammation and regulating miR-21, miR-126, miR-155, miR-132, and miR-20.
Wu et al. 2015 [45]	Tongxinluo capsule	HFD male apoE−/− mice	12 weeks	12 weeks	APA↓; p22↓ p47↓ HO-1↓; NF-κB↓; TC↓ TG↓ LDL↓	Decreasing atherosclerotic plaque formation and inhibiting oxidative stress and inflammation.
Lang et al. 2015 [46]	Tongxinluo capsule	HFD New Zealand rabbits with the silastic collar implantation around the right carotid artery	4 weeks	4 weeks	IT↓; CD34↓; microvascular blood flow volume↓; VAGF↓ VEGFR-2↓	Inhibiting VV proliferation.
Kang et al. 2015 [47]	Compound Chuanxiong capsule	HFD male apoE−/− mice	13 weeks	7 weeks	TC↓ TG↓ LDL-C↓; AI↓ APA↓; CPA↑; PI3K↓ Akt↓ NF-κB↓ IL-6↓ TNF-α↓	Preventing AS and inhibiting the expression of IL-6 and TNF-α by regulating the PI3K/Akt/NF-κB signaling pathway.
Cheng et al. 2015 [48]	Yindanxinnaotong soft capsule	HFD male SD rats with vitamin D3 injection	9 weeks	12 weeks	APA↓ TC↓ TG↓ LDL-C↓; MDA↓ SOD↑ GSH↑ GSH-px↑; NF-κB↓ IkB↑; IL-1β↓ CRP↓ TNF-α↓; NO↑ TXB2↓	Relieving AS through regulating lipids, reducing lipid particle deposition in the endothelial layer of artery, enhancing antioxidant power, and repressing inflammation activity by inhibiting the NF-κB signal pathway.
Zhang et al. 2014 [49]	Tongxinluo capsule	Male C57BL/6 mice with the left common carotid artery ligation	0	21 days	IA/MA ratio↓ IA↓; TNF-α↓ IL-1β↓; miR-155↓	Inhibiting the vascular inflammatory response and neointimal hyperplasia.
Zhang et al. 2014 [50]	Suxiaojiuxin pill	HFD male apoE−/− mice	13 weeks	8 weeks	TG↓ APA↓; CPA↑ FCT↑; VEGF↓ α-SMA↑; MMP-2↓ MMP-9↓ TIMP-1↑ TIMP-2↑	Enhancing atherosclerotic plaque stability associated with modulating the MMPs/TIMPs balance.
Yao et al. 2014 [51]	Tongxinluo capsule	Male SD rats with the left carotid artery balloon injury	0	2 weeks	Serum ET-1↓ MCP-1↓ sICAM-1↓ NO↑; artery: ICAM-1↓ MCP-1↓; the neointimal thickening↓	Improving endothelial function, attenuating neointimal formation, and reducing inflammation.
Wang et al. 2014 [52]	Tongxinluo capsule	HFD male apoE−/− mice	12 weeks	12 weeks	TC↓ HDL↑ TG↓ LDL↓; CRP↓; APA↓; ICAM-1↓ VCAM-1↓ MCP-1↓	Preventing atherosclerotic plaque formation and intimal thickening. Reducing inflammation.
Liu et al. 2014 [53]	Danhong injection	HFD male apoE−/− mice	16 weeks	16 weeks	MCP-1↓ MMP-2↓ MMP-9↓; AAA formation↓; CPA↑	Inhibiting the high-fat diet-induced AAA formation related to the maintenance of the collagen content and the inhibition of expression of AAA-related genes.

Table 1: Continued.

Author, year	Postmarketing Chinese patent formulas	Experimental models	HFD feeding time	Drug intervention time	Outcome measures	Effects and mechanisms
Guo et al. 2014 [54]	Suxiaojiuxin pill	HFD male SD rats with vitamin D3	12 weeks	12 weeks	TG↓ LDL↓ TC↓ HDL↑	Reducing lipids.
Chen et al. 2014 [55]	Danhong injection	HFD male or female apoE−/− or LDLR−/− mice	16 weeks/ 20 weeks	16 weeks/20 weeks	Male apoE−/−: ABCA1↑ TNF-α↓; female apoE−/−: APA↓ LDL-C↓ HMGCR↓ LDLR↑ TNF-α↓; male LDLR−/−: ABCA1↑ TNF-α↓; female LDLR−/−: ABCA1↑ APA↓ HMGCR↓ TNF-α↓ TG↓ LDL-C↓; aorta caveolin-1↓; MDA↓ SOD↑ T-AOC↑; eNOS↑, plasma NOx↑, cGMP in erythrocyte plasma and aorta wall↑; EDI↓ blood viscosity↓	Inhibiting AS through amelioration of lipid profiles.
Zhu et al. 2013 [56]	Xuezhikang	HFD male Wistar rats with vitamin D3 injection	12 weeks	12 weeks		Elevating eNOS/NO, improving hemorheology, and inhibiting oxidative stress.
Zhong et al. 2013 [57]	Naoxintong capsule	HFD New Zealand rabbits	12 weeks	12 weeks	LDL-C↓ TC↓; aorta: iNOS mRNA↓ NO↓	Reducing iNOS expression in AS lesions
Zhao et al. 2013 [58]	Naoxintong capsule	HFD male LDLR−/− mice	8 weeks	8 weeks	TC↓ TG↓; APA↓; CD68↓; DCs↓ CD40↓ CD86↓ CD80↓ plasma IL-12p70↓	Protecting against AS through lipid lowering and inhibiting DCs maturation.
Li et al. 2011 [59]	Xuezhikang	HFD male Wistar rats with vitamin D3 injection	12 weeks	12 weeks	LDL-C↓ TC↓; APTT↑ PT↑ TT↑ fibrinogen↓ tissue factor↓ SOD↑ MDA↓	Inhibiting the tissue factor expression and reducing oxidative stress.
Han et al. 2011 [60]	Dahuang Zhechong pill	HFD male New Zealand rabbits with balloon injury in aorta.	60 days	60 days	Serum: MDA↓SOD↑ NO↑. Aorta: MPO↓. VSMCs: PCNA↓ Bcl-2↓	Inhibiting AS through antilipid peroxidation, protection of vascular endothelium, inhibition of VSMCs proliferation, and promotion of VSMCs apoptosis
Li et al. 2011 [61]	Suxiaojiuxin pill	HFD male SD rats with vitamin D3 injection	12 weeks	12 weeks	Serum: MDA↓ SOD↑ ox-LDL↓; PPAR γ↓; NF-κB↓	Anti-inflammation and inhibition of oxidative stress.
Song et al. 2010 [62]	Tongxinluo capsule	HFD male Japanese rabbits	14 weeks	14 weeks	TC↓ LDL↓; PAI-1↓ VCAM-1↓	Inhibiting AS related to the reduction of blood lipid and inflammation.
Fu et al. 2009 [63]	Danhong injection	HFD male New Zealand rabbits	14 weeks	14 weeks	TC↓ TG↓ LDL-C↓; MDA↓ iNOS↓ COX-2↓; APA↓	Inhibiting AS related to the reduction of blood lipid, the inhibition of arterial wall inflammation, and the regulation of oxidative stress level.
Cao et al. 2009 [64]	Tongxinluo capsule	HFD male Japanese rabbits	14 weeks	14 weeks	APA↓; MMP-3↓ MMP-9↓ PPARγ↑	Inhibiting the expression of MMP-3 and MMP-9 and increasing the expression of PPARγ.
Yu et al. 2006 [65]	Tongxinluo capsule	HFD male New Zealand rabbits	16 weeks	16 weeks	APA↓; TC↓ LDL↓; macrophage↓; LOX-1↓	Inhibiting AS related to the reduction of blood lipid and LOX-1.
Xie et al. 2006 [66]	Xuezhikang	HFD Japanese rabbits	12 weeks	12 weeks	APA↓; TC↓ HDL-C↑ TG↓ LDL-C↓; serum NO↑ CRP↓	Inhibiting AS related to the reduction of blood lipid and inflammation.

Table 1: Continued.

Author, year	Postmarketing Chinese patent formulas	Experimental models	HFD feeding time	Drug intervention time	Outcome measures	Effects and mechanisms
Li et al. 2006 [67]	Tongxinluo capsule	HFD male Japanese rabbits with balloon injury	16 weeks	16 weeks	ET↓ NO↑; IT↓; CPA↑; MMP-1↓, COX-2↓; Bcl-2↑; FasL↓; macrophage↓	Reducing endothelial injury and intima thickness, inhibiting apoptosis, and stabilizing plaques.
Tian et al. 2004 [68]	Fufang Danshen dropping pill	HFD male New Zealand rabbits	12 weeks	12 weeks	TC↓ HDL-C↑ TG↓ LDL-C↓; IT↓	Reducing the blood lipid.
Chen et al. 2004 [69]	Fufang Danshen dropping pill	HFD male New Zealand rabbits	12 weeks	12 weeks	LO↓ APA↓; VCAM-1↓	Inhibiting VCAM-1 expression.
Guan et al. 2015 [70]	Tongxinluo capsule	Male Wistar rats with the silicone collar around the left carotid artery	0	4 weeks	pERK1/2↑ nNOS↑; LO↓	Improving the blood flow and attenuating the chronic vasoconstriction through the activation of ERK1/2 signaling.
Chen et al. 2009 [71]	Tongxinluo capsule	HFD New Zealand rabbits with balloon-induced abdominal aortic endothelial injury, undergoing plaques triggering by Chinese Russell viper venom	20 weeks	12 weeks	Serum TC↓ LDL-C↓ TG↓; MCP-1↓ hs-CRP↓ IL-8↓ IL-18↓ MMP-1↓ P-selectin↓; ultrasonography measurements: IMT↓; corrected AII ↑ APA↓ EEMA↓; MCP-1↓ MMP-1↓ MMP-3↓ MMP-12↓ P-selectin↓; vulnerability index↓ α-SMCs↑ CPA↓ lipid↓ RAM-11↓	Enhancing the stability of vulnerable plaques via effects on lipid lowering and anti-inflammation.
Zhang et al. 2009 [72]	Tongxinluo capsule	HFD New Zealand rabbits with balloon-induced abdominal aortic endothelial injury, undergoing an adenovirus-containing p53 and plaques triggering by Chinese Russell viper venom	10 weeks	8 weeks	Serum TC↓ LDL↓ TG↓ HDL↑; MCP-1↓ hs-CRP↓ sICAM-1↓ ox-LDL↓; ultrasonography measurements: corrected AII ↑ APA↓ EEMA↓; MCP-1↓ MMP-1↓ MMP-3↓ MMP-12↓ P-selectin↓; vulnerability index↓ α-SMCs↑ CPA↓ lipids↓ macrophages↓ fibrous cap thickness↓; LOX-1↓ MMP-1↓ MMP-3↓ TIMP-1↓ NF-κB↓	Enhancing the stability of plaque and preventing plaque rupture via lipid lowering, anti-inflammation, and anti-oxidation.
Liu et al. 2019 [73]	Shexiang Baoxin pill	HFD LDLR−/− mice	14 weeks	14 weeks	α-SMA↓ SM22α↓ OPN↓	Reversing the dedifferentiation of VSMCs.
Meng et al. 2019 [74]	Xuezhitong capsule	HFD male apoE−/− mice	34 weeks	34 weeks	Serum TC↓ LDL↓ TG↓ HDL↑; APA↓; plasma FFA↓ ox-LDL↓ LCAT↑ ApoB↓; liver ox-LDL↓ FAS↓ LDLR↑ ABCA1↑ SR-B1↑ LCAT↑ ApoA1↑ APA↓; serum IL-8↓ MMP-1↓ MMP-2↓	Activating RCT and increasing HDL levels.
Gao et al. 2020 [75]	Danlou tablet	HFD male apoE−/− mice	10 weeks	10 weeks		Protecting against AS by reducing inflammation.

Table 1: Continued.

Author, year	Postmarketing Chinese patent formulas	Experimental models	HFD feeding time	Drug intervention time	Outcome measures	Effects and mechanisms
Lu et al. 2020 [76]	Guanxinshutong capsule	HFD male apoE−/− mice	10 weeks	10 weeks	Serum TC↓ LDL-C↓ TG↓ HDL-C↑; APA↓; CPA↑; CD68↓; serum TNF-α↓ IL-6↓ SOD↑ GSH↑ MDA↓; aortic sinus TNF-α↓ IL-6↓ NF-κB↓ HO-1↑ Nrf2↑	Attenuating AS by reducing lipid deposition, modulating oxidative stress, and inflammatory responses
Sun et al. 2020 [77]	Danlou tablet	HFD male apoE−/− mice	32 weeks	8 weeks	Serum TC↓ TG↓ LDL-C↓; APA↓; aorta mRNA TNF-α↓ IL-1β↓ ICAM-1↓	Inhibiting AS through lipid lowering and modulating inflammation
Zhai et al. 2020 [78]	Zhixiong capsule	HFD male SD mice + vitamin D3	18 weeks	6 weeks	APA↓ IA/MA ratio↓ CPA↑ mineralization↓; serum TC↓ LDL↓ HDL↑; thoracic arteries IL-4↑ IL-13↑ MAPK1↓ MAPK14↓ p53↑	Inhibiting AS plaque progression related to the reduction of blood lipid, macrophage content, and macrophage transformation.

AAA, abdominal aortic aneurysms; ABCA1, ATP binding cassette transporter A1; ABCG1, ATP binding cassette transporter G1; ACAT, acyl coenzyme A: cholesterol acyltransferase; ANGPT-1, angiopoietin-1; APOA1, apolipoprotein A I; APOB, apolipoprotein B; AS, atherosclerosis; APA, atherosclerotic plaque area; AI, atherosclerosis index values; AII, acoustic intensities; Akt, serine/threonine kinase; AMPK, adenosine monophosphate-activated protein kinase; CHOP, CCAAT-enhancer-binding protein homologous protein; CPA, collagen-positive area; DC, dendritic cell; EDI, erythrocyte deformation index; EEMA, external elastic membrane area; FAS, fatty acid synthase; FBG, fasting blood glucose; FCA, fibrous cap area; FCT, fibrous cap thickness; FFA, free fatty acid; FINS, fasting insulin; GLUT-4, glucose transporter-4; GSH-PX, glutathione peroxidase; GSH, glutathione; HHcy, hyper-homocysteinemia; HMGCR, HMG-CoA reductase; HMGCS, HMG-CoA synthase; HO-1, heme oxygenase-1; hs-CRP, high-sensitivity C-reactive protein; ICAM-1, intercellular adhesion molecules-1; IL-6, interleukin-6; IR: insulin resistance; IA, intimal area; IT, intima thickness; IMT, intima-media thickness; LA, luminal area; LCAT, lecithin-cholesterol acyltransferase; LDH, lactate dehydrogenase; LOX-1, lectin-like oxidized low-density lipoprotein receptor-1; LO, luminal occlusion; LP-PLA2, lipoprotein-associated phospholipase A2; LXRα, liver X receptor α; MA, medial area; MDA, malondialdehyde; NADPH, nicotinamide adenine dinucleotide phosphate; NQO1, NADPH quinone oxidoreductase-1; NCA, necrotic core area; NEFA, nonesterified fatty acid; NF-κB, nuclear factor-kappa B; Nrf2, nuclear factor erythroid-2-related factor 2; OPN, osteopontin; ox-LDL, oxidized low-density lipoprotein; PAI-1, plasminogen activator inhibitor 1; PI3K, phosphatidylinositol-3-kinases; PPARγ, peroxisome proliferator-activated receptor γ; RCT, reverse cholesterol transport; SD, Sprague–Dawley; α-SMA, alpha smooth muscle actin; SM22α, smooth muscle 22 alpha; SR-B1, scavenger receptor class B type 1; SR-A1, scavenger receptor class A type 1; SOD, superoxide dismutase; sPLA2, secretory phospholipase A2; TNF-α, tumor necrosis factor-α; VV, vasa vasorum; VEGF-A, vascular endothelial growth factor-A; VCAM-1, vascular cell adhesion molecule-1; VSMCs, vascular smooth muscle cells; VEGF, vascular endothelial growth factor.

missing data, while 18 articles [22, 24, 25, 27–31, 38, 41, 49, 54, 57, 64, 70–72, 78] were unclear of the attrition bias. Although none of the studies provided any protocol, almost all had reported the expected outcome indicators, and most of them were evaluated as the low-risk bias. Moreover, other risks were not detected in the whole studies. The results showed that the methodology of the 60 studies included in this review was incomplete, and the quality was generally low.

3.4. Outcome Analysis

3.4.1. Models of AS. A total of 15 primary AS models were utilized in these studies, including HFD ApoE$^{-/-}$ mice, HFD LDLR$^{-/-}$ mice, HFD New Zealand or Japanese rabbits, HFD SD rats, HFD SD or Wistar rats with vitamin D3 injection, HFD Wistar rats with vitamin D3 injection and balloon injury in aorta, SD rats with the carotid artery balloon injury, HFD New Zealand rabbits or Japanese rabbits with balloon injury in aorta, HFD ApoE$^{-/-}$ mice with silastic collar implantation, Wistar rats with the silicone collar around the carotid artery, HFD Japanese rabbits or New Zealand rabbits with the silastic collar implantation around the carotid artery, C57BL/6 mice with the common carotid artery ligation, ApoE$^{-/-}$ mice combined partial ligation of the left common carotid artery and left renal artery, HFD New Zealand rabbits with balloon injury and plaques triggering by Chinese Russell viper venom (RVV), and HFD New Zealand rabbits with balloon injury, transfected with adenovirus-containing p53 and plaques triggered by RVV.

Among these, mice and rabbits were common animal species that accounted for 70% of the included studies. The HFD ApoE$^{-/-}$ mice model constituted 45% (27/60) of the studies, and rabbits made up 25% (15/60) of the studies. The models established by extra injection of adenovirus-containing p53 or triggered with RVV aimed to aggravate local inflammation and led to vulnerable plaques in rabbits [71, 72]. Despite the varied content of fat feeding, HFD was fed in most (93.3%, 56/60) of the animal models to promote the formation of AS. Furthermore, studies using only male animals constituted 81.7% (49/60) of the series.

3.4.2. Amelioration of Plaque Area and Artery Structure. In summary, most of the included studies [19–24, 26, 28, 30–42, 44–52], [55, 58, 63–66, 68–72, 74–78] showed that the drugs, including 22 drugs of Danhong

injection, Zhixiong capsule, Longshengzhi capsule, Tongxinluo capsule, Shexiang Baoxin pill, Danlou tablet, Angong Niuhuang pill, Longxuetongluo capsule, Longhu Rendan, Naoxintong pill/capsule, Di'ao Xinxuekang capsule, Xuezhikang, Qishenyiqi pill, ginkgo biloba tablet, Xuefu Zhuyu granule, Shexiang Tongxin dropping pill, compound Chuanxiong capsule, Yindanxinnaotong soft capsule, Fufang Danshen dropping pill, Suxiaojiuxin pill, Xuezhitong capsule, and Guanxinshutong capsule, significantly reduce the atherosclerotic plaque area (APA) in different AS models.

In addition to the reduction in APA, Zhixiong capsule altered the artery structure of attenuating intima thickening (IT), intimal area (IA), and IA/MA (intimal area/medial area) ratio [20, 78]; Danlou tablet reduced luminal occlusion (LO) and lipid content in the artery [24, 75, 77]; Naoxintong capsule, ginkgo biloba tablet, Tongxinluo capsule, and Fufang Danshen dropping pill also decreased LO [32, 37, 69, 70]; Angong Niuhuang pill attenuated IT and media thickness (MT) [35]; ginkgo biloba tablet, Danlou tablet, Tongxinluo capsule, Fufang Danshen dropping pill, and Xuefu Zhuyu granule reduced IT [37, 40, 46, 68]; Tongxinluo capsule decreased IA and the IA/MA ratio [49] and attenuated the external elastic membrane area (EEMA) and intima-media thickness (IMT) [71, 72].

3.4.3. Modification of Blood Lipid Level. Among these studies, 20 formulas, including Danhong injection, Zhixiong capsule, Danlou tablet, Longxuetongluo capsule, Naoxintong, Qishenyiqi pill, Angong Niuhuang pill, ginkgo biloba tablet, Xuefu Zhuyu granule, Yindanxinnaotong capsule, Longhu Rendan, Di'ao Xinxuekang capsule, compound Chuanxiong capsule, Tongxinluo, Shexiang Tongxin dropping pill, Fufang Danshen dropping pill, Xuezhikang, Suxiaojiuxin pill, Xuezhitong capsule, and Guanxinshutong capsule, showed the potential lipid-lowing property.

Furthermore, Danhong injection significantly suppressed the serum total triglyceride (TG) and low-density lipoprotein cholesterol (LDL-C) levels, upregulated the serum high-density lipoprotein cholesterol (HDL-C) level of HFD ApoE$^{-/-}$ mice [19], and downregulated the serum total cholesterol (TC), TG, and LDL-C levels of HFD New Zealand rabbits [63]. Zhixiong capsule administration showed a significant plasma lipid-lowering effect of the decreased TC level, LDL level, TC/HDL-C ratio, and log(TG/HDL-C) value and elevated HDL-C content [20, 78]. Danlou tablet also significantly reduced the TC, TG, and LDL-C levels in HFD ApoE$^{-/-}$ mice [77] and HFD Wistar rats with vitamin D3 injection [42] and increased the HDL-C levels in HFD ApoE$^{-/-}$ mice [24]. Longxuetongluo capsule decreased the serum TC, TG, and LDL-C levels and increased HDL-C levels in HFD male SD rats [26]. Naoxintong inhibited the serum LDL-C and TC in HFD New Zealand rabbits [57], reduced TC and TG in HFD LDLR$^{-/-}$ mice [58], and promoted the HDL-C level in HFD ApoE$^{-/-}$ mice [32]. Qishenyiqi pill decreased the level of blood LDL-C in HFD ApoE$^{-/-}$ mice [34]. Angong Niuhuang pill significantly reduced the serum content of TC, LDL-C, and the ratio of LDL-C to HDL-C in HFD male SD rats with vitamin D3 injection [35]. Ginkgo biloba tablet treatment significantly reduced serum levels of TC, TG, and LDL-C in HFD Wistar male rats with vitamin D3 injection and balloon injury in the aorta [37]. Xuefu Zhuyu granule reduced the serum level of TC in HFD Wistar male rats with vitamin D3 injection [40]. Yindanxinnaotong capsule also decreased the levels of blood TC, TG, and LDL-C in HFD SD male rats with vitamin D3 injection [48]. Longhu Rendan, Di'ao Xinxuekang capsule, or compound Chuanxiong capsule treatment ameliorated AS by significantly reducing serum levels of TC, TG, and LDL-C in HFD ApoE$^{-/-}$ mice [28, 30, 47]. Tongxinluo, Shexiang Tongxin dropping pill, Fufang Danshen dropping pill, Xuezhikang, Suxiaojiuxin pill, Guanxinshutong capsule, or Xuezhitong capsule treatment reduced serum levels of TC, TG, and LDL-C and increased HDL-C in different models [44, 52, 54, 66, 68, 72, 74, 76]. In addition, Danhong injection and compound Chuanxiong capsule decreased the atherosclerotic index (AI) [19, 47], which could be calculated as the ratio of non-HDL-C and HDL-C.

3.4.4. Modification of Plaque Stability. To summarize, nine formulas, including Longshengzhi capsule, Tongxinluo capsule, Naoxintong, Danhong injection, Xuezhikang, compound Chuanxiong capsule, Suxiaojiuxin pill, Zhixiong capsule, and Guanxinshutong capsule, could stabilize the plaques in different models.

Longshengzhi capsule maintained the integrity of the arterial wall and enhanced plaque stability by decreasing necrotic core areas (NCAs); increasing collagen-positive areas (CPAs), smooth muscle cell (SMC) content, and fibrous cap areas (FCAs); and inhibiting cell apoptosis in the lesion areas [21]. Tongxinluo capsule treatment increased the stability of plaques by increasing the intraplaque contents of SMC, CPA, and fibrous cap thickness (FCT) and reducing that of macrophages and lipids [22, 41]. The vulnerability index (VI) was calculated as follows: (lipids staining% + macrophages (MOMA-2) staining%)/(SMCs staining% + collagen staining%). Tongxinluo capsule treatment also stabilized atherosclerotic plaques by significantly attenuating VI and macrophage apoptosis and enhancing Beclin-1-induced autophagy [31]. In the plaque rupture models, Tongxinluo capsule treatment prevented vulnerable plaques from rupture by downregulating VI, reducing macrophages and lipids, increasing CPA and SMC, lowering the levels of matrix metalloproteinase-1 (MMP-1), MMP-3, and MMP-12, and upregulating tissue inhibitor of metalloproteinase-1 (TIMP-1) protein in plaques [71, 72]. Furthermore, Tongxinluo capsule treatment downregulated MMP-9 [64] and MMP-2 in plaques [22]. Naoxintong treatment enhanced plaque stability by increasing CPA, FCT, FCA, and SMC content and reducing the MMP-2 level, macrophage accumulation, and calcification events in lesion areas [32, 39]. Danhong injection maintained the content of CPA in the arterial wall and reduced the expression of MMP-2 and MMP-9 [53]. Xuezhikang treatment also increased CPA and SMC and decreased NCA, MMP-8, and MMP-13, thereby stabilizing the atherosclerotic plaques and

rupture by the suppression of macrophage endoplasmic reticulum (ER) stress-mediated apoptosis and the NF-κB pathway [33]. Compound Chuanxiong capsule increased collagen proportion in plaques [47]. Suxiaojiuxin pill enhanced atherosclerotic plaque stability by increasing SMC, TIMP-1, and TIMP-2 proteins while decreasing MMP-2 and MMP-9 proteins, which might be associated with the mechanism of modulating the MMPs/TIMPs balance [50]. Both Zhixiong and Guanxinshutong capsules enhanced plaque stability by increasing the content of CPA [76, 78]. In addition, Zhixiong capsule decreased vascular mineralization [78] and Guanxinshutong reduced the accumulation of macrophages in aortic root sections [76].

3.4.5. Amelioration of Lipid Metabolism and Lipid Accumulation. The disorder of hepatic lipid metabolism induced fatty liver and increased the risk of AS. Excessive accumulation of lipid in aortas and oxidative low-density lipoprotein (ox-LDL) taken in by macrophages could also lead to AS. A total of 14 formulas involving Longshengzhi capsule, Naoxintong, Shexiang Baoxin pill, Danlou tablet, Longhu Rendan, ginkgo biloba tablet, Di'ao Xinxuekang capsule, Xuezhitong capsule, Qishenyiqi pill, Danhong injection, Tongxinluo capsule, Shexiang Tongxin dropping pill, Zhixiong capsule, and Suxiaojiuxin pill described the related mechanisms.

Longshengzhi capsule ameliorated hepatic lipid metabolism by activating the sterol regulatory element binding protein (SREBP) 2 pathway and regulating the expression of SREBP1c protein, low-density lipoprotein receptor (LDLR), hydroxymethylglutaryl coenzyme A synthase (HMGCS), diacylglycerol acyltransferase-1 (DGAT1), adipose triglyceride lipase (ATGL), microsomal triglyceride transporter protein (MTTP), and apolipoprotein C II (APOC2) related to lipogenesis, cholesterol, and TG metabolism in the liver. Longshengzhi capsule also reduced AS lesions associated with the reduction of macrophage and foam cell accumulation by triggering the expression of ATP binding cassette transporter A1 (ABCA1) and ATP binding cassette transporter G1 (ABCG1) [21]. Naoxintong capsule reduced hepatic TG levels by the inhibition of TG synthesis and the activation of TG hydrolysis, including downregulation of DGAT1 while activating AMPKα, ATGL, and comparative gene identification-58 (CGI-58) expression in the liver [32]; Naoxintong treatment also significantly reduced foam cell accumulation in atherosclerotic plaques [29, 32]. Shexiang Baoxin pill treatment inhibited lipid accumulation by elevating the levels of liver X receptor α (LXRα), ABCA1, and ABCG1 and reducing the content of scavenger receptor class A (SR-A) and lectin-like oxidized low-density lipoprotein receptor-1 (LOX-1) in the arterial wall [23]. The mechanism of Danlou tablet in accelerating cholesterol efflux was to activate the peroxisome proliferator-activated receptor α (PPARα)/ABCA1 signaling pathway by upregulating the expression of PPARα, PGC-1α, and ABCA1 [24]. Longhu Rendan ameliorated AS via downregulating the protein expression of LOX-1 in the aortic root, subsequently attenuating AS and lipid deposition [28]. Ginkgo biloba tablet decreased the content of SR-A in the arterial wall [37]. Di'ao Xinxuekang capsule treatment demonstrated lipid-lowering and antiatherosclerotic mechanisms via the downregulation of proprotein convertase subtilisin/kexin type 9 (PCSK9) and upregulation of the LDLR signaling pathway in the liver tissue [30]. It also facilitated reverse cholesterol transport (RCT) via enhanced cholesterol efflux through ABCA1 and ABCG1 in aortas, the upregulation of HDL synthesis modulated by the PPARγ-LXRα-ABCA1 pathway, the modification of HDL maturation by increasing serum lecithin-cholesterol acyltransferase (LCAT) activity, and the promotion of scavenger receptor class B type 1 (SR-B1)-mediated HDL-cholesteryl ester uptake [33]. Xuezhitong capsule improved blood lipid dysfunction via the activation of RCT and the accompanying increase in the HDL levels, as characterized by improved ABCA1, SR-B1, LCAT, apolipoprotein A I (ApoA1), and apolipoprotein B (ApoB) [74]. Qishenyiqi pill treatment removed blood cholesterol by promoting the LDLR-LXR-α-ABCG5 pathway in the liver, and it also blocked phagocytosis of ox-LDL by macrophages by inhibiting the expression of CD36 in the aorta [34]. Danhong injection treatment reduced the AS by inhibiting HMG-CoA reductase (HMGCR), activating the LDLR in the liver, and reducing macrophage accumulation while increasing ABCA1 expression in the aortic root in various AS models [55]. Tongxinluo capsule administration promoted the antiatherosclerotic effects by increasing the level of PPARγ in aortas [64] and lowering the expression of macrophages and LOX-1 in vascular walls [65, 67, 72]. Zhixiong capsule blocked the proliferation of macrophages and monocytes, thereby reducing the formation of foam cells by upregulating p53 expression and decreasing MAPK14 expression [78]. Moreover, all these formulas, including Danlou tablet, Shexiang Tongxin dropping pill, Suxiaojiuxin pill, Tongxinluo capsule, and Xuezhitong capsule treatment, led to a significant reduction in the serum level of ox-LDL [42, 44, 61, 72, 74].

3.4.6. Anti-inflammation and Antioxidant Stress. The development and progression of AS were associated with oxidative stress and chronic inflammation. In summary, a total of 18 formulas, including Zhixiong capsule, Longshengzhi capsule, Tongxinluo capsule, Shexiang Baoxin pill, Danlou tablet, Angong Niuhuang pill, Longxuetongluo capsule, Xuezhikang, Qishenyiqi pill, ginkgo biloba tablet, Naoxintong capsule, Shexiang Tongxin dropping pill, compound Chuanxiong capsule, Yindanxinnaotong capsule, Danhong injection, Fufang Danshen dropping pill, Suxiaojiuxin pill, and Guanxinshutong capsule, have potential anti-inflammatory properties. Nine formulas, including Tongxinluo capsule, Shexiang Baoxin pill, Angong Niuhuang pill, Xuezhikang, Shexiang Tongxin dropping pill, Yindanxinnaotong capsule, Dahuang Zhechong pill, Suxiaojiuxin pill, and Guanxinshutong capsule, were related to antioxidant stress functions.

Zhixiong capsule intervened AS progression by blocking the proinflammatory process and increasing the plasma level of interleukin-4 (IL-4) and IL-13 [20, 78]. Longshengzhi

capsule reduced AS lesions related to potent anti-inflammatory effects, including decreasing the expression of serum tumor necrosis factor-α (TNF-α), the number of Kupffer cells, and the levels of C-C chemokine receptors-2 (CCR2), IL-6, monocyte chemoattractant protein-1 (MCP-1), and TNF-α in liver sections [21]. Tongxinluo capsule inhibited inflammation by reducing the expressions of IL-6, MMP-2, IL-1β, intercellular adhesion molecule-1 (ICAM-1), MCP-1, vascular cell adhesion molecule-1 (VCAM-1), and TNF-α in the arterial wall [22, 27, 49, 51, 52, 62, 71, 72]. Moreover, Tongxinluo also decreased the serum proinflammatory levels of IL-8, IL-18, high-sensitivity C-reactive protein (hs-CRP), MCP-1, MMP-1, ICAM-1, and VCAM-1 [51, 52, 62, 71, 72]. It may also reduce inflammation by inhibiting NF-κB expression in arteries [27, 45, 72]. Shexiang Baoxin pill regulated the serum levels of proinflammatory and anti-inflammatory cytokines, including MCP-1, interferon-γ (IFN-γ), IL-17A, IL-10, and transformed growth factor-β1 (TGF-β1), but decreased the levels of proinflammatory factors, including VCAM-1, ICAM-1, IL-6, and IL-2, in the vascular wall; moreover, it suppressed the activities of inflammation-related pathways by elevating the level of Mfn2 and reducing the phosphorylation of NF-κB, JNK, and p38 in the aorta [23]. Danlou tablet treatment attenuated AS by downregulating the NF-κB signaling pathway and decreasing the levels of IL-1β, MCP-1, IL-18, and IL-33 in plaques [24, 77] and suppressing the serum levels of IL-6, TNF-α, MCP-1, IL-8, MMP-1, MMP-2, ICAM-1, TNF-α, IL-1β, lipoprotein-associated phospholipase A2 (LP-PLA2), and secretory phospholipase A2 (sPLA2) in the aorta [42, 75]. Angong Niuhuang pill prevented AS associated with the anti-inflammatory effects and the immunoregulatory functions via multiple targets: the ratio of splenic T helper 17 cells (Th17) to regulatory T cell (Treg), cytokines (IL-6, TGF-β1, and IL-17), chemokines (MCP-1, MCP-2, MCP-3, CCR2, and CXCR3), cell adhesion molecules (ICAM-1 and VCAM-1) in the aorta [25], and serum CRP [35]. The underlying mechanism of the Longxuetongluo capsule for AS may be attributed to its anti-inflammatory effects of reducing serum levels of VCAM-1, ICAM-1, and MCP-1 and decreasing NF-κB expression in the aorta [26]. Xuezhikang treatment was also associated with the NF-κB proinflammatory pathway in ApoE$^{-/-}$ mice combined with artery ligations [33]. Qishenyiqi pill inhibited AS by promoting Treg immigration into atherosclerotic plaques and inhibiting the secretion of IL-17 via Th17 in the spleen and plaques [34]. Ginkgo biloba tablet also promoted the anti-inflammatory effects in reducing serum CRP, ICAM-1, and VCAM-1 levels [37]. Naoxintong capsule inhibited the expression of proinflammatory molecules MMP-2 and TNF-α in the aorta [39]. Shexiang Tongxin dropping pill treatment significantly decreased the serum levels of the proinflammatory cytokines IL-2, IL-6, TNF-α, and INF-γ [43, 44]. Compound Chuanxiong capsule prevented AS by regulating the PI3K/Akt/NF-κB signaling pathway and inhibiting the expression of IL-6 and TNF-α [47]. Yindanxinnaotong capsule relieved AS lesions by repressing the inflammation activity of inhibiting the NF-κB signaling pathway and serum proinflammatory cytokines IL-1β, CRP, and TNF-α [48]. Danhong injection administration reduced the proinflammatory cytokines, MCP-1 [53] and TNF-α [55]. Fufang Danshen dropping pill reduced VCAM-1 in the aorta [69], and Suxiaojiuxin pill reduced NF-κB protein expression in the aorta [61]. Guanxinshutong capsule also regulated AS progression by inhibiting TNF-α, IL-6, and NF-κB expression [76].

Tongxinluo inhibited oxidative stress injury by downregulating serum malondialdehyde (MDA), while upregulating the levels of nuclear factor erythroid-2-related factor 2 (Nrf2) and NADPH quinone oxidoreductase-1 (NQO1) in the arterial wall and increasing the serum levels of superoxide dismutase (SOD) and total antioxidant capacity (T-AOC) [27]. Shexiang Baoxin pill enhanced the antioxidative abilities by increasing SOD, catalase (CAT), and glutathione (GSH) in the circulation of ApoE$^{-/-}$ mice and improved the oxidative injury by reducing serum MDA, hydrogen peroxide (H_2O_2), and myeloperoxidase (MPO) content [23]. Angong Niuhuang pill also exerted the antioxidant effect of decreasing the serum MDA level [35]. Xuezhikang regulated the blood levels of MDA, SOD, CRP, and T-AOC [56, 59, 66]. Shexiang Tongxin dropping pill increased the serum levels of GSH and SOD and decreased MDA, which also reduced reactive oxygen species (ROS) generation in the aortic root lesions [43, 44]. Yindanxinnaotong capsule enhanced the antioxidative effect by regulating SOD, MDA, GSH, and glutathione peroxidase (GSH-PX) [48]. Guanxinshutong capsule improved serum SOD, MDA, and GSH and upregulated the expression of heme oxygenase-1 (HO-1) and Nrf2 in the aortic sinus [76]. Both Dahuang Zhechong and Suxiaojiuxin pills attenuated AS via the regulation of SOD and MDA levels in the serum [60, 61] and inhibited MPO in the arterial wall [60].

3.4.7. Other Effects and Mechanisms. Other mechanisms were mainly related to improved endothelial dysfunction, the inhibition of angiogenic factors, the regulation of VSMCs proliferation, and apoptosis.

Tongxinluo administration alleviated early AS and inhibited adventitial vasa vasorum (VV) angiogenesis by regulating the angiogenic expression of vascular endothelial growth factor-A (VEGF-A), its receptor VEGF-R2, angiopoietin-1 (ANGPT-1), and CD34 in the artery [27, 41, 46]. Tongxinluo also inhibited neointimal hyperplasia via the overexpression of miR-155 [49]. Moreover, Tongxinluo attenuated the chronic vasoconstriction in the regulation of neuronal nitric oxide synthase (nNOS) by stimulating the ERK1/2 signaling pathway [70]; it also improved endothelial functions by reducing serum ET-1 and upregulated nitric oxide (NO) [51]. In addition, Tongxinluo also inhibited monocyte adhesion via reduced plasminogen activator inhibitor type-1 (PAI-1) [62]. Xuezhikang inhibited AS lesions probably by elevating endothelial nitric oxide synthase (eNOS)/NO production in the aortic wall and improving hemorheology [56]; it also reduced blood hypercoagulation and inhibited the tissue factor expression [59]. Dahuang Zhechong pill inhibited AS by exerting a protective effect on

vascular endothelium, inhibiting VSMCs proliferation, and promoting VSMC apoptosis [60]. Both Danlou tablet and Xuefu Zhuyu granule decreased the serum level of platelet-derived growth factor (PDGF) and inhibited ERK1/2 signaling pathway activation and VSMCs proliferation [40]. Shexiang Baoxin pill reversed the dedifferentiation of VSMCs from the synthetic phenotype to the contractile phenotype [73]. Danhong injection treatment ameliorated HFD-induced AS and insulin resistance by activating the PI3K/AKT insulin pathway induced by insulin receptor substance-1 (IRS-1) [19]. The Danhong injection treatment also protected the endothelial function by inhibiting the expression of inducible nitric oxide synthase (iNOS) and COX-2 in the aortic wall [63]. Yindanxinnaotong inhibited AS on the vascular endothelial function markers, including thromboxane B2 (TXB2) and NO [48]. Shexiang Tongxin dropping pill regulated the expression of miR-21, miR-126, miR-155, miR-132, and miR-20 in the aorta, which might attenuate AS [43, 44]. Naoxintong capsule also showed potent atheroprotective power in reducing iNOS expression in AS lesions and inhibiting dendritic cell (DC) maturation [57, 58].

4. Discussion

In this review, we have summarized 60 studies, including 23 Chinese patent formulas in treating AS. The animal models, effects, and mechanisms were listed via a critical systematic review. Opposite to Western medicine, traditional Chinese herbs are aimed at multiple targets for various pharmaceutical ingredients. TCM also has the potential to increase the therapeutic efficacy of AS.

4.1. Choice of AS Models. Herein, we presented well-established animal models related to AS. The HFD ApoE−/− mice pattern might be a long-desired AS model owing to its high plasma TC level, foam cell-rich depositions in the proximal aortas, and easy breeding and handling procedures [79, 80]. Rabbits are also commonly used in AS models; both $ApoE^{-/-}$ mice and rabbits are suitable models for the studies of plaque stability and lipid accumulation in vascular walls. Despite the sensitivity to dietary cholesterol induction, the locations of AS lesions in rabbits are different from those of humans [81], and prolonged cholesterol feeding in rabbits may result in hepatic toxicity [82]. The major limitation of $ApoE^{-/-}$ mice is the rare occurrence of thrombosis and plaque rupture, which is common in humans [16]. Owing to the studies of vulnerable plaques, the rabbit model is successfully established through the overexpression of p53 in local plaques and triggered by RVV [83]. Rats and C57BL/6 mice are used in the included studies; these animals are naturally resistant to atherogenesis and lack plasma cholesteryl ester transfer protein (CETP) activity [79, 84]. In addition, the rat and mouse models established by HFD, vitamin D3 injection, balloon injury, and artery ligation may be valuable methods to promote AS; however, the fibrous plaques in the vascular wall lack lipid depositions and are different from those of $ApoE^{-/-}$ mice and rabbits [79]. Typically, there is no perfect model for any experimental condition, and an appropriate animal model should be considered based on the sample size, docility, feeding and housing, specific genetic profile, aims of the pathological aspects, costs, and analogy with humans [85].

4.2. Methodological Quality of the Results. We also assessed the methodological quality of the included studies and evaluated all of them as generally low. Although many entries were judged as unclear risk of bias, the reporting of essential details still needs to be emphasized. Sequence generation, baseline characteristics, and random outcome assessment are necessary to be reported in an animal experiment in order to make the results adequately comparable. Regarding random housing conditions, the pharmacological agents could be influenced because of inconsistent temperature, lighting, humidity, and non-randomized shelves or different rooms for animals [18]. For the judgment of attrition bias, the incomplete outcome data should be noticed and addressed adequately. SYRCLE's ROB is an adapted tool based on the Cochrane ROB tool that facilitates critical appraisal in a systematic review and improves the reporting quality of animal experiments. However, during the actual animal experiment, random methods should be considered with respect to animal weight, modeling parameters, and high-fat intake that would impact grouping. Although it is an effective method to improve internal validity and avoid subjectivity in interpreting the results, the blinding of caregivers, investigators, and outcome assessors in animal studies is often hard to achieve. Considering the practical difficulties in some items, we propose that SYRCLE's ROB could be further updated to better evaluate the animal experiments.

4.3. Effects and Mechanisms in All Formulas. Based on the outcome analysis, we summarized the effects and mechanisms involved in plaque formation and stability, the changes in the lipid level, lipid metabolism and accumulation, anti-inflammation, and antioxidative stress *in vivo*. Interestingly, most of the included drugs in different models reduce the areas of plaques, which are directly related to AS procession. Regarding the stability of plaques, the relevant factors are the areas of plaque necrotic core and fibrous cap, the content of collagen and SMCs, macrophage accumulation and apoptosis, and the synthesis and balance of MMPs/TIMPs in lesion areas. In addition, hyperlipidemia is the independent risk in AS, and over three-quarters of the drugs have reported the lipid-lowing property related to the downregulation of TC, TG, and LDL-C and upregulation of HDL-C in the serum level. The in-depth studies further found the mechanisms in the modification of hepatic lipid disorders and promoted lipid efflux from macrophages, which reduce the lipid deposition and indirectly inhibit AS development. Excessive phagocytosis of ox-LDL into macrophages depends on the scavenger receptors, such as SR-A, CD36, and LOX-1, and ultimately leads to foam cell formation and AS procession. In the current review, some formulas have also been identified for the property of

reducing the scavenger receptors. In addition, chronic inflammation and oxidative stress are the major contributors throughout the whole AS progression [86, 87]; some formulas have been verified to suppress the proinflammatory and pro-oxidative stress while activating the anti-inflammation and antioxidative stress, including the NF-κB signaling pathway and the related cytokines, chemokines, cell adhesion molecules, and oxidant enzymes. Moreover, some studies have listed other atheroprotective mechanisms in protecting endothelial injury and inhibiting VSMCs proliferation and migration.

4.4. Multiple Components and Targets in Chinese Patent Formulas. Statins are the first choice for AS that can reduce plasma cholesterol levels due to their effects on the synthesis, reuptake, and intestinal absorption of cholesterol [88]. Different from statins, Chinese patent formulas contain many active components with multiple targets and functions in AS. In this review, 16 studies of Tongxinluo capsules elucidated the effects and mechanisms of ameliorating APA, recovering the serum lipid level, inhibiting macrophage accumulation, stabilizing atherosclerotic plaques, reducing inflammation, and antioxidant stress, and protecting endothelial dysfunction in $ApoE^{-/-}$ mice and rabbit models. Especially in the vulnerable plaque rabbit model, Tongxinluo capsule treatment exerts protective effects in plaque rupture, and the mechanisms in the amelioration of MMPs and TIMPs were explored [31]. The bioactive ingredients from Tongxinluo also supported the evidence in the prevention and treatment of AS. According to the major extracts, ginsenoside Rb1 has anti-AS effects in reducing inflammation and oxidative stress responses, stabilizing plaques and attenuating the plaque formation. Additionally, it prevents endothelial dysfunction by upregulating the eNOS expression and improves the balance between apoptosis and autophagy; ginsenoside Rg1 has also been reported to inhibit AS by activating the AMPK/mTOR signaling pathway in the macrophages [89, 90]. Paeoniflorin is one of the aqueous extracts of Tongxinluo that could ameliorate AS by inhibiting the inflammation of the TLR4/MyD88/NF-κB pathway [91]. The combination of bioactive ingredients in a formula has a synergistic role in treating AS and is beneficial to the balance of the whole body.

Unlike other formulas, Xuezhikang extract from red yeast Chinese rice containing lovastatin, unsaturated fatty acids, essential amino acids, and ergosterol [59] naturally. In addition to the lipid-lowering and anti-inflammatory effects of lovastatin, Xuezhikang has also been investigated with respect to stabilizing atherosclerotic plaques and improving endothelial dysfunction, which might be related to other useful substances [33, 56]. In our study, other formulas like Danhong injection, Danlou tablet, and Naoxintong capsule were also significant. Besides the mechanisms in reducing APA and blood lipids, inhibiting plaque inflammation, and regulating the level of oxidative stress, Danhong injection can maintain the collagen content in the arterial wall and reduce the expression of MCP-1, MMP-2, and MMP-9 mRNAs in the aortic wall [53]; ethanol extracts of Danlou tablet plays a key role in anti-inflammation and preventing lipid deposition in macrophages of AS via suppressing the NF-κB signaling pathway and triggering the PPARα/ABCA1 signaling pathway [24]; Naoxintong has shown its ability in inhibiting dendritic cells maturation, improving endothelial function, and enhancing plaque stability [29, 32, 39, 57, 58]. In summary, multiple components with multiple targets in Chinese patent formulas are beneficial in AS and may surpass single Western therapies.

4.5. Limitations. Nevertheless, the present study has several limitations. Firstly, we used the qualitative synthesis rather than the quantitative method due to the varied models and inconsistent interventions, and hence, we could not draw specific conclusions from the meta-analysis. Owing to the stringent inclusion and exclusion criteria in the systematic review, relevant cell experiments were excluded, necessitating further investigation of the mechanisms *in vitro*. In addition, to elucidate the effects and mechanisms of action, HPLC/MS analysis for compound identification should be employed.

5. Conclusions

In summary, our analysis revealed the atheroprotective effects and mechanisms of 23 postmarketing Chinese patent formulas *in vivo*. In this systematic review, we first summarized the roles of the amelioration of plaques, the improvement of plaque stability, the modification of lipid level and metabolisms, and the anti-inflammation and antioxidant stress in alleviating AS lesions. Also, the methodological quality was found to be low in the included literature. Thus, additional high-quality evidence is essential through a broad perspective of postmarketing Chinese patent formulas in treating AS.

Abbreviations

ABCA1: ATP binding cassette transporter A1
ABCG1: ATP binding cassette transporter G1
ACAT: Acyl coenzyme A:cholesterol acyltransferase
AI: Atherosclerosis index
Akt: Serine/threonine kinase
AMPK: Adenosine monophosphate-activated protein kinase
ANGPT-1: Angiopoietin-1
APA: Atherosclerotic plaque area
APOA1: Apolipoprotein A I
APOB: Apolipoprotein B
AS: Atherosclerosis
CPA: Collagen-positive area
EEMA: External elastic membrane area
FAS: Fatty acid synthase
FCA: Fibrous cap area
FCT: Fibrous cap thickness
GSH-PX: Glutathione peroxidase
GSH: Glutathione
HMGCR: HMG-CoA reductase
HMGCS: HMG-CoA synthase

HO-1: Heme oxygenase-1
hs-CRP: High-sensitivity C-reactive protein
ICAM-1: Intercellular adhesion molecules-1
IL-6: Interleukin-6
IR: Insulin resistance
IA: Intimal area
IT: Intima thickness
IMT: Intima-media thickness
LA: Luminal area
LCAT: Lecithin-cholesterol acyltransferase
LDH: Lactate dehydrogenase
LDLR: Low-density lipoprotein receptor
LOX-1: Lectin-like oxidized low-density lipoprotein receptor-1
LO: Luminal occlusion
LP-PLA2: Lipoprotein-associated phospholipase A2
LXRα: Liver X receptor α
MA: Medial area
MDA: Malondialdehyde
NADPH: Nicotinamide adenine dinucleotide phosphate
NQO1: NADPH quinone oxidoreductase-1
NCA: Necrotic core area
NF-κB: Nuclear factor-kappa B
Nrf2: Nuclear factor erythroid-2-related factor 2
ox-LDL: Oxidized low-density lipoprotein
PI3K: Phosphatidylinositol-3-kinases
PPARγ: Peroxisome proliferator-activated receptor γ
RCT: Reverse cholesterol transport
SD: Sprague–Dawley
SREBP: Sterol regulatory element binding protein
SR-B1: Scavenger receptor class B type 1
SR-A1: Scavenger receptor class A type 1
SOD: Superoxide dismutase
sPLA2: Secretory phospholipase A2
TNF-α: Tumor necrosis factor-alpha
VCAM-1: Vascular cell adhesion molecule-1
VSMCs: Vascular smooth muscle cells.

Data Availability

All the data generated or analyzed during this study are included in this published article and its additional files.

Disclosure

Shiqi Chen and Xiaoxiao Wu are co-first authors. Yahong Wang and Mingjing Zhao are the corresponding authors.

Conflicts of Interest

The authors declare that there are no conflicts of interest regarding the publication of this article.

Authors' Contributions

YHW and MJZ designed the research and supervised the whole process. SQC and XXW conducted the literature searching and selection. TL, YL, and BFW extracted and analyzed the outcomes. WTC, YT, and JJY assessed the risk of bias. SQC drafted the manuscript with the help of HM, LW, ZWL, and YYJ. YHW and MJZ detected any mistakes in the entire process. All the authors have approved the final manuscript for submission.

Acknowledgments

This work was supported by the National Natural Science Foundation Project of China (grant no. 81774127) and the 2020 Science and Technology Innovation Project of Dongzhimen Hospital (grant no. DZMKJCX-2020-012).

Supplementary Materials

Table S1. Classification of the postmarketing Chinese patent formulas *in vivo*. Table S2. Classification of the AS models *in vivo*. Table S3. Details of herbal drugs of the included formulas. Table S4. The bias of included animal studies according to SYRCLE's ROB tool. (*Supplementary Materials*)

References

[1] World Health Organization, *Key Facts of Cardiovascular Diseases (CVDs)*, WHO, Geneva, Switzerland, 2021, https://www.who.int/en/news-room/fact-sheets/detail/cardiovascular-diseases-cvds.
[2] S. Feijóo-Bandín, A. Aragón-Herrera, and S. Moraña-Fernández, "Adipokines and inflammation: focus on cardiovascular diseases," *International Journal of Molecular Sciences*, vol. 21, no. 20, 2020.
[3] J. Han, H. Tan, Y. Duan et al., "The cardioprotective properties and the involved mechanisms of NaoXinTong Capsule," *Pharmacological Research*, vol. 141, pp. 409–417, 2019.
[4] L. Qiao and W. Chen, "Atheroprotective effects and molecular targets of bioactive compounds from traditional Chinese medicine," *Pharmacological Research*, vol. 135, pp. 212–229, 2018.
[5] M. C. S. Wong, D. X. Zhang, and H. H. X. Wang, "Rapid emergence of atherosclerosis in Asia," *Current Opinion in Lipidology*, vol. 26, no. 4, pp. 257–269, 2015.
[6] P. Bhatnagar, K. Wickramasinghe, E. Wilkins, and N. Townsend, "Trends in the epidemiology of cardiovascular disease in the UK," *Heart*, vol. 102, no. 24, pp. 1945–1952, 2016.
[7] F. Abdolmaleki, S. M. Gheibi Hayat, V. Bianconi, T. P. Johnston, and A. Sahebkar, "Atherosclerosis and immunity: a perspective," *Trends in Cardiovascular Medicine*, vol. 29, no. 6, pp. 363–371, 2019.
[8] G. K. Hansson and P. Libby, "The immune response in atherosclerosis: a double-edged sword," *Nature Reviews Immunology*, vol. 6, no. 7, pp. 508–519, 2006.
[9] N. C. Ward, G. F. Watts, and R. H. Eckel, "Statin toxicity," *Circulation Research*, vol. 124, no. 2, pp. 328–350, 2019.
[10] P.-P. Hao, F. Jiang, Y.-G. Chen et al., "Traditional Chinese medication for cardiovascular disease," *Nature Reviews Cardiology*, vol. 12, no. 2, pp. 115–122, 2015.
[11] C. Liu and Y. Huang, "Chinese herbal medicine on cardiovascular diseases and the mechanisms of action," *Frontiers in Pharmacology*, vol. 7, p. 469, 2016.

[12] P. Hao, F. Jiang, J. Cheng, L. Ma, Y. Zhang, and Y. Zhao, "Traditional Chinese medicine for cardiovascular disease," *Journal of the American College of Cardiology*, vol. 69, no. 24, pp. 2952–2966, 2017.

[13] L. Lu, X. Sun, C. Chen, Y. Qin, and X. Guo, "Shexiang baoxin pill, derived from the traditional Chinese medicine, provides protective roles against cardiovascular diseases," *Frontiers in Pharmacology*, vol. 9, p. 1161, 2018.

[14] C. Wang, M. Niimi, T. Watanabe, Y. Wang, J. Liang, and J. Fan, "Treatment of atherosclerosis by traditional Chinese medicine: questions and quandaries," *Atherosclerosis*, vol. 277, pp. 136–144, 2018.

[15] C. R. Hooijmans, A. Tillema, M. Leenaars, and M. Ritskes-Hoitinga, "Enhancing search efficiency by means of a search filter for finding all studies on animal experimentation in PubMed," *Laboratory Animals*, vol. 44, no. 3, pp. 170–175, 2010.

[16] B. Emini Veseli, P. Perrotta, G. R. A. De Meyer et al., "Animal models of atherosclerosis," *European Journal of Pharmacology*, vol. 816, pp. 3–13, 2017.

[17] A. Huang, R. Huang, X. Huang, J. Huang, and Y. Zhou, "Establishing animal models of atherosclerosis," *Chinese Journal of Tissue Engineering Research*, vol. 19, no. 27, pp. 4423–4428, 2015.

[18] C. R. Hooijmans, M. M. Rovers, R. B. de Vries, M. Leenaars, M. Ritskes-Hoitinga, and M. W. Langendam, "SYRCLE's risk of bias tool for animal studies," *BMC Medical Research Methodology*, vol. 14, no. 43, p. 43, 2014.

[19] M. Zhou, P. Ren, S. Li et al., "Danhong injection attenuates high-fat-induced atherosclerosis and macrophage lipid accumulation by regulating the PI3K/AKT insulin pathway," *Journal of Cardiovascular Pharmacology*, vol. 74, no. 2, pp. 152–161, 2019.

[20] J. Zhai, Z. Song, Y. Wang et al., "Zhixiong Capsule (ZXC), a traditional Chinese patent medicine, prevents atherosclerotic plaque formation in rabbit carotid artery and the related mechanism investigation based on network pharmacology and biological research," *Phytomedicine: International Journal of Phytotherapy and Phytopharmacology*, vol. 59, Article ID 152776, 2019.

[21] J. Ma, D. Zhao, X. Wang et al., "LongShengZhi capsule reduces established atherosclerotic lesions in apoe-deficient mice by ameliorating hepatic lipid metabolism and inhibiting inflammation," *Journal of Cardiovascular Pharmacology*, vol. 73, no. 2, pp. 105–117, 2019.

[22] J. Ma, L. Qiao, L. Meng et al., "Tongxinluo may stabilize atherosclerotic plaque via multiple mechanisms scanning by genechip," *Biomedicine & pharmacotherapy = Biomedecine & pharmacotherapie*, vol. 113, Article ID 108767, 2019.

[23] L. Lu, Y. Qin, and X. Zhang, "Shexiang baoxin pill alleviates the atherosclerotic lesions in mice via improving inflammation response and inhibiting lipid accumulation in the arterial wall," *Mediators of Inflammation*, vol. 2019, Article ID 6710759, 2019.

[24] D. Hao, W. Danbin, G. Maojuan et al., "Ethanol extracts of Danlou tablet attenuate atherosclerosis via inhibiting inflammation and promoting lipid effluent," *Pharmacological Research*, vol. 146, Article ID 104306, 2019.

[25] Y. Chai, Z. Yin, Q. Fan et al., "Protective effects of Angong Niuhuang pill on early atherosclerosis in ApoE-/- mice by reducing the inflammatory response," *Evidence-based Complementary and Alternative Medicine*, vol. 2019, Article ID 9747212, 2019.

[26] J. M. Zhou, H. M. Wang, Y. Z. Lv, Z. Z. Wang, and W. Xiao, "Anti-atherosclerotic effect of Longxuetongluo Capsule in high cholesterol diet induced atherosclerosis model rats," *Biomedicine & Pharmacotherapy*, vol. 97, pp. 793–801, 2018.

[27] Y. J. Yin, L. Y. Ma, and Z. H. Jia, "Tongxinluo alleviates adventitial vasa vasorum angiogenesis via regulating oxidative stress and inflammation in early carotid atherosclerosis," *International Journal of Clinical and Experimental Medicine*, vol. 11, no. 4, pp. 3368–3377, 2018.

[28] S. Yan, T. Wu, N. Li et al., "Protective effects of Chinese traditional medicine longhu rendan against atherosclerosis via negative regulation of LOX-1," *Evidence-based Complementary and Alternative Medicine*, vol. 2018, Article ID 4812639, 2018.

[29] Z. Wang, H. Shi, and H. Zhao, "Naoxintong retards atherosclerosis by inhibiting foam cell formation through activating pparalpha pathway," *Current Molecular Medicine*, vol. 18, no. 10, pp. 698–710, 2018.

[30] L. Qu, D. Li, X. Gao, Y. Li, J. Wu, and W. Zou, "Di'ao xinxuekang capsule, a Chinese medicinal product, decreases serum lipids levels in high-fat diet-fed apoE-/- mice by downregulating PCSK9," *Frontiers in Pharmacology*, vol. 9, p. 1170, 2018.

[31] Y. Chen, M. Li, Y. Zhang et al., "Traditional Chinese medication Tongxinluo attenuates apoptosis in ox-LDL-stimulated macrophages by enhancing Beclin-1-induced autophagy," *Biochemical and Biophysical Research Communications*, vol. 501, no. 2, pp. 336–342, 2018.

[32] X. Yang, Y. Li, L. Sun et al., "NaoXinTong enhances atorvastatin-induced plaque stability while ameliorating atorvastatin-induced hepatic inflammation," *Journal of Cardiovascular Pharmacology*, vol. 69, no. 1, pp. 55–64, 2017.

[33] L. Shen, Z. Sun, S. Chu et al., "Xuezhikang, an extract from red yeast rice, attenuates vulnerable plaque progression by suppressing endoplasmic reticulum stress-mediated apoptosis and inflammation," *PLoS One*, vol. 12, no. 11, Article ID e0188841, 2017.

[34] L. Peng, C.-S. Lv, Y. Zhao et al., "QiShenYiQi pill attenuates atherosclerosis by promoting regulatory T cells, inhibiting T helper 17 cells and accelerating cholesterol excretion," *Oncotarget*, vol. 8, no. 47, pp. 82196–82206, 2017.

[35] W.-J. Fu, T. Lei, Z. Yin et al., "Anti-atherosclerosis and cardioprotective effects of the Angong Niuhuang Pill on a high fat and vitamin D3 induced rodent model of atherosclerosis," *Journal of Ethnopharmacology*, vol. 195, pp. 118–126, 2017.

[36] G.-x. Dong, W.-w. Li, R.-z. Wang, W.-j. Zou, Z.-d. Zhong, and B.-g. Li, "Xinxuekang regulates reverse cholesterol transport by improving high-density lipoprotein synthesis, maturation, and catabolism," *Journal of Cardiovascular Pharmacology*, vol. 70, no. 2, pp. 110–118, 2017.

[37] G. Y. Zhu, W. Zhu, L. Y. Pan, X. J. Ma, H. T. Yuan, and G. Yang, "Effect of ginkgo biloba tablet on the expression of scavenger receptor A of the aortic wall in atherosclerotic rats," *Chinese Journal of Integrated Traditional and Western Medicine*, vol. 36, no. 4, pp. 449–453, 2016.

[38] J. Zheng, B. Liu, Q. Lun et al., "Longxuetongluo capsule inhibits atherosclerosis progression in high-fat diet-induced ApoE−/− mice by improving endothelial dysfunction," *Atherosclerosis*, vol. 255, pp. 156–163, 2016.

[39] X. Yang, L. Sun, Y. Li et al., "NaoXinTong inhibits the advanced atherosclerosis and enhances the plaque stability in apolipoprotein e deficient mice," *Journal of Cardiovascular Pharmacology*, vol. 67, no. 3, pp. 203–211, 2016.

[40] J. Miao, X. B. Zhou, W. Mao, J. Chen, and X. M. Xu, "Effects of xuefu zhuyu granule and danlou tablet on anti-atherosclerosis rats and potential mechanisms," *Chinese Journal of Integrated Traditional and Western Medicine*, vol. 36, no. 1, pp. 80–84, 2016.

[41] L. Ma, M. Ni, P. Hao et al., "Tongxinluo mitigates atherogenesis by regulating angiogenic factors and inhibiting vasa vasorum neovascularization in apolipoprotein E-deficient mice," *Oncotarget*, vol. 7, no. 13, pp. 16194–16204, 2016.

[42] J. Chen, H. W. Cai, J. Miao, X. M. Xu, and W. Mao, "Danlou tablet fought against inflammatory reaction in atherosclerosis rats with intermingled phlegm and blood stasis syndrome and its mechanism study," *Chinese Journal of Integrated Traditional and Western Medicine*, vol. 36, no. 6, pp. 703–708, 2016.

[43] M. Q. Xiong, C. L. Jia, and J. G. Cui, "Anti-atherosclerotic effects of bear bile powder in shexiang tongxin dripping pill: a mechanism study," *Chinese Journal of Integrated Traditional and Western Medicine*, vol. 35, no. 9, pp. 1083–1089, 2015.

[44] M. Xiong, C. Jia, J. Cui et al., "Shexiang Tongxin dropping pill attenuates atherosclerotic lesions in ApoE deficient mouse model," *Journal of Ethnopharmacology*, vol. 159, pp. 84–92, 2015.

[45] X. L. Wu, B. Zheng, L. S. Jin et al., "Chinese medicine Tongxinluo reduces atherosclerotic lesion by attenuating oxidative stress and inflammation in microvascular endothelial cells," *International Journal of Clinical and Experimental Pathology*, vol. 8, no. 6, pp. 6323–6333, 2015.

[46] Y. S. Lang, H. Y. Mi, H. L. Liu, and G. Q. Yuan, "Interventional effects of Tongxinluo combined with Atorvastatin and Aspirin (ATS) on the angiogenesis of vasa vasorum in the early stage of atherosclerosis," *Chinese Pharmacological Bulletin*, vol. 31, no. 1, pp. 71–76, 2015.

[47] Q. Kang, W. Liu, H. Liu, and M. Zhou, "Effect of compound Chuanxiong capsule on inflammatory reaction and PI3K/Akt/NF-kappaB signaling pathway in atherosclerosis," *Evidence-based Complementary and Alternative Medicine*, vol. 2015, Article ID 584596, 2015.

[48] L. Cheng, G. F. Pan, X. D. Zhang et al., "Yindanxinnaotong, a Chinese compound medicine, synergistically attenuates atherosclerosis progress," *Scientific Reports*, vol. 5, Article ID 12333, 2015.

[49] R.-n. Zhang, B. Zheng, L.-m. Li, J. Zhang, X.-h. Zhang, and J.-k. Wen, "Tongxinluo inhibits vascular inflammation and neointimal hyperplasia through blockade of the positive feedback loop between miR-155 and TNF-α," *American Journal of Physiology - Heart and Circulatory Physiology*, vol. 307, no. 4, pp. H552–H562, 2014.

[50] J. Zhang, P. Zhuang, Z. Lu et al., "Suxiaojiuxin pill enhances atherosclerotic plaque stability by modulating the MMPs/TIMPs balance in ApoE-deficient mice," *Journal of Cardiovascular Pharmacology*, vol. 64, no. 2, pp. 120–126, 2014.

[51] E.-H. Yao, H.-J. Wang, and C.-S. Xu, "Effects of tongxinluo on the neointima formation and expression of inflammatory cytokines in rats after carotid artery balloon injury," *Indian Journal of Pharmacology*, vol. 46, no. 5, pp. 510–514, 2014.

[52] L. Wang, H. T. Wang, C. Wei, J. F. Zhang, S. W. Tang, and W. G. Xiao, "Effects of Tongxinluo combined with atorvastatin and aspirin on atherosclerotic lesions in ApoE-/-mice," *Chinese Pharmacological Bulletin*, vol. 30, no. 1, pp. 135–139, 2014.

[53] M. Liu, Y. Chen, X. Yang et al., "DanHong Injection inhibits the development of primary abdominal aortic aneurysms in apoE knockout mice," *Chinese Science Bulletin*, vol. 59, no. 13, pp. 1366–1373, 2014.

[54] Q. X. Guo, J. Zhang, Y. Q. Li, and G. F. Zhang, "Study on anti-atherosclerotic effect of suxiao jiuxin pill and its mechanism," *African Journal of Traditional, Complementary, and Alternative Medicines*, vol. 11, no. 1, pp. 97–102, 2014.

[55] Y. Chen, M. Liu, T. Zhao et al., "Danhong Injection inhibits the development of atherosclerosis in both apoe−/− and Ldlr−/− Mice," *Journal of Cardiovascular Pharmacology*, vol. 63, no. 5, pp. 441–452, 2014.

[56] X. Y. Zhu, P. Li, Y. B. Yang, and M. L. Liu, "Xuezhikang, extract of red yeast rice, improved abnormal hemorheology, suppressed caveolin-1 and increased eNOS expression in atherosclerotic rats," *PLoS One*, vol. 8, no. 5, Article ID e62731, 2013.

[57] X. N. Zhong, H. H. Wang, Z. Q. Lu et al., "Effects of Naoxintong on atherosclerosis and inducible nitric oxide synthase expression in atherosclerotic rabbit," *Chinese Medical Journal*, vol. 126, no. 6, pp. 1166–1170, 2013.

[58] J. Zhao, H. Zhu, S. Wang et al., "Naoxintong protects against atherosclerosis through lipid-lowering and inhibiting maturation of dendritic cells in LDL receptor knockout mice fed a high-fat diet," *Current Pharmaceutical Design*, vol. 19, no. 33, pp. 5891–5896, 2013.

[59] P. Li, Y. Yang, and M. Liu, "Xuezhikang, extract of red yeast rice, inhibited tissue factor and hypercoagulable state through suppressing nicotinamide adenine dinucleotide phosphate oxidase and extracellular signal-regulated kinase activation," *Journal of Cardiovascular Pharmacology*, vol. 58, no. 3, pp. 307–318, 2011.

[60] C. J. Han, J. T. Liu, Y. Zhang, M. Li, X. M. Pang, and J. J. Mao, "Mechanism of Dahuang Zhechong pill against atherosclerosis induced by balloon angioplasty in rabbits," *Journal of Chinese Medicinal Materials*, vol. 34, no. 12, pp. 1919–1922, 2011.

[61] C.-s. Li, Z.-q. Qu, S.-s. Wang et al., "Effects of suxiao jiuxin pill () on oxidative stress and inflammatory response in rats with experimental atherosclerosis," *Journal of Traditional Chinese Medicine*, vol. 31, no. 2, pp. 107–111, 2011.

[62] Z. K. Song, R. Qu, L. Qin, and K. X. Huang, "Anti-atherosclerosis effect of Tongxinluo in rabbits and its mechanism," *Journal of Jilin University - Medicine Edition*, vol. 36, no. 1, pp. 119–122, 2010.

[63] T. T. Fu, C. J. Wang, C. Y. Min, and X. H. Huang, "Effects of danhong injection on experimental atherosclerosis rabbit model and its mechanism," *Journal of Traditional Chinese Medicine*, vol. 32, no. 11, pp. 1720–1722, 2009.

[64] H. Y. Cao, L. Qin, and K. X. Huang, "Effects of Tongxinluo on MMP-3, 9 and PPARgamma expressions in atherosclerotic rabbits," *Journal of Southern Medical University*, vol. 29, no. 9, pp. 1887–1889, 2009.

[65] Y. H. Yu, X. Q. Xu, Y. Wang, S. Z. Sun, and Y. Chen, "Intervention of Tongxinluo capsule against vascular lesion of atherosclerosis and its effect on lectin-like oxidized low density lipoprotein receptor-1 expression in rabbits," *Chinese Journal of Integrative Medicine*, vol. 12, no. 1, pp. 32–36, 2006.

[66] Y. G. Xie and X. L. Yu, "Inhibitory effects of Xuezhi Kang, folic acid and their combination on the progression of atherosclerosis in rabbits," *Chinese Journal of Clinical Rehabilitation*, vol. 10, no. 43, pp. 64–66, 2006.

[67] Z. Li, Y. J. Yang, and X. W. Qin, "Effects of Tongxinluo and Simvastatin on the stabilization of vulnerable atherosclerotic plaques of aorta in aortic atherosclerosis and molecular mechanism thereof: a comparative study with rabbits," *National Medical Journal of China*, vol. 86, no. 44, pp. 3146–3150, 2006.

[68] J. Y. Tian, J. Z. Chen, Y. Gu, and S. F. Xi, "Effect of fufang danshen diwan on blood lipid level and carotid atherosclerosis plaque in rabbits," *Chinese Journal of Clinical Rehabilitation*, vol. 8, no. 9, pp. 1708-1709, 2004.

[69] J. Z. Chen, J. Y. Tian, Y. Gu, S. F. Xi, K. Q. Fang, and X. P. Zhu, "Effect of fufang danshen diwan on the expression of vascular cell adhesion molecule-1 in the carotid artery wall of rabbits with atherosclerosis," *Chinese Journal of Clinical Rehabilitation*, vol. 8, no. 24, pp. 5048-5049, 2004.

[70] Q. Guan, M. Liu, R. Liu et al., "Tongxinluo induces nNOS expression through ERK activation," *Journal of Cardiovascular Pharmacology*, vol. 66, no. 1, pp. 9–15, 2015.

[71] W. Q. Chen, L. Zhong, L. Zhang et al., "Chinese medicine tongxinluo significantly lowers serum lipid levels and stabilizes vulnerable plaques in a rabbit model," *Journal of Ethnopharmacology*, vol. 124, no. 1, pp. 103–110, 2009.

[72] L. Zhang, Y. Liu, X. T. Lu et al., "Traditional Chinese medication Tongxinluo dose-dependently enhances stability of vulnerable plaques: a comparison with a high-dose simvastatin therapy," *American Journal of Physiology - Heart and Circulatory Physiology*, vol. 297, no. 6, pp. H2004–H2014, 2009.

[73] L. B. Liu, H. F. Shen, W. Cha et al., "SXBX pill suppresses homocysteine-induced vascular smooth muscle cells dedifferentiation by inhibiting NLRP3 inflammasomes activation via ERK/p38 MAPK pathways," *American Journal of Tourism Research*, vol. 11, no. 2, pp. 806–818, 2019.

[74] X. B. Meng, T. Zhu, D. H. Yang, W. Liang, G. B. Sun, and X. B. Sun, "Xuezhitong capsule, an extract of Allium macrostemon Bunge, exhibits reverse cholesterol transport and accompanies high-density lipoprotein levels to protect against hyperlipidemia in ApoE-/- mice," *Annals of Translational Medicine*, vol. 7, no. 11, p. 239, 2019.

[75] S. Gao, X. Xue, J. Yin et al., "Danlou tablet inhibits the inflammatory reaction of high-fat diet-induced atherosclerosis in ApoE knockout mice with myocardial ischemia via the NF-κB signaling pathway," *Journal of Ethnopharmacology*, vol. 263, Article ID 113158, 2020.

[76] Y. Lu, Y. Sun, and Z. Jiang, "Guanxinshutong alleviates atherosclerosis by suppressing oxidative stress and proinflammation in ApoE-/-mice," *Evidence-Based Complementary and Alternative Medicine*, vol. 2020, Article ID 1219371, 2020.

[77] Y. X. Sun, Y. Huang, and M. Zeng, "Based on "intestinal flora-inflammation" pathway to investigate effect and mechanism of Danlou Tablet on atherosclerosis of ApoE-/- mice," *Chinese Traditional and Herbal Drugs*, vol. 51, no. 9, pp. 2492–2500, 2020.

[78] J. Zhai, Z. Ren, Y. Wang et al., "Traditional Chinese patent medicine Zhixiong Capsule (ZXC) alleviated formed atherosclerotic plaque in rat thoracic artery and the mechanism investigation including blood-dissolved-component-based network pharmacology analysis and biochemical validation," *Journal of Ethnopharmacology*, vol. 254, Article ID 112523, 2020.

[79] X. F. Leong, C. Y. Ng, and K. Jaarin, "Animal models in cardiovascular research: hypertension and atherosclerosis," *BioMed Research International*, vol. 2015, Article ID 528757, 2015.

[80] S. H. Zhang, R. L. Reddick, J. A. Piedrahita, and N. Maeda, "Spontaneous hypercholesterolemia and arterial lesions in mice lacking apolipoprotein E," *Science*, vol. 258, no. 5081, pp. 468–471, 1992.

[81] M. H. Moghadasian, J. J. Frohlich, and B. M. McManus, "Advances in experimental dyslipidemia and atherosclerosis," *Laboratory Investigation*, vol. 81, no. 9, pp. 1173–1183, 2001.

[82] A. E. Yanni, "The laboratory rabbit: an animal model of atherosclerosis research," *Laboratory Animals*, vol. 38, no. 3, pp. 246–256, 2004.

[83] C.-m. Qi, L. Du, W.-h. Wu et al., "Detection of vulnerable atherosclerotic plaques in experimental atherosclerosis with the USPIO-enhanced MRI," *Cell Biochemistry and Biophysics*, vol. 73, no. 2, pp. 331–337, 2015.

[84] Y. C. Haa and P. J. Barter, "Differences in plasma cholesteryl ester transfer activity in sixteen vertebrate species," *Comparative Biochemistry and Physiology A Part B: Comparative Biochemistry*, vol. 71, no. 2, pp. 265–269, 1982.

[85] Y. T. Lee, H. Y. Lin, Y. W. Chan et al., "Mouse models of atherosclerosis: a historical perspective and recent advances," *Lipids in Health and Disease*, vol. 16, no. 12, p. 12, 2017.

[86] J. Viola and O. Soehnlein, "Atherosclerosis - a matter of unresolved inflammation," *Seminars in Immunology*, vol. 27, no. 3, pp. 184–193, 2015.

[87] J. F. Keaney and J. A. Vita, "Atherosclerosis, oxidative stress, and antioxidant protection in endothelium-derived relaxing factor action," *Progress in Cardiovascular Diseases*, vol. 38, no. 2, pp. 129–154, 1995.

[88] A. H. Ali, N. Younis, and R. Abdallah, "Lipid-lowering therapies for atherosclerosis: statins, fibrates, ezetimibe and PCSK9 monoclonal antibodies," *Current Medicinal Chemistry*, 2021.

[89] T.-T. Li, Z.-B. Wang, Y. Li, F. Cao, B.-Y. Yang, and H.-X. Kuang, "The mechanisms of traditional Chinese medicine underlying the prevention and treatment of atherosclerosis," *Chinese Journal of Natural Medicines*, vol. 17, no. 6, pp. 401–412, 2019.

[90] Q. Xue, N. He, Z. Wang et al., "Functional roles and mechanisms of ginsenosides from Panax ginseng in atherosclerosis," *Journal of Ginseng Research*, vol. 45, no. 1, pp. 22–31, 2021.

[91] H. Li, Y. Jiao, and M. Xie, "Paeoniflorin ameliorates atherosclerosis by suppressing TLR4-Mediated NF-κB activation," *Inflammation*, vol. 40, no. 6, pp. 2042–2051, 2017.

Hindawi
Evidence-Based Complementary and Alternative Medicine
Volume 2021, Article ID 6704798, 8 pages
https://doi.org/10.1155/2021/6704798

Research Article

Network Pharmacology and Molecular Docking-Based Analysis on Bioactive Anticoronary Heart Disease Compounds in *Trichosanthes kirilowii* Maxim and *Bulbus allii* Macrostemi

Yi-Ding Yu,[1] Wang-Jun Hou,[1] Juan Zhang,[2] Yi-Tao Xue,[2] and Yan Li[1,2]

[1]*Shandong University of Traditional Chinese Medicine, Jinan 250014, China*
[2]*Affiliated Hospital of Shandong University of Traditional Chinese Medicine, Jinan 250014, China*

Correspondence should be addressed to Yi-Tao Xue; xytsdzydfy@126.com and Yan Li; liyan88130@163.com

Received 15 September 2021; Accepted 5 November 2021; Published 16 November 2021

Academic Editor: Arquimedes Gasparotto Junior

Trichosanthes kirilowii Maxim. and *Bulbus allii* Macrostemi are the components of Gualou Xiebai decoction (GLXB), a commonly used herbal combination for the treatment of coronary heart disease (CHD) in traditional Chinese medicine. Although GLXB is associated with a good clinical effect, its active compounds and mechanism of action remain unclear, which limits its clinical application and the development of novel drugs. In this study, we explored key compounds, targets, and mechanisms of action for GLXB in the treatment of CHD using the network pharmacology approach. We identified 18 compounds and 21 action targets via database screening. Enrichment analysis indicated that the effects of GLXB in patients with CHD are primarily associated with the regulation of signalling pathways for tumour necrosis factor, nuclear factor-kappa B, hypoxia-inducible factor-1, arachidonic acid metabolism, and insulin resistance. GLXB thus exerts anti-inflammatory, antihypoxic, and antiagglutinating effects; regulates lipid metabolism; and combats insulin resistance in CHD via these pathways, respectively. After reverse targeting, we observed that the main active compounds of GLXB in the treatment of CHD were quercetin, naringenin, β-sitosterol, ethyl linolenate, ethyl linoleate, and prostaglandin B1. To explore the potential of these compounds in the treatment of CHD, we verified the affinity of the compounds and targets via molecular docking analysis. Our study provides a bridge for the transformation of natural herbs and molecular compounds into novel drug therapies for CHD.

1. Introduction

Coronary heart disease (CHD) is characterised by atherosclerosis in the coronary arteries, leading to blockage of the vascular lumen and subsequent myocardial ischaemia, hypoxia, and necrosis. In the 2016 update on Heart Disease and Stroke Statistics, the American Heart Association reported that 15.5 million individuals aged ≥20 years in the USA have CHD [1]. Thus, in addition to its severe effects on patient quality of life, CHD is associated with a significant societal and economic burden. Moreover, long-term use of aspirin, statins, and other drugs can have adverse effects on health [2, 3], making it necessary to identify alternative treatment strategies with a reduced risk of side effects.

In recent years, the field of drug research and development has placed an emphasis on identifying natural herbal medicines that can improve patient outcomes without the adverse effects of standard pharmacological agents. Gualou Xiebai decoction (GLXB) has long been used as a treatment for symptoms of chest pain in traditional Chinese medicine (TCM). However, due to the complexity of TCM compounds, multiple target sites, and diverse pathways of action, the previous research model—in which studies aim to identify unique compounds that exhibit regulatory activity at exclusive sites—cannot be used to adequately explain the overall role of TCM.

In 2008, British pharmacologist Andrew Hopkins proposed the idea of network pharmacology, which integrates

bioinformatics, multimodal pharmacology, network data analysis, and computer technology to update the current research model from "one target, one drug" to a network-based model. This "drug-compound-target" model offers an improved strategy for exploring associations between various drugs and diseases [4]. Therefore, in the current study, we aimed to analyse the mechanism by which GLXB exerts beneficial effects in the treatment of CHD using a network pharmacology approach. We also performed molecular docking analyses to verify the affinity between the compound and the target. Figure 1 is the schematic representation of the study workflow.

2. Methods

2.1. Data Collection and Processing. The Traditional Chinese Medicine Systems Pharmacology Platform (TCMSP) (http://lsp.nwu.edu.cn/) is an open database containing information regarding oral bioavailability (OB), drug similarity (DL), equal-reference values, targets of action, participating pathways, and related diseases for nearly 500 Chinese herbal medicines and their bioactive compounds [5]. The TCMSP was used to screen for GLXB compounds. According to the pharmacokinetic absorption, distribution, metabolism, and excretion parameters, $OB \geq 30\%$, and $DL \geq 0.18$ were the conditions used to screen out the active ingredients.

Bencao Zujian (HERB) (http://herb.ac.cn/) is a high-throughput database established by Professor Zhao Yi and his team [6]. They reanalysed the expression profiles of 6,164 genes in 1,037 high-throughput experiments evaluating herbs/ingredients and manually selected 1,241 gene targets and 494 modern diseases from 1,966 recently published articles. The HERB database is based on objective data and experiments, and relevant experimental support can be found for the interaction between each drug and target, with high reliability. We searched the database using "gualou" and "xiebai" as keywords to obtain the targets of GLXB.

Similarly, we searched the HERB and GeneCards (https://www.genecards.org/) databases using the term "coronary heart diseases" as a keyword to obtain the target of CHD.

2.2. Network Construction. We used the graphical software Cytoscape3.6.1 to construct the "compound-target" network diagram for GLXB. In the network diagram, "nodes" represent compounds or action targets, and "edges" represent the association between compounds and targets. First, we obtained the data input software from the TCMSP database to generate the basic network. Next, we examined the intersections of targets in all the databases to obtain the key targets. Finally, we selected the key target in the basic network and the compounds connected to it to obtain the key network.

2.3. Enrichment Analysis. Key targets were recorded in the DAVID6.8 database (https://david.ncifcrf.gov/summary.jsp) to obtain the Kyoto Encyclopedia of Genes and Genomes (KEGG) signalling pathway data. Results with P values less than 0.05 were considered significant and subjected to further analysis.

2.4. Molecular Docking. AutoDock Vina_1.1.2 software was used to conduct molecular docking analyses between major compounds and key targets of potential pathways. AutoDock Vina uses a semiflexible molecular docking model, in which the pharmacophore is flexible while the protein remains rigid during docking. The docking results were evaluated using a semiempirical free energy function.

The specific steps of molecular docking analysis were as follows: first, we downloaded the three-dimensional structure of the active ingredient file ("Spatial Data File" format) from the PubChem website (https://pubchem.ncbi.nlm.nih.gov/). We then downloaded the crystal structure of the key target molecule from the Protein Data Bank website (http://www.rcsb.org/). Subsequently, we used AutoDock tools to separate the target protein and its ligand, added a hydrogen atom, calculated the electric charge, and exported it to the PDBQT format file. Finally, we used Vina to connect the active ingredients with the target protein, and affinity data were extracted. PyMOL was used to analyse and plot the results [7].

3. Results

3.1. Data Collection. Analysis of the TCMSP database revealed that GL had 11 active compounds and 32 predicted targets, while XB had 21 active compounds and 32 predicted targets. From the HERB database, we identified 78 high-throughput targets for GL and 36 high-throughput targets for XB. We obtained 1,225 and 7,100 CHD targets in the HERB and GeneCards databases, respectively.

3.2. Network Diagram. We input the TCMSP data into the graphical software Cytoscape3.6.1 to generate the basic network. Subsequently, we intersected the targets extracted from all databases, which resulted in 21 key targets. Eighteen key compounds were identified and used to establish a key network by selecting the nodes connected to the key targets. The key network filtering process is illustrated in Figure 2.

3.3. Enrichment Analysis. KEGG analysis indicated that the key targets of GLXB in the treatment of CHD were enriched in 26 pathways, and 21 of them had P values less than 0.05. Among these pathways, the tumour necrosis factor (TNF) signalling pathway, nuclear factor (NF) kappa B signalling pathway, hypoxia-inducible factor (HIF) 1 signalling pathway, arachidonic acid metabolism, and insulin resistance were closely associated with GLXB treatment for CHD. The top 20 pathways identified in the enrichment analysis are shown in Figure 3. We also identified six key targets via reverse targeting in these five pathways: interleukin 6 (1ALU), TNF (2AZ5), prostaglandin-endoperoxide synthase 2 (PTGS2) (5KIR), B-cell leukaemia/lymphoma 2 (BCL2) (4LVT), nitric oxide synthase 3 (3EAH), and vascular cell adhesion molecule-1 (VCAM1) (1VCA).

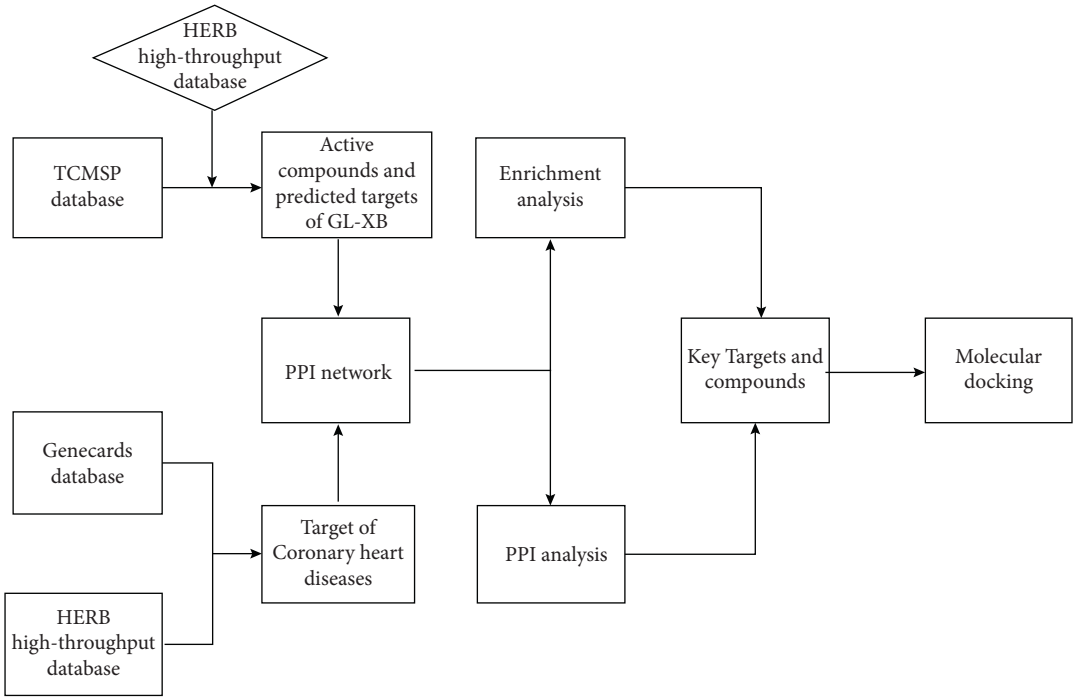

Figure 1: The workflow of our study. TCMSP: Traditional Chinese Medicine Systems Pharmacology Platform; GXLB: Gualou Xiebai decoction; HERB: Bencao Zujian; PPI: psychophysiological interaction.

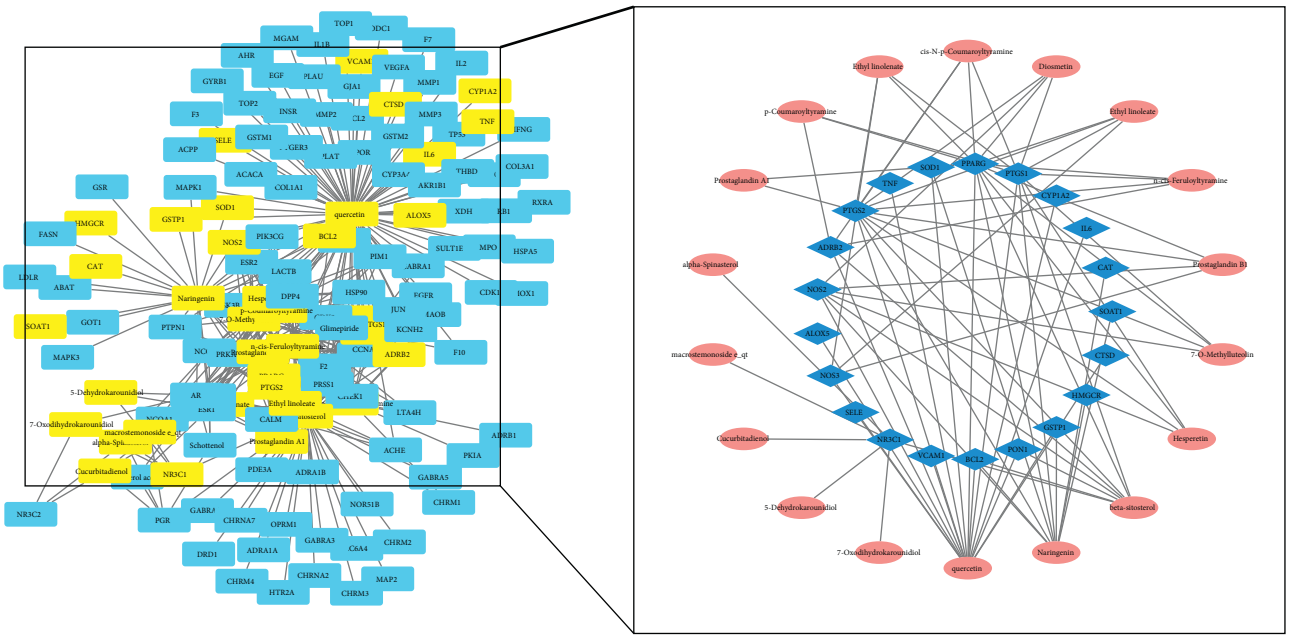

Figure 2: Filtering process for the network diagram. In the figure on the left, the squares represent all compound and protein targets. Among them, yellow squares represent intersection targets and intersection compounds. We extracted the yellow squares and arranged them to obtain the network diagram on the right, in which red ovals and blue diamonds represent the compounds and the targets, respectively.

3.4. Molecular Docking Results. AutoDock Vina evaluates the binding ability of small molecules to proteins mainly based on affinity. An affinity of less than 0 indicates that the ligand can spontaneously bind to the receptor, and smaller values are indicative of higher binding energy, meaning that the active compound is more easily associated with the receptor. We obtained the compounds associated with the key targets through the network diagram, which included quercetin, naringenin, β-sitosterol, ethyl linolenate, ethyl linoleate, and prostaglandin B1. The docking results are shown in Table 1. The compounds with the highest affinity are shown in Figure 4.

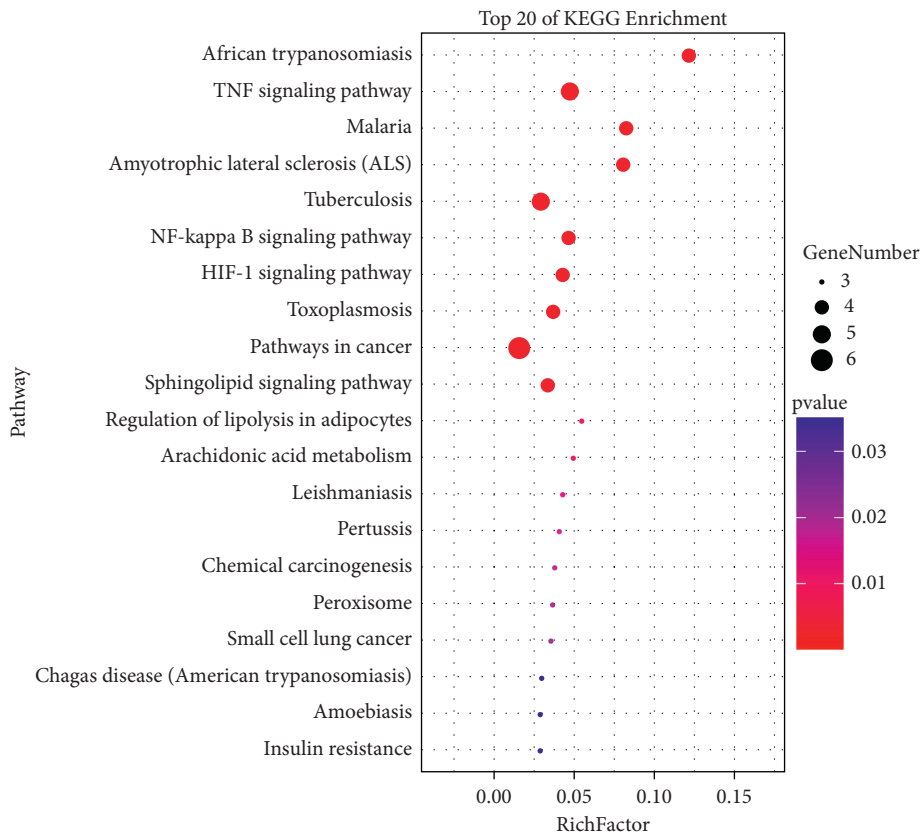

Figure 3: The top 20 results in the enrichment analysis. Among them, the tumour necrosis factor signalling pathway, nuclear factor-kappa B signalling pathway, hypoxia-inducible factor signalling pathway, arachidonic acid metabolism, and insulin resistance were closely associated with coronary heart disease.

Table 1: Molecular docking results.

	BCL2	IL-6	NOS3	PTGS2	TNF	VCAM1
Naringenin	−7.2	−6.2	−8.2	−9.4	−7.5	−6.6
Quercetin	−6.9	−6.3	−8.6	−9.7	−7.8	−6.4
β-Sitosterol	−7.6	−6.3	−9	−1.4	−8.3	−5.6
Prostaglandin B1	−6.3	−4.7	−7	−7.7	−6.5	−4.2
Ethyl linolenate	−5.4	−4.5	−6.4	−7.3	−5.6	−3.7
Ethyl linoleate	−5.8	−4.7	−6.2	−6.6	−5.4	−3.5

The figures in the table represent the affinity determined in the molecular docking analysis (kcal/mol).

4. Discussion

In previous centuries, in the absence of modern medical tests, doctors could only diagnose a patient's illness based on his/her appearance. The outward manifestation of CHD is chest discomfort associated with physical activity. TCM works indicate that the herbal medicine GLXB has been used to treat the external manifestations of chest discomfort. In traditional medicine, GLXB is believed to ease the symptoms of chest discomfort by smoothing the meridians. Our study suggests that the beneficial effects of GLXB in patients with CHD may be associated with intervention in pathways related to TNF signalling, NF-kappa B signalling, HIF-1 signalling, arachidonic acid metabolism, and insulin resistance.

Our understanding of CHD has deeply changed in recent years: atherosclerosis is no longer considered a simple lipid storage disorder but is instead regarded as a systemic inflammatory disease. Indeed, inflammation plays a pivotal role in all stages of atherogenesis, including foam cell accumulation, fatty streak organisation, fibrous plaque formation, acute plaque fissuring, rupture, and thrombosis [8].

The NF-kappa B signalling pathway is activated when the organism is stimulated or when reactive oxygen species become unbalanced, thus leading to the release of proinflammatory factors, such as IL-6, IL-8, TNF-α, iNOS, ICAM-1, VCAM-1, and cyclooxygenase (COX) 2. At the same time, increased production and release of proinflammatory factors further activate NF-kappa B, which in turn induces NOD-like receptor protein-3 inflammasomes, leading to continuous amplification of initial inflammatory signals and the inflammatory cascade effect [9, 10]. NF-kappa B also plays a central role in the activation of chemotactic cytokines, which contribute to the recruitment of monocytes/macrophages. Research has also indicated that NF-kappa B promotes the transcription and translation of monocyte chemotactic protein-1 and its receptor (chemotactic factor receptor), thereby activating VCAM-1 [11].

VCAM-1 attracts monocytes, which then migrate through the endothelial layer under the influence of various proinflammatory chemoattractants. Once within the arterial

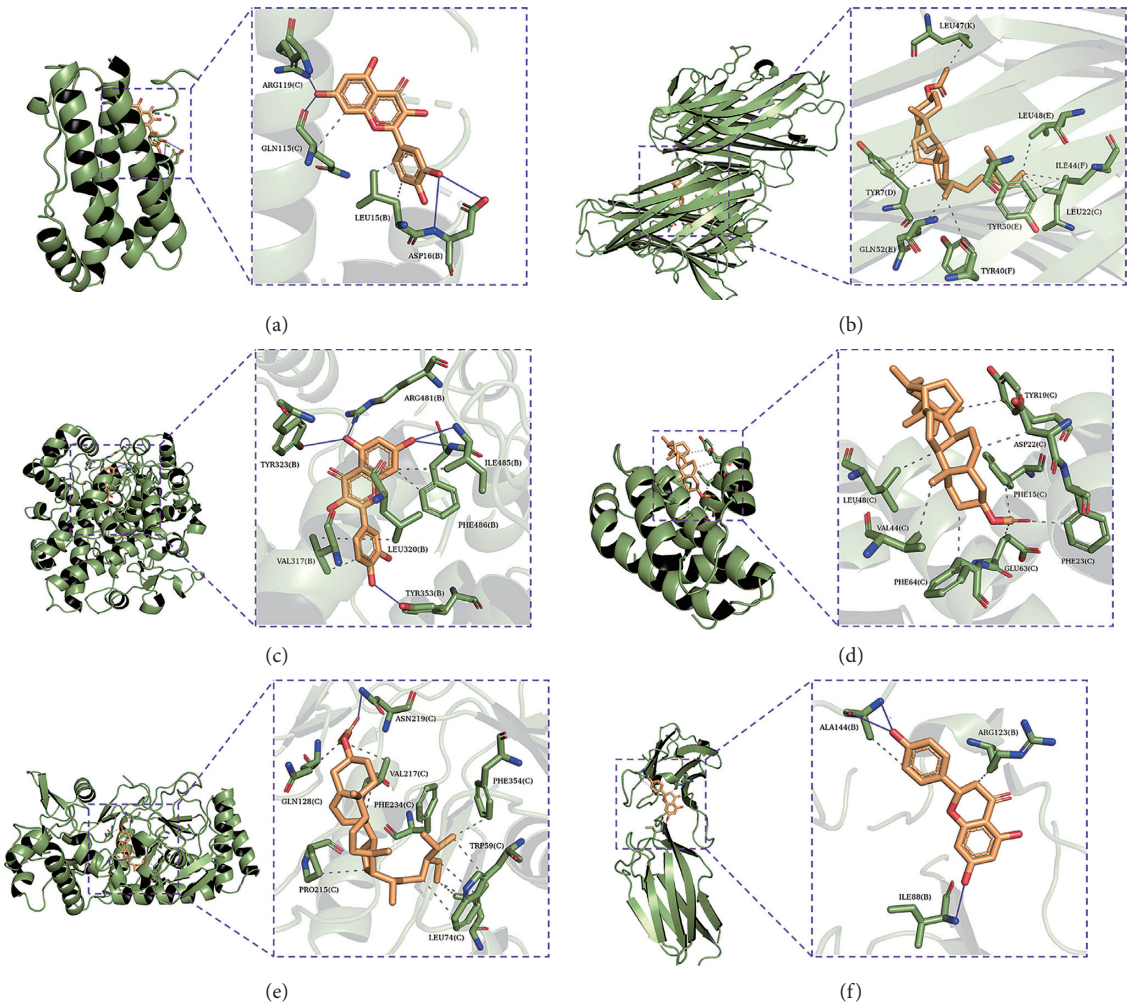

Figure 4: Components with the highest affinity in the molecular docking analysis. (a) Interleukin 6 and quercetin, affinity = −6.3 kcal/mol. (b) Tumour necrosis factor and β-sitosterol, affinity = −8.3 kcal/mol. (c) Prostaglandin-endoperoxide synthase 2 and quercetin, affinity = −9.7 kcal/mol. (d) B-cell leukaemia/lymphoma 2 and β-sitosterol, affinity = −7.6 kcal/mol. (e) Nitric oxide synthase 3 and β-sitosterol, affinity = −9 kcal/mol. (f) Vascular cell adhesion molecule-1 and naringenin, affinity = −6.6 kcal/mol. Solid blue lines represent hydrogen bonds, while dotted grey lines represent hydrophobic interactions.

intima, the monocytes continue to undergo inflammatory changes, transform into macrophages, engulf lipids, and become foam cells. T lymphocytes also migrate into the intima, where they release proinflammatory cytokines that amplify the inflammatory activity. Inflammatory cells then attach and cross the blood vessel wall into the ischaemic areas of the heart, where they cleave proteases to produce reactive oxygen species and block microvessels, resulting in damage to the heart cells [12].

IL-6 is secreted by T cells, macrophages, and endothelial cells and propagates inflammatory cascades in response to inflammatory stimuli [13]. An animal study has demonstrated that IL-6 administration to apolipoprotein $E^{-/-}$ mice on a high-fat diet can promote plaque formation [14]. In addition, animal studies have found elevated levels of IL-6 in mast cell-deficient mice, suggesting that IL-6 is a mediator of CHD. IL-6 may promote a procoagulant state by upregulating the expression of fibrinogen [15], which is considered a downstream marker of the inflammatory response. In addition to participating in the clotting cascade, fibrinogen is hypothesised to stimulate smooth muscle cell migration, promote platelet aggregation, and increase blood viscosity [16]. Previous studies have shown that fibrin may bind to lipoproteins in blood vessel walls, promoting lipid accumulation in fibrous plaques, and leading to plaque growth [17].

TNF-α is a proinflammatory cytokine that can lead to tumour cell necrosis. TNF-α is involved in the pathological process of atherosclerosis by increasing inflammatory cells in injured tissues and assisting vascular smooth muscle remodeling [18]. Meanwhile, TNF-α can decrease the expression of endothelial NOS, reduce the bioavailability of nitric oxide, and promote oxidative stress by decreasing levels of nitric oxide and endothelial NOS expression. This process intensifies oxidative damage to vascular endothelial cells and promotes plaque formation [19]. TNF-α is also an exogenous activator of cell apoptosis [20], and the inhibition of vascular smooth muscle cell death during the

development of CHD plays a significant role in reducing the lesion area and promoting cardiac recovery [21].

BCL2 is a key antiapoptotic protein. Studies have shown that apoptotic cells induce an inflammatory response by releasing inflammatory cytokines and an immune response by directly activating dendritic cells. These results suggest that CHD can be treated by overexpressing BCL2 in cardiomyocytes to protect them from apoptosis and inhibit local inflammation [22].

The HIF-1 signalling pathway involves the expression of more than 100 genes that coordinate the adaptive response of tissues to hypoxia. HIF-1, a transcriptional regulator produced in response to hypoxia, is degraded by proteasome action on proline hydroxylase (PHD) under normoxic conditions. However, PHD activity is inhibited under hypoxic conditions; thus, HIF-1 cannot be degraded [23]. HIF-1 plays an important role in angiogenesis, and its downstream genes can induce the production of a variety of angiogenic signalling molecules, including vascular endothelial growth factor, angiotensin (Ang) I, and Ang-II [24]. Therefore, HIF-1 can improve exercise tolerance and quality of life in patients with CHD by promoting the formation of ischaemic myocardial collateral circulation [25]. In addition, studies have shown that HIF-1 can reduce the expression of NF kappa-B and inflammatory factors, thereby reducing the inflammatory response in the myocardium [26].

Arachidonic acid (AA) is the precursor of a series of proinflammatory/proaggregating mediators that are metabolised by COX and lipoxygenases into prostaglandins, thromboalkanes, leukotrienes, and other oxidative derivatives [27]. Among them, prostaglandin E2 and leukotriene B4 can promote the production of IL-6 and increase vascular permeability. Thrombosis A2 affects blood pressure and blood flow and promotes platelet activation and aggregation [28]. COX, which plays an important role in this process, has been identified in three subtypes, but only COX-1 and COX-2 are functional. The former, which is structurally expressed in most normal tissues, is a housekeeping enzyme responsible for a variety of physiological functions and is involved in the formation of thromboxane A2. The latter is rarely expressed in normal tissues but is rapidly induced by cytokines and growth factors [29]. COX-2 is involved in angiogenesis, inhibition of apoptosis, and suppression of the immune response, which are closely associated with CHD. The risk of cardiovascular events associated with COX-2 is correlated with polymorphisms in the gene promoter PTGS2 [30]. Meanwhile, as an antagonist of eicosapentaenoic acid (EPA), AA blocks the regulation of lipid metabolism and the anti-inflammatory and antiplatelet effects of EPA. Evidence suggests that reducing the intravascular level of AA can reduce the risk of adverse cardiovascular events [31].

Resistance of muscle and adipose tissue to insulin regulation leads to elevated plasma insulin and free fatty acid concentrations. This combination stimulates liver very low-density lipoprotein (LDL) triglyceride (TG) secretion, leading to increased plasma TG concentrations and hypertriglyceridemia in insulin-resistant nondiabetic individuals [32]. Elevated levels of IL-6 and TNF-α also induce insulin resistance and promote the development of CHD. Accordingly, reducing insulin resistance has proven beneficial in patients with CHD [33].

The current results indicate that the active components of GLXB in the treatment of CHD are mainly quercetin, naringenin, β-sitosterol, ethyl linolenate, ethyl linoleate, and prostaglandin B1. Molecular docking results revealed that these components have affinity values less than 0, indicating that they can spontaneously bind to their key targets, thus inhibiting the function of the protein.

Flavonoids have been shown to have significant cardiac benefits, such as inhibiting LDL oxidation and endothelial-dependent vasodilation, reducing levels of adhesion molecules, and other inflammatory markers while protecting nitric oxide and endothelial function under conditions of oxidative stress and preventing oxidation and inflammatory damage to neurons and platelet aggregation [34]. Quercetin and naringenin are flavonoids. Some studies have shown that treatment with 120 mg of quercetin daily can inhibit inflammation and reduce NF-kappa B transcription activity in patients with CHD [35]. Naringenin also inhibits the production of inflammatory factors and NF-kappa B activation [36]. In terms of metabolism, naringenin has been shown to reduce plasma triglyceride and cholesterol levels as well as insulin resistance [37].

The European Food Safety Authority and US Food and Drug Administration recommend that individuals consume 1.5 to 2.4 g of phytosterols daily to lower blood cholesterol levels, as this reduces the risk of heart disease [38]. β-Sitosterol is a phytosterol that exerts anti-inflammatory and immunomodulatory effects by reducing plasma IL-6 and TNF-α levels [39]. Although few studies have investigated the effects of ethyl linoleate, ethyl linolenic acid, and prostaglandin B1, the current study highlights the potential of these three compounds in the treatment of CHD based on their modes of action and the results of the molecular docking analysis. Further studies are required to determine whether these compounds have clinical significance in the treatment of CHD.

This study had some limitations. Despite the integration of information from the databases screened in our study, we may have missed some compounds that exert positive effects in patients with CHD. At the same time, due to the limitations of network pharmacology, additional studies are required to determine the dose-effect relationships of the compounds identified in the current study.

5. Conclusion

Using a network pharmacology approach, the current study identified the material basis and potential mechanisms by which GLXB exerts its effects in the treatment of CHD. This approach conforms to the scenario observed for many TCM formulations, which include multiple compounds that act on multiple targets. Our molecular docking analyses allowed us to determine the affinity between the compounds and their targets, providing preliminary evidence regarding the potential of these compounds in the treatment of CHD. Our study thus provides new insight into screening for active small molecular compounds contained in natural herbs, which is beneficial for the development of new drugs.

Data Availability

The data used to support the findings of this study are available from the corresponding author upon request.

Conflicts of Interest

The authors declare no conflicts of interest in this work.

Authors' Contributions

Yu YD drafted the manuscript, contributed to data analysis, and revised the final manuscript. Hou WJ and Zhang J provided the data and theoretical support. Xue YT and Li Y provided advice during the study and manuscript preparation. All authors read and approved the final manuscript.

Acknowledgments

The authors sincerely thank the National Natural Science Foundation of China (grant nos. 81804045 and 81774247) for their support.

References

[1] F. Sanchis-Gomar, C. Perez-Quilis, R. Leischik, and A. Lucia, "Epidemiology of coronary heart disease and acute coronary syndrome," *Annals of Translational Medicine*, vol. 4, no. 13, p. 256, 2016.

[2] A. A. White and D. D. Stevenson, "Side effects from daily aspirin treatment in patients with AERD: identification and management," *Allergy and Asthma Proceedings*, vol. 32, no. 5, pp. 333-334, 2011.

[3] F. A. Wood, J. P. Howard, J. A. Finegold et al., "N-of-1 trial of a statin, placebo, or no treatment to assess side effects," *New England Journal of Medicine*, vol. 383, no. 22, pp. 2182–2184, 2020.

[4] A. L. Hopkins, "Network pharmacology: the next paradigm in drug discovery," *Nature Chemical Biology*, vol. 4, no. 11, pp. 682–690, 2008.

[5] J. Ru, P. Li, J. Wang et al., "TCMSP: a database of systems pharmacology for drug discovery from herbal medicines," *Journal of Cheminformatics*, vol. 6, no. 1, p. 13, 2014.

[6] S. Fang, L. Dong, L. Liu et al., "HERB: a high-throughput experiment- and reference-guided database of traditional Chinese medicine," *Nucleic Acids Research*, vol. 49, no. D1, pp. D1197–D1206, 2021.

[7] Y. D. Yu, Y. P. Xiu, Y. F. Li, and Y. T. Xue, "To explore the mechanism and equivalent molecular group of fuxin mixture in treating heart failure based on network pharmacology," *Evidence-Based Complementary and Alternative Medicine: eCAM*, vol. 2020, Article ID 8852877, 10 pages, 2020.

[8] M. Fioranelli, A. G. Bottaccioli, F. Bottaccioli, M. Bianchi, M. Rovesti, and M. G. Roccia, "Stress and inflammation in coronary artery disease: a review Psychoneuroendocrineimmunology-based," *Frontiers in Immunology*, vol. 9, p. 2031, 2018.

[9] J. E. Barbosa, M. B. Stockler-Pinto, B. O. D. Cruz et al., "Nrf2, NF-κB and pparβ/δ mRNA expression profile in patients with coronary artery disease," *Arquivos Brasileiros de Cardiologia*, vol. 113, no. 6, pp. 1121–1127, 2019.

[10] Q. Su, L. Li, Y. Sun, H. Yang, Z. Ye, and J. Zhao, "Effects of the TLR4/Myd88/NF-κB signaling pathway on NLRP3 inflammasome in coronary microembolization-induced myocardial injury," *Cellular Physiology and Biochemistry*, vol. 47, no. 4, pp. 1497–1508, 2018.

[11] N. S. Rial, K. Choi, T. Nguyen, B. Snyder, and M. J. Slepian, "Nuclear factor kappa B (NF-κB): a novel cause for diabetes, coronary artery disease and cancer initiation and promotion?" *Medical Hypotheses*, vol. 78, no. 1, pp. 29–32, 2012.

[12] P. Libby, "Inflammation and cardiovascular disease mechanisms," *The American Journal of Clinical Nutrition*, vol. 83, no. 2, pp. 456S–460S, 2006.

[13] J. S. Yudkin, M. Kumari, S. E. Humphries, and V. Mohamed-Ali, "Inflammation, obesity, stress and coronary heart disease: is interleukin-6 the link?" *Atherosclerosis*, vol. 148, no. 2, pp. 209–214, 2000.

[14] E. Bernberg, M. A. Ulleryd, M. E. Johansson, and G. M. L. Bergström, "Social disruption stress increases IL-6 levels and accelerates atherosclerosis in ApoE−/− mice," *Atherosclerosis*, vol. 221, no. 2, pp. 359–365, 2012.

[15] K. Ganeshan and P. J. Bryce, "Regulatory T cells enhance mast cell production of IL-6 via surface-bound TGF-β," *The Journal of Immunology*, vol. 188, no. 2, pp. 594–603, 2012.

[16] M. W. Mosesson, "Fibrinogen and fibrin structure and functions," *Journal of Thrombosis and Haemostasis*, vol. 3, no. 8, pp. 1894–1904, 2005.

[17] E. Ernst and W. Koenig, "Fibrinogen and cardiovascular risk," *Vascular Medicine*, vol. 2, no. 2, pp. 115–125, 1997.

[18] J. Xing, Y. Liu, and T. Chen, "Correlations of chemokine CXCL16 and TNF-α with coronary atherosclerotic heart disease," *Experimental and Therapeutic Medicine*, vol. 15, no. 1, pp. 773–776, 2018.

[19] X. Li, F. Zhang, H. Zhou et al., "Interplay of TNF-α, soluble TNF receptors and oxidative stress in coronary chronic total occlusion of the oldest patients with coronary heart disease," *Cytokine*, vol. 125, Article ID 154836, 2020.

[20] Y. Dong, H. Chen, J. Gao, Y. Liu, J. Li, and J. Wang, "Molecular machinery and interplay of apoptosis and autophagy in coronary heart disease," *Journal of Molecular and Cellular Cardiology*, vol. 136, pp. 27–41, 2019.

[21] S. Wang, Z. Cheng, and X. Chen, "Promotion of PTEN on apoptosis through PI3K/Akt signal in vascular smooth muscle cells of mice model of coronary heart disease," *Journal of Cellular Biochemistry*, vol. 120, no. 9, pp. 14636–14644, 2019.

[22] M. Tanaka, S. Nakae, R. D. Terry et al., "Cardiomyocyte-specific Bcl-2 overexpression attenuates ischemia-reperfusion injury, immune response during acute rejection, and graft coronary artery disease," *Blood*, vol. 104, no. 12, pp. 3789–3796, 2004.

[23] D. Tekin, A. D. Dursun, and L. Xi, "Hypoxia inducible factor 1 (HIF-1) and cardioprotection," *Acta Pharmacologica Sinica*, vol. 31, no. 9, pp. 1085–1094, 2010.

[24] G. L. Semenza, "Regulation of vascularization by hypoxia-inducible factor 1," *Annals of the New York Academy of Sciences*, vol. 1177, no. 1, pp. 2–8, 2009.

[25] C. Song-Ming, L. Yu-Guang, Z. Hong-xuan et al., "Hypoxia-inducible factor-1α induces the coronary collaterals for coronary artery disease," *Coronary Artery Disease*, vol. 19, no. 3, pp. 173–179, 2008.

[26] D. Bandarra, J. Biddlestone, S. Mudie, H. A. Muller, and S. Rocha, "HIF-1α restricts NF-κB dependent gene expression to control innate immunity signals," *Disease Models & Mechanisms*, vol. 8, no. 2, pp. 169–181, 2015.

[27] P. C. Calder, "n−3 Polyunsaturated fatty acids, inflammation, and inflammatory diseases," *The American Journal of Clinical Nutrition*, vol. 83, no. 6, pp. 1505S–1519S, 2006.

[28] T. Sonnweber, A. Pizzini, M. Nairz, G. Weiss, and I. Tancevski, "Arachidonic acid metabolites in cardiovascular and metabolic diseases," *International Journal of Molecular Sciences*, vol. 19, no. 11, p. 3285, 2018.

[29] C.-L. Xuan, W. Yan, L. Xuan, and R.-H. Xu, "PTGS2 gene polymorphism -765G>C is associated with coronary artery disease: a meta-analysis," *Genetics and Molecular Research*, vol. 13, no. 1, pp. 1491–1496, 2014.

[30] S. Ross, J. Eikelboom, S. S. Anand et al., "Association of cyclooxygenase-2 genetic variant with cardiovascular disease," *European Heart Journal*, vol. 35, no. 33, pp. 2242–2248, 2014.

[31] M. Kanoh, K. Inai, T. Shinohara, H. Tomimatsu, and T. Nakanishi, "Clinical implications of eicosapentaenoic acid/arachidonic acid ratio (EPA/AA) in adult patients with congenital heart disease," *Heart and Vessels*, vol. 32, no. 12, pp. 1513–1522, 2017.

[32] G. Reaven, "Insulin resistance and coronary heart disease in nondiabetic individuals," *Arteriosclerosis, Thrombosis, and Vascular Biology*, vol. 32, no. 8, pp. 1754–1759, 2012.

[33] V. Rotter, I. Nagaev, and U. Smith, "Interleukin-6 (IL-6) induces insulin resistance in 3T3-L1 adipocytes and is, like IL-8 and tumor necrosis factor-α, overexpressed in human fat cells from insulin-resistant subjects," *Journal of Biological Chemistry*, vol. 278, no. 46, pp. 45777–45784, 2003.

[34] R. V. Patel, B. M. Mistry, S. K. Shinde, R. Syed, V. Singh, and H.-S. Shin, "Therapeutic potential of quercetin as a cardiovascular agent," *European Journal of Medicinal Chemistry*, vol. 155, pp. 889–904, 2018.

[35] N. Chekalina, Y. Burmak, Y. Petrov et al., "Quercetin reduces the transcriptional activity of NF-kB in stable coronary artery disease," *Indian Heart Journal*, vol. 70, no. 5, pp. 593–597, 2018.

[36] F. A. Pinho-Ribeiro, A. C. Zarpelon, V. Fattori et al., "Naringenin reduces inflammatory pain in mice," *Neuropharmacology*, vol. 105, pp. 508–519, 2016.

[37] A. C. Burke, B. G. Sutherland, D. E. Telford et al., "Naringenin enhances the regression of atherosclerosis induced by a chow diet in Ldlr mice," *Atherosclerosis*, vol. 286, pp. 60–70, 2019.

[38] S. Babu and S. Jayaraman, "An update on β-sitosterol: a potential herbal nutraceutical for diabetic management," *Biomedicine & Pharmacotherapy*, vol. 131, Article ID 110702, 2020.

[39] Q. Yang, D. Yu, and Y. Zhang, "β-Sitosterol attenuates the intracranial aneurysm growth by suppressing TNF-α-mediated mechanism," *Pharmacology*, vol. 104, no. 5-6, pp. 303–311, 2019.

Hindawi
Evidence-Based Complementary and Alternative Medicine
Volume 2021, Article ID 6580458, 11 pages
https://doi.org/10.1155/2021/6580458

Research Article

Multiple Risk Factors for Heart Disease: A Challenge to the Ethnopharmacological Use of *Croton urucurana* Baill.

Priscila Megda João Job Zago,[1] Gustavo Ratti da Silva,[2] Eduarda Carolina Amaral,[1] Lorena Neris Barboza,[1] Fernanda de Abreu Braga,[1] Bethânia Rosa Lorençone,[3] Aline Aparecida Macedo Marques,[3] Karyne Garcia Tafarelo Moreno,[3] Patrícia Regina Terço Leite,[3] Alan de Almeida Veiga,[4] Lauro Mera de Souza,[4] Roosevelt Isaias Carvalho Souza,[5] Ariany Carvalho dos Santos,[5] João Tadeu Ribeiro-Paes,[6] Arquimedes Gasparotto Junior,[3] and Francislaine Aparecida dos Reis Lívero[7]

[1]*Laboratory of Preclinical Research of Natural Products, Post-Graduate Program in Medicinal Plants and Phytotherapeutics in Basic Attention, Paranaense University, Umuarama, Paraná, Brazil*
[2]*Laboratory of Preclinical Research of Natural Products, Post-Graduate Program in Animal Science with Emphasis on Bioactive Products, Paranaense University, Umuarama, Paraná, Brazil*
[3]*Laboratory of Cardiovascular Pharmacology, Faculty of Health Sciences, Federal University of Grande Dourados, Dourados, Mato Grosso do Sul, Brazil*
[4]*Institute of Research Pelé Pequeno Príncipe, Pequeno Príncipe Faculty, Curitiba, Paraná, Brazil*
[5]*Laboratory of Histology, Faculty of Health Sciences, Federal University of Grande Dourados, Dourados, Mato Grosso do Sul, Brazil*
[6]*Laboratory of Genetics and Cell Therapy, São Paulo State University, Assis, São Paulo, Brazil*
[7]*Laboratory of Preclinical Research of Natural Products, Post-Graduate Program in Medicinal Plants and Phytotherapeutics in Basic Attention, Post-Graduate Program in Animal Science with Emphasis on Bioactive Products, Paranaense University, Umuarama, Paraná, Brazil*

Correspondence should be addressed to Francislaine Aparecida dos Reis Lívero; francislaine@prof.unipar.br

Received 4 September 2021; Revised 15 October 2021; Accepted 28 October 2021; Published 15 November 2021

Academic Editor: Daniel Kam Wah Mok

Croton urucurana Baill. is a native Brazilian tree, popularly known as "sangra-d'água" or "sangue-de-dragão," based on the red resinous sap of the trunk. Its use has been transmitted through generations based on popular tradition that attributes analgesic, anti-inflammatory, and cardioprotective properties to the tree. However, its cardioprotective effects have not yet been scientifically investigated. Thus, the present study investigated the pharmacological response to an ethanol-soluble fraction from the leaves of *C. urucurana* in Wistar rats exposed to smoking and dyslipidemia, two important cardiovascular risk factors. The extract was evaluated by high-performance liquid chromatography. Wistar rats received a 0.5% cholesterol-enriched diet and were exposed to cigarette smoke (9 cigarettes/day for 10 weeks). During the last 5 weeks, the animals were orally treated with vehicle (negative control group), *C. urucurana* extract (30, 100, and 300 mg/kg), or simvastatin (2.5 mg/kg) + enalapril (15 mg/kg). One group of rats that was not exposed to these risk factors was also evaluated (basal group). Electrocardiograms and systolic, diastolic, and mean blood pressure were measured. Blood was collected to measure total cholesterol, triglycerides, urea, and creatinine. The heart and kidneys were collected and processed for oxidative status and histopathological evaluation. The phytochemical analysis revealed different classes of flavonoids and condensed tannins. The model induced dyslipidemia and cardiac and renal oxidative stress and increased

levels of urea and creatinine in the negative control group. Treatment with the *C. urucurana* extract (300 mg/kg) and simvastatin + enalapril decreased cholesterol and triglyceride levels. In contrast to simvastatin + enalapril treatment, the *C. urucurana* extract exerted cardiac and renal antioxidant effects. No alterations of electrocardiograms, blood pressure, or histopathology were observed between groups. These findings indicate that *C. urucurana* exerts lipid-lowering, renal, and cardioprotective effects against oxidative stress in a preclinical model of multiple risk factors for heart disease.

1. Introduction

Because of the high risk of morbidity and mortality associated with cardiovascular disease, finding ways to mitigate such risk has become paramount in public healthcare. The presence of classic risk factors, such as hypertension, dyslipidemia, obesity, sedentary lifestyle, smoking, diabetes, and family history, increases the risk of developing cardiovascular disease. Dyslipidemia is an important cardiovascular risk factor. Low-density lipoprotein cholesterol (LDL-c) is the most relevant modifiable risk factor for coronary artery disease [1]. Ample evidence indicates that low LDL-c levels are associated with a proportional reduction of cardiovascular outcomes, including myocardial infarction, stroke, and cardiovascular-related death [2].

Another cardiovascular risk factor is smoking, a disease that is caused by nicotine addiction. An estimated 1.25 billion smokers worldwide are at risk of early death from smoking [3]. The health consequences of smoking are disastrous, given long-term exposure of the body to harmful components in cigarettes. The long-term continued use of tobacco and its derivatives leads to the appearance of cardiovascular, oncological, and respiratory diseases, making it one of the main causes of preventable death worldwide [4].

Despite the high morbidity and mortality of cardiovascular disease, animal models that combine its main risk factors are scarce. Despite the existence of effective and low-cost pharmacological therapies, some new drugs that are recommended by recent guidelines are expensive or unavailable in public healthcare systems [5]. Thus, the search for new therapeutic agents that are less expensive and safe and act effectively for the management of cardiovascular risk factors is essential. Plants remain an important source of potential medicines and the development of new therapies.

One important native tree in Brazil is *Croton urucurana* Baill. (Euphorbiaceae), popularly known as "sangra-d'água" or "sangue-de-dragão." This species is widely used by the Brazilian native population as a natural source of medicines. The leaves and bark of *C. urucurana* are popularly used to treat various conditions, including rheumatism, wounds, gastric ulcers, liver disorders, diarrhea, cancer, and cardiovascular diseases [6, 7]. The main active constituents of *C. urucurana* are tannins, lignans, and alkaloids [8]. Preclinical studies have shown that *C. urucurana* has antifungal [9], antibacterial [8], anti-inflammatory [10], antinociceptive [6, 11], antitumoral [12, 13], wound healing [12, 14], antiulcerogenic [15, 16], antidiarrheal [17, 18], and antihemorrhagic [19] effects. Toxicological studies reported that *C. urucurana* is potentially nontoxic, with an oral lethal dose 50 (LD50) above 5 g/kg in mice [9].

However, despite the popular use of *C. urucurana* for the treatment of cardiovascular diseases [7], the cardioprotective actions of this species have not yet been pharmacologically investigated. Thus, the present study investigated the lipid-lowering and antioxidant effects of an ethanol-soluble fraction obtained from leaves of *C. urucurana* in Wistar rats in a model of a combination of risk factors (exposure to tobacco smoke and dyslipidemia) for heart disease.

2. Material and Methods

2.1. Drugs. Bovine serum albumin, 5,5′-dithiobis(2-nitrobenzoic acid), reduced glutathione (GSH), xylenol orange, K_2HPO_4, KH_2PO_4, 1 M Tris, 5 mM ethylenediaminetetraacetic acid, Tris HCl (all from Sigma, St. Louis, MO, USA), pyrogallol, absolute ethanol, absolute methanol, ferrous ammonium sulfate, trichloroacetic acid, formaldehyde (all from Vetec, Rio de Janeiro, Brazil), and ultra-pure water from a Milli-Q system were used for eluent preparation.

2.2. Extract Preparation and Phytochemical Profile. Leaves of *Croton urucurana* Baill. were collected in May 2020 at Dourados, Mato Grosso do Sul (″22°20.9299′ south, 54°83.7713 west), and a voucher specimen (no. 5536) was deposited in the Herbarium of the Federal University of Grande Dourados. The plant was dried in an oven at 50°C for 5 days and pulverized. The extract was prepared by infusion using the methodology of Barbosa et al. [20], in which the pulverized material (100 g) was subjected to the extraction process by infusion with 1 L of boiling water. The resulting infusion was kept in an amber flask for 5 h, filtered, and then treated with 95% ethanol (1 : 3, v/v) to precipitate proteins and polysaccharides, giving rise to the heterogeneous phase that was removed by filtration. The ethanol-soluble fraction was concentrated on a rotary evaporator and lyophilized. The final yield of the dried extract of *C. urucurana* was 11.31%. Phytochemical characterization was performed using high-performance liquid chromatography (HPLC) with a diode-array detector (DAD; Shimadzu, Prominence LC-20A). Chromatography was conducted in the reverse-phase on a C18-PCP column (Ascentis Express; 150×4.6 mm, 2.7 μm particle size) using mobile phases that were composed of (A) 0.1% formic acid in water and (B) 0.05% formic acid in acetonitrile. The separation was obtained by a gradient of B that increased from 5% to 30% in 15 min then to 80% in 20 min, with a return to 5% in 21 min and then 5 min at the initial condition for solvent reequilibration. The flow rate was 0.5 ml/min. The column temperature was held at 40°C. Compound detection was accompanied by ultraviolet (UV) light at 190–400 nm.

2.3. Animals. Wistar rats, weighing 150–200 g, were obtained from the central vivarium of the Federal University of Grande Dourados. The animals were housed in the vivarium of the

Laboratory for Pre-Clinical Research of Natural Products, Paranaense University, with free access to food and water. The animals were housed under controlled environmental conditions (20° ± 2°C temperature, 50% ± 10% relative humidity, and 12 h/12 h light/dark cycle) with environmental enrichment. The total number of animals in the experiment was 48 ($n = 8$/group). The animals were weighed weekly on an analytical balance. The experimental protocol was approved by the Ethics Committee on the Use of Animals of Paranaense University (protocol no. 1000/2020). All national and international guidelines on animal welfare were followed. The reporting of animal investigations conformed to Animal Research Reporting of *In Vivo* Experiments (ARRIVE) guidelines [21].

2.4. Experimental Design. The choice of the animal species, sample size, and extract doses was based on Mendes et al. [22]. For 10 weeks, the animals received standard commercial food that was enriched with 0.5% cholesterol *ad libitum*. They were exposed to smoke from nine commercial cigarettes (0.8 mg nicotine, 10 mg tar, and 10 mg carbon monoxide) for 1 h daily, 5 days weekly, for 10 weeks, as proposed by Mendes et al. [22]. During the last 5 weeks of the experiment, the animals were treated orally by gavage with vehicle (0.1 ml of filtered water/100 g body weight; negative control [C−] group), the ethanol-soluble fraction of *Croton urucurana* (30, 100, and 300 mg/kg), or enalapril (15 mg/kg) + simvastatin (2.5 mg/kg) once daily. Non-dyslipidemic and nonsmoke-exposed Wistar rats were treated with vehicle (filtered water) and served as the basal group ($n = 8$). The final groups were the following: (1) basal (rats not exposed to any risk factor and treated with vehicle), (2) negative control (C−; dyslipidemic rats exposed to cigarette smoke and treated for 5 weeks with vehicle), (3) *C. urucurana* 30 (dyslipidemic rats exposed to cigarette smoke and treated with 30 mg/kg *C. urucurana* extract for 5 weeks), (4) *C. urucurana* 100 (dyslipidemic rats exposed to cigarette smoke and treated with 100 mg/kg *C. urucurana* extract for 5 weeks), (5) *C. urucurana* 300 (dyslipidemic rats exposed to cigarette smoke and treated with 300 mg/kg *C. urucurana* extract for 5 weeks), and (6) simvastatin + enalapril (dyslipidemic rats exposed to cigarette smoke and treated with 2.5 mg/kg simvastatin plus 15 mg/kg enalapril for 5 weeks).

2.5. Electrocardiography and Heart Rate and Blood Pressure Measurements. On the last day of the experiment, the rats were intramuscularly anesthetized with ketamine (100 mg/kg) + xylazine (20 mg/kg). A bolus injection of heparin (15 IU) was administered subcutaneously. Electrocardiography (ECG) was recorded using a 12-lead ECG recorder (WinCardio, Micromed, Brasília, Brazil) according to Romão et al. [23]. Electrocardiographic waves were recorded for 5 min. After ECG, the left carotid artery was isolated, cannulated, and connected to a pressure transducer that was coupled to a PowerLab recording system. Chart 4.1 software (ADI Instruments, Castle Hill, Australia) was used to record heart rate, systolic blood pressure (SBP), diastolic blood pressure (DBP), and mean arterial pressure (MAP). After 15 min of stabilization, changes in heart rate and blood pressure were recorded for 5 min.

2.6. Blood Collection and Biochemical Analysis. Blood samples were collected from the left carotid artery using heparinized syringes. Plasma was separated by centrifugation at 1,500 × g for 10 min and stored at −80°C for biochemical analyses. Total cholesterol, triglyceride, creatinine, and urea levels were measured using commercial kits and an automated analyzer (Quick Lab).

2.7. Euthanasia and Organ Collection. The rats were euthanized by puncture of the diaphragm while under anesthesia. The heart and left kidney were removed, carefully dissected, and weighed on an analytical balance. The weights of the heart and kidney were multiplied by 100 and divided by the animal's body weight before euthanasia to obtain the relative organ weight (%). A sample of the heart and kidney was rapidly separated and frozen in liquid nitrogen to evaluate oxidative stress. Other organ samples were stored in a 10% formalin solution for further histological analysis.

2.8. Tissue Redox Status. To investigate the tissue antioxidant system, the heart and kidney samples were homogenized in a 1 : 10 dilution of potassium phosphate buffer (0.1 M, pH 6.5). Afterward, 100 μl was separated, suspended in 80 μl of trichloroacetic acid (12.5%), vortexed, and centrifuged at 6000 × g for 15 min at 4°C. Reduced glutathione levels were measured according to Sedlak and Lindsay [24]. The remaining homogenate was centrifuged at 9000 × g for 20 min at 4°C for the determination of superoxide dismutase (SOD) activity and lipoperoxidation (LPO) levels according to Gao et al. [25] and Jiang et al. [26], respectively.

2.9. Histopathological Analysis. Samples of the heart and kidney were fixed in buffered 10% formalin solution (distilled water, 35–40% formaldehyde, and monobasic and dibasic sodium phosphate), dehydrated with alcohol and xylene, embedded in paraffin, sectioned at 6 μm, and stained with hematoxylin/eosin. The slides were analyzed by optical microscopy (Leica DM 2500) to evaluate cellular alterations.

2.10. Statistical Analysis. The data were analyzed for homogeneity of variance and a normal distribution. Differences between means were determined by one-way analysis of variance (ANOVA) followed by the Newman–Keuls *post hoc* test. The level of significance was set at 95% ($p < 0.05$). The data are expressed as the mean ± standard error of the mean (SEM).

3. Results

3.1. Phytochemical Profile. The phytochemicals in the ethanol-soluble fraction from the leaf extract of *Croton urucurana* are described in Table 1. *C. urucurana* was previously investigated for the chemical composition of its leaves and stem bark. Different compounds were reported in this plant,

Table 1: Phytochemicals in ethanol-soluble fraction from the leaf extract of *C. urucurana*.

Peak	R^t	UV λ_{max}	Tentative identification	Reference
1	2.58	264	n.i.	—
2	2.81	200, 280	n.i.	—
3	3.31	261	n.i.	—
4	3.45	254, 278 (Sh)	n.i.	—
5	8.06	277	Condensed tannin	[27]
6	9.07	279	Condensed tannin	[27]
7	9.66	278	Condensed tannin	[27]
8	10.26	279	Condensed tannin	[27]
9	11.39	221, 268, 301	n.i.	—
10	14.36	255, 353	Flavonol-*O*-glycoside	[27]
11	14.51	255, 353	Rutin	Std. [27]
12	14.75	269, 337	Apigenin-*C*-glycoside	[27]
13	14.83	269, 337	Apigenin-*C*-glycoside	[27]
14	15.13	255, 353	Isoquercitrin	Std. [27]
15	15.33	265, 346	Flavone *C*-glycoside	[27]
16	15.81	265, 346	Flavone *C*-glycoside	[27]
17	16.46	245, 333 (Sh), 348	n.i.	—
18	20.35	229, 266, 316	n.i.	—
19	20.53	229, 266, 316	n.i.	—
20	20.87	254, 366	Quercetin	Std.
21	22.06	254, 366	Kaempferol	Std.

n.i.: not identified; Std.: compound confirmed by a comparison with authentic standard.

including flavan-3-ols, proanthocyanidins (condensed tannins), flavonols, *O*-glycosides, hydroxyflavones, *C*-glycosides [14, 27], alkaloids, terpenes, and phenolic acids [10], which were obtained with different extraction solvents. In the present study, comparisons with authentic standards identified some main compounds in the extract of the leaves of *C. urucurana*, despite the lack of information to confirm the identification of some low-abundance peaks (e.g., 1, 2, 3, and 4). Other compounds were tentatively identified based on UV spectra, supported by previous reports, but some compounds were not observed in the current extract. Alves et al. [27] performed a more comprehensive phytochemical analysis of the leaves of *C. urucurana*. They identified different classes of flavonoids, such as condensed tannins (e.g., proanthocyanidins). In the current extract, we identified peaks 5, 6, and 7 with UV spectra which were consistent with these compounds, with λ_{max} at 277–279 nm. Condensed tannins have been reported in all investigated parts of *C. urucurana* [10, 14, 27].

In addition to condensed tannins, Alves et al. [27] also described the presence of catechin. In the present study, comparisons with the catechin standard did not reveal catechin, but peak 9 was eluted close to catechin and had a similar UV spectrum, with λ_{max} at 279 nm. Although unconfirmed, the isomer epicatechin has a chromatographic elution profile that is close to catechin [28] and should be considered because it was previously reported in the bark of *C. urucurana* [10].

Flavonol-*O*-glycosides were also reported in the leaves of *C. urucurana* [27]. These compounds have characteristic UV spectra, with an absorbance λ_{max} range of 350–365 nm from band B and 255–265 nm from band A [29]. Compound 10 had this characteristic UV spectrum and was identified as from this class of flavonoid. In contrast, the main compound that was observed on the chromatogram was identified as rutin (peak 11, λ_{max} at 255 and 353 nm), confirmed by comparisons with the authentic standard. Isoquercitrin was also identified based on the authentic standard comparison at an Rt of 15.13 min, with a UV spectrum that was similar to rutin.

Two other compounds (12 and 13) had λ_{max} at 269 and 337 nm, which was slightly different from the characteristic UV absorption of flavonols. Alves et al. [27] described the presence of *C*-glycosides of apigenin, and these compounds have similar UV spectra as peaks 12 and 13, suggesting they belong to this flavonoid class [30]. Peaks 15 and 16 also had characteristic UV spectra that indicated flavonoid-glycosides with λ_{max} at 265 and 346 nm. These compounds could not be accurately identified because in addition to rutin and isoquercitrin, Alves et al. [27] found other di- and triglycosides that were attached to myricetin, quercetin, and kaempferol. These compounds commonly appear with different glycan distributions, including several isomers, thereby hindering their identification [28, 29]. Although several glycosides were identified in the leaves of *C. urucurana*, no free aglycones were reported previously. Here, based on UV spectra and authentic standards, quercetin (peak 20) and kaempferol (peak 21) were also confirmed in the extract (Figure 1).

3.2. Electrocardiographic Profile, Heart Rate, and Blood Pressure. Electrocardiograms, heart rate, and blood pressure are shown in Table 2. No significant changes were found in the amplitude of the P-, Q-, R-, or S-waves or in the PR-, QRS-, QT-, and QTC-segments between experimental groups ($p > 0.05$). No significant alterations of heart rate or blood pressure were observed between groups ($p > 0.05$).

3.3. Body and Organ Weight. The median body weight of rats in the basal group at the end of the experiment was 166.30 ± 3.51 g. No differences were observed in body weight between groups ($p > 0.05$). For organ weights, we observed increases in relative weights (%) of the heart ($p < 0.01$) and kidney ($p < 0.01$) in the C− group compared with the basal group ($0.36\% \pm 0.02\%$ and $0.42\% \pm 0.01\%$, respectively). Treatment with 30, 100, and 300 mg/kg of the *C. urucurana* extract normalized relative heart weights ($p < 0.05$, 0.01, and 0.01, respectively) and relative kidney weights ($p < 0.05$, 0.01, and 0.001, respectively), whereas treatment with simvastatin + enalapril normalized only relative heart weights ($p < 0.01$). Body and organ weight are shown in Table 3.

3.4. Biochemical Profile. Dyslipidemia and smoking increased plasma triglyceride and total cholesterol levels by 117.17% ($p < 0.001$) and 160.60% ($p < 0.001$), respectively, compared with the basal group. Treatment with 300 mg/kg of the *C. urucurana* extract and simvastatin + enalapril completely reversed these changes in cholesterol ($p < 0.001$)

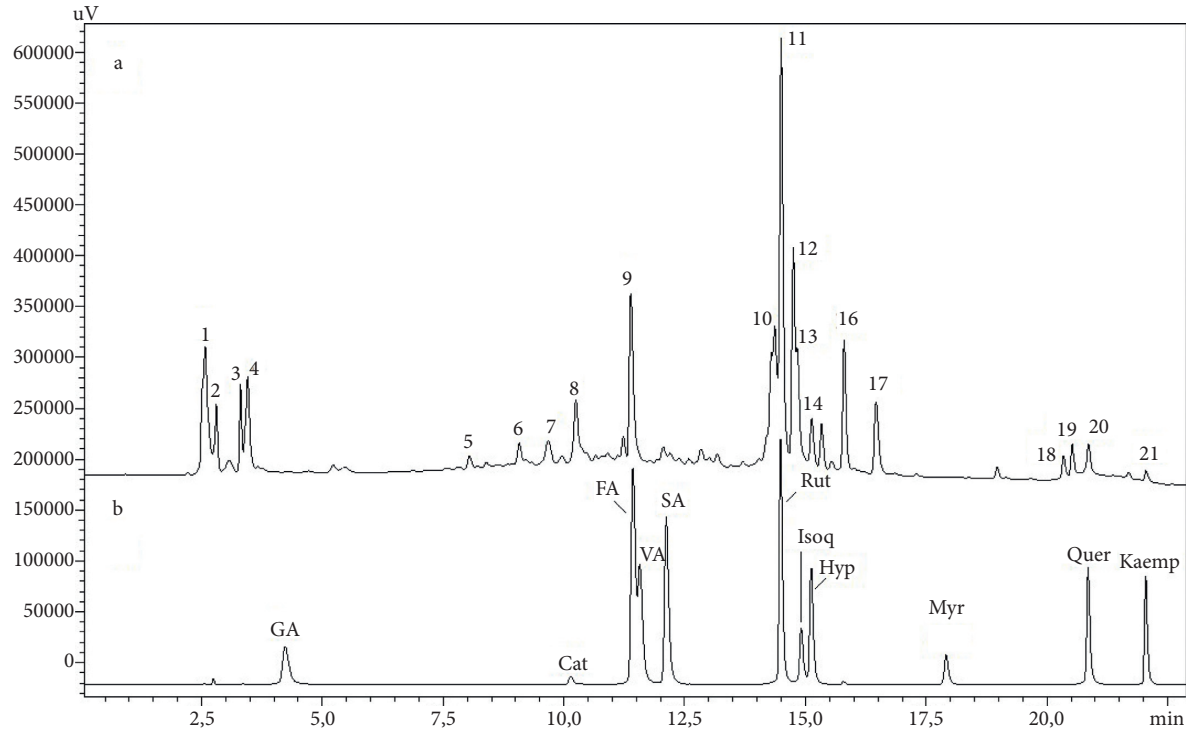

Figure 1: HPLC analysis of the ethanol-soluble fraction of the leaf extract of *C. urucurana* (A) and authentic standards (B). GA: gallic acid; cat: catechin; FA: ferulic acid; VA: vanillic acid; SA: syringic acid; rut: rutin; Isoq: isoquercitrin; Hyp: hyperoside; Myr: myricetin; Quer: quercetin; Kaemp: kaempferol.

Table 2: Electrocardiogram, heart rate, and blood pressure in dyslipidemic and smoking rats that were treated with vehicle, *Croton urucurana* extract, and simvastatin + enalapril.

		Basal	C–	*Croton urucurana* (mg/kg)			SIM + ENAL
				30	100	300	
HR (BPM)		160.8 ± 5.2	152.4 ± 7.0	151.6 ± 5.6	152.3 ± 5.6	140.9 ± 20.2	171.6 ± 3.3
SBP (mm Hg)		94.0 ± 6.8	107.6 ± 11.9	100.3 ± 4.1	107.2 ± 6.2	104.6 ± 2.9	95.6 ± 11.9
DBP (mm Hg)		52.7 ± 5.2	50.4 ± 2.2	52.4 ± 3.0	58.2 ± 4.0	56.9 ± 3.7	52.6 ± 3.0
MAP (mm Hg)		73.5 ± 5.7	81.1 ± 8.8	79.1 ± 4.0	84.1 ± 5.1	82.2 ± 3.3	77.1 ± 8.9
Electrocardiogram							
Wave (mV)	P	0.07 ± 0.01	0.07 ± 0.01	0.06 ± 0.01	0.07 ± 0.01	0.07 ± 0.005	0.07 ± 0.01
	Q	−0.02 ± 0.01	−0.02 ± 0.01	−0.02 ± 0.01	−0.02 ± 0.01	−0.02 ± 0.01	−0.02 ± 0.01
	R	0.35 ± 0.01	0.34 ± 0.02	0.37 ± 0.20	0.35 ± 0.02	0.33 ± 0.02	0.31 ± 0.02
	S	−0.04 ± 0.01	−0.05 ± 0.01	−0.04 ± 0.01	−0.05 ± 0.01	−0.05 ± 0.01	−0.05 ± 0.01
Segment (ms)	PR	47.8 ± 3.5	43.5 ± 1.0	45.1 ± 2.7	45.5 ± 4.1	44.7 ± 4.0	43.5 ± 2.4
	QRS	42.1 ± 1.5	37.2 ± 1.7	40.3 ± 1.8	38.1 ± 2.8	37.6 ± 2.0	36.8 ± 1.6
	QT	105.8 ± 5.3	97.8 ± 3.6	96.1 ± 3.8	92.1 ± 4.4	102.3 ± 4.9	97.38 ± 5.86
	QTC	185.8 ± 7.2	183.3 ± 7.2	188.6 ± 8.4	178.4 ± 9.6	198.2 ± 7.9	187.0 ± 11.8

BPM: beats per minute; C–: negative control; DBP: diastolic blood pressure; HR: heart rate; MAP: mean arterial pressure; SBP: systolic blood pressure; SIM + ENAL: simvastatin + enalapril. $n = 8$/group. The data are expressed as mean ± SEM. One-way ANOVA followed by Newman–Keuls *post hoc* test.

and triglycerides ($p < 0.001$), whereas treatment with 30 and 100 mg/kg of the *C. urucurana* extract only partially reversed triglyceride and total cholesterol levels. The risk factors also increased urea and creatinine levels compared with the basal group (8.83 ± 1.22 mg/dl, $p < 0.001$, and 8.50 ± 1.25 mg/dl, $p < 0.001$, respectively). Treatment with 300 mg/kg of the *C. urucurana* extract completely reversed the increases in urea ($p < 0.001$) and creatinine ($p < 0.001$) levels. Treatment with 30 and 100 mg/kg of the *C. urucurana* extract and simvastatin + enalapril partially reversed these changes (Figure 2).

3.5. Cardiac and Renal Redox State. The combination of smoking and dyslipidemia induced significant cardiac and renal oxidative stress in Wistar rats (Figure 3). Significant decreases in cardiac and renal GSH levels were observed compared with the basal group (150.50 ± 4.32 μg GSH/g

Table 3: Body weight and relative heart and kidney weight in dyslipidemic and smoking rats that were treated with vehicle, *Croton urucurana* extract, and simvastatin + enalapril.

	Basal	C−	*Croton urucurana* (mg/kg)			SIM + ENAL
			30	100	300	
Body weight (g)	166.3 ± 3.5	176.0 ± 1.1	174.0 ± 3.1	177.7 ± 2.5	174.9 ± 3.2	175.4 ± 1.9
Heart (%)	0.36 ± 0.02	0.48 ± 0.02[a]	0.42 ± 0.01[b]	0.39 ± 0.01[b]	0.37 ± 0.01[b]	0.37 ± 0.01[b]
Kidney (%)	0.42 ± 0.01	0.49 ± 0.01[a]	0.44 ± 0.01[b]	0.42 ± 0.01[b]	0.40 ± 0.01[b]	0.46 ± 0.01

SIM + ENAL: simvastatin + enalapril. $n = 8$/group. The data are expressed as mean ± SEM. [a] $p < 0.05$ versus basal; [b] $p < 0.05$ versus C− (one-way ANOVA followed by Newman–Keuls *post hoc* test).

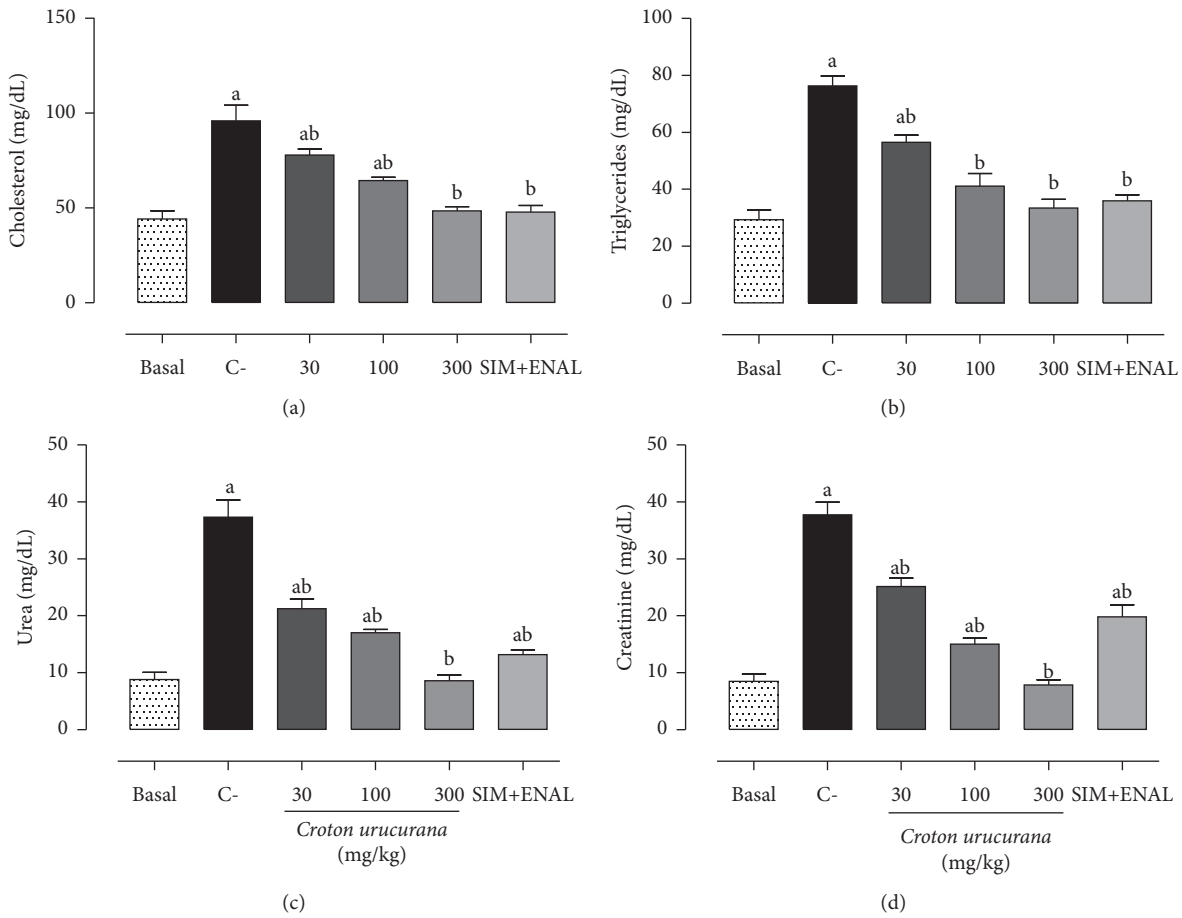

Figure 2: Effects of *Croton urucurana* on biochemical profile. Plasma levels of (a) cholesterol (mg/dl), (b) triglycerides (mg/dl), (c) urea (mg/dl), and (d) creatinine (mg/dl) in nondyslipidemic and nonsmoking rats (basal group) and dyslipidemic and smoking rats that were treated with vehicle (negative control (C−)), *Croton urucurana* extract (30, 100, and 300 mg/kg), or simvastatin + enalapril (SIM + ENAL). The data are expressed as mean ± SEM. [a] $p < 0.05$ versus basal group; [b] $p < 0.05$ versus C− group (one-way ANOVA followed by Newman–Keuls *post hoc* test).

tissue, $p < 0.001$, and 139.30 ± 1.58 μg GSH/g tissue, $p < 0.001$, respectively). These risk factors decreased cardiac ($p < 0.001$) and renal SOD ($p < 0.001$) activity and increased LPO levels compared with the basal group. Treatment with 300 mg/kg of the *C. urucurana* extract completely reversed these changes ($p < 0.001$), whereas treatment with 30 and 100 mg/kg of the *C. urucurana* extract and simvastatin + enalapril only partially reversed cardiac and renal oxidative stress.

3.6. Histopathological Evaluation. Heart and kidney samples stained with hematoxylin/eosin did not reveal any significant histopathological changes in any of the experimental groups (Figure 4).

4. Discussion

The present study investigated cardiac and renal effects of an extract of *Croton urucurana* using an experimental

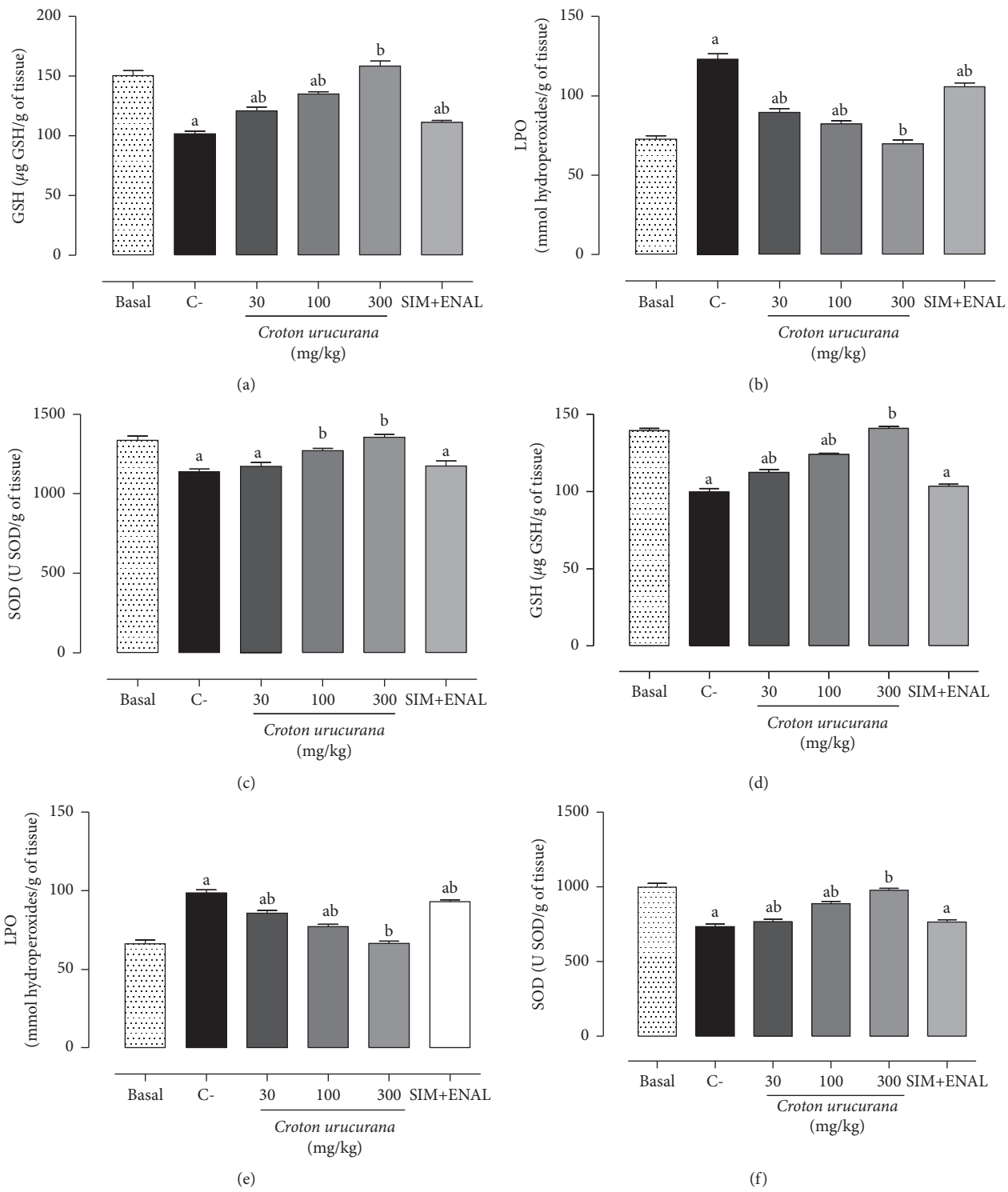

Figure 3: Antioxidant effects of *Croton urucurana* extract. Cardiac levels of (a) reduced glutathione, (b) lipoperoxidation, and (c) superoxide dismutase and renal levels of (d) reduced glutathione, (e) lipoperoxidation, and (f) superoxide dismutase in nondyslipidemic and nonsmoking Wistar rats (basal group) and dyslipidemic and smoking rats that were treated with vehicle (negative control (C−)), *Croton urucurana* extract (30, 100, and 300 mg/kg), or simvastatin + enalapril (SIM + ENAL). The data are expressed as mean ± SEM. $^{a}p < 0.05$ versus basal group; $^{b}p < 0.05$ versus C− group (one-way ANOVA followed by Newman–Keuls *post hoc* test).

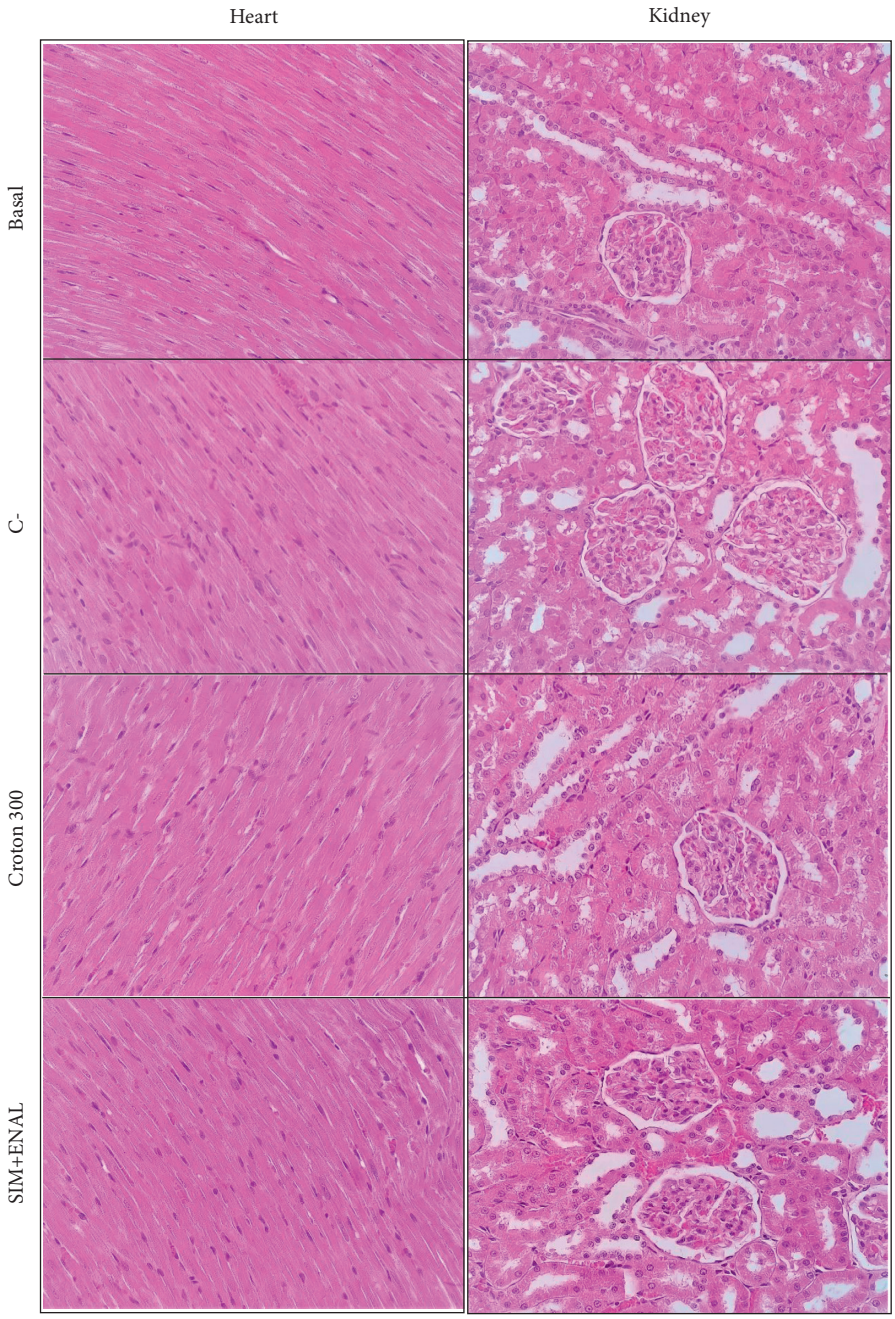

Figure 4: Cardiac and renal histopathological analysis. Hematoxylin/eosin staining of the heart and kidney from nondyslipidemic and nonsmoking rats (basal group) and dyslipidemic and smoking rats that were treated with vehicle (negative control (C−)), 300 mg/kg *Croton urucurana* extract (croton 300), and simvastatin + enalapril (SIM + ENAL). 40 × magnification.

model that combined dyslipidemia and tobacco smoking, both of which are important risk factors for cardiovascular diseases. Rats exposed to a high-cholesterol diet and cigarette smoke for 10 weeks exhibited dyslipidemia, cardiac and renal oxidative stress, and high plasma levels of urea and creatinine. Daily treatment with an ethanol-soluble fraction of *C. urucurana* for 5 weeks effectively reversed these changes.

Because of the high morbidity and mortality of heart diseases, finding ways to prevent them has become essential in public healthcare [31]. The presence of such risk factors as hypertension, dyslipidemia, obesity, physical inactivity, smoking, diabetes, and family history significantly increases the likelihood of heart disease. When combinations of these risk factors are present, synergistic effects can occur that further aggravate the course of cardiovascular disease [32, 33]. Despite the well-established association between multiple risk factors and heart disease, animal models that combine the main risk factors are scarce [20, 22, 33]. Thus, the use of scientifically validated preclinical models is essential to investigate and validate potential ethnobotanical candidates.

The Western medical system has a wide range of classic drugs used to prevent and control heart disease. However, their high cost and side effects limit patients' adherence to treatment. Thus, the search is ongoing for new therapeutic agents that are effective and have a more favorable side effect profile to improve treatment adherence [34]. Given the therapeutic potential of *C. urucurana* for heart disease, we performed a series of preclinical studies to validate its popular usage. The results of the present study further demonstrate the potential beneficial effects of a *C. urucurana* extract in an animal model that utilizes a combination of two well-known cardiovascular risk factors: smoking and dyslipidemia.

The HPLC-DAD analyses identified several secondary metabolites in the *C. urucurana* extract, including flavonoids (i.e., rutin) and tannins (i.e., catechin). Several studies have been conducted to determine biological effects of rutin and catechin. The preventive effects of catechins on cardiovascular disease were shown to occur through the regulation of lipid metabolism, vascular endothelial protection, and blood pressure reduction [35]. In a rat model of obesity that was induced by a high-fat diet, supplementation with rutin decreased cholesterol and triglyceride levels [36, 37]. Supplementation with rutin also exerted lipid-lowering effects (i.e., a decrease in plasma triglyceride levels) in a Golden Syrian hamster model of diet-induced hypercholesterolemia [38]. Furthermore, supplementation with rutin (100 mg/kg) improved kidney and heart morphology and function in a rat model of chronic kidney disease, promoting reno- and cardioprotective effects [39]. Antioxidant effects of rutin were also previously reported in preclinical studies [36, 40, 41]. Evidence from preclinical and clinical studies also revealed antioxidant effects of catechin [42–46]. Despite strong evidence of the participation of rutin and catechin in the lipid-lowering, antioxidant, and renoprotective effects of *C. urucurana*, we do exclude the possibility that other compounds may also be involved in its beneficial effects. We speculate that the pharmacological effects that were observed in the present study may be attributable to an integrated action of several secondary metabolites that act both independently and in a coordinated manner on different molecular targets.

The antioxidant and renoprotective effects of *C. urucurana* were superior to the simvastatin + enalapril-treated group. Although some studies showed that simvastatin exerted antioxidant effects [47, 48], we did not observe such a significant effect in the present model. Furthermore, previous studies indicated that enalapril worsened renal function in patients with heart disease by inhibiting the angiotensin-converting enzyme. Thus, enalapril appears to cause direct intrarenal vasoconstriction, reducing perfusion pressure of the renal afferent arteriole, decreasing glomerular filtration, and worsening kidney function [49–51]. Treatment with the *C. urucurana* extract did not alter renal function and instead had antioxidant actions, thus highlighting the advantage of this treatment relative to simvastatin and enalapril.

In summary, we found that treatment with the *C. urucurana* extract, mainly at the highest dose, exerted reno- and cardioprotective effects against smoking- and dyslipidemia-induced damage in Wistar rats. These results will likely contribute to further studies to validate these preclinical effects in human patients. Despite these encouraging data, the important limitations of this study are worth mentioning. First, we did not determine the molecular mechanisms by which the *C. urucurana* extract exerted its pharmacological effects. Furthermore, we did not evaluate the possible synergistic or additive effects of *C. urucurana* combined with simvastatin or enalapril. Future studies should investigate whether the cardioprotective effects of *C. urucurana* could be improved by the concomitant administration of a classic cardioprotective drug.

5. Conclusion

The *Croton urucurana* extract exerted reno- and cardioprotective effects in a rat model of smoking- and dyslipidemia-induced heart disease.

Abbreviations

ANOVA: Analysis of variance
DAD: Diode-array detector
DBP: Diastolic blood pressure
ECG: Electrocardiography
GSH: Reduced glutathione
HPLC: High-performance liquid chromatography
LD50: Lethal dose 50
LDL-c: Low-density lipoprotein cholesterol
LPO: Lipoperoxidation
MAP: Mean arterial pressure
SBP: Systolic blood pressure
SEM: Standard error of the mean
SOD: Superoxide dismutase
UV: Ultraviolet.

Data Availability

Data will be available upon request to the corresponding author (e-mail: francislaine@prof.unipar.br).

Conflicts of Interest

The authors declare that they have no conflicts of interest related to this research.

Authors' Contributions

PMJJZ, GRS, ECA, LNB, FAB, BRL, AAMM, KGTM, PRTL, and FARL were responsible for the animal experiments and extract preparation. RICS and ACS contributed to the histological analyses. AAV and LMS performed the phytochemical analyses. PMJJZ, AGJ, and FARL were responsible for data discussion and manuscript elaboration. JTRP, AGJ, and FARL contributed to data interpretation and manuscript preparation. FARL was the senior researcher who was responsible for the project.

Acknowledgments

The authors thank students in the Laboratory of Preclinical Research of Natural Products (Paranaense University) and Laboratory of Cardiovascular Pharmacology (Federal University of Grande Dourados) for help with the experiments and Michael Arends for proofreading the manuscript. This research was supported by grants from Coordenadoria de Pós-Graduação (COPG, Paranaense University, Brazil), Conselho Nacional de Desenvolvimento Científico e Tecnológico (CNPq), and Fundação Araucária, Paraná/SETI (Brazil, CP 20/2018, 014/2020).

References

[1] D. J. Aggarwal, M. G. Kathariya, and D. P. K. Verma, "LDL-C, NON-HDL-C and APO-B for cardiovascular risk assessment: looking for the ideal marker," *Indian Heart Journal*, vol. 73, no. 5, pp. 544–548, 2021.

[2] K. C. Koskinas, G. C. M. Siontis, R. Piccolo et al., "Effect of statins and non-statin LDL-lowering medications on cardiovascular outcomes in secondary prevention: a meta-analysis of randomized trials," *European Heart Journal*, vol. 39, no. 14, pp. 1172–1180, 2018.

[3] T. Münzel, O. Hahad, M. Kuntic, J. F. Keaney, J. E. Deanfield, and A. Daiber, "Effects of tobacco cigarettes, e-cigarettes, and waterpipe smoking on endothelial function and clinical outcomes," *European Heart Journal*, vol. 41, no. 41, pp. 4057–4070, 2020.

[4] W. K. Balwan and S. Kour, "Lifestyle diseases: the link between modern lifestyle and threat to public health," *Saudi Journal of Medical and Pharmaceutical Sciences*, vol. 7, no. 4, pp. 179–184, 2021.

[5] Y. Zhu, J. P. Moriarty, K. M. Swanson et al., "A model-based cost-effectiveness analysis of pharmacogenomic panel testing in cardiovascular disease management: preemptive, reactive, or none?" *Genetics in Medicine*, vol. 23, no. 3, pp. 461–470, 2021.

[6] V. S. Rao, L. A. Gurgel, R. C. P. Lima-Júnior, D. T. O. Martins, V. Cechinel-Filho, and F. A. Santos, "Dragon's blood from *Croton urucurana* (Baill.) attenuates visceral nociception in mice," *Journal of Ethnopharmacology*, vol. 113, no. 2, pp. 357–360, 2007.

[7] F. C. Coelho, C. A. S. Tirloni, A. A. M. Marques, F. M. Gasparotto, F. A. D. R. Lívero, and A. Gasparotto Junior, "Traditional plants used by remaining healers from the region of Grande Dourados, Mato Grosso do Sul, Brazil," *Journal of Religion and Health*, vol. 58, no. 2, pp. 572–588, 2019.

[8] M. T. L. P. Peres, F. D. Monache, A. B. Cruz, M. G. Pizzolatti, and R. A. Yunes, "Chemical composition and antimicrobial activity of *Croton urucurana* Baillon (Euphorbiaceae)," *Journal of Ethnopharmacology*, vol. 56, no. 3, pp. 223–226, 1997.

[9] L. A. Gurgel, J. J. C. Sidrim, D. T. Martins, V. C. Filho, and V. S. Rao, "*In vitro* antifungal activity of dragon's blood from *Croton urucurana* against dermatophytes," *Journal of Ethnopharmacology*, vol. 97, no. 2, pp. 409–412, 2005.

[10] K. W. Cordeiro, J. L. Felipe, K. F. Malange et al., "Anti-inflammatory and antinociceptive activities of *Croton urucurana* Baillon bark," *Journal of Ethnopharmacology*, vol. 183, pp. 128–135, 2016.

[11] M. T. L. P. Peres, F. D. Monache, M. G. Pizzolatti et al., "Analgesic compounds of *Croton urucurana* Baillon. Pharmaco-chemical criteria used in their isolation," *Phytotherapy Research*, vol. 12, no. 3, pp. 209–211, 1998.

[12] Z.-P. Chen, Y. Cai, and J. Phillipson, "Studies on the anti-tumour, anti-bacterial, and wound-healing properties of dragon's Blood1," *Planta Medica*, vol. 60, no. 6, pp. 541–545, 1994.

[13] P. de Matos Cândido-Bacani, F. Ezan, P. de Oliveira Figueiredo et al., "[1-9-NαC]-crourorb A1 isolated from *Croton urucurana* latex induces G2/M cell cycle arrest and apoptosis in human hepatocarcinoma cells," *Toxicology Letters*, vol. 273, pp. 44–54, 2017.

[14] T. D. R. L. Casao, C. G. Pinheiro, M. M. Sarandy et al., "*Croton urucurana* Baillon stem bark ointment accelerates the closure of cutaneous wounds in knockout IL-10 mice," *Journal of Ethnopharmacology*, vol. 261, Article ID 113042, 2020.

[15] M. J. S. Miller, W. K. MacNaughton, X.-J. Zhang et al., "Treatment of gastric ulcers and diarrhea with the Amazonian herbal medicine sangre de grado," *American Journal of Physiology-Gastrointestinal and Liver Physiology*, vol. 279, no. 1, pp. G192–G200, 2000.

[16] K. Wolff Cordeiro, L. Aparecida Pinto, A. S. Nazari Formagio, S. Faloni de Andrade, C. A. Leite Kassuya, and K. de Cássia Freitas, "Antiulcerogenic effect of *Croton urucurana* Baillon bark," *Journal of Ethnopharmacology*, vol. 143, no. 1, pp. 331–337, 2012.

[17] L. A. Gurgel, R. M. Silva, F. A. Santos, D. T. O. Martins, P. O. Mattos, and V. S. N. Rao, "Studies on the antidiarrhoeal effect of dragon's blood from *Croton urucurana*," *Phytotherapy Research*, vol. 15, no. 4, pp. 319–322, 2001.

[18] D. S. V. Barbieri, F. Tonial, P. V. A. Lopez et al., "Antiadherent activity of *Schinus terebinthifolius* and *Croton urucurana* extracts on in vitro biofilm formation of Candida albicans and Streptococcus mutans," *Archives of Oral Biology*, vol. 59, no. 9, pp. 887–896, 2014.

[19] L. E. Esmeraldino, A. M. Souza, and S. V. Sampaio, "Evaluation of the effect of aqueous extract of *Croton urucurana* Baillon (Euphorbiaceae) on the hemorrhagic activity induced by the venom of *Bothrops jararaca*, using new techniques to quantify hemorrhagic activity in rat skin," *Phytomedicine*, vol. 12, no. 8, pp. 570–576, 2005.

[20] R. J. Barbosa, G. R. Silva, I. M. Cola et al., "Promising therapeutic use of *Baccharis trimera* (Less.) DC. as a natural hepatoprotective agent against hepatic lesions that are caused by multiple risk factors," *Journal of Ethnopharmacology*, vol. 254, Article ID 112729, 2020.

[21] N. Percie du Sert, V. Hurst, A. Ahluwalia et al., "The ARRIVE guidelines 2.0: updated guidelines for reporting animal research," *PLoS Biology*, vol. 18, no. 7, Article ID e3000410, 2020.

[22] T. C. Mendes, G. R. Silva, A. O. Silva et al., "Hepato- and cardioprotective effects of *Baccharis trimera* (Less.) DC. against multiple risk factors for chronic noncommunicable diseases," *Anais da Academia Brasileira de Ciências*, vol. 93, Article ID e20200899, 2021.

[23] P. V. M. Romão, R. A. C. Palozi, L. P. Guarnier et al., "Cardioprotective effects of *Plinia cauliflora* (Mart.) Kausel in a rabbit model of doxorubicin-induced heart failure," *Journal of Ethnopharmacology*, vol. 242, Article ID 112042, 2019.

[24] J. Sedlak and R. H. Lindsay, "Estimation of total, protein-bound, and nonprotein sulfhydryl groups in tissue with Ellman´s reagent," *Analytical Biochemistry*, vol. 25, pp. 192–205, 1968.

[25] R. Gao, Z. Yuan, Z. Zhao, and X. Gao, "Mechanism of pyrogallol autoxidation and determination of superoxide

dismutase enzyme activity," *Bioelectrochemistry and Bioenergetics*, vol. 45, no. 1, pp. 41–45, 1998.

[26] J. Jiang, D. Kosman, Y. T. Ip, and M. Levine, "The dorsal morphogen gradient regulates the mesoderm determinant twist in early Drosophila embryos," *Genes & Development*, vol. 5, no. 10, pp. 1881–1891, 1991.

[27] J. J. L. Alves, M. I. Dias, J. C. M. Barreira et al., "Phenolic profile of *Croton urucurana* Baill. leaves, stems and bark: pairwise influence of drying temperature and extraction solvent," *Molecules*, vol. 25, no. 9, p. 2032, 2020.

[28] L. M. Souza, T. R. Cipriani, M. Iacomini, P. A. J. Gorin, and G. L. Sassaki, "HPLC/ESI-MS and NMR analysis of flavonoids and tannins in bioactive extract from leaves of Maytenus ilicifolia," *Journal of Pharmaceutical and Biomedical Analysis*, vol. 47, no. 1, pp. 59–67, 2008.

[29] L. M. Souza, T. R. Cipriani, C. F. Sant'Ana, M. Iacomini, P. A. J. Gorin, and G. L. Sassaki, "Heart-cutting two-dimensional (size exclusion × reversed phase) liquid chromatography–mass spectrometry analysis of flavonol glycosides from leaves of Maytenus ilicifolia," *Journal of Chromatography A*, vol. 1216, no. 1, pp. 99–105, 2009.

[30] T. B. L. Prando, L. N. Barboza, V. O. Araújo et al., "Involvement of bradykinin B2 and muscarinic receptors in the prolonged diuretic and antihypertensive properties of *Echinodorus grandiflorus* (Cham. & Schltdl.)," *Phytomedicine*, vol. 23, no. 11, pp. 1249–1258, 2016.

[31] D. P Leong, P. G. Joseph, M. McKee et al., "Reducing the global burden of cardiovascular disease, part 2: prevention and treatment of cardiovascular disease," *Circulation Research*, vol. 121, no. 6, pp. 695–710, 2017.

[32] S. Francula-Zaninovic and I. A. Nola, "Management of measurable variable cardiovascular disease' risk factors," *Current Cardiology Reviews*, vol. 14, no. 3, pp. 153–163, 2018.

[33] M. M. Q. Souza, G. R. Silva, I. M. Cola et al., "*Baccharis trimera* (Less.) DC: an innovative cardioprotective herbal medicine against multiple risk factors for cardiovascular disease," *Journal of Medicinal Food*, vol. 23, no. 6, pp. 676–684, 2020.

[34] M. Aggarwal, B. Aggarwal, and J. Rao, "Integrative medicine for cardiovascular disease and prevention," *Medical Clinics of North America*, vol. 101, no. 5, pp. 895–923, 2017.

[35] X. Q. Chen, T. Hu, Y. Han et al., "Preventive effects of catechins on cardiovascular disease," *Molecules*, vol. 21, no. 12, p. 1759, 2016.

[36] C. L. Hsu, C. H. Wu, S. L. Huang, and G. C. Yen, "Phenolic compounds rutin and o-coumaric acid ameliorate obesity induced by high-fat diet in rats," *Journal of Agricultural and Food Chemistry*, vol. 57, no. 2, pp. 425–431, 2009.

[37] A. Ziaee, F. Zamansoltani, M. Nassiri-Asl, and E. Abbasi, "Effects of rutin on lipid profile in hypercholesterolaemic rats," *Basic and Clinical Pharmacology and Toxicology*, vol. 104, no. 3, pp. 253–258, 2009.

[38] A. Kanashiro, D. C. Andrade, L. M. Kabeya et al., "Modulatory effects of rutin on biochemical and hematological parameters in hypercholesterolemic Golden Syrian hamsters," *Anais da Academia Brasileira de Ciências*, vol. 81, pp. 67–72, 2009.

[39] V. Diwan, L. Brown, and G. C. Gobe, "The flavonoid rutin improves kidney and heart structure and function in an adenine-induced rat model of chronic kidney disease," *Journal of Functional Foods*, vol. 33, pp. 85–93, 2017.

[40] M. Karthick, P. Stanely, and M. Prince, "Preventive effect of rutin, a bioflavonoid, on lipid peroxides and antioxidants in isoproterenol-induced myocardial infarction in rats," *Journal of Pharmacy and Pharmacology*, vol. 58, no. 5, pp. 701–707, 2006.

[41] İ. Topal, A. Ö. Bilgin, F. K. Çimen et al., "The effect of rutin on cisplatin-induced oxidative cardiac damage in rats," *The Anatolian Journal of Cardiology*, vol. 20, no. 3, pp. 136–142, 2018.

[42] D. L. McKay and J. B. Blumberg, "Roles for epigallocatechin gallate in cardiovascular disease and obesity: an introduction," *Journal of the American College of Nutrition*, vol. 26, no. 4, pp. 362S–365S, 2013.

[43] A. Chowdhury, J. Sarkar, T. Chakraborti, P. K. Pramanik, and S. Chakraborti, "Protective role of epigallocatechin-3-gallate in health and disease: a perspective," *Biomedicine & Pharmacotherapy*, vol. 78, pp. 50–59, 2016.

[44] M. Grzesik, K. Naparło, G. Bartosz, and I. Sadowska-Bartosz, "Antioxidant properties of catechins: comparison with other antioxidants," *Food Chemistry*, vol. 241, pp. 480–492, 2018.

[45] M. P. Mudagal and K. Swathi, "Role of quercetin and catechin in attenuation of isoproterenol induced bioflavonoids, myocardial infarction in rats," *Asian Journal of Pharmacy and Pharmacology*, vol. 4, no. 5, pp. 662–667, 2018.

[46] K. Venkatakrishnan, H. F. Chiu, J. C. Cheng et al., "Comparative studies on the hypolipidemic, antioxidant and hepatoprotective activities of catechin-enriched green and oolong tea in a double-blind clinical trial," *Food & Function*, vol. 9, no. 1, pp. 1205–1213, 2018.

[47] T. Nikolic, V. Zivkovic, I. Srejovic et al., "Effects of atorvastatin and simvastatin on oxidative stress in diet-induced hyperhomocysteinemia in Wistar albino rats: a comparative study," *Molecular and Cellular Biochemistry*, vol. 437, no. 1, pp. 109–118, 2018.

[48] H. A. Abd El Aal, L. A. Ahmed, W. A. Hassan, H. M. Fawzy, and H. Moawad, "Combination of carvacrol with simvastatin improves the lipid-lowering efficacy and alleviates simvastatin side effects," *Journal of Biochemical and Molecular Toxicology*, vol. 31, no. 12, Article ID e21981, 2017.

[49] H. C. Rayner, M. E. Thomas, and D. V. Milford, "What have you been taking? Nephrotoxicity from medications and other chemicals," in *Understanding Kidney Diseases*Springer, Berlin, Germany, 2020.

[50] Z. Kanic, V. Kanic, and T. Hojnik, "Enalapril and Acute Kidney Injury in a hypertensive premature newborn–should it be used or not?" *Journal of Pediatric Pharmacology and Therapeutics*, vol. 26, no. 6, pp. 638–642, 2021.

[51] W. McCallum, H. Tighiouart, E. Ku, D. Salem, and M. J. Sarnak, "Trends in kidney function outcomes following RAAS inhibition in patients with heart failure with reduced ejection fraction," *American Journal of Kidney Diseases*, vol. 75, no. 1, pp. 21–29, 2020.

Hindawi
Evidence-Based Complementary and Alternative Medicine
Volume 2021, Article ID 7203934, 11 pages
https://doi.org/10.1155/2021/7203934

Research Article

Ethyl Acetate Fraction from *Leandra dasytricha* (A. Gray) Cong. Leaves Promotes Vasodilatation and Reduces Blood Pressure in Normotensive and Hypertensive Rats

Rita de Cassia Vilhena da Silva,[1] Luísa Nathália Bolda Mariano,[1] Eleine Renata Bidinha,[1] Camila Leandra Bueno de Almeida,[1] Valdir Cechinel-Filho,[1] Vanessa Samudio Santos Zanuncio,[2] Denise Brentan Silva,[2] Arquimedes Gasparotto Junior,[3] and Priscila de Souza[1]

[1]*Postgraduate Program in Pharmaceutical Sciences, Nucleus of Chemical-Pharmaceutical Investigations, University of Vale do Itajaí, Itajaí, Brazil*
[2]*Laboratory of Natural Products and Mass Spectrometry, Faculty of Pharmaceutical Sciences, Food and Nutrition, Federal University of Mato Grosso do Sul, Campo Grande, MatoGrosso do Sul, Brazil*
[3]*Laboratory of Cardiovascular Pharmacology, Faculty of Health Sciences, Federal University of Grande Dourados, Dourados, MatoGrosso do Sul, Brazil*

Correspondence should be addressed to Priscila de Souza; priscilasouza_rc@yahoo.com.br

Received 5 September 2021; Accepted 28 October 2021; Published 15 November 2021

Academic Editor: Eliana Rodrigues

Leandra dasytricha (A. Gray) Cong. is widely distributed in the south of Brazil and is commonly used for cardiovascular and kidney ailments. For this study, we used male Wistar normotensive rats (NTRs) and spontaneously hypertensive rats (SHRs) to verify the effects of the ethyl acetate fraction (EAF) obtained from *L. dasytricha* leaves on isolated aorta relaxation and in the arterial blood pressure. The EAF was analyzed by LC-DAD-MS, and several components were annotated, including hydrolysable tannins, triterpenes, and *O*- and *C*-glycosylated dihydrochalcones, such as the most intense ion peak relative to *C*-hexosyl phloretin (nothofagin; compound number **13**). The EAF caused a concentration and endothelium-dependent relaxation of the aorta in both NTRs and SHRs. This effect was abolished in the endothelium-denuded aorta. L-NAME, a nonselective nitric oxide synthase inhibitor, and ODQ, a soluble guanylate cyclase inhibitor, entirely blocked the EAF-induced relaxation. The presence of a muscarinic receptor antagonist or a cyclooxygenase inhibitor did not alter the EAF's effectiveness in relaxing the aorta. The preincubation with tetraethylammonium, a Ca^{2+}-activated K^+ channel blocker, and with 4-aminopyridine, a voltage-dependent K^+ channel blocker, significantly interfered with the EAF's relaxation. However, the incubation with glibenclamide, an ATP-sensitive K^+ channel blocker, and barium chloride, an inward-rectifier K^+ channel blocker, did not interfere with the EAF-induced relaxation. The EAF treatment also caused a dose-dependent decrease in the mean arterial pressure, systolic arterial pressure, and diastolic arterial pressure of both NTRs and SHRs, without significantly interfering with heart rate values. In conclusion, this study demonstrated the EAF-induced vasorelaxant and hypotensive actions, primarily dependent on the endothelium function and mainly with the participation of the nitric oxide and Ca^{2+}-activated and voltage-dependent K^+ channels.

1. Introduction

According to data from the American Heart Association (AHA), heart diseases are the leading causes of death globally. In 2019, nearly 18.6 million people worldwide died from cardiovascular diseases (CVDs) [1], hypertension being the most common risk factor [2]. The pathogenesis of hypertension involves many factors, and the treatment requires a healthy lifestyle and multiple therapies in a large majority of patients. The main objective in the treatment of

hypertension is to prevent the occurrence of damage to the blood vessels and heart caused by sustained high blood pressure levels. A slight reduction in systolic blood pressure is enough to decrease mortality levels and cardiovascular risks [3]. There are several classes of antihypertensive drugs; however, the failure to effectively control blood pressure can occur for several reasons, including suboptimal treatment and disease progression, with nonadherence to the treatment being responsible for 50 to 80% of unsatisfactory pressure reduction [4–6]. For these reasons, cardiovascular disease risks remain increased in hypertensive patients. Alternative approaches, such as herbal preparations with higher efficacy and lower toxicity, are sought to improve treatments and are also used to prevent cardiovascular complications [7].

Leandra dasytricha (A. Gray) Cong., popularly known as "pixirica," belongs to the Melastomataceae family, which is widely distributed in the south of Brazil [8]. In addition to *L. dasytricha,* other species of *Leandra* have also shown pharmacological effects. *L. lacunosa* had a hypoglycemic effect in alloxan-induced diabetes in rats, and *L. chaetodon* revealed an antifungal activity [9, 10]. Recently, the ethyl acetate fraction isolated from *L. dasytricha* leaves exhibited the ability to increase the urine volume when orally given to rats. Its isolated compound nothofagin presented diuretic, natriuretic, and renal protective effects in both normotensive and hypertensive rats [11, 12]. In addition, nothofagin induced endothelium-dependent vasodilation in renal arteries [13].

Although *L. dasytricha* is commonly used for cardiovascular and kidney ailments [11, 12], studies with its preparations are still scarce. Based on the premise of developing new therapeutic alternatives for the treatment of cardiovascular diseases, this study extends the investigations from a semipurified fraction obtained from the leaves of *L. dasytricha* and demonstrates the chemical profile of this preparation. In this context, it became interesting to evaluate the possible vasodilator and hypotensive properties in both normotensive and hypertensive rats. Spontaneously hypertensive rats (SHRs) are developed by selective breeding of Wistar Kyoto rats for high blood pressure to develop hypertension [14]; they are considered a suitable animal model of essential or primary human hypertension and have been widely used to study cardiovascular diseases [15].

2. Materials and Methods

2.1. Drugs and Chemicals. Atropine, acetylcholine chloride (ACh), indomethacin, Nω-nitro-l-arginine methyl ester (L-NAME), H-[1,2,3]oxadiazolo[4,3-alpha]quinoxalin (ODQ), phenylephrine hydrochloride (PE), tetraethylammonium (TEA), glibenclamide (GLI), 4-aminopyridine (4-AP), barium chloride ($BaCl_2$), and all salts used to prepare the Krebs solution were purchased from Merck & Co. (Kenilworth, New Jersey, USA).

2.2. Phytochemical Procedures. The leaves of *Leandra dasytricha* (A. Gray) Cong. were collected from Camboriú, SC, Brazil (May 2014). Prof. Dr. Oscar Iza (UNIVALI) identified the plant species, and a voucher specimen has been deposited in the Barbosa Rodrigues Herbarium under number VCF 145. The preparation of the extract and the fractions were described by de Almeida et al. [11]. Briefly, fresh leaves of *L. dasytricha* were macerated at room temperature in methanol for 7 days. The ethyl acetate fraction (EAF) was obtained from the partition of the crude methanolic extract of *L. dasytricha* leaves by adding the ethyl acetate solvent.

2.3. LC-DAD-MS Analysis of L. dasytricha. The ethyl acetate fraction (EAF) of *L. dasytricha* leaves was solubilized in methanol and water (7 : 3, v/v) at a concentration of 2 mg/mL. Subsequently, this solution was filtered through a syringe filter (0.22 μM pore, membrane PTFE, Millex® filters) and analyzed by liquid chromatography coupled to a diode array detector and mass spectrometer (LC-DAD-MS) using a Kinetex C-18 column (2.6 μm, 150 × 2.2 mm, Phenomenex) with a precolumn of the same stationary phase material. The mass spectrometer MicrOTOF-Q III (Bruker Daltonics) was provided with an electrospray ionization source and quadrupole-time-of-flight analyzers. The elution gradient profile was the same reported by Tolouei et al. [16]. The mobile phase was composed by acetonitrile and ultrapure water with 0.1% formic acid. The oven temperature was 50°C, and the volume of injection was 2 μL.

The analyses were obtained by positive and negative ion modes (*m/z* 120–1200). Additionally, the compounds were monitored at wavelengths ranging from 240 to 800 nm. The annotation of the constituents from EAF was based on MS data (accurate mass and the ion fragmentation pathway) and UV data compared to data reported in the literature. The molecular formula of each compound was determined based on the mass errors within ±5 ppm and mSigma below 30. The authentic standards (gallic acid, catechin, and ellagic acid) were injected to confirm the identification of some metabolites.

2.4. Animals. Male normotensive Wistar rats (NTRs) and male spontaneously hypertensive rats (SHRs), twelve weeks old (250–300 g), provided by Universidade do Vale do Itajaí (UNIVALI), were kept at a constant temperature (22 ± °C) under a 12 h light/12 h dark cycle. The animal had free access to water and feed. The experiments were approved by the Ethical Committee for the Care and Use of animals of UNIVALI (authorization *n*°. 045/16 and 014/21), which followed the guidelines of the Brazilian National Council for Control of Animal Experimentation.

2.5. Isolation, Preparation of Rat Aorta, and Vascular Reactivity Studies. The thoracic aorta was isolated from male NTR and male SHR as previously described by Da Silva et al. [17].Briefly, the thoracic aorta was removed under anesthesia, cleaned of fat and connective tissue, and cut into rings (3-4 mm length). They were kept in organ baths containing Krebs solution (composition in mM : NaCl 115.3, KCl 4.9,

$CaCl_2 \cdot 2H_2O$ 1.46, KH_2PO_4 1.2, $MgSO_4$ 1.2, d-glucose 11.1, and $NaHCO_3$ 25), pH 7.4, maintained at 37°C under a resting tension of 1 g, and continuously aerated with 95% O_2 and 5% CO_2. Tension changes were obtained through isometric transducers coupled to DATAQ Instruments data acquisition hardware connected to a computer with specific software integration (WinDaq software, DATAQ Instruments, Akron, Ohio, USA). The rings remained at an equilibrium period of 60 min, with solution changes every 15 min. Then, the preparations were contracted with a potassium chloride solution (KCl: 60 mM) to test their responsiveness. To confirm the presence of a functional endothelium, a further 30 min stabilization period was expected. A new contraction was induced by adding phenylephrine (PE: 1 μM), followed by administering 1 μM acetylcholine (ACh). Only rings that showed relaxation equal to or greater than 80% were considered with functional endothelium. For preparations devoid of endothelium, this was mechanically removed by gently scraping the endothelial cells away from the intima. A new 30 min interval was expected for stabilization, and the aortic rings were then exposed to cumulative concentrations of EAF (10 to 500 μg/mL) in preparations with and without functional endothelium at the plateau of the PE-induced contraction. To study the mechanisms involved in the vasorelaxant effect induced by the EAF, the rings were preincubated (30 min) before the addition of PE, with the following drugs: L-NAME (100 μM, a nonselective NO synthase inhibitor), ODQ (100 μM, an inhibitor of soluble guanylyl cyclase), atropine (1 μM, a muscarinic receptor antagonist), indomethacin (1 µM, a cyclooxygenase inhibitor), and with the K^+ channel blockers, which are as follows: tetraethylammonium (TEA, 1 mM, a calcium-activated K^+ channel blocker) or TEA (10 mM, a nonselective K^+ channel blocker), glibenclamide (10 μM, an ATP-sensitive K^+ channel blocker), 4-aminopyridine (4-AP, 1 mM, a voltage-sensitive K^+ channel blocker), or barium chloride ($BaCl_2$, 10 μM, a nonselective inward-rectifier K^+ channel blocker). The cumulative concentration curve of EAF was obtained in the presence of these drugs or just the vehicle.

2.6. Blood Pressure Analysis. The blood pressure study was conducted, as previously described by Da Silva et al. [18]. After anesthesia with ketamine/xylazine (80/10 mg/kg; by intramuscular route), the left femoral vein was cannulated with a polyethylene catheter filled with physiological saline solution (0.9%) for administration of heparin to prevent clot formation. The left carotid artery was isolated from the vagus nerve for insertion of a polyethylene catheter, which was connected to a pressure transducer coupled to an AECAD 04P recording system, running the software AQCAD 2.3.7 (Bonther, Ribeirão Preto, Brazil). Blood pressure was stabilized for 15 min with continuous real-time blood pressure recording. After that, three doses of EAF (0.3, 1, and 3 mg/kg), acetylcholine (10 nmol/kg), or vehicle were administered to the rats. All doses were given in a 200 µL bolus through duodenal access. Changes in mean arterial pressure (MAP), systolic arterial pressure (SAP), diastolic arterial pressure (DAP), and heart rate (HR) were recorded and compared between groups.

2.7. Statistical Analysis. All data are expressed as the mean ± standard error of the mean (SEM) from six preparations or animals per group. One- or two-way analysis of variance (ANOVA) followed by Bonferroni's multiple comparison test was performed using GraphPad Prism version 8 for Windows (GraphPad Software, La Jolla, CA, USA). A *p*value less than 0.05 was considered statistically significant.

3. Results

3.1. Chemical Analyses by LC-DAD-MS. The EAF was analyzed by LC-DAD-MS, and twenty-one compounds were annotated (Table 1 and Figure 1). The compounds were annotated based on their spectral data (MS, MS/MS, and UV) compared with data reported in the literature, and standards were used to confirm some compounds when possible.

The peaks **1** and **2** were putatively annotated as di-*O*-hexoside and shikimic acid, while the compounds **3**, **5,** and **6** presented similar UV spectra, and from the accurate mass, their molecular formulas were determined as $C_7H_6O_5$, $C_8H_8O_5$, and $C_{15}H_{14}O_6$. In addition, **5** also revealed the product ion at *m/z* 168 $[M\text{-}H\text{-}^{\bullet}CH_3]^{-\bullet}$ [19], suggesting a methoxyl group, and **3** and **6** were confirmed by the authentic standard. Thus, **3**, **5**, and **6** were annotated as gallic acid, methyl gallate, and catechin.

The peaks **4**, **7**, and **8** showed similar UV ($\lambda_{max} \approx 275$ nm), and they revealed a molecular formula with high number of carbons such as $C_{41}H_{26}O_{26}$. They revealed fragment ions at *m/z* 301 and 169 which are relative to ellagic acid, confirming the hexahydroxydiphenoyl (HHDP) and gallic acid (Singh et al., 2016). For example, the successive losses of galloyl (152 *u*) from *m/z* 635 $[M\text{-}H]^-$ (**8**) yielded the fragment ions *m/z* 465 $[M\text{-}H\text{-}152\text{-}H_2O]^-$ and 313 $[M\text{-}H\text{-}152\text{-}2xH_2O]^-$. The compounds **4**, **7,** and **8** were annotated as the hydrolysable tannins castalagin isomer, acutissimin A or B, and tri-*O*-galloyl hexoside, respectively.

The peaks **11** and **16** revealed the absorption bands in the UV spectra at the wavelength ≈ 280 and 368 nm, which is compatible with the chromophore of ellagic acid. The compound **11** (*m/z* 300.9996 $[M\text{-}H]^-$, $C_{14}H_6O_8$) was confirmed by ellagic acid as the authentic standard. The protonated ion from **16** revealed losses of 15 *u* (*m/z* 330 $[M + H\text{-}^{\bullet}CH_3]^{+\bullet}$ and 315 $[M + H\text{-}2x^{\bullet}CH_3]^{+\bullet}$), suggesting the methoxyl substituents [19], so it was annotated as tri-O-methyl ellagic acid.

The compounds **9-10**, **12-13**, **15**, and **17-19** revealed spectral data compatible to dihydrochalcones, such as the UV data. The characteristics of losses of 180 (hexosyl + H_2O molecules) and 152 (galloyl), 42 *u* (cetene) and subsequent losses of 90 and 120 *u* suggest the substituents *O*-hexosyl, galloyl, acetyl, and *C*-hexosyl [20–23]. They were annotated as *O*-hexosyl phloretin (**9**), *C*-hexosyl hydroxyphlorizin (**10**), di-*C*-hexosyl phloretin (**12**), *C*-hexosyl phloretin (nothofagin) (**13**), *C*-hexosyl phloretin (**15**), *O*-galloyl *C*-hexosyl

Table 1: Chemical constituents from the ethyl acetate fraction (EAF) of *L. dasytricha*.

Peak	Compound	RT (min)	MF	UV (nm)	*m/z* $[M+H]^+$	*m/z* $[M-H]^-$	MS/MS
1	Di-O-hexoside	1.1	$C_{12}H_{22}O_{11}$	—	365.1044^{Na}	341.1028	—
2	Shikimic acid	1.2	$C_7H_{10}O_5$	—	—	173.0459	—
3	Gallic acidst	2.4	$C_7H_6O_5$	270	—	169.0125	—
4	Castalagin isomer	4.5	$C_{41}H_{26}O_{26}$	285	935.0803	466.0275^{-2}	466 ⟶ 301, 275, 231, 191, 169
5	Methyl gallate	7.8	$C_8H_8O_5$	270	185.0444	183.0299	183 ⟶ 168
6	Catechinst	9.1	$C_{15}H_{14}O_6$	270	291.0855	289.0695	289 ⟶ 221, 203, 151
7	Acutissimin A/B isomer	9.7	$C_{56}H_{38}O_{31}$	285	—	602.0626^{-2}	602 ⟶467, 301, 275, 249, 169
8	Tri-*O*-galloyl hexoside	15.6	$C_{27}H_{24}O_{18}$	270	637.1035	635.089	635 ⟶ 465, 313, 423, 271, 211, 169
9	*O*-hexosyl phloretin	16.0	$C_{21}H_{24}O_{10}$	284	437.1442	435.1297	435 ⟶ 255, 229
10	*C*-hexosyl hydroxyphlorizin	16.6	$C_{21}H_{24}O_{11}$	284	453.1391	451.1246	451 ⟶ 361, 331, 239, 167
11	Ellagic acidst	17.7	$C_{14}H_6O_8$	282, 368	303.0120	300.9996	301 ⟶ 283, 257, 245, 229
12	Di-*C*-hexosyl phloretin	19.1	$C_{27}H_{34}O_{15}$	286	599.1970	597.1825	597 ⟶ 417, 387, 357, 315, 209, 167
13	*C*-hexosyl phloretin (nothofagin)	19.4	$C_{21}H_{24}O_{10}$	286	437.1442	435.1297	435 ⟶ 345, 315, 273, 209, 167
14	Unknown	20.8	$C_{27}H_{28}O_{12}$	280	545.1654	543.1508	543 ⟶ 313, 229, 169
15	*C*-hexosyl phloretin	24.2	$C_{21}H_{24}O_{10}$	285	437.1437	435.1293	435 ⟶ 345, 315, 272, 209, 179, 167
16	Tri-*O*-methyl ellagic acid	24.4	$C_{17}H_{12}O_8$	285, 368	345.0605	343.0459	345 ⟶ 330, 315, 285
17	*O*-galloyl *C*-hexosyl phloretin	24.8	$C_{28}H_{28}O_{14}$	284	589.1536	587.1412	587 ⟶ 345, 315, 273, 209, 167
18	*O*-acetyl *C*-hexosyl phloretin	25.6	$C_{23}H_{26}O_{11}$	284	479.1525	477.1407	477 ⟶ 345, 315, 273, 167
19	Phloretin	28.4	$C_{15}H_{14}O_5$	285	275.0914	273.0768	273 ⟶ 189, 167, 151
20	Triterpene	33.8	$C_{30}H_{48}O_5$	—	489.3575	487.3429	—
21	Triterpene	34.6	$C_{30}H_{48}O_5$	—	489.3564	487.3445	—

MF: molecular formula; RT: retention time; ^{Na}: $[M+Na]^+$; $^{-2}$: $[M-2H]^{-2}$; st: confirmed by authentic standard.

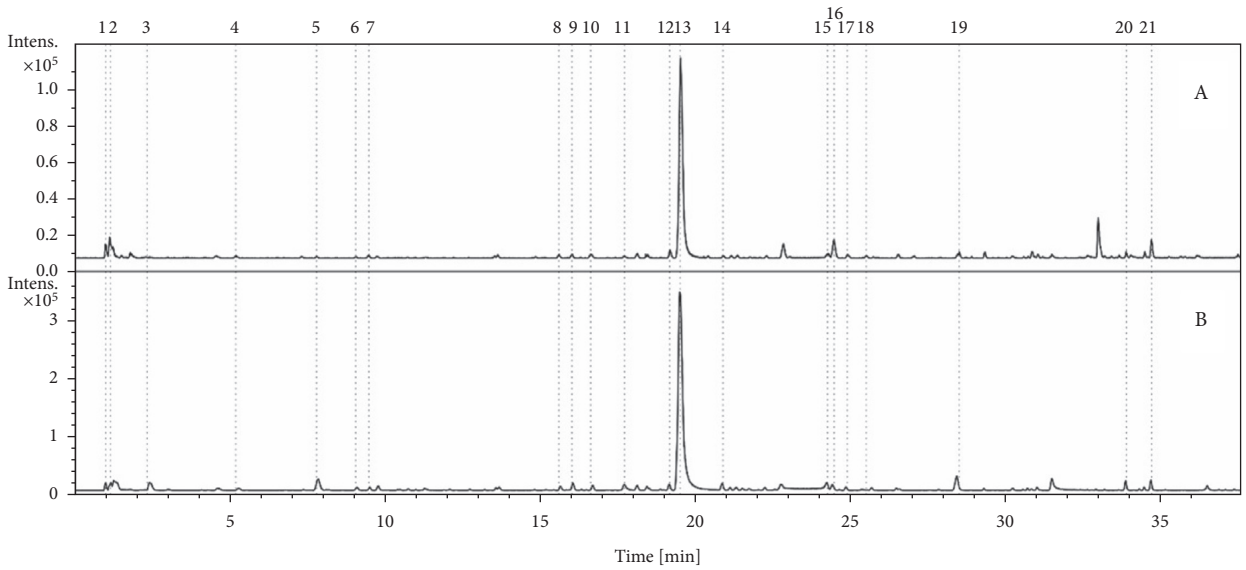

Figure 1: Base peak chromatograms obtained in positive (a) and negative ion mode (b) chromatograms from EAF.

phloretin (**17**), *O*-acetyl *C*-hexosyl phloretin (**18**), and phloretin (**19**). The molecular structure of the major peak identified in the ethyl acetate fraction from *L. dasytricha* , nothofagin (13), can be seen in Figure S1 (supplementary material).

3.2. Effect of EAF from L. dasytricha in Thoracic Aorta Rings Precontracted with Phenylephrine. The cumulative addition of EAF caused a concentration-dependent vasorelaxant effect in the endothelium intact aortic rings of both NTRs and SHRs. The maximal relaxation (R_{max}) values in endothelium intact preparations were $83.22 \pm 9.05\%$ in NTRs and $74.87 \pm 7.30\%$ in SHRs (Figures 2(a) and 2(b), respectively). The vasodilator effect in the endothelium-denuded aorta was only $27.07 \pm 16.54\%$ in NTRs and $16.80 \pm 8.09\%$ in SHRs, indicating that the endothelium is essential for the relaxation induced by EAF. The vehicle (Krebs solution), represented in all images by the closed rectangle symbol, did not affect the aortic rings tonus.

3.3. Involvement of Nitric Oxide in the Vasorelaxant Activity of EAF. The nonselective nitric oxide synthase inhibitor

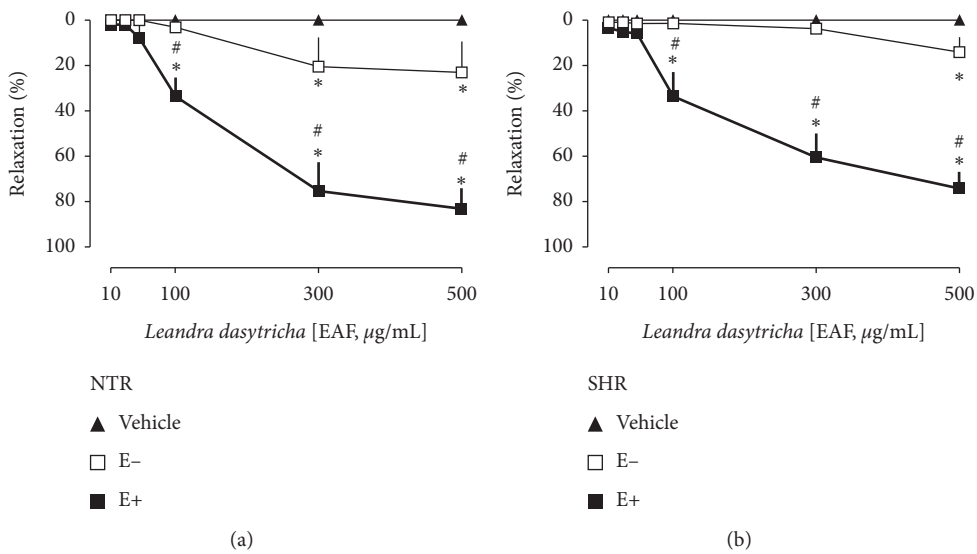

Figure 2: Vasorelaxation induced by EAF in the aorta of Wistar normotensive rats (NTRs) and spontaneously hypertensive rats (SHRs). Concentration-response curves were determined in endothelium-intact (E+) or endothelium-denuded (E-) rings. (a) The EAF-induced vasorelaxation in the NTR aorta. (b) EAF-induced vasorelaxation in the SHR aorta. Statistical analyses were performed using a two-way analysis of variance followed by Bonferroni's multiple comparison test. $^{*}p < 0.05$ when compared to the vehicle (closed triangles), and $^{\#}p < 0.05$ when compared to E- (opened squares).

L-NAME, as well as the soluble guanylate cyclase inhibitor ODQ, entirely blocked the EAF-induced relaxation in both NTR and SHR aorta rings (Figure 3). Besides, it can be seen in Figure 4 that neither atropine nor indomethacin modified the EAF-induced vasodilation response in the aorta of NTRs and SHRs.

3.4. Effect of K^+ Channel Blockers on EAF-Induced Relaxation. The EAF-induced relaxation was significantly reduced in the presence of the nonselective potassium channel blocker (TEA, 10 mM) in both NTR and SHR preparations (Figures 5(a) and 5(b), respectively). Besides, TEA at a concentration of 1 mM (Figures 5(c) and 5(d)), which acts as a Ca^{2+}-activated K^+ channel blocker, reduced the relaxation response of EAF in both NTR and SHR aortas. The pre-incubation with 4-aminopyridine (4-AP), a voltage-dependent K^+ channel blocker, significantly interfered with the EAF's relaxation in both NTR and SHR preparations (Figures 6(a) and 6(b), respectively). However, the incubation with glibenclamide (10 μM), an ATP-sensitive K^+ channel blocker, and barium chloride (10 μM), an inward-rectifier K^+ channel blocker, did not interfere with the EAF-induced relaxation (Figures 6(c)–6(f)).

3.5. EAF Reduces Mean and Systolic Blood Pressure in Both Normotensive and Hypertensive Rats. As depicted in Table 2, the EAF treatment at doses of 1 and 3 mg/kg, but not 0.3 mg/kg, triggered a dose-dependent decrease in the blood pressure of NTRs, with a reduction of~24 mm Hg (at the highest dose tested) in the values of MAP, SAP, and DAP. Regarding the EAF treatment in SHR, a dose-dependent decrease in the blood pressure was also observed, with a reduction of ~21 mm Hg in the values of MAP, SAP, and DAP at the highest dose tested. The values obtained with the administration of acetylcholine (10 nmol/kg) are also shown in Table 2 as the positive control of the experiment. None of the treatments significantly interfered with heart rate values (data not shown).

4. Discussion

In the present study, we showed that a semipurified fraction obtained from the leaves of *Leandra dasytricha* (A. Gray) Cong. induced a concentration-dependent relaxation in the aorta preparations, as well as dose-dependent hypotensive and antihypertensive effects in NTRs and SHRs, respectively. Due to the similarity with human arterial hypertension pathogenesis, SHRs have become the animals of choice for screening antihypertensive agents [15, 24]; thus, our study evidences a meaningful fraction-mediated action in an established disease model with translation into clinical practice.

The analyses by LC-DAD-MS from EAF revealed several compounds that had not been reported previously in *L. dasytricha*; thus, we here expanded the chemical knowledge of this medicinal species. Between the compounds annotated, we highlighted hydrolysable tannins, triterpenes, and mainly dihydrochalcones, such as the most intense ion peak C-hexosyl phloretin (nothofagin). This dihydrochalcone has been reported as a diuretic and natriuretic with potassium-sparing effects [11, 12].

The EAF-induced vasorelaxation was blunted with the endothelium removal, indicating that the integrity of the

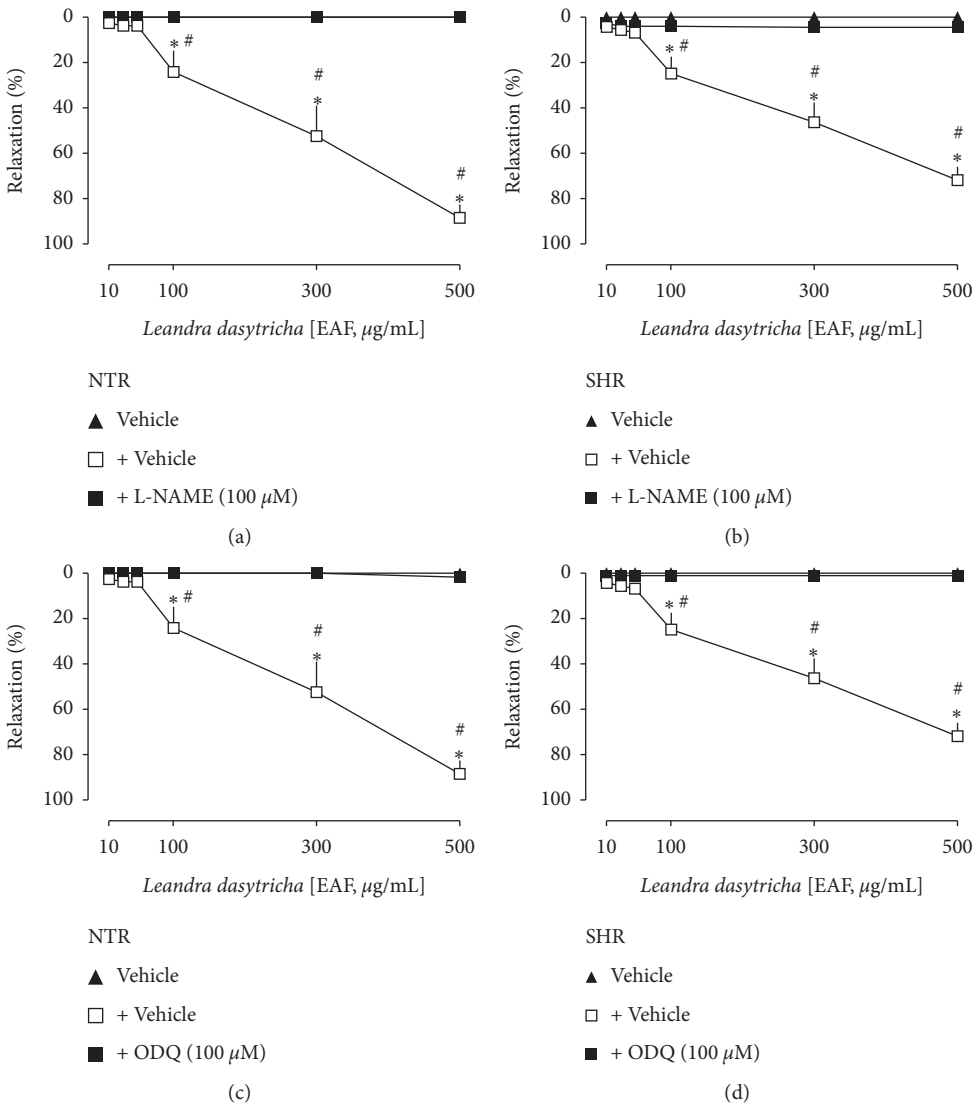

Figure 3: Vasorelaxation induced by EAF in the aorta of Wistar normotensive rats (NTRs) and spontaneously hypertensive rats (SHRs) in the absence or presence of L-NAME (a, b) and ODQ (c, d). Statistical analyses were performed using a two-way analysis of variance followed by Bonferroni's multiple comparison test. $^{*}p < 0.05$ when compared to the vehicle (closed triangles), and $^{\#}p < 0.05$ when compared to the vehicle-only incubation (opened squares).

endothelium is necessary to EAF's vasodilation. To investigate the mechanism of endothelium-dependent relaxation, the vessels were pretreated with L-NAME, which completely blocked the vasorelaxation response, indicating NO's participation in the vasodilator response produced by EAF. Endothelial cells may cause vasorelaxation by releasing vasoactive substances called endothelium-derived relaxing factor (EDRF), identified as NO [25]. NO production and release is mediated through the upregulation of the endothelium nitric oxide synthase (eNOS) activity. NO diffuses into the vascular smooth muscle cells where it stimulates the soluble guanylate cyclase (sGC) that increases cyclic guanosine monophosphate (cGMP) concentration, which in turn activates a GMP-dependent protein kinase (PKG) that can phosphorylate and inhibit the myosin light chain kinase (MLCK), reducing myosin phosphorylation and consequently promoting vascular smooth muscle relaxation [26, 27]. The selective inhibitor of the sGC enzyme ODQ also inhibited the EAF-induced vasorelaxation. These results confirm the involvement of the NO/cGMP pathway in the EAF-induced endothelium-dependent relaxation.

In addition to NO production through the muscarinic receptor, endothelium cells can also induce relaxation by releasing prostaglandin I_2 (PGI_2, prostacyclin) through the cyclooxygenase pathway. PGI_2 activates the prostaglandin I2 receptor, or just IP receptor, on the vascular smooth muscle cell membrane, coupled to adenylate cyclase through the protein (Gs), promoting an increase in cyclic adenosine monophosphate (cAMP) levels. cAMP levels have been a key cellular event to trigger blood vessel

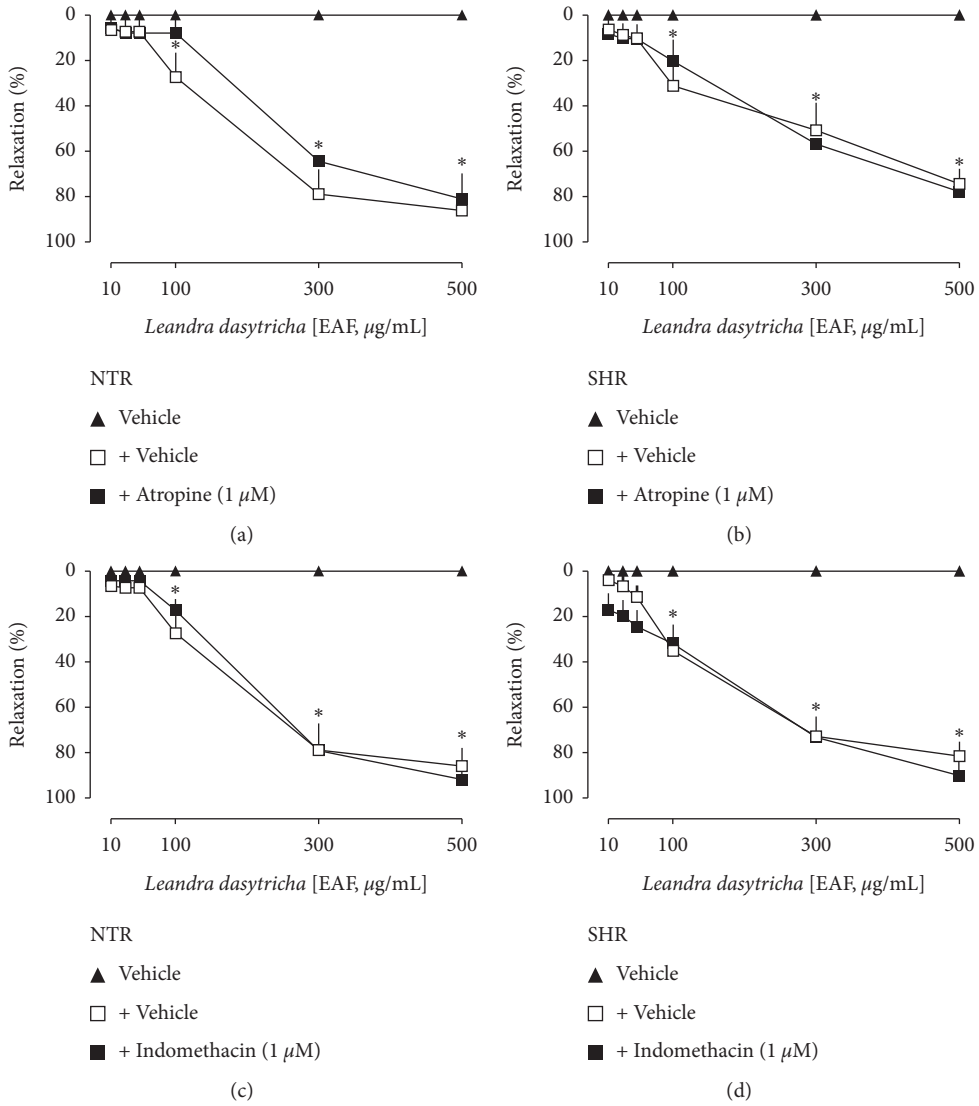

Figure 4: Vasorelaxation induced by EAF in the aorta of Wistar normotensive rats (NTRs) and spontaneously hypertensive rats (SHRs) in the absence or presence of atropine (a, b) and indomethacin (c, d). Statistical analyses were performed using a two-way analysis of variance followed by Bonferroni's multiple comparison test. $^{*}p < 0.05$ when compared to the vehicle (closed triangles).

relaxation by IP agonists [25]. Increased concentrations of cGMP or cAMP are correlated with smooth muscle relaxation induced by various drugs and phytochemicals [28, 29]. However, neither the muscarinic receptor antagonism nor the cyclooxygenase inhibition was able to modify the EAF-induced vasodilation, suggesting that these pathways are not pivotal for the relaxant effect of this fraction.

The second pathway of PKG stimulation is the activation of the K^+ channel [30]. The opening of a K^+ channel in the vascular smooth muscle membrane cells causes hyperpolarization, increasing K^+ efflux, leading to the closure of Ca^{2+} channels and, consequently, vasodilation [31]. TEA, at high concentrations, is a nonspecific K^+ channel blocker that inhibits the ATP-, voltage-, and calcium-dependent subtypes of channels. Our results showed that the presence of TEA (10 mM) produced a significant reduction in the aortic relaxant response induced by the EAF, indicating the participation of K^+ channels. Many subtypes of K^+ channels have been identified in smooth muscle cells [32]. The contribution of each channel to vasodilation is estimated from the effect of selective inhibitors. Glibenclamide, which acts as a selective blocker of adenosine triphosphate- (ATP-) dependent K^+ channels, and barium chloride, a selective blocker of inward-rectifier K^+ channels, did not modify the EAF-induced relaxation, indicating that these K^+ channel subtypes are not the main ones responsible for the fraction's actions. On the other hand, TEA (1 mM), which acts as a large-conductance Ca^{2+}-activated K^+ channel blocker, and 4-AP, a selective voltage-dependent K^+ channel blocker,

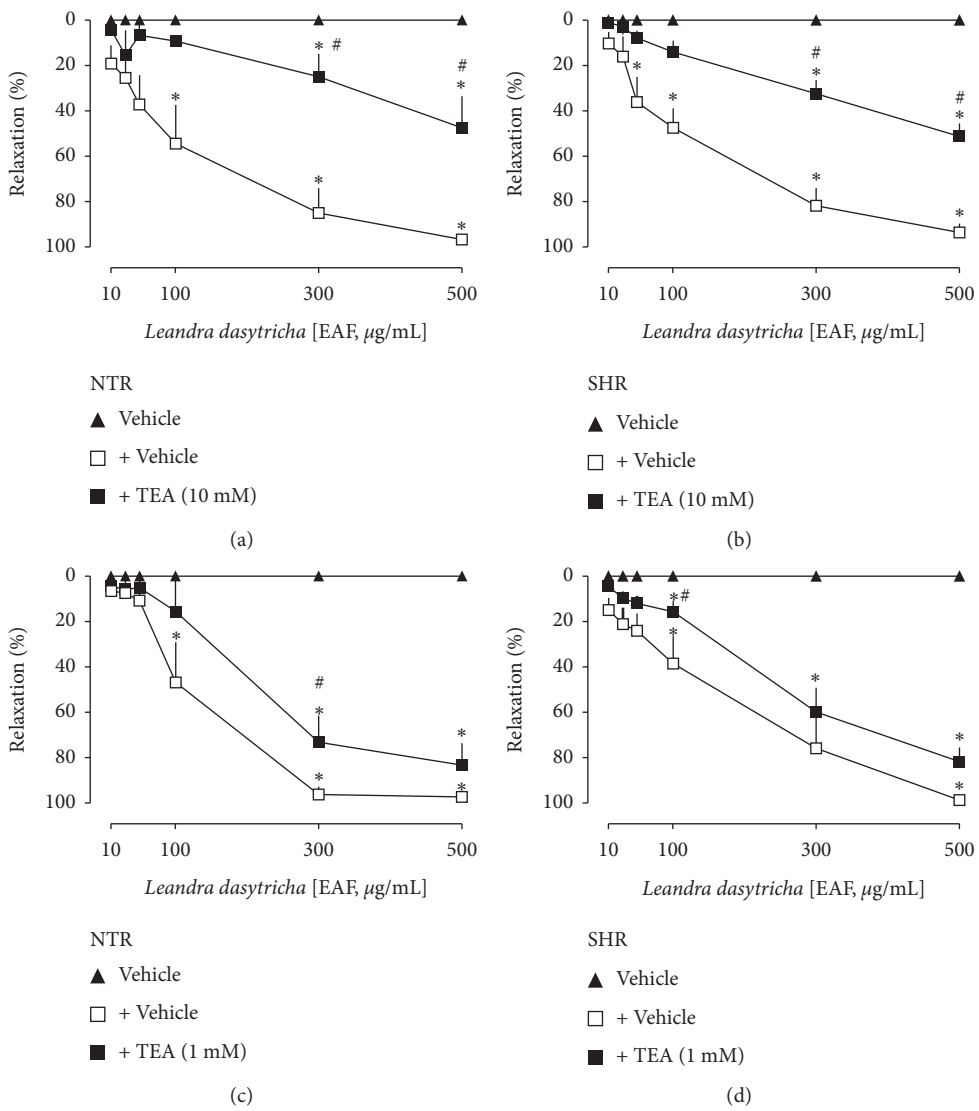

Figure 5: Vasorelaxation induced by EAF in the aorta of Wistar normotensive rats (NTRs) and spontaneously hypertensive rats (SHRs) in the absence or presence of TEA 10 mM (a, b) and TEA 1 mM (c, d). Statistical analyses were performed using a two-way analysis of variance followed by Bonferroni's multiple comparison test. * $p < 0.05$ when compared to the vehicle (closed triangles), and # $p < 0.05$ when compared to the vehicle-only incubation (opened squares).

significantly reduced the vasorelaxation response of EAF. The voltage-dependent K^+ channels are activated by depolarizing the membrane potential, resulting in repolarization and a return to the resting membrane potential, maintaining the resting vascular tone. The Ca^{2+}-activated K^+ channels are activated by either increased intracellular Ca^{2+} or membrane depolarization, resulting in the control of Ca^{2+} influx and K^+ efflux [33]. Indeed, these subtypes of K^+ channels seem to be the main ones for the fraction's vasodilating actions.

Our results suggest that EAF has bioactive compounds, which induce endothelium-dependent vasodilation, mainly through the NO pathway with consequent activation of K^+ channels. The isolated rat aorta model has been a valuable tool to validate the vasoactive properties of extracts and compounds obtained from plants [34]. Extending these findings to the *in vivo* system, it was interesting to evaluate the effect of the EAF on the blood pressure values of rats. The data presented herein revealed that the treatment with EAF reduced the MAP, SAP, and DAP of both normotensive and hypertensive animals. In SHR, hypertension is generally attributed to the increased activity of the sympathetic nervous system, hyperactivation of the renin-angiotensin-aldosterone system, and endothelial dysfunction mainly due to the reduced bioavailability of NO [35, 36]. Thus, strategies aimed at reestablishing some of these pathways are essential tools for the therapeutic management of hypertension and associated conditions.

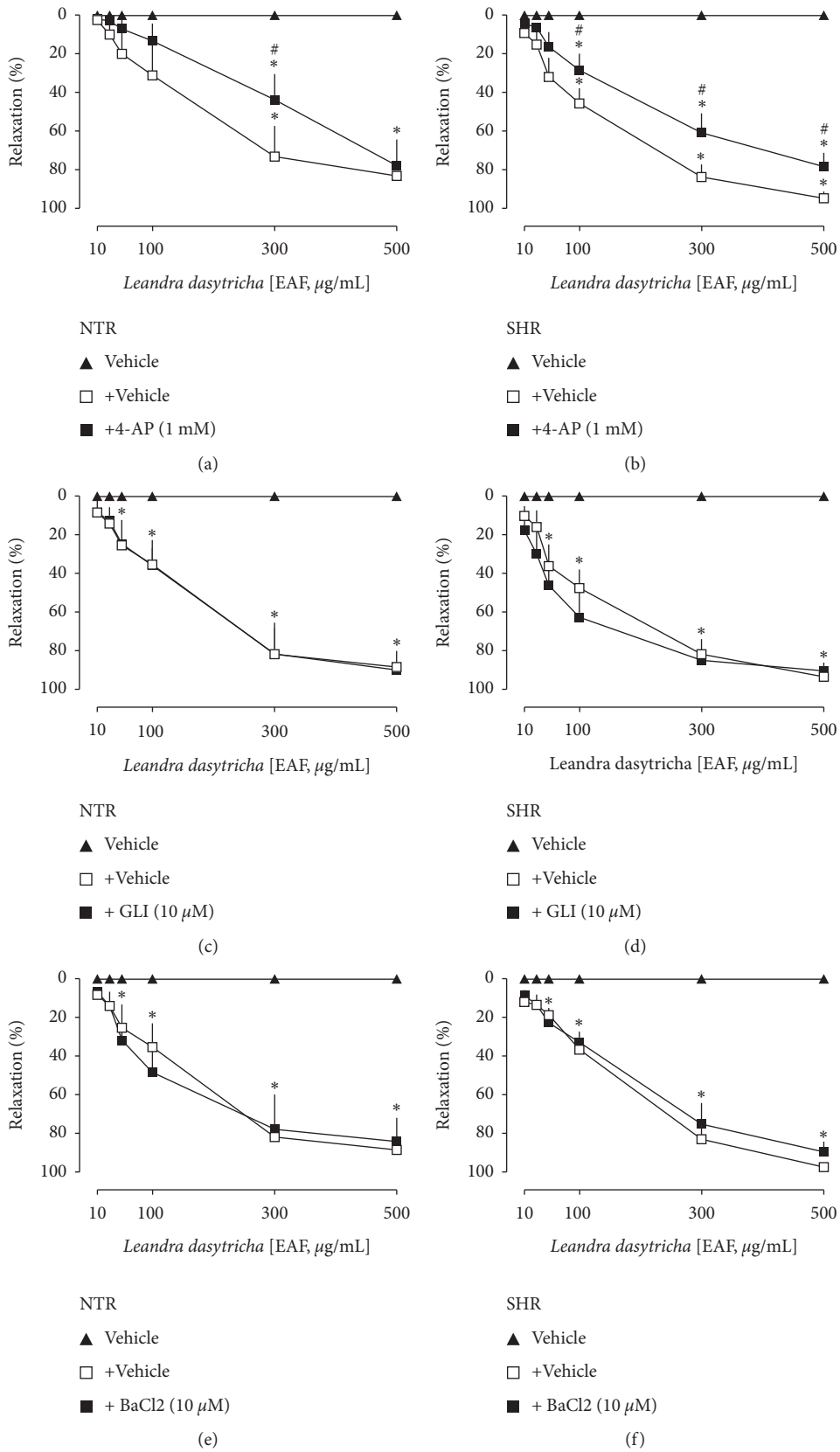

Figure 6: Vasorelaxation induced by EAF in the aorta of Wistar normotensive rats (NTRs) and spontaneously hypertensive rats (SHRs) in the absence or presence of 4-AP (a, b), glibenclamide (c, d), and $BaCl_2$ (e, and f). Statistical analyses were performed using a two-way analysis of variance followed by Bonferroni's multiple comparison test. $^{*}p < 0.05$ when compared to the vehicle (closed triangles), and $^{\#}p < 0.05$ when compared to the vehicle-only incubation (opened squares).

Table 2: Effects of EAF (0.3, 1, and 3 mg/kg) treatment on the blood pressure of normotensive rats (NTRs) and hypertensive rats (SHRs).

Groups	Vehicle	Acetylcholine 10 nmol/kg	EAF 0.3 mg/kg	EAF 1 mg/kg	EAF 3 mg/kg
		NTR			
MAP (mm Hg)	—	$-12.82 \pm 3.07^{*}$	-4.07 ± 1.99	$-11.78 \pm 3.55^{*\#}$	$-24.20 \pm 2.45^{*\#}$
SAP (mm Hg)	—	$-12.44 \pm 4.03^{*}$	-3.47 ± 2.21	$-12.20 \pm 3.56^{*\#}$	$-24.22 \pm 2.30^{*\#}$
DAP (mm Hg)	—	$-13.71 \pm 2.03^{*}$	-2.08 ± 1.49	$-14.08 \pm 3.94^{*\#}$	$-25.36 \pm 2.77^{*\#}$
		SHR			
MAP (mm Hg)	—	$-20.75 \pm 6.86^{*}$	-2.92 ± 1.68	$-10.71 \pm 2.32^{*\#}$	$-21.17 \pm 2.46^{*\#}$
SAP (mm Hg)	—	$-20.92 \pm 5.45^{*}$	-4.09 ± 1.93	$-10.70 \pm 2.67^{*\#}$	$-21.37 \pm 3.29^{*\#}$
DAP (mm Hg)	—	$-21.76 \pm 6.69^{*}$	-4.46 ± 1.33	$-11.19 \pm 1.75^{*\#}$	$-21.35 \pm 1.93^{*\#}$

The results show the mean ± S.E.M. of 6 animals in each group. Statistical analyses were performed by means of a one-way analysis of variance followed by Bonferroni's multiple comparison test. $^{*}p < 0.05$ when compared to a vehicle, and $^{\#}p < 0.05$ when compared to EAF 0.3 mg/kg or EAF 1 mg/kg. MAP, mean arterial pressure; SAP, systolic arterial pressure; and DAP, diastolic arterial pressure.

5. Conclusions

The present study shows that a semipurified fraction obtained from the *Leandra dasytricha* leaves has bioactive compounds that can synergistically induce vascular relaxation and, consequently, reduce blood pressure in normotensive and hypertensive animals. Further studies are required to confirm the mechanisms of action suggested in this study, which point to the involvement of the NO/cGMP pathway and K^{+} channel activation.

Abbreviations

ACh: Acetylcholine
AHA: American Heart Association
4-AP: 4-Aminopyridine
$BaCl_2$: Barium chloride
CVD: Cardiovascular disease
cGMP: Cyclic guanosine monophosphate
cAMP: Cyclic adenosine monophosphate
DAP: Diastolic arterial pressure
eNOS: Endothelium nitric oxide synthase
EDRF: Endothelium-derived relaxing factor
GLI: Glibenclamide
PKG: GMP-dependent protein kinase
ODQ: H-[1,2,3]oxadiazolo[4,3-alpha]quinoxalin
HR: Heart rate
MAP: Mean arterial pressure
MLCK: Myosin light-chain kinase
NO: Nitric oxide
L-NAME: Nω-nitro-l-arginine methyl ester
NTR: Normotensive rat
PE: Phenylephrine
PGI_2: Prostaglandin I_2
SAP: Systolic arterial pressure
sGC: Soluble guanylate cyclase
SHR: Spontaneously hypertensive rat
EAF: Ethyl acetate fraction
TEA: Tetraethylammonium.

Data Availability

Data are available from the corresponding author on request.

Conflicts of Interest

The authors declare no conflicts of interest.

Authors' Contributions

R.C.V. da Silva and P. de Souza wrote the manuscript. The phytochemical procedures and analysis were carried out by C.L.B. Almeida, V. Cechinel-Filho, A. Gasparotto-Junior, V.S.S. Zanuncio, and D.B. Silva. Pharmacological assays were idealized and undertaken by E.R. Bidinha, L.N.B. Mariano, R.C.V. da Silva, and P. de Souza. All authors reviewed and approved the final version of the manuscript.

Acknowledgments

This study was supported by the Conselho Nacional de Desenvolvimento Científico e Tecnológico, Coordenação de Aperfeiçoamento de Pessoal de Nível Superior, Fundação de Amparo à Pesquisa e Inovação do Estado de Santa Catarina, and Universidade do Vale do Itajaí. Dr. Rita de Cássia Vilhena da Silva is grateful for the postdoctoral scholarship and financial support from PNPD/CAPES.

Supplementary Materials

Figure S1: molecular structure of nothofagin (**13**) identified in the ethyl acetate fraction from *L. dasytricha*. (*Supplementary Materials*)

References

[1] American Heart Association, *AHA: Heart Disease Remains Leading Cause of Death Worldwide; Trends Discouraging*, American Heart Association, Dallas, TX, USA, 2021, https://www.healio.com/news/cardiology/20210127/aha-heart-disease-remains-leading-cause-of-death-worldwide-trends-discouraging.

[2] P. C. W. van den Hoogen, "The relation between blood pressure and mortality due to coronary heart disease among men in different parts of the world," *New England Journal of Medicine*, vol. 342, pp. 1–81, 2000.

[3] A. V. Chobanian, G. L. Bakris, H. R. Black et al., "Seventh report of the joint national committee on prevention, detection, evaluation, and treatment of high blood pressure," *Hypertension*, vol. 42, pp. 1206–1252, 2003.

[4] B. Williams, G. Mancia, W. Spiering et al., "ESC/ESH Guidelines for themanagement of arterial hypertension," *European Heart Journal*, vol. 39, pp. 3021–3104, 2018.

[5] M. G. Saklayen and N. V. Deshpande, "Timeline of history of hypertension treatment," *Frontiers in Cardiovascular Medicine*, vol. 3, 2016.

[6] C. Cuspidi, M. Tadic, G. Grassi, and G. Mancia, "Treatment of hypertension: the ESH/ESC guidelines recommendations," *Pharmacological Research*, vol. 128, pp. 315–321, 2018.

[7] WHO, *WHO Traditional Medicine Strategy: 2014-2023*, WHO, Geneva, Switzerland, 2015.

[8] M. Sobral, J. A. Jarenkow, P. Brack, B. E. Irgang, J. Larocca, and R. S. Rodrigues, *Flora Arbórea e Arborescente do rio Grande do Sul*, RiMa Editora, São Paulo, Brazil, 1 edition, 2006.

[9] W. R. Cunha, G. M. Arantes, D. S. Ferreira et al., "Hypoglicemic effect of Leandra lacunosa in normal and alloxan-induced diabetic rats," *Fitoterapia*, vol. 79, pp. 356–360, 2008.

[10] Q. Zhang, H. N. ElSohly, X. C. Li, and L. A. Walker, "A new triterpene from Leandra chaetodon," *Planta Medica*, vol. 69, pp. 582–584, 2003.

[11] C. L. B. de Almeida, T. Boeing, L. Bordignon Somensi et al., "Diuretic, natriuretic and potassium-sparing effect of nothofagin isolated from Leandra dasytricha (A. Gray) Cogn. leaves in normotensive and hypertensive rats," *Chemico-Biological Interactions*, vol. 268, pp. 103–110, 2017.

[12] C. L. B. de Almeida, V. Cechinel-Filho, T. Boeing et al., "Prolonged diuretic and saluretic effect of nothofagin isolated from Leandra dasytricha (A. Gray) Cogn. leaves in normotensive and hypertensive rats: role of antioxidant system and renal protection," *Chemico-Biological Interactions*, vol. 279, pp. 227–233, 2018.

[13] A. A. M. Marques, C. Henrique Francisconi da Silva, P. de Souza et al., "Nitric oxide and Ca2+-activated high-conductance K+ channels mediate nothofagin-induced endothelium-dependent vasodilation in the perfused rat kidney," *Chemico-Biological Interactions*, vol. 327, 2020.

[14] K. Okamoto and K. Aoki, "Development of a strain of spontaneously hypertensive rats," *Japanese Circulation Journal*, vol. 27, pp. 282–293, 1963.

[15] N. C. Trippodo and E. D. Frohlich, "Similarities of genetic (spontaneous) hypertension. Man and rat," *Circulation Research*, vol. 48, pp. 309–319, 1981.

[16] S. E. L. Tolouei, C. Adriane Signor Tirloni, R. Alan Calloi Palozi et al., "*Celosia argentea* L. (Amaranthaceae) a vasodilator species from the Brazilian Cerrado–An ethnopharmacological report," *Journal of Ethnopharmacology*, vol. 229, pp. 115–126, 2019.

[17] R. Da Silva, S. Crestani, P. de Souza et al., "Endothelium-dependent and independent vasorelaxation induced by an n-butanolic fraction of bark of Scutia buxifolia Reiss (Rhamanaceae)," *Journal of Ethnopharmacology*, vol. 141, pp. 997–1004, 2012.

[18] R. Da Silva, P. de Souza, S. Crestani et al., "Hypotensive and diuretic effect of the butanolic soluble fraction of the hydroethanolic extract of bark of Scutia buxifolia Reissek in rats," *Journal of Ethnopharmacology*, vol. 172, pp. 395–401, 2015.

[19] A. M. Mustafa, S. Angeloni, D. Abouelenein et al., "A new HPLC-MS/MS method for the simultaneous determination of 36 polyphenols in blueberry, strawberry and their commercial products and determination of antioxidant activity," *Food Chemistry*, vol. 367, Article ID 130743, 2022.

[20] Z. Fan, Y. Wang, M. Yang, J. Cao, A. Khan, and G. Cheng, "UHPLC-ESI-HRMS/MS analysis on phenolic compositions of different E Se tea extracts and their antioxidant and cytoprotective activities," *Food Chemistry*, vol. 318, Article ID 126512, 2020.

[21] I. M. Abu-Reidah, D. Arráez-Román, I. Warad, A. Fernández-Gutiérrez, and A. Segura-Carretero, "UHPLC/MS2-based approach for the comprehensive metabolite profiling of bean (*Vicia faba* L.) by-products: a promising source of bioactive constituents," *Food Research International*, vol. 93, pp. 87–96, 2017.

[22] M. F. Mahomoodally, S. Jugreet, K. I. Sinan et al., "Pharmacological potential and chemical characterization of *Bridelia ferruginea* benth.—a native tropical african medicinal plant," *Antibiotics*, vol. 10, no. 2, p. 223, 2021.

[23] G. Baeza, B. Sarriá, L. Bravo, and R. Mateos, "Exhaustive qualitative LC-DAD-MSn analysis of arabica green coffee beans: cinnamoyl-glycosides and cinnamoylshikimic acids as new polyphenols in green coffee," *Journal of Agricultural and Food Chemistry*, vol. 64, no. 51, pp. 9663–9674, 2016.

[24] A. Singh, V. Bajpai, S. Kumar, K. R. Sharma, and B. Kumara, "Profiling of gallic and ellagic acid derivatives in different plant parts of *Terminalia arjuna* by HPLC-ESI-QTOF-MS/MS," *Natural Products Communications*, vol. 11, pp. 239–244, 2016.

[25] G. Gendron, F. Gobeil, J. Morin, P. D'Orléans-Juste, and D. Regoli, "Contractile responses of aortae from WKY and SHR to vasoconstrictors," *Clinical and Experimental Hypertension*, vol. 26, pp. 511–523, 2004.

[26] M. Félétou, R. Köhler, and P. M. Vanhoutte, "Nitric oxide: orchestrator of endothelium-dependent responses," *Annals of Medicine*, vol. 44, pp. 694–716, 2012.

[27] R. M. J. Palmer, A. G. Ferrige, and S. Moncada, "Nitric oxide release accounts for the biological activity of endothelium-derived relaxing factor," *Nature*, vol. 327, pp. 524–526, 1987.

[28] P. M. Vanhoutte, H. Shimokawa, M. Feletou, and E. H. C. Tang, "Endothelial dysfunction and vascular disease-a thirthieth anniversary update," *Acta Physiologica*, vol. 219, 2015.

[29] F. Murad, "Cyclic guanosine monophosphate as a mediator of vasodilation," *Journal of Clinical Investigation*, vol. 78, pp. 1–5, 1986.

[30] M. Knox, R. Vinet, L. Fuentes, B. Morales, and J. L. Martínez, "A review of endothelium-dependent and -independent vasodilation induced by phytochemicals in isolated rat aorta," *Animals*, vol. 9, p. 623, 2019.

[31] S. L. Archer, J. M. Huang, V. Hampl, D. P. Nelson, P. J. Shultz, and E. K. Weir, "Nitric oxide and cGMP cause vasorelaxation by activation of a charybdotoxin-sensitive K channel by cGMP-dependent protein kinase," *Proceedings of the National Academy of Sciences of the United States of America*, vol. 91, pp. 7583–7587, 1994.

[32] M. T. Nelson and J. M. Quayle, "Physiological roles and properties of potassium channels in arterial smooth muscle," *American Journal of Physiology*, vol. 268, pp. C799–C822, 1995.

[33] N. B. Standen and J. M. Quayle, "K^+ channel modulation in arterial smooth muscle," *Acta Physiologica Scandinavica*, vol. 164, pp. 549–557, 1998.

[34] M. Rameshrad, H. Babaei, Y. Azarmi, and R. F. Fouladi, "Rat aorta as a pharmacological tool for in vitro and in vivo studies," *Life Sciences*, vol. 145, pp. 190–204, 2016.

[35] R. J. Head, "Hypernoradrenergic innervation: its relationship to functional and hyperplastic changes in the vasculature of the spontaneously hypertensive rat," *Blood Vessels*, vol. 26, pp. 1–20, 1989.

[36] J. de Champlain, "Pre- and postsynaptic adrenergic dysfunctions in hypertension," *Journal of Hypertension-Supplement*, vol. 8, 1990.

Hindawi
Evidence-Based Complementary and Alternative Medicine
Volume 2021, Article ID 4471944, 19 pages
https://doi.org/10.1155/2021/4471944

Research Article

Efficacy and Safety of Curcumin Supplement on Improvement of Insulin Resistance in People with Type 2 Diabetes Mellitus: A Systematic Review and Meta-Analysis of Randomized Controlled Trials

Tianqing Zhang,[1] Qi He,[2] Yao Liu,[1] Zhenrong Chen,[1] and Hengjing Hu[1,3]

[1]*The First Affiliated Hospital, Department of Cardiovascular Medicine, Hengyang Medical School, University of South China, Hengyang, Hunan Province, China*
[2]*People's Hospital of Ningxiang City, Ningxiang City, Hunan Province, China*
[3]*Institute of Cardiovascular Disease and Key Lab for Arteriosclerology of Hunan Province, University of South China, Hengyang, Hunan, China*

Correspondence should be addressed to Hengjing Hu; bestmanhhj123@163.com

Received 6 June 2021; Accepted 20 July 2021; Published 25 August 2021

Academic Editor: Denise Brentan Silva

Background. Diabetes is a major public health concern. In addition, there is some evidence to support curcumin as part of a diabetes treatment program. *Methods*. Data from randomized controlled trials were obtained to assess the effects of curcumin versus placebo or western medicine in patients with type 2 diabetes mellitus (T2DM). The study's registration number is CRD42018089528. The primary outcomes included homeostasis model assessment-insulin resistance (HOMA-IR), glycosylated hemoglobin (HbAlc), total cholesterol (TC), and triglyceride (TG). *Results*. Four trials involving 453 patients were included. The HOMA-IR of curcumin group is lower in Asia (WMD: −2.41, 95% CI: −4.44 to −0.39, $P = 0.02$) and the Middle East subgroups (WMD: −0.60, 95% CI: −0.74 to −0.46, $P < 0.00001$). The HbAlc in the curcumin group is lower than that in the control group (WMD: −0.69; 95% CI: −0.91, −0.48; $P < 0.0001$). The TC and TG levels of the curcumin group are lower in the Asia subgroup (TC: WMD: −23.45, 95% CI: −40.04 to −6.84, $P = 0.006$; TG: WMD: −54.14, 95% CI: −95.71 to −12.57, $P = 0.01$), while in the Middle East the difference was of not statistically significant (TC: WMD: 22.91, 95% CI: −16.94 to 62.75, $P = 0.26$; TG: WMD: −4.56, 95% CI: −19.28 to 10.16, $P = 0.54$). *Conclusion*. Based on the current evidence, curcumin may assist in improving the insulin resistance, glycemic control, and decreased TG and TC in patients with T2DM.

1. Introduction

As a serious metabolic disease, diabetes affects about 5% of the world's people. Epidemiological data show that the number of people with diabetes is expected to increase dramatically to 592 million by 2035 [1]. 12% of global health expenditure is spent annually on diabetes and its complications [2]. Diabetes is divided into different types, wherein type 1 and type 2 diabetes accounted for more than 90% of all cases. Among these types of diabetes, type 2 diabetes mellitus (T2DM) causes metabolic abnormalities and serious complications that have a profound impact on the patient's lifespan and quality of life. T2DM is mainly characterized by insulin resistance and hyperglycemia [3]. Its common complications include microvascular disease (diabetic retinopathy, diabetic nephropathy, and diabetic neuropathy), macrovascular disease (diabetic heart disease, diabetic cerebrovascular disease, and peripheral vascular disease) [4, 5], and increased risk of cancer [6, 7]. At present, T2DM has a variety of therapeutic drugs, such as human insulin preparation, alpha glucosidase inhibitor, dipeptidyl peptidase-4 inhibitor, incretin analogue, biguanide, insulin secretagogue, insulin sensitizer, and intestinal lipase inhibitor [8, 9]. However, the currently used therapies have many side effects such as hypoglycemia, gastrointestinal problems, and weight gain [8]. Therefore, new drugs

and natural compounds are constantly being tested to prevent and treat diabetes better [10].

Curcumin is a chemical component extracted from the rhizome of some plants. It has a series of effects such as blood lipid lowering, antitumor, anti-inflammatory, and anti-oxidation [11, 12] and has been used as a food flavoring agent, preservative, and ancillary medication for some diseases (such as heart disease and tumors) [13, 14]. In the treatment of diabetes, there is also evidence to support curcumin as a part of the diabetes treatment program [14, 15]. At present, many randomized controlled trials (RCTs) on the treatment of T2DM with curcumin have been published [11, 16–22], but there is still no systematic review and meta-analysis to assess the effects and safety of curcumin. Therefore, we decide to perform a systematic review and meta-analysis for the first time to evaluate the clinical effects of curcumin on T2DM.

2. Materials and Methods

2.1. Protocol. Study selection, assessment of eligibility criteria, data extraction, and statistical analyses were performed based on a predefined protocol registered on PROSPERO CRD42018089528 (see supplementary materials) [23].

2.2. Search Strategy and Selection Criteria. We searched the English database and the Chinese database from the beginning of their establishment to September 3, 2020. The English database includes EMBASE, Medline Complete, the Cochrane Library (until Issue 9, 2020), ClinicalTrials, PubMed, and Web of Science. The Chinese database includes the Chinese Science and Technology Periodical Database (VIP), Chinese Biomedical Database (CBM), Wan Fang Database (Chinese Ministry of Science and Technology), and China National Knowledge Infrastructure Databases (CNKI). The search strategy for PubMed is presented in Table 1 as an example.

Studies meeting the inclusion criteria would be included in this review: (1) participants: patients with type 2 diabetes mellitus; (2) intervention: curcumin with no limits on the type, dose, frequency, and so on; (3) comparisons: Western medicine, blanks, or placebo; (4) outcomes: primary outcomes: homeostasis model assessment-insulin resistance (HOMA-IR), glycosylated hemoglobin (HbAlc), total cholesterol (TC), and triglyceride (TG); secondary outcomes: body mass index (BMI), low-density lipoprotein cholesterol (LDL-C), high-density lipoprotein cholesterol (HDL-C), fasting glucose, and fasting insulin; (5) study type: randomized controlled trials (RCTs) with no limits on the manner by which randomization has been achieved on blinding or on the language of publication. Studies meeting the exclusion criteria would be excluded: (1) not T2DM patients; (2) the participant is not human; (3) nonoriginal research literature; and (4) non-RCT.

2.3. Data Extraction. Two reviewers independently extracted the data and it was checked by a third reviewer. When there is a disagreement, a consensus is reached through mutual discussion and negotiation with all reviewers. The extracted data include basic information (author, publication time, age of the research object, etc.), sample size, intervention measures, dose, intervention time, outcomes, etc. [24].

2.4. Study Quality Assessment. The risk of bias of RCTs was assessed by using the risk of bias assessment tool based on the Cochrane Handbook [25]. Two reviewers independently assessed the risk of bias. When there is a disagreement, a consensus is reached through mutual discussion and negotiation with all reviewers. The risk of bias is divided into three levels: high risk, low risk, and unclear. The content of the evaluation includes random sequence generation, allocation concealment, blinding, incomplete outcomes, selective reporting, and other bias.

2.5. Statistical Analysis. The data were analyzed by RevMan 5.3 software. Cochrane's Q and I^2 test were used to judge the heterogeneity of different studies. If there is good homology between studies ($I^2 < 50\%$, $P > 0.1$), the fixed-effects model is used for meta-analysis. If there is heterogeneity between studies ($I2 > 50\%$, $P < 0.1$), we first find the source of heterogeneity, conduct subgroup analysis, and then choose random-effects model or give up meta-analysis [26]. The dichotomous variable measure was summarized by risk ratio (RR) with a 95% confidence interval (CI). The continuous outcomes underwent meta-analysis using weight mean differences (WMD) and 95% CI. If the units of outcomes are different, or the value difference between RCTs is more than 10 times, the standard mean differences (SMD) and 95% CI are used according to the situation.

2.6. Sensitivity Analysis and Publication Bias Detection. STATA 15.0 was utilized for sensitivity analysis and publication bias detection. Studies with RCTs ≥5 were evaluated for publication bias. The outcomes with $P > 0.1$ were thought to have publication bias. The outcomes that meet the following conditions are all subjected to sensitivity analysis: (1) random-effects model is used; (2) number of included RCTs ≥ 3; and (3) the results of the fixed-effects model are inconsistent with the results of the random-effects model (whether it is a subgroup result or a summary result).

3. Results

3.1. Results of the Search. The total records identified through database searching and other sources were 431. Sixteen records were included after initial identification. Four records were excluded: Yang et al. is not RCT [27]; and the participants in the remaining 3 records are not only T2DM patients [28–30]. Eventually, 12 records were included to undergo analysis (Figure 1).

3.2. Description of Included Trials. Twelve records met the inclusion criteria [11, 16–22, 31–34]. Of the 12 records, 4 records [16–19] are from one RCT: Panahi et al., 2 records

Table 1: Search strategy for PubMed.

Database	Search strategy
PubMed	(Curcumin OR Turmeric Yellow OR Yellow, Turmeric OR Diferuloylmethane) AND (Type 2 diabetes mellitus OR Diabetes Mellitus, Noninsulin-Dependent OR Diabetes Mellitus, Ketosis-Resistant OR Diabetes Mellitus, Ketosis Resistant OR Ketosis-Resistant Diabetes Mellitus OR Diabetes Mellitus, Non Insulin Dependent OR Diabetes Mellitus, Non-Insulin-Dependent OR Non-Insulin-Dependent Diabetes Mellitus OR Diabetes Mellitus, Stable OR Stable Diabetes Mellitus OR Diabetes Mellitus, Type II OR NIDDM OR Diabetes Mellitus, Noninsulin Dependent OR Diabetes Mellitus, Maturity-Onset OR Diabetes Mellitus, Maturity Onset OR Maturity-Onset Diabetes Mellitus OR Maturity Onset Diabetes Mellitus OR MODY OR Diabetes Mellitus, Slow-Onset OR Diabetes Mellitus, Slow Onset OR Slow-Onset Diabetes Mellitus OR Type 2 Diabetes Mellitus OR Noninsulin-Dependent Diabetes Mellitus OR Noninsulin Dependent Diabetes Mellitus OR Maturity-Onset Diabetes OR Diabetes, Maturity-Onset OR Maturity Onset Diabetes OR Type 2 Diabetes OR Diabetes, Type 2 OR Diabetes Mellitus, Adult-Onset OR Adult-Onset Diabetes Mellitus OR Diabetes Mellitus, Adult Onset) AND (randomized controlled trial [pt] OR controlled clinical trial [pt] OR placebo [tiab] OR drug therapy [sh] OR trial [tiab] OR groups [tiab] OR clinical trials as topic [mesh: noexp] OR Clinical Trial OR random∗ [tiab] OR random allocation [mh] OR single-blind method [mh] OR double-blind method [mh] OR cross-over studies) NOT (animals [mh] NOT humans [mh])

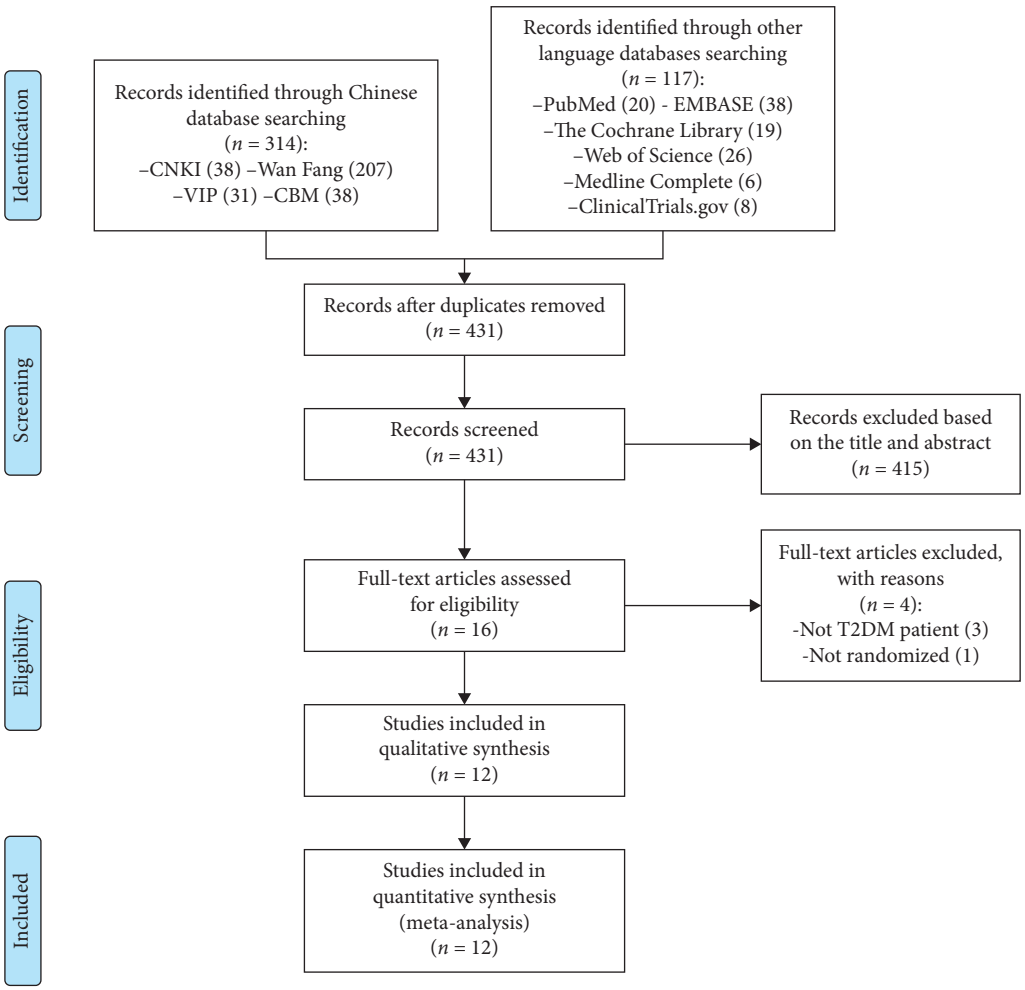

Figure 1: Flow diagram of searching and article selection.

[20, 21] are from the same RCT: Na et al, and 2 records [31, 32] are from one RCT: Asadi et al. Hence, a total of 7 RCTs are included in this review. All of them were parallel-group RCTs. Study characteristics are presented in Table 2.

3.3. Risk of Bias of Included Studies. The summary and graph of risk of bias are shown in Figure 2.

3.3.1. Sequence Generation. Panahi et al. [16–19] and Khajehdehi et al. [22] failed to describe the method of randomization, and we therefore rated it as having an unclear risk of bias. Na et al. [20, 21], Chuengsamarn et al. [11], and Thota et al. [33] utilized a computer-generated random list, and Asadi et al. [31, 32] and Adibian et al. [34] utilized block randomization, so they were thought to have low risks of bias.

Table 2: The characteristics of the included studies.

Study	Register ID	Country	Sample size		Intervention		Relevant outcomes	Duration
			Trial group	Control group	Trial group	Control group		
Panahi et al. [16–19]	IRCT201505301165N4	Iran	50	50	Curcuminoids (C3 Complex®) 1000 mg + 10 mg piperine	Placebo + 10 mg piperine	BMI, TG, TC, LDL-C, HDL-C, HOMA-IR, HbAlc, fasting blood glucose, fasting insulin, adiponectin adverse events	12 weeks
Na et al. [20, 21]	ISRCTN85826075	China	50	50	Curcuminoids 300 mg with no changes to patients' previous drug medication	Placebo with no changes to patients' previous drug medication	TG, TC, LDL-C, HDL-C, HOMA-IR, HbAlc, fasting blood glucose	12 weeks
Chuengsamarn et al. [11]	NCT01052597	Thailand	107	106	Curcumin 1500 mg with no oral antidiabetes or insulin injection	Placebo (starch) 1500 mg with no oral antidiabetes or insulin injection	BMI, TG, TC, LDL-C, HDL-C, HOMA-IR, HbAlc, fasting blood glucose, fasting insulin, adiponectin, adverse events	24 weeks
Khajehdehi et al. [22]	—	Iran	20	20	Turmeric 1500 mg with no changes to patients' previous drug medication	Placebo with no changes to patients' previous drug medication	TG, TC, LDL-C, HDL-C, HOMA-IR, HbAlc, fasting blood glucose, adverse events	8 weeks
Asadi et al. [31, 32]	IRCT20140413017254N5	Iran	40	40	Nanocurcumin 80 mg with no changes to patients' previous hypoglycemic drugs	Placebo with no changes to patients' previous hypoglycemic drugs	BMI, HbAlc, fasting blood glucose, adverse events	8 weeks
Thota et al. [33]	ACTRN12615000559516	Australia	15	16	Curcumin 1000 mg	Placebo (2000 mg corn oil)	HbAlc, TC, LDL-C, HDL-C, fasting blood glucose, adverse events	12 weeks
Adibian et al. [34]	NCT02529969	Iran	21	23	Curcumin 1500 mg with no changes to patients' previous drug medication	Placebo (rice flour) 1332 mg with no changes to patients' previous drug medication	BMI, TG, TC, LDL-C, HDL-C, fasting blood glucose, fasting insulin, adiponectin	10 weeks

Table 2: Continued.

Study	BMI		Mean age (years)		Inclusion criteria	Exclusion criteria
	Trial group	Control group	Trial group	Control group		
Panahi et al. [16–19]	26.53 ± 2.32	27.33 ± 1.58	43 ± 8	41 ± 7	Diagnosis of T2DM based on fasting plasma glucose (FPG) ≥ 126 mg/dL, glycated hemoglobin (HbA1C) ≥ 6.5%, or the use of antidiabetic treatments	Pregnancy or breastfeeding, lack of possibility to give an informed consent, participation in a concomitant trial, presence of malignancies, chronic liver disease (alanine aminotransferase levels three times the upper limit of normal value range), renal failure (serum creatinine ≥ 2.0 mg/dL or being on dialysis), chronic inflammatory diseases such as rheumatoid arthritis and acute infections, endocrine diseases other than T2DM (e.g., hypothyroidism or hyperthyroidism), obsessive compulsive disorder, hyperglycemia due to secondary causes, receiving hormone therapy or other herbal medicines, hypersensitivity to the study medication, and lack of compliance with the study medication
Na et al. [20, 21]	27.12 ± 2.26	27.42 ± 3.04	55.42 ± 6.40	54.72 ± 8.34	(1) Aged 18–65 years, both male and female (2) Type 2 diabetes with fasting blood glucose greater than or equal to 7.0 mmol/L or postprandial blood glucose greater than or equal to 11.1 mmol/L (3) Current optimal therapeutic regimens lasting for at least 6 months	(1) A history of type 1 diabetes, malignancies, thyroid, or any other endocrine diseases likely to interfere with the study (2) Diabetic ketosis acidosis and infection in recent 3 months (3) Pregnancy or breastfeeding (4) Incomplete information or unwillingness to attempt to comply with the intervention
Chuengsamarn et al. [11]	27.09 ± 0.52	26.84 ± 0.42	59.16 ± 11.04	59.58 ± 10.71	(1) Diabetic patients aged 35 years or older and did not use insulin during the first 5 years of treatment after being diagnosed (with or without symptoms listed in the following inclusion criteria) (2) Patients with hyperlipidemia (cholesterol ≥ 200 mg/dl, TG ≥ 150 mg/dl, LDL ≥ 100 mg/dl, and HDL ≥ 35 mg/dl) (3) Patients with hypertension (blood pressure ≥ 130/85 mmHg or take hypertensive drugs) (4) Obesity (BMI ≥ 25)	(1) Current diagnosis of secondary peripheral arterial disease (PAD) (except listed in the inclusion criteria item 1–4) (2) Current diagnosis of cardiovascular disease, i.e., coronary arterial disease and cerebrovascular disease (3) Current diagnosis of end-stage renal function with serum creatinine >2.0 mg/dl or on renal dialysis (4) Current diagnosis of cirrhosis with ALT ≥3 times the normal range
Khajehdehi et al. [22]	—	—	52.9 ± 9.2	52.6 ± 9.7	Patients with overt type 2 diabetic nephropathy (proteinuria ≥500 mg/day), who had normal kidney function and well-controlled blood pressure by ACE-I and/or angiotensin receptor blockers	Patient with recurrent or relapsing urinary tract infection, bacteriuria, pyuria and/or haematuria, or who failed to sign a written informed consent when risks associated with the trial was carefully outlined for them

Table 2: Continued.

Study	BMI		Mean age (years)		Inclusion criteria	Exclusion criteria
	Trial group	Control group	Trial group	Control group		
Asadi et al. [31, 32]	31.1 ± 4.2	30.8 ± 3.8	53.3 ± 6.5	54.6 ± 6.2	Age between 30 and 60 years, desire to participate in the study, body mass index between 25 and 39.9, noninsulin type 2 diabetic patients, detection of mild sensorimotor polyneuropathy by using the Toronto questionnaire (score 6–8)	Follow a special diet during last month, sensitivity to curcumin, pregnancy and lactation, took any nutritional supplement, vitamin and mineral supplement last month, history of gastrointestinal ulcer and bile duct, neuropathies other than the sensory-motor polyneuropathy diabetic diagnosed by a neurologist, taking gabapentin and any medication, diseases such as cancer, liver, kidney, autoimmune diseases, inflammatory, thyroid and nervous and cardiovascular diseases are diagnosed, and drug use associated with these diseases
Thota et al. [33]	30.9 ± 1.2	31.9 ± 1.7	55 ± 2.8	50 ± 2.5	(1) Age: 30–70; gender: both male and female (2) No participation in any clinical trial for at least 3 months (3) An HbA1c of 5.7%–6.4% (4) Impaired glucose tolerance (IGT) (5) 2-hour OGTT plasma glucose greater than or equal to 7.8 mmol/land <11.1 mmol/L (6) Impaired fasting glucose (IFG) (7) Fasting plasma venous glucose measurement 6.1–6.9 mmol/L (8) 12 or more score or high-risk individuals in AUSDRISK assessment tool (9) BMI between 25 and 45	(1) Pregnancy or lactation (2) Established type 2 diabetes (3) Allergic to sea foods (4) People with gall bladder problems (5) People currently on medication with erythropoietin (6) People with anaemia (7) People with pace maker implants (8) Currently on medication with aspirin and warfarin (9) History of severe neurological diseases or seizures (10) History of new investigational drug three months prior to this trial (11) Consuming more than 2 servings of oily fish per week (12) Taking regular dietary supplements known to influence blood glucose level (13) People taking regular vitamin C supplements (14) Unwilling to fast for 10 hr before obtaining blood sample. People currently on medication with clopidogrel, ibuprofen, naproxen, dalteparin, enoxaparin, and heparin
Adibian et al. [34]	—	—	Around 58	60 ± 7	(1) Tendency to participate (2) Age range of 40–65 (3) Suffering from diabetes type 2 (for 1 to 10 years) (4) BMI 18/5–30 (5) Patients with diabetes who administer oral hypoglycemic agents and who do not use them	(1) Patients with liver diseases (2) Patients with kidney diseases (3) Patients with inflammatory diseases (4) Patients with liver diseases (5) Administering herbal agents (6) Administering multivitamins and minerals in past 3 months

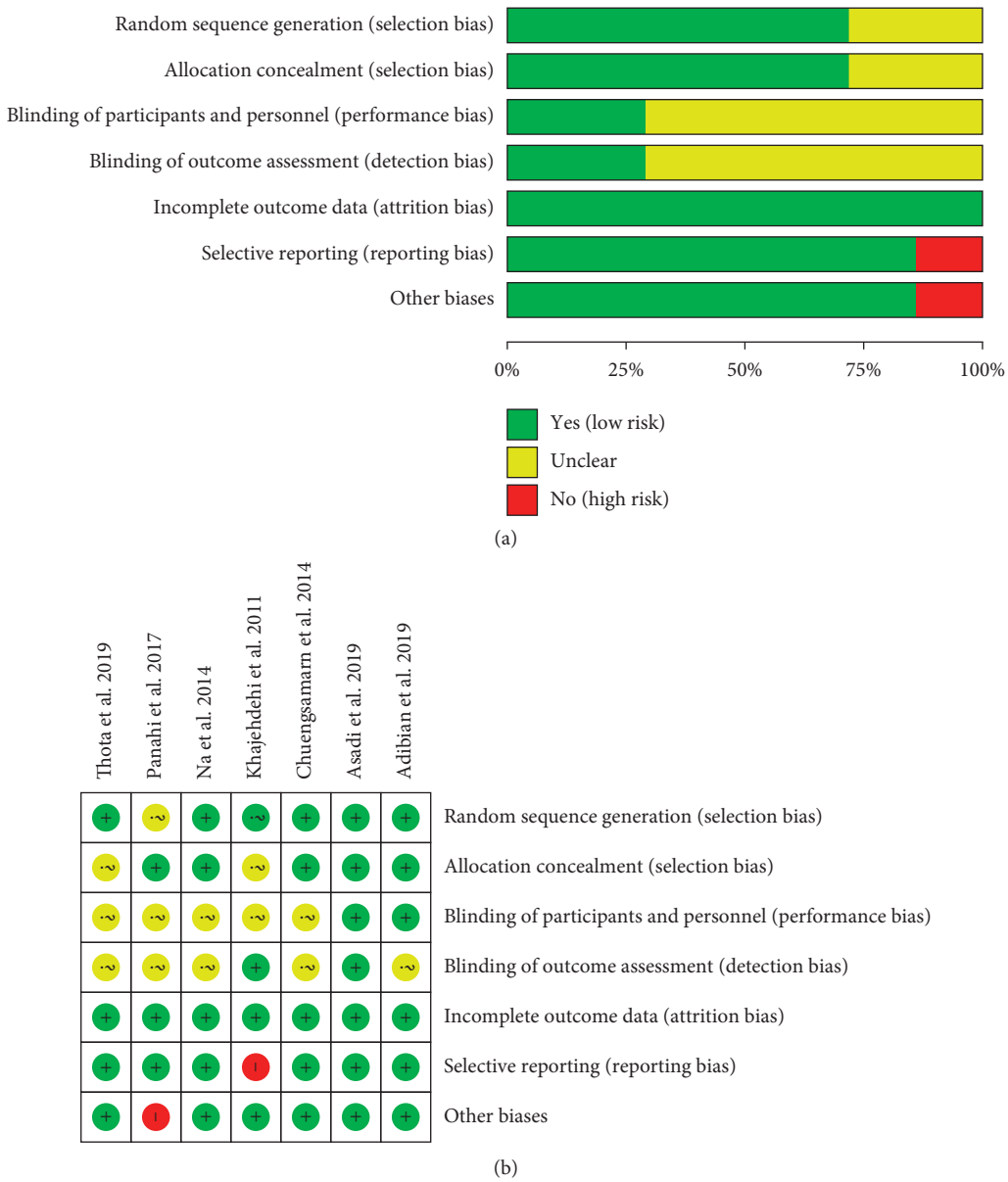

Figure 2: (a) Risk of bias graph. (b) Risk of bias summary.

3.3.2. Allocation Concealment. Khajehdehi et al. [22] and Thota et al. [33] did not describe an acceptable method of allocation concealment; therefore, they were rated as having an unclear risk of bias. Panahi et al. [16–19], Na et al. [20, 21], Asadi et al. [31, 32], and Adibian et al. [34] utilized the capsules in the same shape, size, and color to contain curcumin and placebo; Chuengsamarn et al. [11] used opaque and consecutively numbered envelopes. Hence, these five RCTs considered to have allocation concealment were rated as having low risks of bias.

3.3.3. Blinding, Incomplete Outcome Data, and Selective Reporting. All RCTs claimed to use blinding, but only Asadi et al. [31, 32] described the implementation process for researchers and participants, so only its double blinding was rated as a low risk of bias. Four RCTs [11, 16–21, 33] did not describe the implementation process for both researchers and participants, and they were rated as high risk of bias. Khajehdehi et al. [22] described blinding to researchers, so its blinding of outcome assessment (detection bias) was rated as low risk of bias. Adibian et al. [34] described blinding of participants, so the blinding of participants and personnel (performance bias) was rated as low risk of bias.

3.3.4. Incomplete Outcome Data and Selective Reporting. The incomplete outcome data of all RCTs are rated as low risk of bias because the number of missing persons and the reasons for the missing between groups is balanced. One

RCT (Khajehdehi et al. [22]) failed to provide all outcomes mentioned in its protocols; thus, we thought its risk of bias was high. The others 6 RCTs reported study's prespecified outcomes that are of interest in the review; and their risks of bias were low.

3.3.5. Other Potential Bias. Panahi et al. [16–19] claimed that one of the authors had a conflict of interest and was therefore assessed as a high risk of bias. Other sources of bias in the other 6 RCTs were not found; therefore, the risks of other bias of the RCTs were low.

3.4. Primary Outcomes

3.4.1. Homeostasis Model Assessment-Insulin Resistance. Four RCTs [11, 16–21, 34] reported HOMA-IR. However, the data in Adibian et al. [34] cannot be extracted; hence, the data in four RCTs (207 participants in the curcumin group and 206 participants in the control group) were extracted. Due to the high heterogeneity, three RCTs were subdivided into two subgroups according to the region of the patients. After subdivision, the heterogeneity was still high in each subgroup (Asia Pacific: $I^2 = 86\%$, $P = 0.07$; the Middle East: not applicable) among the RCTs. The random-effects model was used. The HOMA-IR in the curcumin group was lower than that in the control group in the Middle East subgroup (WMD: −0.60, 95% CI:−0.74 to −0.46, $P < 0.00001$) and the Asia subgroup (WMD: −2.41, 95% CI −4.44 to −0.39, $P = 0.02$). However, the summary result showed that the difference in HOMA-IR between two groups was of no significance (WMD: −1.76, 95% CI:−3.65 to 0.13, $P = 0.07$) (Figure 3).

3.4.2. Glycosylated Hemoglobin. Six RCTs [11, 16–21, 31–34] reported HbAlc. However, the data in Adibian et al. [34] cannot be extracted; hence, the data in 5 RCTs including 262 participants in the curcumin group and 262 participants in the control group were extracted. Due to the high heterogeneity ($I^2 = 0\%$, $P = 0.96$), the fixed-effect model was utilized. The results showed that, compared with the control group, curcumin can reduce HbAlc levels (WMD: −0.70; 95% CI: −0.87, −0.54; $P < 0.0001$) (Figure 4).

3.4.3. Total Cholesterol. Five RCTs [11, 16–22, 34] reported TC; however, Adibian et al. [34] used the same symbol for TC and TG, so it is not clear which group of data is TC, and the data cannot be extracted. The data in four RCTs containing 227 participants in the curcumin group and 226 participants in control group were extracted. Due to the high heterogeneity, four RCTs were subdivided into two subgroups according to the region of the patients. After subdivision, the heterogeneity was still high in each subgroup (Asia Pacific: $I^2 = 60\%$, $P = 0.11$; the Middle East: $I^2 = 71\%$, $P = 0.06$) among the RCTs. The random-effects model was used. The difference between two groups in the Asia subgroup has statistical significance (WMD: −23.45, 95% CI: −40.04 to −6.84, $P = 0.006$), but it did not have statistical significance in the Middle East subgroup (WMD: 22.91, 95% CI: −16.94 to 62.75, $P = 0.26$). The summary result also showed that the difference between two groups was of no significance (WMD: −2.00, 95% CI:−39.91 to 35.91, $P = 0.92$) (Figure 5).

3.4.4. Triglyceride. Five RCTs [11, 16–22] reported TG; however, Adibian et al. [34] used the same symbol for TC and TG, so it is not clear which group of data is TG, and the data cannot be extracted. The data in four RCTs involving 227 participants in the curcumin group and 226 participants in the control group were extracted. Due to the high heterogeneity, four RCTs were subdivided into two subgroups according to the region of the patients. After subdivision, the heterogeneity was still high in the Asia subgroup ($I^2 = 80\%$, $P = 0.02$) but low in the Middle East subgroup ($I^2 = 60\%$, $P = 0.11$) among the RCTs. The random-effects model was used in the Asia subgroup. The difference between two groups in the Asia subgroup has statistical significance (WMD: −54.14, 95% CI: −95.71 to −12.57, $P = 0.01$), but it did not have statistical significance in the Middle East subgroup (WMD −4.56, 95% CI: −19.28 to 10.16, $P = 0.54$). The summary result also showed that the difference between two groups was of no significance (WMD: −33.45, 95% CI: −70.60 to 3.71, $P = 0.08$) (Figure 6).

3.5. Secondary Outcomes

3.5.1. Body Mass Index. Three RCTs [11, 16–19, 31, 32] reported BMI. Due to the high heterogeneity ($I^2 = 89\%$, $P = 0.0002$), the statistical analysis was abandoned according to the Cochrane Handbook for Systematic Reviews of Interventions. Panahi et al. [16–19] found that there was a statistically significant difference in BMI changes between the curcumin group and the control group (-0.49 ± 0.52 versus 0.24 ± 0.73; $P < 0.001$). Chuengsamarn et al. [11] also found that there was a statistically significant difference in BMI changes between the curcumin group and the control group (-1.97 ± 5.38 versus 0.16 ± 4.32; $P < 0.001$). However, Asadi et al. [31, 32] found that there were no significant differences in terms of BMI and weight between the two groups.

3.5.2. Fasting Blood Glucose and Fasting Insulin. All RCTs [11, 16–22, 31–34] reported fasting blood glucose. However, the data in Adibian et al. [34] cannot be extracted; hence, the data in 6 RCTs include 282 participants in the curcumin group and 282 participants in the control group. Due to the high heterogeneity, 6 RCTs were subdivided into two subgroups according to the region of the patients. After subdivision, the heterogeneity was low in the Asia Pacific subgroup but high in the Middle East subgroup (Asia:

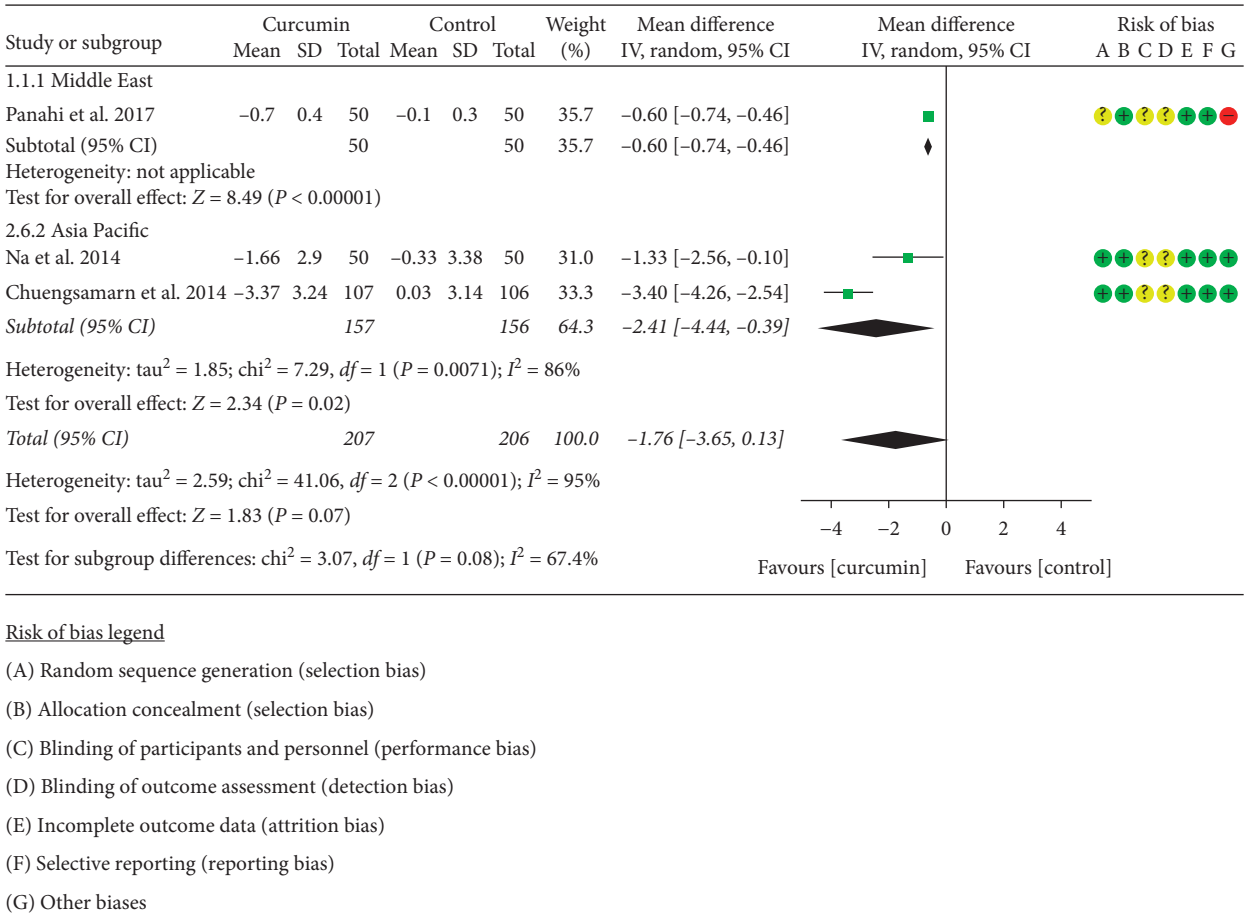

Figure 3: Homeostasis model assessment-insulin resistance.

$I^2 = 0\%$, $P = 0.79$; the Middle East: $I^2 = 74\%$, $P = 0.02$). The random-effects model was used. The fasting blood glucose in the curcumin group was lower than that in the control group Asia subgroup (SMD: −0.57, 95% CI: −0.79 to −0.36, $P < 0.00001$). However, the difference between the curcumin group and the control group in the Middle East subgroup was of no statistical significance (SMD: 0.04, 95% CI: −0.50 to 0.58, $P = 0.89$). The summary results also showed that the difference between two groups was of no statistical significance (SMD: −0.28, 95% CI: −0.62 to 0.06, $P = 0.11$) (Figure 7).

Two RCTs [11, 16–19] reported fasting insulin. Due to the high heterogeneity ($I^2 = 96\%$, $P < 0.00001$), the statistical analysis was abandoned according to the Cochrane Handbook for Systematic Reviews of Interventions. Panahi et al. [16–19] found no significant difference in fasting insulin levels between the two groups ($P > 0.05$), while Chuengsamarn et al. [11] found that the curcumin group had lower fasting insulin levels ($P < 0.05$).

3.5.3. Blood Lipid. Five RCTs [11, 16–22, 34] including 248 participants in the curcumin group and 249 participants in the control group reported LDL-C and HDL-C. Due to the high heterogeneity, 5RCTs were subdivided into two subgroups according to the region of the patients. After subdivision, the heterogeneity was low in each subgroup (Asia: $I^2 = 6\%$, $P = 0.30$; the Middle East: $I^2 = 29\%$, $P = 0.24$) among the RCTs. The fixed-effects model was used. The LDL-C in the curcumin group was lower than that in the control group in the Asia subgroup (WMD: −20.85, 95% CI: −28.78 to −12.92, $P < 0.00001$), but it was higher in the Middle East subgroup (WMD: 15.67, 95% CI: 5.91 to 25.43, $P = 0.002$) (Figure 8).

The RCTs in HDL-C were also subdivided into two subgroups according to the region of the patients for the same sake. After subdivision, the heterogeneity was still high in the two subgroups (Asia Pacific: $I^2 = 91\%$, $P = 0.001$; the Middle East: $I^2 = 76\%$, $P = 0.02$) among the RCTs. The random-effects model was used. The difference in HDL-C between two groups was of no statistical significance in each subgroup (the Middle East: WMD: −0.30, 95% CI: −3.78 to 3.19, $P = 0.87$; Asia: WMD: 6.01, 95% CI: −2.58 to 14.60, $P = 0.17$). The summary result also showed that the difference between two groups was of no statistical significance (WMD: 2.26, 95% CI: −2.03 to 6.55, $P = 0.30$) (Figure 9).

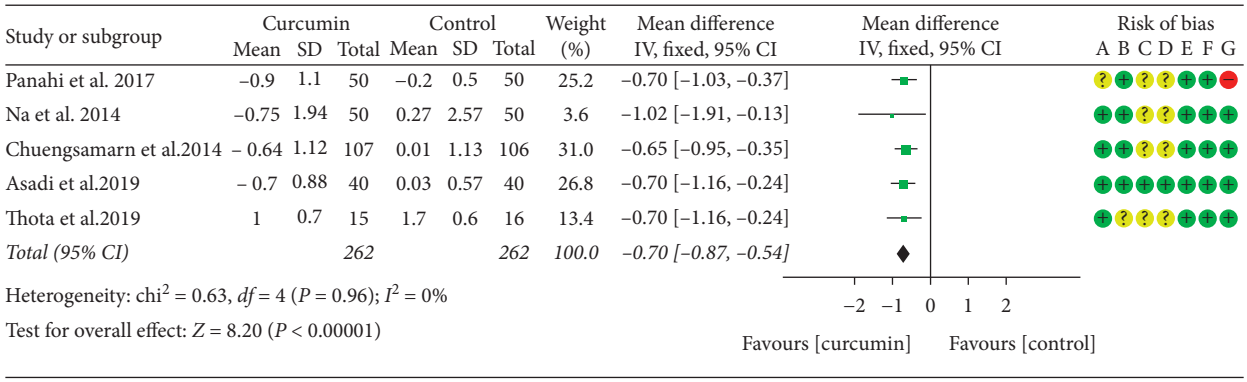

Risk of bias legend

(A) Random sequence generation (selection bias)

(B) Allocation concealment (selection bias)

(C) Blinding of participants and personnel (performance bias)

(D) Blinding of outcome assessment (detection bias)

(E) Incomplete outcome data (attrition bias)

(F) Selective reporting (reporting bias)

(G) Other biases

Figure 4: Glycosylated hemoglobin.

3.5.4. Adiponectin. Three RCTs [11, 16–19, 34] reported adiponectin. The data of Chuengsamarn et al. [11] could not be extracted, so only the data of 2 RCTs were extracted for analysis. The heterogeneity between RCTs is low ($I^2 = 0\%$, $P = 0.49$), so a fixed-effects model is used. Compared with the control group, the curcumin group had higher adiponectin (SMD: 0.50, 95% CI: 0.16 to 0.83, $P = 0.003$) (Figure 10).

3.6. Adverse Events. Four RCTs [11, 16–19, 22, 31, 32] reported adverse events. Two RCTs [16–19, 22] showed that there are no severe related side effects in two groups. One RCT [11] showed that four patients in the curcumin group and four in the control group exhibited adverse events. Asadi et al. [31, 32] reported 2 cases of stomach pain in the first few days, but did not specify the group.

3.7. Sensitivity Analysis Results. Sensitivity analysis was performed for 5 outcomes: HOMA-IR, TC, TG, FBG, and HDL-C. (1) In the outcome "HOMA-IR," after we omitted Na et al. [20, 21], we found that the estimate of the result moved out of the lower limit of 95% CI (Figure 11(a)). (2) In the outcome "TC," after we omitted Panahi et al. [16–19], we found that the estimate of the result moved out of the lower limit of 95% CI, while after omitting Chuengsamarn et al. [11], the estimate of the result moved out of the upper limit of 95% CI (Figure 11(b)). (3) In the outcome "TG," after omitting Chuengsamarn et al. [11], the estimate of the result moved out of the upper limit of 95% CI (Figure 11(c)). (4) In the outcome "FBG," no matter which study was removed, the results were not significantly changed, suggesting that the heterogeneity may not come from RCT (Figure 11(d)). (5) In the outcome "HDL-C," after omitting Chuengsamarn et al. [11], the estimate of the result moved out of the lower limit of 95% CI (Figure 11(e)). The abovementioned RCTs may be the source of heterogeneity of corresponding outcomes.

3.8. Publication Bias Detection. (1) HbA1c:the results of HbA1c indicate that there may be publication bias ($P = 0.061$) (Figure 12(a)). (2) FBG: the publication bias detection suggests that there may be no publication bias ($P = 0.381$) (Figure 12(b)). (3) LDL-C: the publication bias detection suggests that there may be no publication bias ($P = 0.296$) (Figure 12(c)). (4) HDL-C: the publication bias detection suggests that there may be no publication bias ($P = 0.776$) (Figure 12(d)).

4. Discussion

4.1. Main Findings. The HOMA-IR of the curcumin group is lower in Asia and the Middle East subgroups. The HbAlc in the curcumin group is lower than the control group. The TC, TG, and fasting blood glucose level of the curcumin group is lower in the Asia subgroup, while in the Middle East, the difference was of no statistical significance. For BMI, fasting insulin, and HDL-C level, there is no strong evidence that which one is better. Interestingly, although the LDL-C level of the curcumin group in the Asia subgroup is lower than that of the control group, the LDL-C level of the curcumin

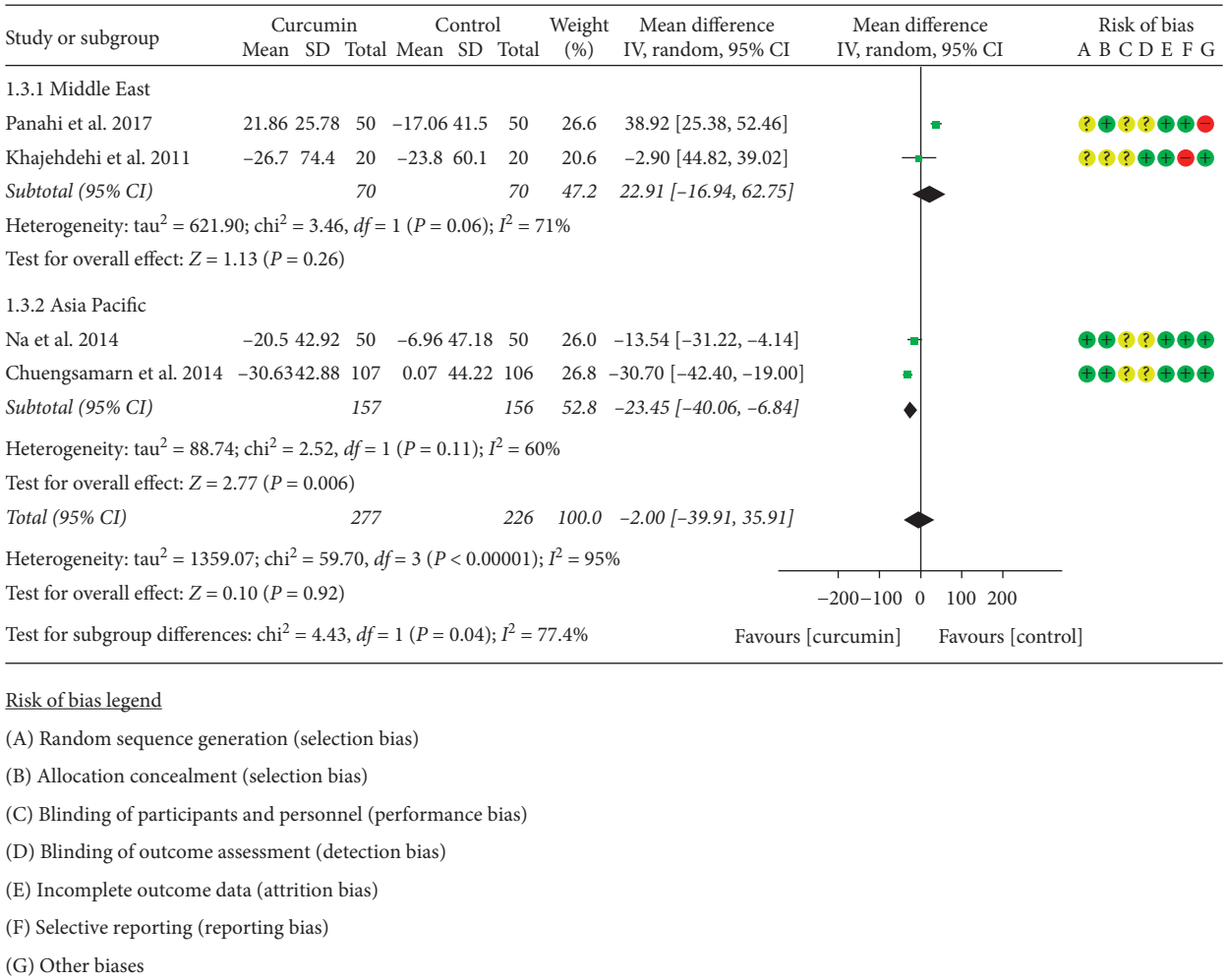

Figure 5: Total cholesterol.

group was higher than the control group in the Middle east subgroup.

4.2. Overall Completeness and Applicability of Evidence. Most of RCTs come from Asia Pacific (especially Southeast Asia, like China and Thailand) and the Middle East (mainly Iran). Due to the lack of RCTs from all over the world, the applicability of the findings is limited.

4.3. Discussion of the Source of Heterogeneity. Most outcomes have heterogeneity, so this study conducted a sensitivity analysis to find the source of heterogeneity. Sensitivity analyses were performed for 5 outcomes: HOMA-IR, TC, TG, FBG, and HDL-C.

For outcome "HOMA-IR," compared with the other two RCTs, the dose of curcuminoids in Na et al. [20, 21] was lower (300 mg), while in Panahi et al. [16–19] it was 1000 mg, and in Chuengsamarn et al. [11] it was 1500 mg. Therefore, the heterogeneity of HOMA-IR may be related to the drug dose. For the outcome "TC," the mean age in Panahi et al. [16–19] is lower, which may be the source of heterogeneity. For the outcome "TC," "TG," and "HDL-C," Chuengsamarn et al. [11] prepared curcumin monomer, while the preparations of several other RCTs are curcuminoids or turmeric, which suggests that different drug preparation methods may be the source of heterogeneity. For the outcome "FBG," no matter which study was removed, the results were not significantly changed, suggesting that the heterogeneity may not come from RCT.

In addition to the above possible sources of heterogeneity, heterogeneity may also come from ethnic differences, regional differences, gender differences, body size differences, and so on. More relevant RCTs are needed to be conducted in more diverse subgroups to reduce the heterogeneity of the research and stabilize the conclusions.

4.4. Novelty of This Research. This systematic review and meta-analysis showed that curcumin can improve HOMA-IR and HbAlc, especially in Asian patients and the Middle Eastern patients. In terms of blood lipids, curcumin can reduce TC, TG, and fasting blood glucose level in Asian patients, but does not improve in the Middle East patients significantly. Curcumin may lower the LDL-C

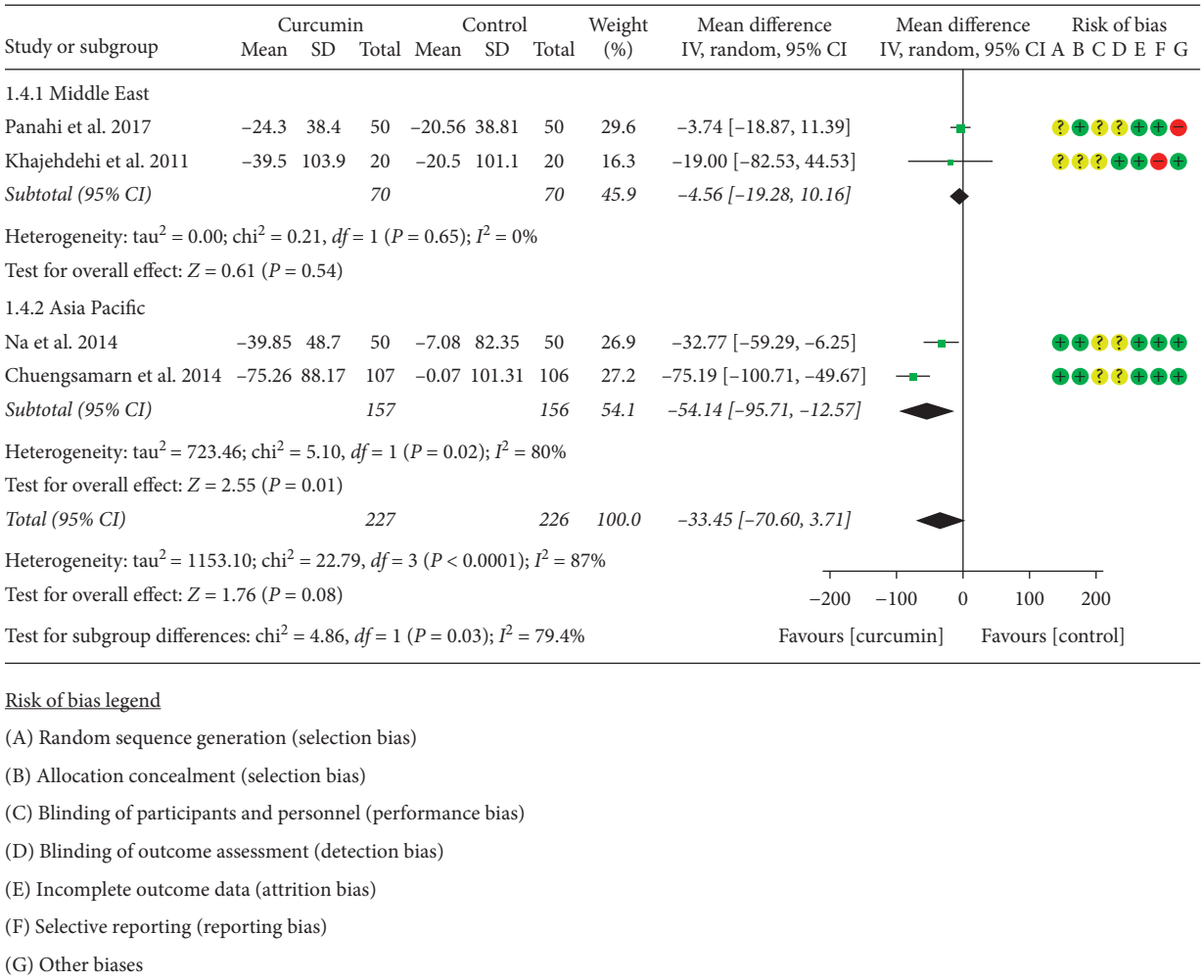

Risk of bias legend

(A) Random sequence generation (selection bias)

(B) Allocation concealment (selection bias)

(C) Blinding of participants and personnel (performance bias)

(D) Blinding of outcome assessment (detection bias)

(E) Incomplete outcome data (attrition bias)

(F) Selective reporting (reporting bias)

(G) Other biases

Figure 6: Triglyceride.

level of Asian patients. Interestingly, after curcumin intervenes in the Middle Eastern patients, their LDL-C level has increased. This is something that needs attention in the future. Demmers et al. [35] estimated the available scientific data on the effectiveness and safety of medicinal food plants in the treatment of impaired glucose tolerance. It included an RCT of curcumin extract intervention for diabetes and found that the fasting blood glucose at 2 hours after intervention showed statistical significance after 3, 6, and 9 months ($P < 0.01$). In addition, the curcumin extract intervention (HbA1c) value showed statistical significance after 3, 6, and 9 months ($P < 0.01$). HOMA-IR after curcumin extract intervention showed statistical significance after 6 months and 9 months ($P < 0.05$ and $P < 0.01$). It shows that curcumin has shown a reliable result that is effective in treating impaired glucose tolerance. Compared with Demmers et al.'s [35] research, our study is mainly devoted to exploring the interventional effects of curcumin and turmeric extracts on T2DM. We included more curcumin in the treatment of T2DM-related RCTs, and the evidence for improving the outcome of multiple related indicators of glucose tolerance is more sufficient. Compared to Marton et al.'s [36] review, (1) in this study, the RCT data (HOMA-IR, HbAlc, and so on) of curcumin treatment of T2DM were statistically analyzed (meta-analysis). (2) This study also conducted a subgroup analysis based on regions. (3) We adopted stricter screening criteria and merged the records belonging to the same RCT. (4) Sensitivity analysis was conducted in this study, which can more accurately locate the main source of heterogeneity. (5) The publication bias assessment was carried out in this study, and the publication bias of outcomes was excluded. In terms of improving metabolism, Roshanravan et al. [37] found the protective effect of supplementing *Crocus sativus* L. on hyperlipidemia and hyperglycemia through systematic reviews and meta-analysis studies. Our research also found that curcumin has the same clinical effect in improving the metabolism of diabetes.

4.5. The Strengths of This Review. This registered systematic review and meta-analysis is the first one that comprehensively evaluated the previous RCT of curcumin on T2DM and underwent a subgroup analysis to assess the applicable

Study or subgroup	Curcumin Mean	Curcumin SD	Curcumin Total	Control Mean	Control SD	Control Total	Weight (%)	Std. Mean difference IV, random, 95% CI	Risk of bias A B C D E F G
2.2.1 Middle East									
Panahi et al. 2017	−9	16	50	−3	11	50	18.3	−0.43 [−0.83, −0.04]	? + ? ? + + −
Asadi et al. 2019	14.8	27.73	40	4.8	31.27	40	17.3	0.34 [−0.11, 0.78]	+ + + + + + +
Khajehdehi et al. 2011	−23.2	108	20	−51.8	89.5	20	13.4	0.28 [−0.34, 0.91]	? ? ? + + − +
Subtotal (95% CI)			*110*			*110*	*49.1*	*0.04 [−0.50, 0.58]*	
Heterogeneity: tau^2 = 0.16; chi^2 = 7.57, *df* = 2 (*P* = 0.02); I^2 = 74%									
Test for overall effect: *Z* = 0.14 (*P* = 0.89)									
2.2.2 Asia Pacific									
Na et al. 2014	−23.4	43.2	50	−4.32	38.16	50	18.3	−0.46 [−0.86, −0.07]	+ + ? ? + + +
Chuengsamarn et al. 2014	−20.6	32.19	107	0.21	36.04	106	21.1	−0.61 [−0.88, −0.33]	+ + ? ? + + +
Thota et al. 2019	−1.9	2.2	15	−0.6	1.3	16	11.5	−0.71 [−1.44, 0.02]	+ ? ? ? + + +
Subtotal (95% CI)			*172*			*172*	*50.9*	*−0.57 [−0.79, −0.36]*	
Heterogeneity: tau^2 = 0.00 chi^2 = 0.47, *df* = 2 (*P* = 0.79); I^2 = 0%									
Test for overall effect: *Z* = 5.21 (*P* < 0.00001)									
Total (95% CI)			*282*			*282*	*100.0*	*−0.28 [−0.62, 0.06]*	
Heterogeneity: tau^2 = 0.12; chi^2 = 17.97, *df* = 5 (*P* = 0.003); I^2 = 72%									
Test for overall effect: *Z* = 1.60 (*P* = 0.11)									
Test for subgroup differences: chi^2 = 4.29, *df* = 1 (*P* < 0.04); I^2 = 76.7%									

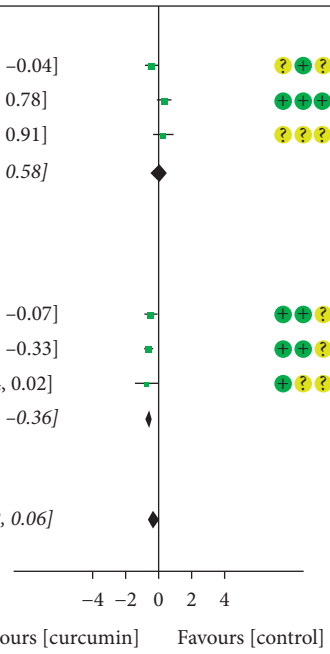

Risk of bias legend

(A) Random sequence generation (selection bias)

(B) Allocation concealment (selection bias)

(C) Blinding of participants and personnel (performance bias)

(D) Blinding of outcome assessment (detection bias)

(E) Incomplete outcome data (attrition bias)

(F) Selective reporting (reporting bias)

(G) Other biases

Figure 7: Fasting blood glucose.

population. It also collected the detailed data from each RCT and a comprehensive assessment of risk of bias was conducted.

4.6. The Limitations of This Review. RCTs from Asia and the Middle East account for a large proportion, which affects the applicability of the findings. The quantity and quality of RCTs are also not high in this review; several subgroups only include one RCT. Only 453 participants were included in this review, which may also impact the applicability of the findings. Meanwhile, half of RCTs [16–19, 22] have an unclear risk of bias in randomization, and one of the RCTs [22] has a high risk of bias in selective reporting; this may also influence the interpretation of the results. In addition, most of the outcomes have a high heterogeneity (such as HOMA-IR, TC, and TG) that cannot be eliminated by appropriate subgroup analysis. This also affected the applicability of the findings. The heterogeneity may come from the potential discrepancies in the pharmacological effects of various curcumin preparations, which may result from different standardizations of curcumin manufacturing process, dosage, duration of treatment, units of laboratory tests, and races of the selected patients or other places.

4.7. Implications for Future. This systematic review and meta-analysis found that curcumin may improve the HOMA-IR and fasting blood glucose of individuals in Asia

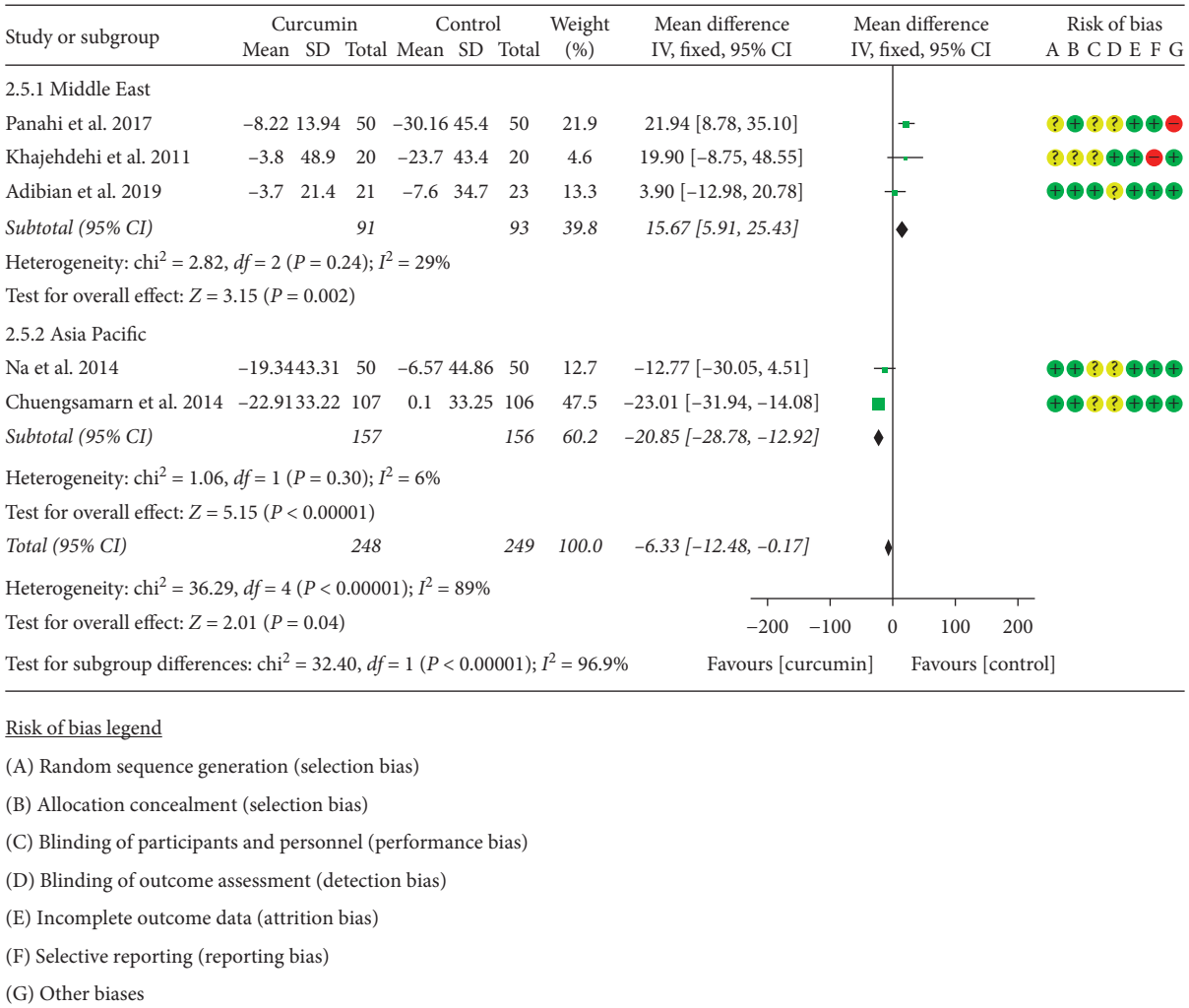

Figure 8: LDL-C.

and the Middle East. Curcumin may also improve the glycemic control in patients with T2DM. For blood lipids, curcumin may decrease the TC and TG in Asian T2DM patients, while its effects on the Middle Eastern T2DM patients may not be as significant as that on Asians; interestingly, according to the results, curcumin may decrease the LDL-C level in Asian T2DM patients, while it has the opposite effect on Middle Eastern patients. This may be related to ethnic differences, and more research is needed to amend or confirm it. In addition, in the aspect of decreasing BMI and fasting insulin, and improving HDL-C, curcumin may not have an advantage over the control group. However, due to the lack of evidence, more RCTs are needed. Last but not the least, for safety, there are no serious adverse events reported in RCTs, and the occurrence of adverse events in curcumin groups is the same as that of the placebo control group; therefore, it can be considered as a safety treatment based on current evidence.

In summary, curcumin may be more effective in Asia. In addition, for clinical practices, curcumin may be recommended as an adjunct to the treatment of T2DM patients to improve insulin resistance and glycemic control and reduce blood lipids. For Middle Eastern T2DM patients, the appropriate dosage, usage, and so on are yet to be confirmed. For future research, more RCTs about the adverse events and the T2DM-related outcomes are needed to revise or validate the findings in this review. The RCTs containing the data of the patients of other

Study or subgroup	Curcumin Mean	Curcumin SD	Curcumin Total	Control Mean	Control SD	Control Total	Weight (%)	Mean difference IV, random, 95% CI
2.6.1 Middle East								
Panahi et al. 2017	1.56	4.25	50	−0.22	4.62	50	23.2	1.78 [0.04, 3.52]
Khajehdehi et al. 2011	−3.4	13.3	20	−2.9	11.6	20	13.5	−0.50 [−8.23, 7.23]
Adibian et al.2019	−0.3	2.2	21	−2.8	5.3	23	22.5	−2.50 [−4.86, −0.14]
Subtotal (95% CI)			*91*			*93*	*59.2*	*−0.30 [−3.78, 3.19]*
Heterogeneity: tau^2 = 6.29; chi^2 = 8.22, *df* = 2 (*P* = 0.02); I^2 = 76%								
Test for overall effect: *Z* = 0.17 (*P* = 0.87)								
2.6.2 Asia Pacific								
Na et al. 2014	1.93	10.83	50	0.39	10.05	50	19.8	1.54 [−2.56, 5.64]
Chuengsamarn et al. 2014	10.19	11.61	107	−0.12	13.08	106	21.1	10.31 [6.99, 13.63]
Subtotal (95% CI)			*157*			*156*	*40.8*	*6.01 [−2.58, 14.60]*
Heterogeneity: tau^2 = 34.84; chi^2 = 10.62, *df* = 1 (*P* = 0.001); I^2 = 91%								
Test for overall effect: *Z* = 1.37 (*P* = 0.17)								
Total (95% CI)			*248*			*249*	*100.0*	*2.26 [−2.03, 6.55]*
Heterogeneity: tau^2 = 19.83; chi^2 = 38.27, *df* = 4 (*P* < 0.00001); I^2 = 90%								
Test for overall effect: *Z* = 1.03 (*P* = 0.30)								
Test for subgroup differences: chi^2 = 1.78, *df* = 1 (*P* = 0.18); I^2 = 43.8%								

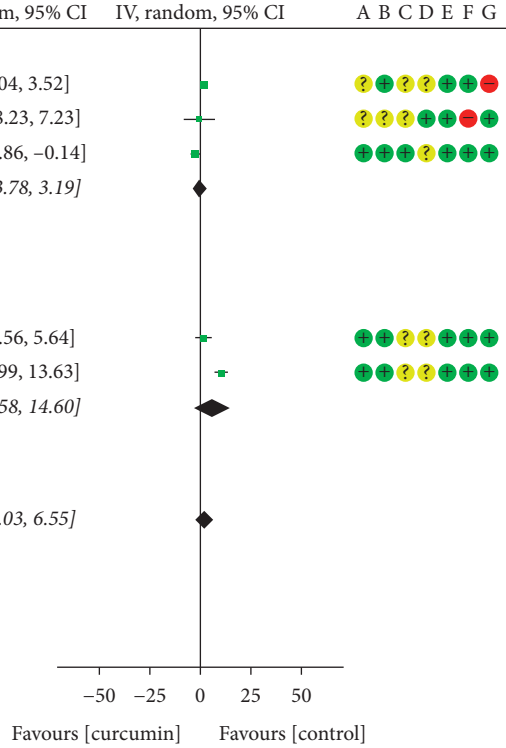

Risk of bias legend

(A) Random sequence generation (selection bias)

(B) Allocation concealment (selection bias)

(C) Blinding of participants and personnel (performance bias)

(D) Blinding of outcome assessment (detection bias)

(E) Incomplete outcome data (attrition bias)

(F) Selective reporting (reporting bias)

(G) Other biases

Figure 9: HDL-C.

Study or subgroup	Curcumin Mean	Curcumin SD	Curcumin Total	Control Mean	Control SD	Control Total	Weight (%)	Std. mean difference IV, fixed, 95% CI
Panahi et al. 2017	0.37	1.15	50	−0.01	0.53	50	70.3	0.42 [0.02, 0.82]
Adibian et al. 2019	12.1	7.7	21	7	7.1	23	29.7	0.68 [0.07, 1.29]
Total (95% CI)			*71*			*73*	*100.0*	*0.50 [0.16, 0.83]*
Heterogeneity: chi^2 = 0.48, *df* = 1 (*P* = 0.49); I^2 = 0%								
Test for overall effect: *Z* = 2.93 (*P* = 0.003)								

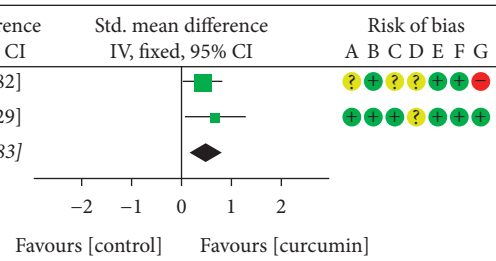

Risk of bias legend

(A) Random sequence generation (selection bias)

(B) Allocation concealment (selection bias)

(C) Blinding of participants and personnel (performance bias)

(D) Blinding of outcome assessment (detection bias)

(E) Incomplete outcome data (attrition bias)

(F) Selective reporting (reporting bias)

(G) Other biases

Figure 10: Adiponectin.

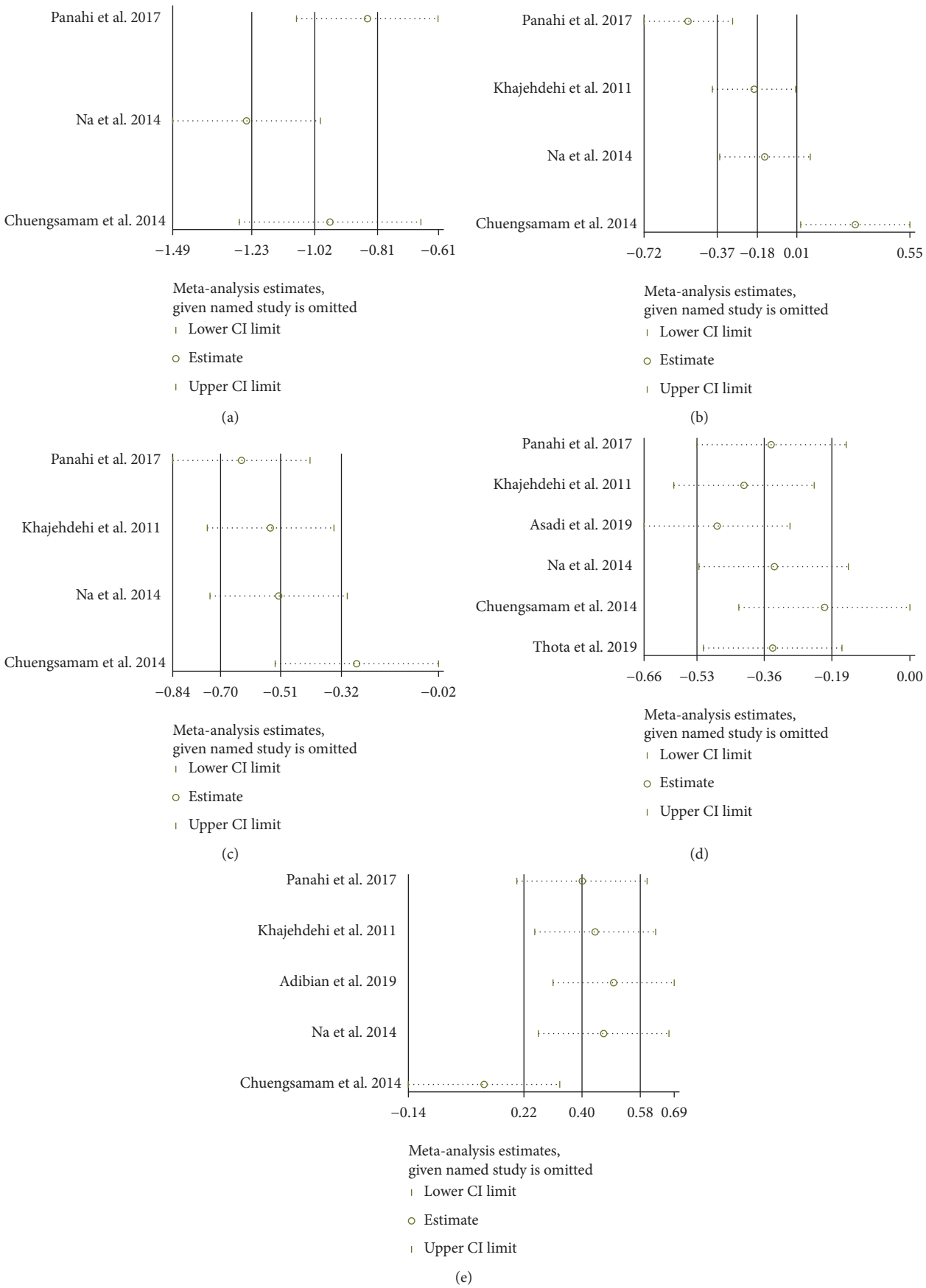

Figure 11: Sensitivity analysis results: (a) HOMA-IR; (b) TC; (c) TG; (d) FBG; (e) HDL-C.

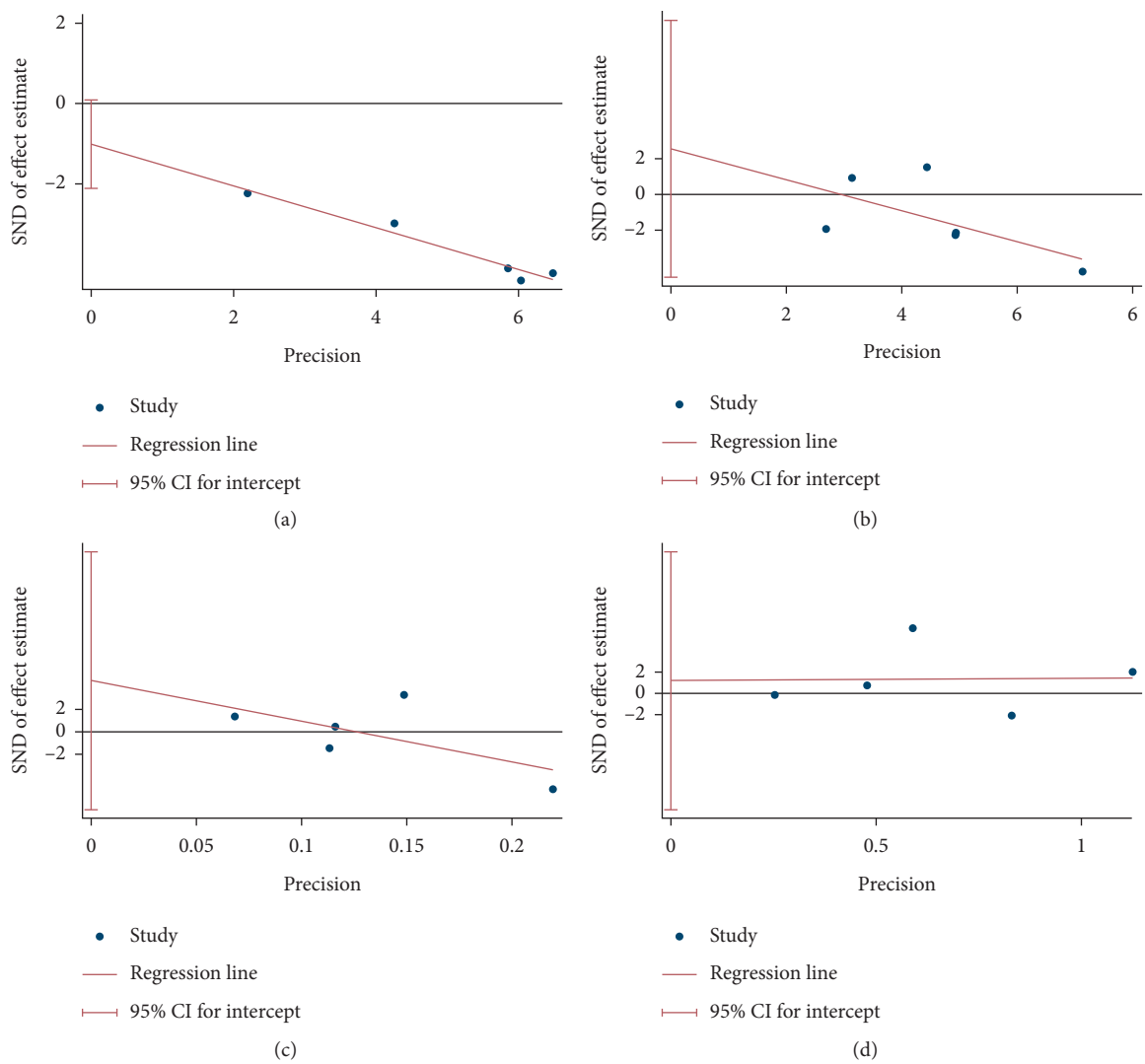

Figure 12: Publication bias detection (a) HbA1c; (b) FBG; (c) LDL-C; (d) HDL-C.

countries or regions around the world are also needed to expand the applicability of the results [38].

5. Conclusion

Based on the current evidence, curcumin may assist in improving insulin resistance, glycemic control, and decrease in TG and TC in patients with T2DM.

Data Availability

All data generated or analyzed during this study are included in this published article.

Disclosure

Tianqing Zhang and Qi He are co-first authors. Hengjing Hu is the corresponding author.

Conflicts of Interest

The authors declare that there are no conflicts of interest.

Authors' Contributions

Tianqing Zhang, Qi He, and Hengjing Hu are responsible for the study concept and design. Tianqing Zhang, Qi He, Yao Liu, Zhenrong Chen, and Hengjing Hu are responsible for the literature searching; Tianqing Zhang, Qi He, Yao Liu, Zhenrong Chen, and Hengjing Hu are responsible for data analysis and interpretation; Tianqing Zhang and Qi He drafted the paper; Hengjing Hu supervised the study; all authors participated in the analysis and interpretation of the data and approved the final manuscript.

Acknowledgments

This work was supported by grants from the National Natural Science Foundation of China (grant no. 81700306), the Natural Science Foundation of Hunan Province (grant no. 2018JJ3469), and the China Postdoctoral Science Foundation (grant no. 2017M622588). The authors thank Kailin Yang for his guidance on system review and meta-analysis.

Supplementary Materials

"CRD42018089528" is the protocol of our systematic review and meta-analysis. The "PRISMA 2009 checklist" is a standardized checklist that make sure that systematic reviews and meta-analyses are implemented according to this standard. (*Supplementary Materials*)

References

[1] International Diabetes Federation, *IDF Diabetes Atlas*, International Diabetes Federation, Brussels, Belgium, 6th edition, 2013.

[2] GBD 2015 Mortality and Causes of Death Collaborators, "Global, regional, and national life expectancy, all-cause mortality, and cause-specific mortality for 249 causes of death, 1980-2015: a systematic analysis for the Global Burden of Disease Study 2015," *Lancet*, vol. 388, pp. 1459–1544, 2016.

[3] A. J. Vegas, O. Veiseh, M. Gürtler et al., "Long-term glycemic control using polymer-encapsulated human stem cell-derived beta cells in immune-competent mice," *Nature Medicine*, vol. 22, no. 3, pp. 306–311, 2016.

[4] J. M. Forbes and M. E. Cooper, "Mechanisms of diabetic complications," *Physiological Reviews*, vol. 93, no. 1, pp. 137–188, 2013.

[5] M. Stolar, "Glycemic control and complications in type 2 diabetes mellitus," *The American Journal of Medicine*, vol. 123, pp. S3–11, 2010.

[6] D. Wu, D. Hu, H. Chen et al., "Glucose-regulated phosphorylation of TET2 by AMPK reveals a pathway linking diabetes to cancer," *Nature*, vol. 559, no. 7715, pp. 637–641, 2018.

[7] J. Pearson-Stuttard, B. Zhou, V. Kontis, J. Bentham, M. J. Gunter, and M. Ezzati, "Worldwide burden of cancer attributable to diabetes and high body-mass index: a comparative risk assessment," *The Lancet Diabetes & Endocrinology*, vol. 6, no. 6, pp. e6–e15, 2018.

[8] A. Y. Y. Cheng and I. G. Fantus, "Oral antihyperglycemic therapy for type 2 diabetes mellitus," *Canadian Medical Association Journal*, vol. 172, no. 2, pp. 213–226, 2005.

[9] G. Nicholson and G. M. Hall, "Diabetes mellitus: new drugs for a new epidemic," *British Journal of Anaesthesia*, vol. 107, no. 1, pp. 65–73, 2011.

[10] E. J. Verspohl, "Novel pharmacological approaches to the treatment of type 2 diabetes," *Pharmacological Reviews*, vol. 64, no. 2, pp. 188–237, 2012.

[11] S. Chuengsamarn, S. Rattanamongkolgul, B. Phonrat, R. Tungtrongchitr, and S. Jirawatnotai, "Reduction of atherogenic risk in patients with type 2 diabetes by curcuminoid extract: a randomized controlled trial," *The Journal of Nutritional Biochemistry*, vol. 25, no. 2, pp. 144–150, 2014.

[12] V. Karuppagounder, S. Arumugam, V. V. Giridharan et al., "Tiny molecule, big power: multi-target approach for curcumin in diabetic cardiomyopathy," *Nutrition*, vol. 34, pp. 47–54, 2017.

[13] S. J. Hewlings and D. S. Kalman, "Curcumin: a review of its' effects on human health," *Foods*, vol. 22, no. 10, p. 6, 2017 pii: E92.

[14] J. Zheng, J. Cheng, S. Zheng, Q. Feng, and X. Xiao, "Curcumin, A polyphenolic curcuminoid with its protective effects and molecular mechanisms in diabetes and diabetic cardiomyopathy," *Frontiers in Pharmacology*, vol. 9, p. 472, 2018.

[15] N. Parsamanesh, M. Moossavi, A. Bahrami, A. E. Butler, and A. Sahebkar, "Therapeutic potential of curcumin in diabetic complications," *Pharmacological Research*, vol. 136, pp. 181–193, 2018.

[16] Y. Panahi, N. Khalili, E. Sahebi et al., "Curcuminoids modify lipid profile in type 2 diabetes mellitus: a randomized controlled trial," *Complementary Therapies in Medicine*, vol. 33, pp. 1–5, 2017.

[17] Y. Panahi, N. Khalili, E. Sahebi et al., "Antioxidant effects of curcuminoids in patients with type 2 diabetes mellitus: a randomized controlled trial," *Inflammopharmacology*, vol. 25, no. 1, pp. 25–31, 2017.

[18] Y. Panahi, N. Khalili, E. Sahebi et al., "Curcuminoids plus piperine modulate adipokines in type 2 diabetes mellitus," *Current Clinical Pharmacology*, vol. 12, no. 4, pp. 253–258, 2018.

[19] Y. Panahi, N. Khalili, E. Sahebi et al., "Effects of curcuminoids plus piperine on glycemic, hepatic and inflammatory biomarkers in patients with type 2 diabetes mellitus: a randomized double-blind placebo-controlled trial," *Drug Research*, vol. 68, no. 07, pp. 403–409, 2018.

[20] L. X. Na, B. L. Yan, S. Jiang, H. L. Cui, Y. Li, and C. H. Sun, "Curcuminoids target decreasing serum adipocyte-fatty acid binding protein levels in their glucose-lowering effect in patients with type 2 diabetes," *Biomedical and Environmental Sciences: BES*, vol. 27, no. 11, pp. 902–906, 2014.

[21] L.-X. Na, Y. Li, H.-Z. Pan et al., "Curcuminoids exert glucose-lowering effect in type 2 diabetes by decreasing serum free fatty acids: a double-blind, placebo-controlled trial," *Molecular Nutrition & Food Research*, vol. 57, no. 9, pp. 1569–1577, 2013.

[22] P. Khajehdehi, M. Pakfetrat, K. Javidnia et al., "Oral supplementation of turmeric attenuates proteinuria, transforming growth factor-β and interleukin-8 levels in patients with overt type 2 diabetic nephropathy: a randomized, double-blind and placebo-controlled study," *Scandinavian Journal of Urology and Nephrology*, vol. 45, no. 5, pp. 365–370, 2011.

[23] D. Moher, A. Liberati, J. Tetzlaff, D. G. Altman, and The PRISMA Group, "Preferred reporting items for systematic reviews and meta-analyses: the PRISMA statement," *Annals of Internal Medicine*, vol. 151, no. 4, pp. 264–269, 2009.

[24] J. J. Deeks, J. P. Higgins, and D. G. Altman, "Chapter 16: special topics in statistics," in *Cochrane Handbook for Systematic Reviews of Interventions*, J. P. Higgins and S. Green, Eds., The Cochrane Collaboration, London, UK, 2011.

[25] J. J. Deeks, J. P. Higgins, and D. G. Altman, "Chapter 8: assessing risk of bias in included studies," in *Cochrane Handbook or Systematic Reviews of Interventions Version 5.1.0*, J. P. Higgins and S. Green, Eds., The Cochrane Collaboration, London, UK, 2011.

[26] J. J. Deeks, J. P. Higgins, and D. G. Altman, "Chapter 9: analyzing data and undertaking meta-analyses," in *Cochrane Handbook for Systematic Reviews of Interventions*, J. P. Higgins and S. Green, Eds., The Cochrane Collaboration, London, UK, 2011.

[27] H. Yang, W. Xu, Z. Zhou et al., "Curcumin attenuates urinary excretion of albumin in type II diabetic patients with enhancing nuclear factor erythroid-derived 2-like 2 (Nrf2) system and repressing inflammatory signaling efficacies," *Experimental and Clinical Endocrinology & Diabetes*, vol. 123, no. 06, pp. 360–367, 2015.

[28] H. R. Rahimi, A. H. Mohammadpour, M Dastani et al., "The effect of nano-curcumin on HbA1c, fasting blood glucose, and lipid profile in diabetic subjects: a randomized clinical trial,"

Avicenna Journal of Phytomedicine, vol. 6, no. 5, pp. 567–577, 2016.

[29] M. Funamoto, K. Shimizu, Y. Sunagawa et al., "Effects of highly absorbable curcumin in patients with impaired glucose tolerance and non-insulin-dependent diabetes mellitus," *Journal of Diabetes Research*, vol. 2019, 7 pages, 2019, PMC6906884, Article ID 8208237.

[30] R. N. Thota, J. I. Rosato, C. B. Dias, T. L. Burrows, R. N. Martins, and M. L. Garg, "Dietary supplementation with curcumin reduce circulating levels of glycogen synthase kinase-3β and islet amyloid polypeptide in adults with high risk of type 2 diabetes and alzheimer's disease," *Nutrients*, vol. 12, no. 4, p. 1032, 2020 PMID: 32283762.

[31] S. Asadi, M. S. Gholami, F. Siassi, M. Qorbani, and G. Sotoudeh, "Beneficial effects of nano-curcumin supplement on depression and anxiety in diabetic patients with peripheral neuropathy: a randomized, double-blind, placebo-controlled clinical trial," *Phytotherapy Research*, vol. 34, no. 4, pp. 896–903, 2020, PMID: 31788880.

[32] S. Asadi, M. S. Gholami, F. Siassi, M. Qorbani, K. Khamoshian, and G. Sotoudeh, "Nano curcumin supplementation reduced the severity of diabetic sensorimotor polyneuropathy in patients with type 2 diabetes mellitus: a randomized double-blind placebo- controlled clinical trial," *Complementary Therapies in Medicine*, vol. 43, pp. 253–260, 2019, PMID: 30935539.

[33] R. N. Thota, S. H. Acharya, and M. L. Garg, "Curcumin and/or omega-3 polyunsaturated fatty acids supplementation reduces insulin resistance and blood lipids in individuals with high risk of type 2 diabetes: a randomised controlled trial," *Lipids in Health and Disease*, vol. 18, no. 1, p. 31, 2019 PMID: 30684965.

[34] M. Adibian, H. Hodaei, O. Nikpayam, G. Sohrab, A. Hekmatdoost, and M. Hedayati, "The effects of curcumin supplementation on high-sensitivity C-reactive protein, serum adiponectin, and lipid profile in patients with type 2 diabetes: a randomized, double-blind, placebo-controlled trial," *Phytotherapy Research*, vol. 33, no. 5, pp. 1374–1383, 2019, Epub 2019 Mar 12. PMID: 30864188.

[35] A. Demmers, H. Korthout, F. S. Van Etten-Jamaludin, F. Kortekaas, and J. M. Maaskant, "Effects of medicinal food plants on impaired glucose tolerance: a systematic review of randomized controlled trials," *Diabetes Research and Clinical Practice*, vol. 131, pp. 91–106, 2017.

[36] L. T. Marton, L. M. Pescinini-E-Salzedas, M. E. C. Camargo et al., "The effects of curcumin on diabetes mellitus: a systematic review," *Frontiers in Endocrinology*, vol. 12, Article ID 669448, 2021.

[37] B. Roshanravan, S. Samarghandian, M. Ashrafizadeh, A. Amirabadizadeh, F. Saeedi, and T. Farkhondeh, "Metabolic impact of saffron and crocin: an updated systematic and meta-analysis of randomised clinical trials," *Archives of Physiology and Biochemistry*, vol. 2020, Article ID 1716020, 13 pages, 2020.

[38] S.-Y. Zhang, K.-L. Yang, L.-T. Zeng, X.-H. Wu, and H.-Y. Huang, "Effectiveness of coenzyme Q10 supplementation for type 2 diabetes mellitus: a systematic review and meta-analysis," *International Journal of Endocrinology*, vol. 2018, Article ID 6484839, 11 pages, 2018.